

DISS. ETH No. 22527

# **Halogen Effects in Organocatalysis**

A thesis submitted to attain the degree of  
DOCTOR OF SCIENCES of ETH ZURICH  
(Dr. sc. ETH Zurich)

presented by

**Yannick Pierre Rey**

Master of Science ETH in Chemistry

born on 10.11.1985

citizen of Geltwil (AG)

accepted on the recommendation of  
Prof. Dr. Ryan Gilmour, co-examiner  
Prof. Dr. Erick M. Carreira, examiner  
Prof. Dr. Antonio Togni, co-examiner

2015



*Meiner Familie*



## Acknowledgements

First of all I would like to thank Prof. Ryan Gilmour for giving me the opportunity to carry out my Ph.D. thesis in his group and also for his encouragement, support and patience.

Special thanks go to Prof. Erick M. Carreira for agreeing to take over my supervision from ETH Zürich when we moved to Münster, and to Prof. Antonio Togni for kindly agreeing to be my co-examinor.

I am very grateful to everyone I worked with, in Zürich: Dr. Christof Sparr, Dr. Christoph Bucher, Dr. Susann Paul, Dr. Eva-Maria Tanzer, Dr. Lucie Zimmer, Estelle Durantie and Dr. Mareike Holland and in Münster: Istvan Molnar, Patrick Bentler, Andrea Kapries, Dr. Nico Santschi, Dr. Randy Benedict, Christian Thiehoff, Jan Metternich, Dr. Nuria Aiguabella and Anna Sadurni. Thank you all for creating a great atmosphere inside and outside the lab during these years.

I am especially grateful to Dr. Mareike Holland for moving to Münster and doing a great deal of the organisational work for the move. It would have been a lot harder without you!

Special thanks go to Dr. Nico Santschi and Sonja Kohrt for the many dinner invitations.

I would also like to thank Dr. Hans Martin Senn for performing the calculations on the DMAP derived systems and Dr. Sami Lakhdar for the kinetic studies.

To the students I had the opportunity to work with: Karin Glansberg, Vanessa Lewe, Georg Radermacher and David Schnieders, thank you very much!

Furthermore, I thank the ETH- and the WWU-services for their support in analysis, mechanical problems and chemical supply.

And last but not least special thanks go to my parents Michèle and Max as well as to my sister Stéphanie for their guidance and endless support.

Merci vill mal!

## List of Publications

Parts of this thesis were published:

### *Modulating NHC catalysis with fluorine*

Yannick P. Rey and Ryan Gilmour,  
*Beilstein J. Org. Chem.* **2013**, 9, 2812-2820.

### *Molecular Design Exploiting a Fluorine gauche Effect as a Stereoelectronic Trigger*

Yannick P. Rey, Lucie E. Zimmer, Christof Sparr, Eva-Maria Tanzer, W. Bernd Schweizer,  
Hans Martin Senn, Sami Lakhdar and Ryan Gilmour,  
*Eur. J. Org. Chem.* **2014**, 1202-1211.

### *The Fluorine Gauche Effect in Molecular Design: A Personal Perspective*

Yannick P. Rey and Ryan Gilmour, *Seminars in Organic Synthesis* (book chapter), **2014**, 90-98.

## Poster Presentations

### *Molecular Design Exploiting a Fluorine gauche Effect as a Stereoelectronic Trigger*

Yannick P. Rey, Lucie E. Zimmer, Christof Sparr, Eva-Maria Tanzer, W. Bernd Schweizer,  
Hans Martin Senn, Sami Lakhdar and Ryan Gilmour,  
Presented at the Syngenta Symposium 2013 in Stein (AG), Switzerland.

### *Molecular Design Exploiting a Fluorine gauche Effect as a Stereoelectronic Trigger*

Yannick P. Rey, Lucie E. Zimmer, Christof Sparr, Eva-Maria Tanzer, W. Bernd Schweizer,  
Hans Martin Senn, Sami Lakhdar and Ryan Gilmour,  
Presented at the Münster Symposium on Cooperative Effects in Chemistry 2013.

### Cooperative Effects in Organocatalysis

Yannick P. Rey and Ryan Gilmour,  
Presented at the SFB evaluation in Münster. 2013.

## Table of Contents

1	Summary .....	1
2	Zusammenfassung .....	3
3	Introduction .....	5
3.1	Stereoelectronic Effects .....	5
3.2	Brominated and Iodinated Organocatalysts .....	15
4	Fluorinated <i>N</i> -Heterocyclic Carbenes .....	20
4.1	Introduction .....	20
4.2	Synthesis of Appropriate NHC Precursors .....	22
4.3	X-ray Structure of Compound <b>1</b> .....	25
4.4	Analysis of the Solution Phase Conformation of the Triazolium Salts .....	26
4.4.1	Introduction .....	26
4.4.2	Analysis of the Solution Phase Conformations of Compounds <b>1</b> and <b>2</b> .....	27
4.5	Asymmetric Steglich Rearrangement Catalysed by Fluorinated NHCs .....	29
4.5.1	Optimisation of Reaction Conditions .....	29
4.5.2	Effect of Differently Substituted NHC Precursors on the Model Reaction .....	31
4.5.3	Conclusion .....	33
5	Fluorinated 4-Aminopyridine Derivatives .....	34
5.1	Introduction .....	34
5.2	Diarylfluoromethyl Derivatives .....	35
5.2.1	Computational Studies .....	35
5.2.2	Synthesis of Fluorinated DMAP Derivatives Part I .....	37
5.2.3	Kinetic Studies by Means of Reaction with Benzhydrylium Ions .....	38
5.2.4	Catalysis Studies Part I .....	40
5.2.5	Synthesis of Fluorinated DMAP Derivatives Part II .....	41
5.2.6	Catalysis Studies Part II .....	43

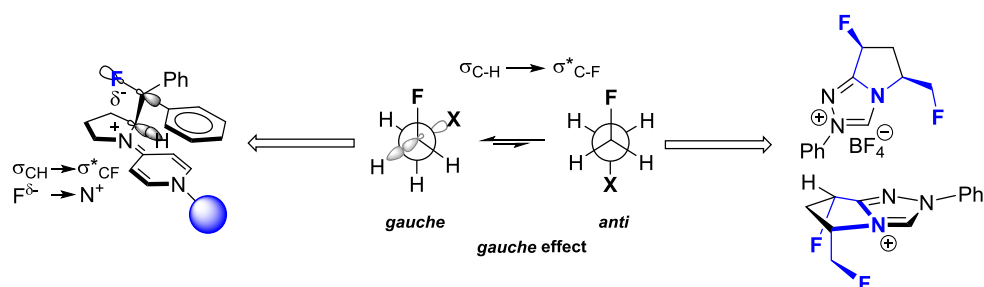
5.2.7	Towards a $C_2$ -Symmetric, Difluorinated DMAP Analogue.....	45
5.2.8	Attempted Photochemical Route to a $C_2$ -Symmetric DMAP Analogue.....	48
5.3	$\alpha$ -Fluorosulfones.....	50
5.3.1	Introduction.....	50
5.3.2	Synthesis of DMAP Derived $\alpha$ -Fluorosulfones.....	51
5.3.3	Crystal Structures of Fluorinated and Non-Fluorinated Compounds <b>98-100</b> . ...	52
5.4	Conclusion and Outlook.....	54
6	Halogenated Borondipyrromethenes (BODIPY).....	55
6.1	Introduction.....	55
6.2	Investigation of The Internal Heavy Atom Effect in Singlet Oxygen Generation ....	59
6.2.1	Synthesis of BODIPY Derived Sensitisers.....	59
6.2.2	UV-visible Spectra of the Synthesised Compounds <b>105-114</b> .....	60
6.2.3	Application of Compound <b>108</b> in the Schenck-Ene Reaction.....	63
6.2.4	Investigating (-)- $\beta$ -Pinene as a Substrate in the Schenck-Ene Reaction.....	65
6.2.5	Application of the Acetoxyated BODIPY Sensitisers in the Photosensitised Oxidation of Anthracene.....	67
6.2.6	Application of the Methylated BODIPY Sensitisers in the Photosensitised Oxidation of Anthracene.....	69
6.2.7	Application of the Pyridine Derived BODIPY Sensitisers in the Photosensitised Oxidation of Anthracene.....	71
6.2.8	Correlation of the Initial Rates with the Spin Orbit Coupling Constants.....	73
6.3	Conclusion and Outlook.....	74
7	Imidazolidinones as Photoredoxcatalysts.....	75
7.1	Introduction.....	75
7.2	Synthesis of a Phenylalanine Derived Photoredoxcatalyst.....	77
7.3	Application of the Phenylalanine Derived Catalysts in the $\alpha$ -Alkylation of Octanal	78
7.4	Conclusion and Outlook.....	80
8	Conclusion and Outlook.....	81



9	Abbreviations .....	82
10	Experimental Part .....	84
11	References .....	143

## 1 Summary

The incorporation of halogen atoms in organic compounds can have various effects. Due to fluorine's high electronegativity ( $\chi = 4$ ) a carbon-fluorine bond is highly polarised which can lead to interesting electrostatic interactions. Moreover, the associated antibonding molecular orbital ( $\sigma^*_{\text{CF}}$ ) is comparatively low in energy which allows for efficient interactions with filled orbitals such as lone pairs (n) or bonding molecular orbitals (*e.g.*  $\sigma_{\text{CH}}$ ). The prerequisite of spatial overlap for orbitals involved in such hyperconjugative interactions can lead to an influence on the fluorinated molecule's conformation (stereoelectronic effect). Importantly, when a C-F bond is placed in a vicinal position to an electron withdrawing or formally positively charged group (X), the electrostatic and stereoelectronic effects lead to a preference for the *synclinal* conformation in which the dihedral angle ( $\Phi$ ) between the two substituents is roughly  $60^\circ$  (*gauche* effect). Herein, this principle was applied to organocatalysis by introducing fluorine atoms in  $\beta$ -position to a nitrogen atom in dimethylaminopyridine (DMAP) derived systems as well as triazolium salts which are used as *N*-heterocyclic carbene (NHC) precursors.



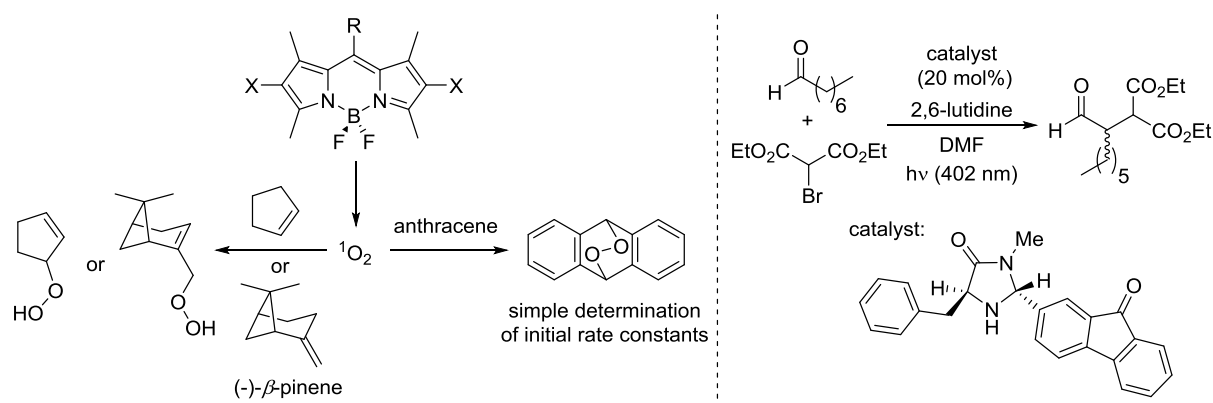
The effect of fluorination on the conformation of fluorinated DMAP derivatives was studied by computational methods (in a collaboration with Dr. Hans Martin Senn), kinetics (with Dr. Sami Lakhdar) and the application in nucleophilic catalysis. It was found that upon reaction with the substrate (acetic anhydride) a conformational change is triggered which places one phenyl ring above the reactive centre. Additionally, kinetic studies revealed a similar nucleophilicity for the fluorinated system ( $N = 14.57$ ) and 4-pyrrolidinopyridine ( $N = 15.90$ ). The application in the kinetic resolution of ( $\pm$ )-1-phenylethanol showed the importance of conformational control of the acetyl group in the acetylpyridinium salt. To this end, a modified structure containing a cyclopentenopyridine moiety was investigated and found to lead to improved selectivities.

An alternative DMAP derived structure containing an  $\alpha$ -fluorosulfone sidechain was proposed and synthesised. X-ray analysis confirmed the expected conformational effects (fluorine

*synclinal* to the nitrogen of the pyrrolidine ring and *antiperiplanar* to one oxygen atom of the sulfonyl group).

The effect of fluorination was also studied by strategically introducing two fluorine atoms in a triazolium salt structure. This compound was applied as a catalyst precursor in the NHC catalysed asymmetric Steglich rearrangement. By comparison with the monofluorinated and non-fluorinated analogues it was found that fluorination has a large effect on the enantioselectivity of this reaction (*e.r.* = 62.5:37.5 for the non-fluorinated compound, *e.r.* = 87.0:13.0 for the difluorinated structure).

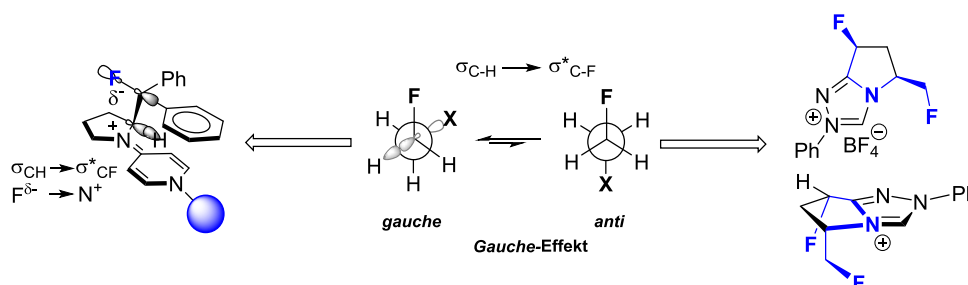
The introduction of heavier halogen atoms like bromine and iodine has a different effect on organic compounds. By the so-called heavy atom effect the behaviour of chromophores upon absorption of light can be influenced. In general, the incorporation of heavy halogens increases the probability of intersystem crossing which can lead to more efficient sensitizers and photoredoxcatalysts. The effect of chlorination, bromination and iodination was studied in the photosensitised generation of singlet oxygen by borondipyrrromethene (BODIPY) derivatives. Using a simple, GC based procedure initial rate constants for the oxidation of anthracene could be obtained and compared.



Light induced reactions were further studied on the example of the known  $\alpha$ -alkylation of aldehydes. Novel catalyst structures that incorporate both a secondary amine moiety and a photochemically active substituent (fluorenone) were synthesised and tested in this reaction. It was found that these compounds deliver the desired product with an *e.r.* of up to 86.5:13.5.

## 2 Zusammenfassung

Das Einfügen von Halogenatomen in organische Verbindungen kann verschiedene Effekte haben. Wegen der hohen Elektronegativität von Fluor ( $\chi = 4$ ) ist eine Kohlenstoff-Fluor-Bindung stark polarisiert, was zu interessanten elektrostatischen Wechselwirkungen führen kann. Des Weiteren liegt das entsprechende antibindende Molekülorbital ( $\sigma^*_{CF}$ ) energetisch tief, was eine effiziente Wechselwirkung mit gefüllten Orbitalen, wie zum Beispiel freien Elektronenpaaren ( $n$ ) oder bindenden Molekülorbitalen (z.B.  $\sigma_{CH}$ ) erlaubt. Die Voraussetzung der räumlichen Überlappung der in einer solchen Hyperkonjugation beteiligten Orbitale kann einen Einfluss auf die Konformation des fluorierten Moleküls haben (stereoelektronischer Effekt). Wichtig ist, dass wenn eine C-F-Bindung vicinal zu einer elektronenziehenden oder formell positiv geladenen Gruppe eingesetzt wird, die elektrostatischen und stereoelektronischen Effekte zu einer Bevorzugung der *synklinalen* Konformation führen. In dieser Konformation besteht ein Diederwinkel ( $\Phi$ ) von ungefähr  $60^\circ$  zwischen den Substituenten (*Gauche*-Effekt). In dieser Arbeit wurde dieses Prinzip durch Einführung von Fluoratomen in  $\beta$ -Position zu einem Stickstoffatom in Dimethylaminopyridin (DMAP)-Derivaten und Triazoliumsalzen (die als Vorläufer von *N*-Heterozyklischen Carbenen (NHC) dienen) auf die Organokatalyse angewendet.



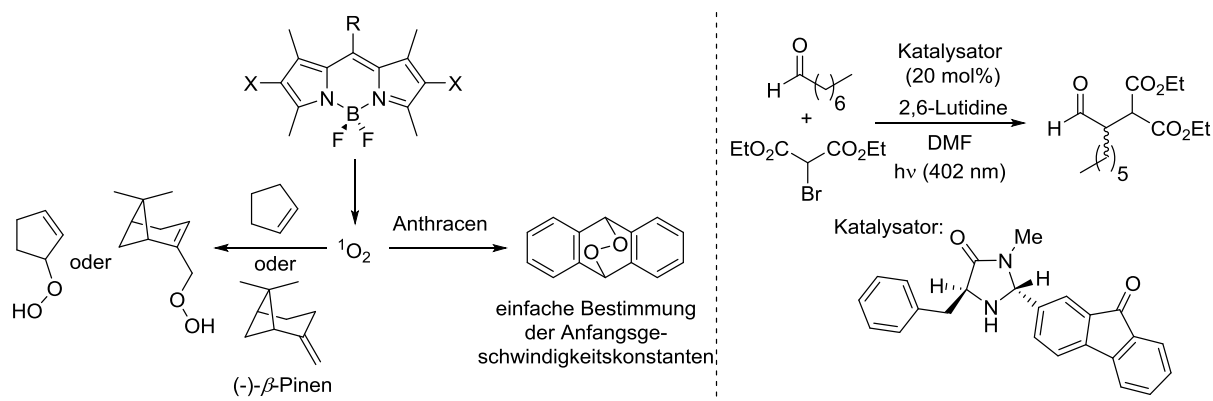
Der Effekt der Fluorierung auf die Konformation von fluorierten DMAP-Derivaten wurde anhand von rechnergestützten Methoden (in Kollaboration mit Dr. Hans Martin Senn), Kinetik (mit Dr. Sami Lakhdar) und der Anwendung in der nukleophilen Katalyse studiert. Es wurde herausgefunden, dass nach der Reaktion mit dem Substrat (Essigsäureanhydrid) eine Änderung der Konformation stattfindet, sodass eine Phenylgruppe über das reaktive Zentrum gesetzt wird. Zusätzlich zeigten kinetische Studien eine ähnlich hohe Nukleophilie des fluorierten Systems ( $N = 14.57$ ) und 4-Pyrrolidinpyridin ( $N = 15.90$ ) auf. Die Anwendung in der kinetischen Racematspaltung von  $(\pm)$ -1-Phenylethanol zeigte die Wichtigkeit der Kontrolle der Acetylgruppenkonformation im Acetylpyridiniumsalz auf.

Dafür wurde eine modifizierte Struktur studiert, die eine Cyclopentenopyridin-Einheit enthielt. Diese führte zu verbesserten Selektivitäten.

Eine alternative, von DMAP abgeleitete Struktur, die eine  $\alpha$ -Fluorosulfon-Seitenkette enthält wurde vorgeschlagen und synthetisiert. Röntgenstrukturanalyse bestätigte die erwarteten konformationellen Effekte (Fluoratom *synklinal* zum Stickstoffatom des Pyrollidinrings und *antiperiplanar* zu einem Sauerstoffatom der Sulfonylgruppe).

Der Effekt der Fluorierung wurde auch anhand der strategischen Einführung zweier Fluoratome in ein Triazoliumsals studiert. Dieser Verbindung wurde als Katalysatorvorläufer in der NHC-katalysierten Steglich-Umlagerung verwendet. Durch einen Vergleich mit den einfach-fluorierten und nicht-fluorierten Analoga wurde ein grosser Effekt auf die Enantioselektivität dieser Reaktion festgestellt (*e.r.* = 62.5:37.5 für die nicht-fluorierte Verbindung, *e.r.* = 87.0:13.0 für die difluorierte Struktur).

Das Einführen von schwereren Halogenatomen, wie Brom und Iod, hat einen anderen Effekt auf organische Verbindungen. Durch den sogenannten „Heavy-Atom-Effect“ kann das Verhalten von Chromophoren nach der Lichtabsorption beeinflusst werden. Generell erhöhen schwere Halogene die Wahrscheinlichkeit eines „Intersystem Crossings“, was zu effizienteren Sensitisatoren und Photoredoxkatalysatoren führen kann. Der Effekt der Chlorierung, Bromierung und Iodierung wurde anhand der photosensitisierten Erzeugung von Singulett-Sauerstoff durch Bordipyrrromethen (BODIPY) - Derivaten untersucht. Durch eine einfache, auf GC basierende Vorgehensweise konnten Anfangsgeschwindigkeitskonstanten für die Oxidation von Anthracen erhalten und verglichen werden.



Lichtinduzierte Reaktionen wurden zudem am Beispiel der bekannten  $\alpha$ -Alkylierung von Aldehyden studiert. Neue Katalysatorstrukturen, die sowohl eine sekundäre Amin-Einheit als auch einen photochemisch aktiven Substituenten (Fluorenon) beinhalten wurden synthetisiert und in dieser Reaktion getestet. Es wurde beobachtet, dass diese Verbindungen das erwartete Produkt mit einem *e.r.* von bis zu 86.5:13.5 ergaben.

### 3 Introduction

#### 3.1 Stereoelectronic Effects

In general, the interaction of orbitals depends on their separation in energy as well as on their spatial overlap. If the difference in energy is small and the overlap is large, interaction between the two orbitals will be significant. This does not only hold true for intermolecular interactions (*e.g.* bond formation) but also for the intramolecular scenario. As the intramolecular overlap depends on the relative orientation of the orbitals, effects arising from such an interaction are intimately related to the conformation of the molecule (hence the name stereoelectronic effects).<sup>[1]</sup> As a consequence, the dihedral angle ( $\Phi$ ) between substituents is crucial for any discussion of such interactions. A schematic representation of the orbital interactions at various dihedral angles, along with the appropriate terms used to describe conformational relationships between vicinal groups is shown in Figure 1. It becomes clear that when two adjacent substituents adopt a conformation with a dihedral angle of  $180^\circ$  (*anti*) the corresponding orbital overlap will be maximal. The closer  $\Phi$  gets to  $90^\circ$ , the smaller the interaction will be. It will then increase again when approaching  $\Phi = 0^\circ$  (*syn*) but will not reach the same value as for  $180^\circ$ . Angles of  $0^\circ \pm 30^\circ$  are referred to as *synperiplanar* and angles of  $180^\circ \pm 30^\circ$  are described as *antiperiplanar*.

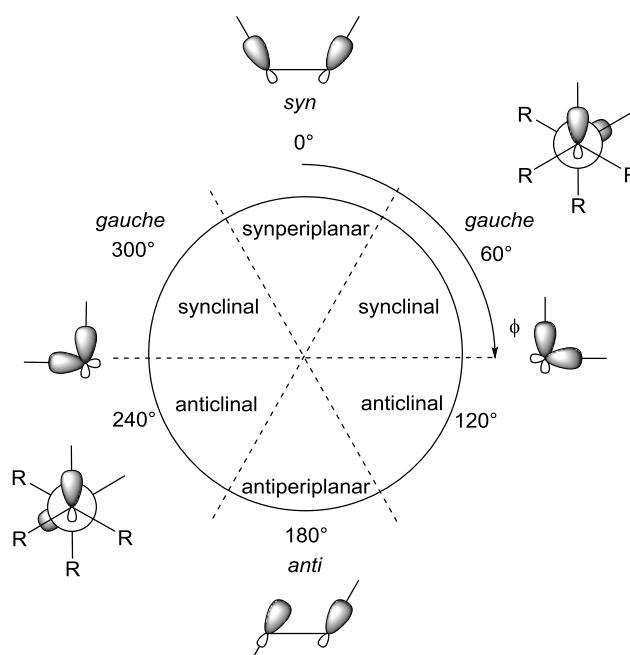


Figure 1: Orbital interactions between vicinal groups depending on the dihedral angle  $\Phi$ .

By extension angles of  $60^\circ$  are referred to as *gauche* ( $60^\circ$ ) or *synclinal* ( $60^\circ \pm 30^\circ$ ). Depending on the occupancy of the orbitals (filled or empty) their interaction can be stabilising or destabilising. Two filled orbitals will interact in a net destabilising manner (Figure 2, left). Pertinent examples include hydrazine derivatives such as tetramethylhydrazine and 1,5-diazabicyclo[3.3.0]octane.<sup>[2]</sup>

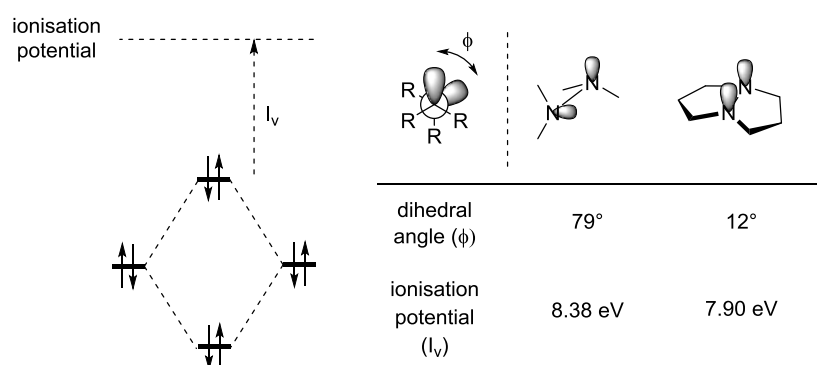


Figure 2: The destabilising stereoelectronic effect in hydrazine derivatives.

Due to the free rotation about the N-N bond in acyclic compounds the lone pairs can be arranged in an almost perpendicular fashion (dihedral angle  $\Phi = 79^\circ$ ) so that the interaction (and therefore the destabilisation) is significantly reduced. In the bicyclic structure the rotation is hindered and therefore the lone pairs are forced to interact ( $\Phi = 12^\circ$ ) which leads to a notably decreased ionisation potential ( $I_v = 7.90$  eV vs. 8.38 eV).<sup>[2]</sup> This is contrasted by stereoelectronic effects that lead to a net stabilisation of the system. Most commonly, these involve the interaction of a filled and an empty orbital. An example in which the prerequisite of a small difference in energy is fulfilled is given by the interaction of a lone pair ( $n$ ) with a low lying antibonding sigma orbital ( $\sigma^*$ ). Arguably, the most prominent example thereof is found in carbohydrates and is commonly referred to as the anomeric effect (Figure 3, left).<sup>[3][4][5]</sup> It can be clearly seen that in a carbohydrate derivative, the axial lone pair is perfectly aligned to interact with the adjacent C-O bond ( $n_o \rightarrow \sigma^*_{co}$ ), thus favouring this conformation.

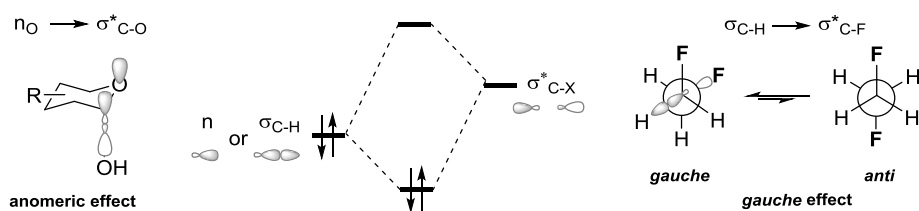
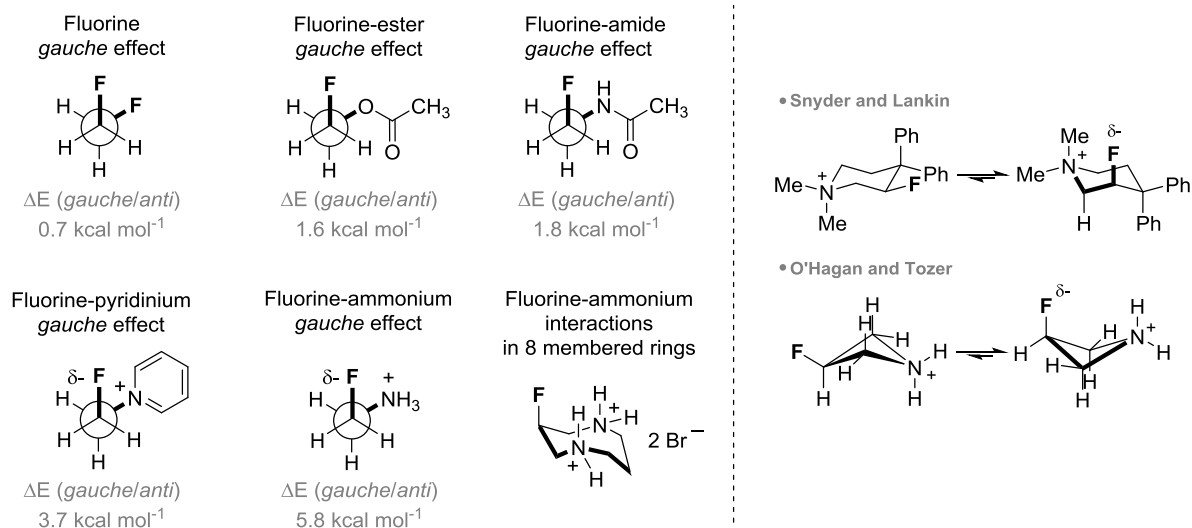


Figure 3: Stabilising stereoelectronic effects: The anomeric and the *gauche* effect.

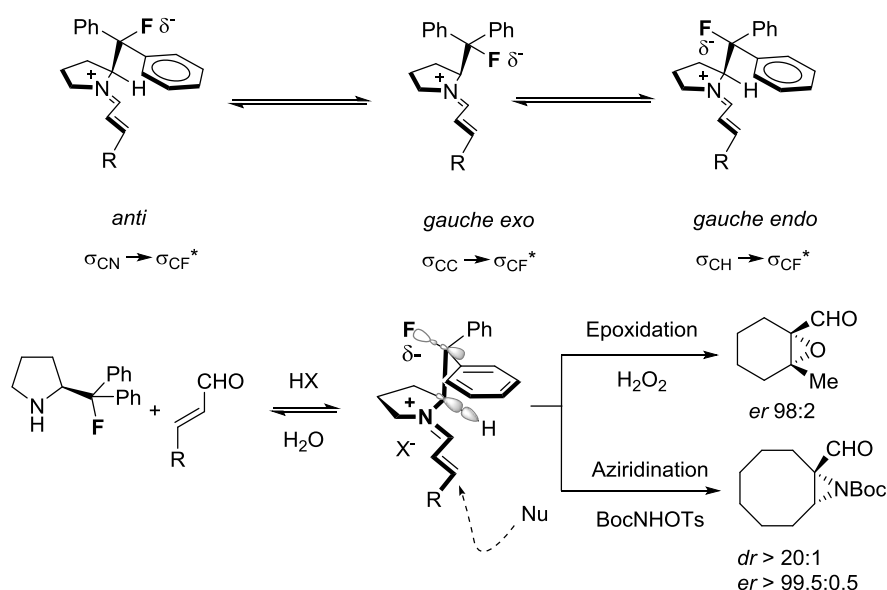
In general, the energy of a molecular orbital depends on the electronegativity of the elements involved (high electronegativity leads to low lying orbitals). Therefore, the antibonding orbital of a C-F bond ( $\sigma^*_{CF}$ ) will typically interact well with donor orbitals. A striking example thereof is the *gauche* effect observed in 1,2-difluoroethane (Figure 3, right).<sup>[6][7][8]</sup> In order to ensure good overlap of the C-H bonding orbitals with the C-F antibonding orbitals in a vicinal relationship ( $2 \times \sigma_{CH} \rightarrow \sigma^*_{CF}$ ) the two fluorine atoms must be placed in a *gauche* relationship ( $\Phi_{FCCF} = 60^\circ$ ). This effect overrides the stabilisation that is expected due to dipole minimisation in the *anti* conformer.

Importantly, the *gauche* effect is also operational in other fluorinated systems bearing a vicinal electron withdrawing group. When one fluorine atom is replaced by a positively charged substituent the conformational preference will be enhanced even more due to a stabilising coulombic interaction of the type ( $F^{\delta-} \cdots N^+$ ). The stabilisation of the *gauche* conformer over the *anti* ranges from  $0.7 \text{ kcal}\cdot\text{mol}^{-1}$  in 1,2-difluoroethane<sup>[9]</sup> to  $5.8 \text{ kcal}\cdot\text{mol}^{-1}$  in protonated 2-fluoroethylamine<sup>[10]</sup> (Figure 4). Importantly, the same conformational preference is observed when an ester<sup>[11]</sup> or an amide<sup>[12][13]</sup> group is placed in a vicinal position to the fluorine atom. Moreover, the conformation of cyclic systems can also be influenced by fluorine incorporation: When placed in  $\beta$ -position to an ammonium ion the combination of the hyperconjugative effect ( $\sigma_{CH} \rightarrow \sigma^*_{CF}$ ) and the coulombic interaction leads to a preference for the fluorine atom in the *pseudo* axial position<sup>[14][15]</sup> (Figure 4). It can therefore be concluded that the fluorine *gauche* effect constitutes a valuable tool for conformational control especially when it is reinforced by an electrostatic component. In general, such a stereoelectronic effect can be expected for systems fulfilling the pattern [F-C-C-X], where X is an electron withdrawing group or an electronegative heteroatom. However, it should be noted that steric effects can always override a stereoelectronic preference.



Figure 4: Various fluorine *gauche* effects.

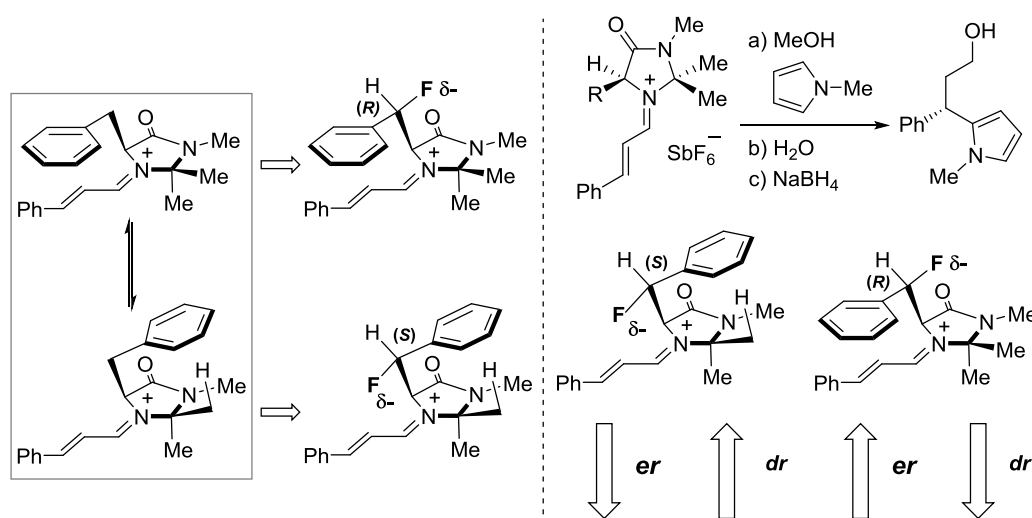
Application of this strategy in organocatalysis was first introduced by this laboratory in 2009 and has successfully been demonstrated in several settings. For example, by introducing a fluorine atom in the  $\beta$ -position to the nitrogen atom of a secondary amine catalyst such as (*S*)-2-(fluorodiphenylmethyl)-pyrrolidine,<sup>[16]</sup> a slight preference for the *gauche* conformers over the *anti* conformer can be expected (Scheme 1). However, upon condensation with an aldehyde the corresponding iminium ion is formed and the *synclinal* conformation is further stabilised. Moreover, this can be rationalised by invoking a  $\sigma_{\text{CH}} \rightarrow \sigma^*_{\text{CF}}$  interaction, but the *synclinal-endo* conformation also allows for a charge-dipole interaction [ $\text{F}^{\delta-} \cdots \text{N}^+$ ]. The consequence of this fluorine effect is to position one of the aryl rings on the fluorine bearing carbon over the  $\pi$  system, thus forming the basis of an enantioinduction strategy. Due to the delocalised nature of the positive charge over the conjugated system an interaction with one of the shielding groups (Ph; cation- $\pi$ ) is thought to further favour the *synclinal-endo* conformer where the fluorine atom is placed over the pyrrolidine ring. This conformational change upon reaction of the catalyst with the substrate is reminiscent of the “induced fit” in enzyme catalysis. As shown in Scheme 1, the conformationally locked iminium ion allows a nucleophile to attack from the bottom face, only (i.e. the *Si*-face). Clearly, the control of the iminium ion chain geometry is important to ensure that only one face is presented to the incoming nucleophile. To this end,  $A^{1,3}$  strain<sup>[17]</sup> is thought to favour the (*E*)-conformer.<sup>[18]</sup> This principle has been showcased by the application in enantioselective epoxidation with hydrogen peroxide as the nucleophile<sup>[16]</sup> as well as in aziridination chemistry<sup>[19]</sup> using BocNHOTs, both with high levels of enantioselectivity.



Scheme 1: Application of the fluorine-iminium ion *gauche* effect in secondary amine catalysis.

Another popular class of secondary amine organocatalysts are the amino acid derived imidazolidinones, in which enantioinduction is proposed to be induced by the shielding effect from the amino acid residue.<sup>[20][21][22]</sup> Consequently, phenylalanine derivatives have proven to be valuable structures for example in the enantioselective Friedel-Crafts alkylation of pyrroles as shown in Scheme 2.<sup>[23]</sup> However, the influence of the orientation of the phenyl group on the reaction outcome required clarification. It was proposed that two geometries of the catalyst-substrate complex would predominate: one in which the phenyl group is placed over the iminium chain (possibly stabilised by a cation- $\pi$  type interaction) and an other where the aromatic group interacts with a C-H bond of the *syn*-methyl group of the 2-position (CH- $\pi$  interaction). Conveniently, each of these conformers can be favoured by introducing a configurationally defined fluorine atom in the benzylic position of the side chain.<sup>[24]</sup> By synthesising the diastereomer in which the fluorinated centre is (*R*)-configured the conformer with the phenyl group above the iminium chain was postulated to be favoured due to two stabilising effects (cation- $\pi$  and  $\sigma_{\text{CH}} \rightarrow \sigma_{\text{CF}}^*$ ). In contrast, the other diastereomer ((*S*)-configuration of the benzylic position) benefits from a CH- $\pi$  interaction reinforced by a hyperconjugative effect of the type  $\sigma_{\text{CC}} \rightarrow \sigma_{\text{CF}}^*$ , thus favouring the other conformer. The analysis of the geometry of the iminium chain ((*E*) vs. (*Z*)) and the reaction outcome (*e.r.*) using these fluorinated analogues revealed that the “CH- $\pi$  conformer equivalent” gave a high diastereomeric ratio for the iminium ion but essentially racemic product. However, the other

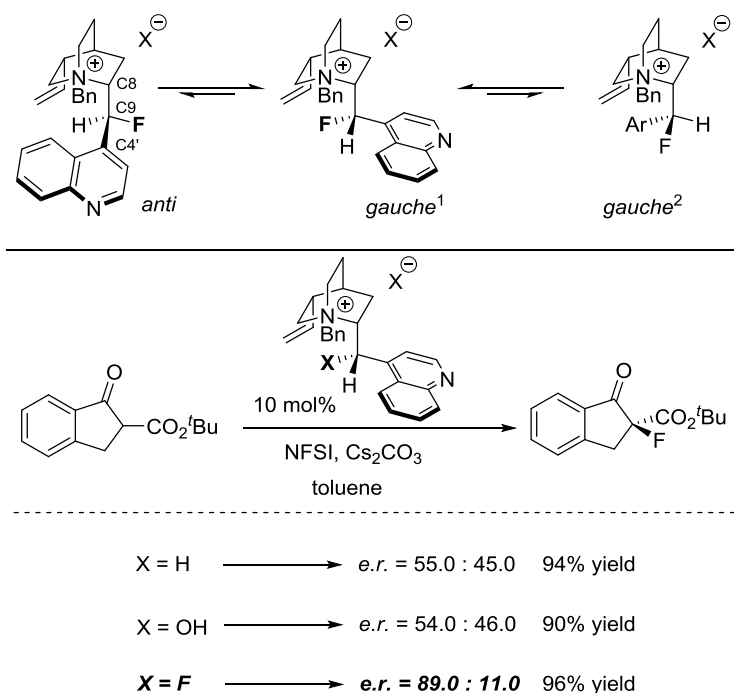
conformer equivalent was found to lead to a reduced (*E*)/(*Z*) ratio of the intermediate but delivered the alkylated compound with an enantioselectivity approaching the one obtained when the non-fluorinated parent compound was used as a catalyst. These results suggest that interplay of the two conformers is important for high levels of enantioselectivity. While one of the geometries leads to a highly preorganised iminium chain the other is responsible for efficient shielding of the *Re*-face of the electrophile. This example serves to demonstrate that systems where two *gauche* conformations are possible can be biased by a secondary, stabilising non-covalent interaction (*e.g.* CH- $\pi$  or  $\pi$ - $\pi$ ).



Scheme 2: Conformer equivalents of phenylalanine derived imidazolidinone catalysts.

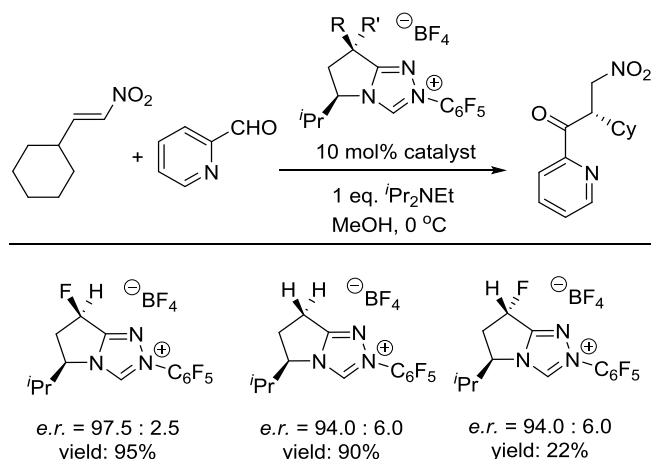
Conformational control by fluorination has also found application in cinchona alkaloids thus addressing an age old problem of internal rotation about C8-C9 and C9-C4'.<sup>[25]</sup> This is particularly useful for the class of phase transfer catalysts<sup>[26]</sup> in which the tertiary nitrogen of the quinuclidine moiety is alkylated and the prerequisite for a strong *gauche* effect (F-C-C-X<sup>+</sup>) is fulfilled. Consequently, the rotation about the exocyclic C-C bond can be influenced by introducing a fluorine atom in a diastereoselective manner.<sup>[27]</sup> As shown in Scheme 3 (upper) fluorination of cinchonine on the 9-position is expected to favour the *synclinal endo* conformation due to hyperconjugative stabilisation ( $\sigma_{\text{CH}} \rightarrow \sigma_{\text{CF}}^*$ ) and the absence of steric interactions (compare with the *synclinal exo* conformer). This catalyst was applied in the enantioselective fluorination of  $\beta$ -ketoesters, a transformation which was conducted in a catalytic fashion for the first time by the group of Togni.<sup>[28]</sup> The most striking effect of fluorination is seen when comparing the outcome of the reaction catalysed by the deoxygenated compound, cinchonine and the fluorinated structure: The enantioselectivity is

increased from *e.r.* = 55.0:45.0 ( $X = \text{H}$ ) and *e.r.* = 54.0:46.0 ( $X = \text{OH}$ ) to *e.r.* = 89.0:11.0 ( $X = \text{F}$ ). All reactions delivered the product in excellent yields (Scheme 3, lower). What is noteworthy in this example is that the conformational lock is sterically non-demanding and so the conformation is different to what is obtained by a more classic approach using bulky groups (e.g.  $t\text{Bu}$ ).



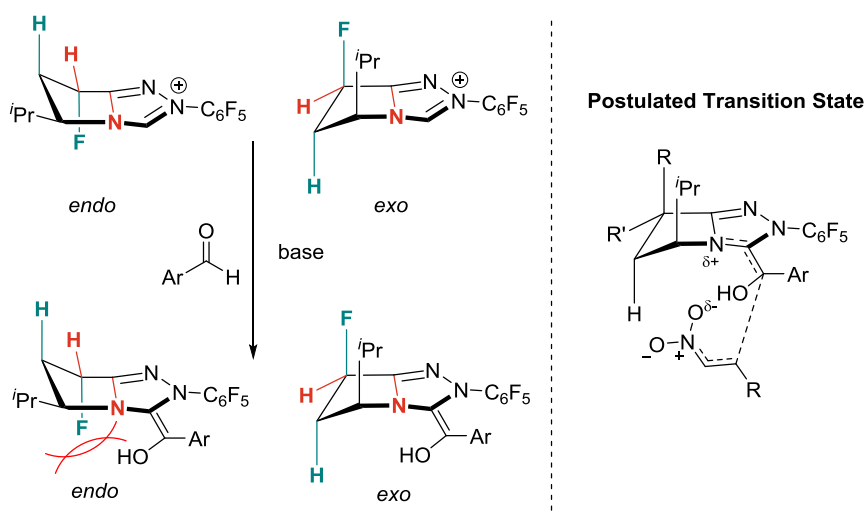
Scheme 3: Influencing cinchona alkaloid conformation using the  $\beta$ -fluoro ammonium ion *gauche* effect.

In addition to these three types of organocatalysts, fluorination has also proven to lead to enhanced selectivities in *N*-heterocyclic carbene (NHC) catalysis. The major difference of this example is that the fluorine atom is introduced in the ring system; this is in contrast to the previous examples in which fluorination was used to control an exocyclic torsion. The group of Rovis has reported a fluorinated triazolium salt which was employed in the enantioselective Stetter reaction of nitroalkenes with aromatic aldehydes (Scheme 4).<sup>[29]</sup> This finding was investigated by computational studies.<sup>[30]</sup> Upon reaction of the NHC with the aldehyde the corresponding Breslow intermediate is formed. For these structures it was calculated that the *exo* conformer is favoured for both diastereomers due to a steric interaction in the *endo* conformer.



Scheme 4: Rovis' enantioselective Stetter reaction of nitroalkenes with aromatic aldehydes using a fluorinated NHC precursor.

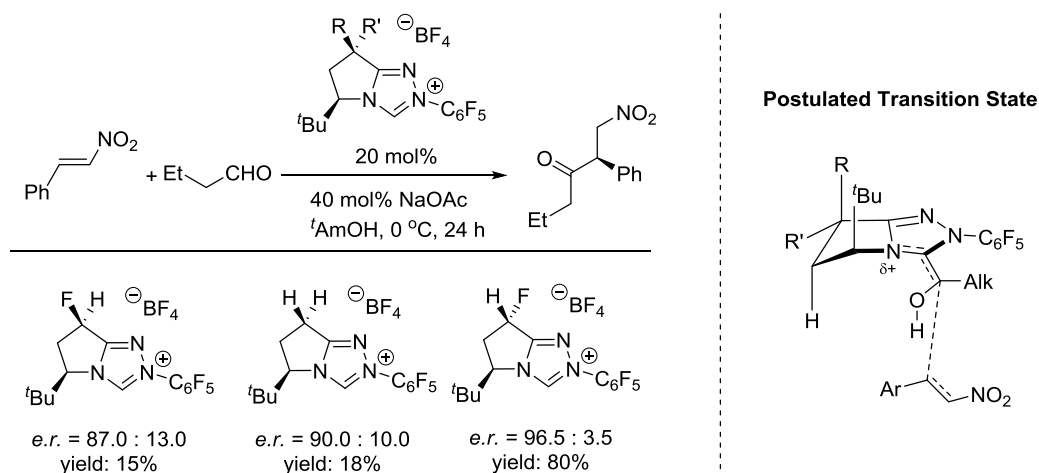
According to Seebach's topological rule<sup>[31]</sup> the electrophile was calculated to approach in such a way that the developing negative charge on its nitro group can efficiently interact with the developing positive charge on the NHC. From the calculated transition state structures it was concluded that in the *syn* diastereomer (R = F) the nitro group can more easily interact with the catalyst structure thus augmenting both selectivity and reactivity (Scheme 5).



Scheme 5: Conformational preference of the two diastereomers in the triazolium salt and in the Breslow intermediates.

The same group also reported the Stetter reaction of aryl substituted nitroolefins with aliphatic aldehydes catalysed by fluorinated NHCs.<sup>[32]</sup> Interestingly, in this case it was found that the *anti* diastereomer was more efficient in terms of reactivity and selectivity than the *syn* diastereomer (Scheme 6). For this reaction the  $\text{iPr}$  group on the triazolium salt was exchanged for a  $\text{tBu}$  sidechain. With these structures the same preference for the *exo* conformation of the

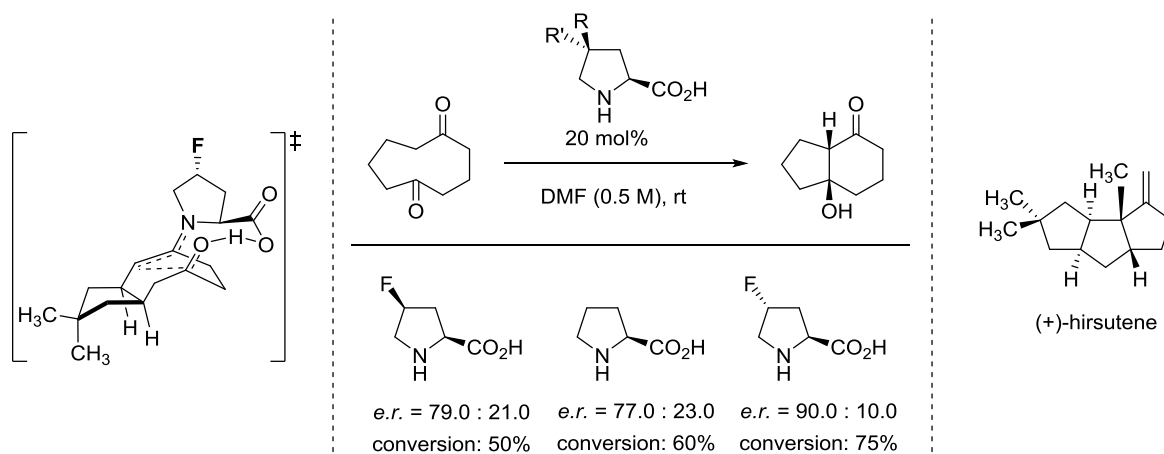
Breslow intermediates was found. An explanation for the higher selectivity of the *anti* diastereomer was found, again supported by calculation to be a stabilising interaction between the fluorine atom and the positively charged component of the phenyl ring, which is not present in the *syn* diastereomer. It should be noted that in this reaction the attack of the Breslow intermediate takes place from the *Re*-face of the nitroolefin which leads to the opposite enantiomer as in the Stetter reaction of aromatic aldehydes with non-aromatic nitroolefins. This observation was attributed to interactions of the alkyl chain of the Breslow intermediate with the nitrogroup of the electrophile as well as an interaction of the hydroxyl group with the carbon atom in  $\alpha$ -position to the nitro group. This beautiful example illustrates the influence that introduction of this small group can have, and that the configuration of the centre is crucial in enantioselective catalysis.



Scheme 6: Rovis' enantioselective Stetter reaction of aromatic nitroolefins with aliphatic aldehydes catalysed by fluorinated NHCs.

Further evidence that incorporation of fluorine in cyclic systems can have profound effects on catalysis comes from the group of List. In 2008 the group reported the enantioselective transannular aldol reaction catalysed by 4-fluoroproline (Scheme 7).<sup>[33]</sup> The reaction proved to be most efficient in both conversion and enantioselectivity when the *trans*-diastereomer was applied (*e.r.* = 90.0:10.0, 75% conversion). When using the C4-epimer, selectivity dropped to *e.r.* = 79.0:21.0 and the conversion to 50%. The non-fluorinated parent compound [(L)-proline] gave slightly lower enantioselectivity (*e.r.* = 77.0:23.0) but higher conversion (60%). The reaction was further optimised and DMSO was found to be the solvent of choice. These conditions were applied in the enantioselective synthesis of (+)-hirsutene. The proposed transition state of the key step is shown in Scheme 7 (left). Although stabilising

hyperconjugative effects of the type  $\sigma_{\text{CH}} \rightarrow \sigma_{\text{CF}}^*$  can be expected the authors did not rationalise the dependence of the reaction outcome on the relative configuration of the catalyst. However, in the case of *trans*-4-fluoroproline, it is reasonable to expect a fluorine-amine gauche *effect* that puckers the ring. This is evident from the X-ray structure of the catalyst. The resulting conformation allows for a hydrogen-bond network required for high levels of enantioselectivity to be obtained. This is not possible with the corresponding *cis*-4-fluoroproline.



Scheme 7: Effect of diastereoselective fluorination of proline on the outcome of a catalyzed transannular aldol reaction.

### 3.2 Brominated and Iodinated Organocatalysts

Although fluorine has very interesting effects on the conformation of organic compounds, it is not the only halogen that has been used to alter the properties of an organocatalytic system. Iodine and bromine are encountered in organic dyes commonly used for the generation of singlet oxygen ( $^1\text{O}_2$ ) such as eosin Y, rose bengal or borondipyrromethene (BODIPY) derived structures (Figure 5).<sup>[34][35]</sup>

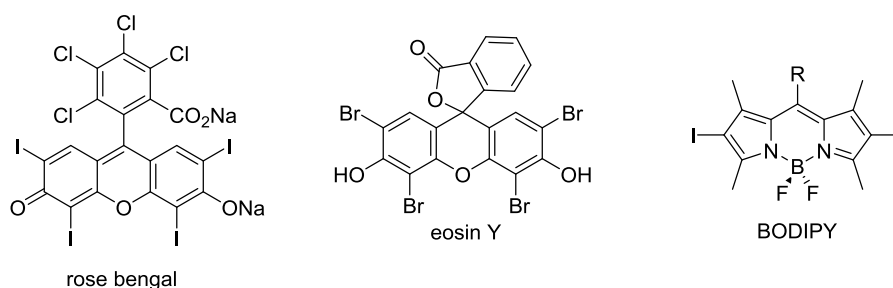
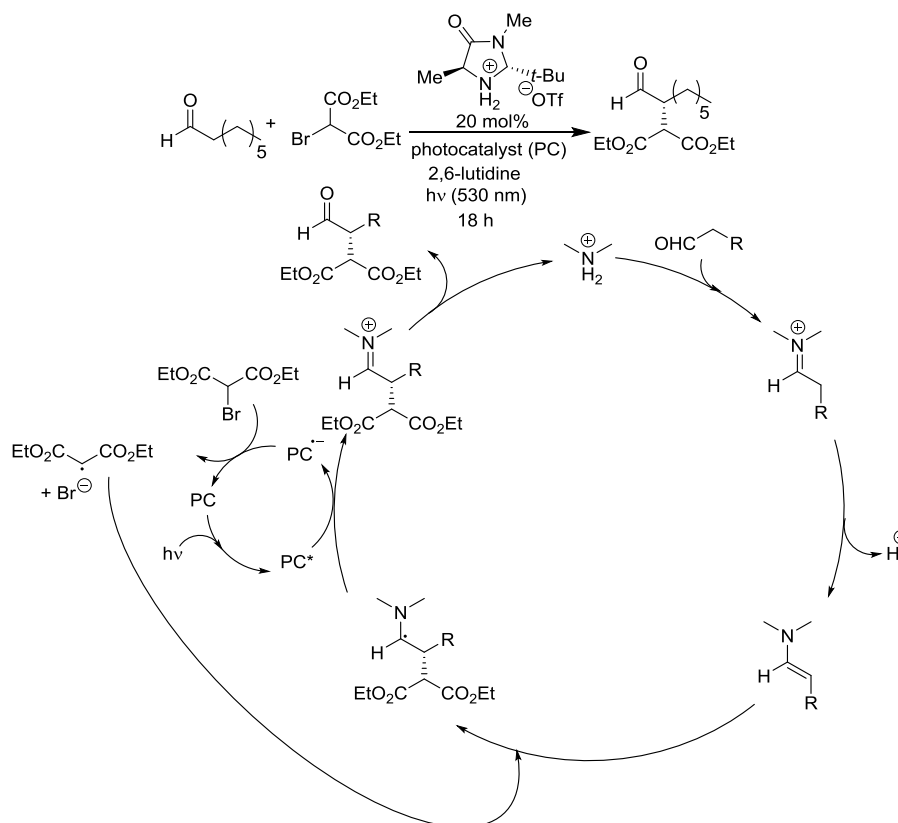


Figure 5: The structures of rose bengal, eosin Y and BODIPY.

Upon irradiation with light of an appropriate wavelength (*i.e.* visible light, 400-800 nm) these compounds reach an electronically excited singlet state. In order to efficiently transfer energy to a substrate (sensitisation) an excited state of longer lifetime is needed.<sup>[36]</sup> A possibility is the so called intersystem crossing (ISC) to a triplet state. Interestingly, substituents with a high atomic number such as bromine and iodine favour this transition between the singlet and the triplet state due to the “heavy atom effect”.<sup>[37]</sup> A more detailed explanation thereof is presented in chapter 6.1. Especially water soluble, iodinated BODIPY structures have obtained a lot of attention because of their potential in the application in photodynamic therapy.<sup>[38]</sup> Although these structures are most commonly used as singlet oxygen sensitisers there are also reports in which eosin Y<sup>[39]</sup> or iodinated BODIPY<sup>[40]</sup> derivatives are used for single electron transfer upon excitation with light. When the chromophores can be used in catalytic amounts the process is often called “photoredoxcatalysis”.<sup>[41][42][43]</sup> An interesting example thereof has been reported by the group of MacMillan in 2008:<sup>[44]</sup> By combining enamine activation with photoredoxcatalysis the challenging enantioselective  $\alpha$ -alkylation of aldehydes has been achieved. The proposed mechanism for the photochemical reaction of octanal with diethylbromomalonate using an imidazolidinone derived catalyst together with a



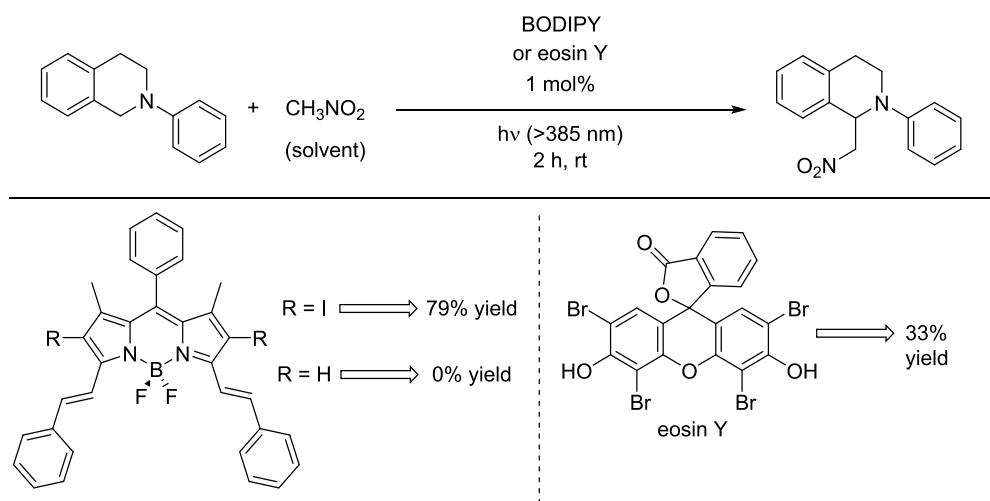
photocatalyst is shown in Scheme 8. Upon condensation of the aldehyde with the secondary amine the corresponding enamine is formed.



Scheme 8: Proposed mechanism of the light mediated enantioselective  $\alpha$ -alkylation of aldehydes.

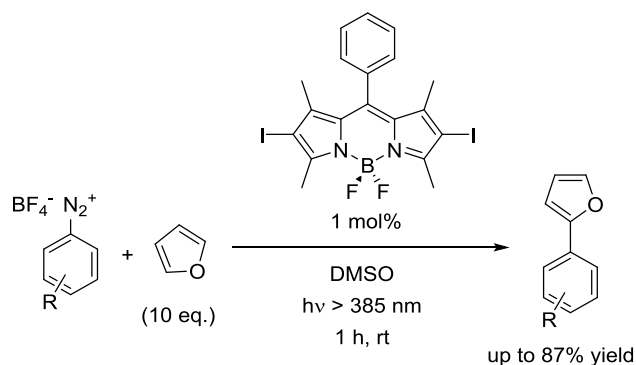
This electron rich system can be expected to efficiently react with an electron poor radical such as the one derived from diethylbromomalonate later on in the catalytic cycle. The resulting  $\alpha$ -amino radical then needs to be oxidised to give the iminium ion which can be hydrolysed to liberate the product and regenerate the catalyst. This is proposed to be achieved by the excited state of the photocatalyst which is a strong oxidant (as well as a strong reductant). The generated radical anion is thought to transfer an electron to the diethylbromomalonate which results in cleavage of the carbon bromine bond to give a bromide anion along with the required radical and the regenerated photocatalyst. The group of MacMillan employed widely used  $\text{Ru}(\text{bipy})_3\text{Cl}_2$  as photoredoxcatalyst.<sup>[43]</sup> However, in 2010 the group of Zeitler could show that eosin Y is also capable of catalysing this transformation.<sup>[45]</sup>

Another iodinated organocatalyst that has recently been applied in the realm of photocatalysis is the BODIPY derived structure shown in Scheme 9. The group of Zhao reported on the dehydrogenative coupling of tetrahydroisoquinolines with nitromethane mediated by photocatalysis under an air atmosphere.<sup>[40]</sup> Amongst various catalysts that were tested, this iodinated BODIPY derivative gave the highest yield (79%). Most strikingly, when the noniodinated analogue was used no product was isolated (in agreement with the absence of a heavy atom effect). In this reaction eosin Y could also be used as catalyst but it led to significantly decreased yield (33%). These results not only demonstrate the importance of halogens in photoredoxcatalysis but also the potential of BODIPY derived structures as valuable compounds for light induced reactions besides singlet oxygen generation.



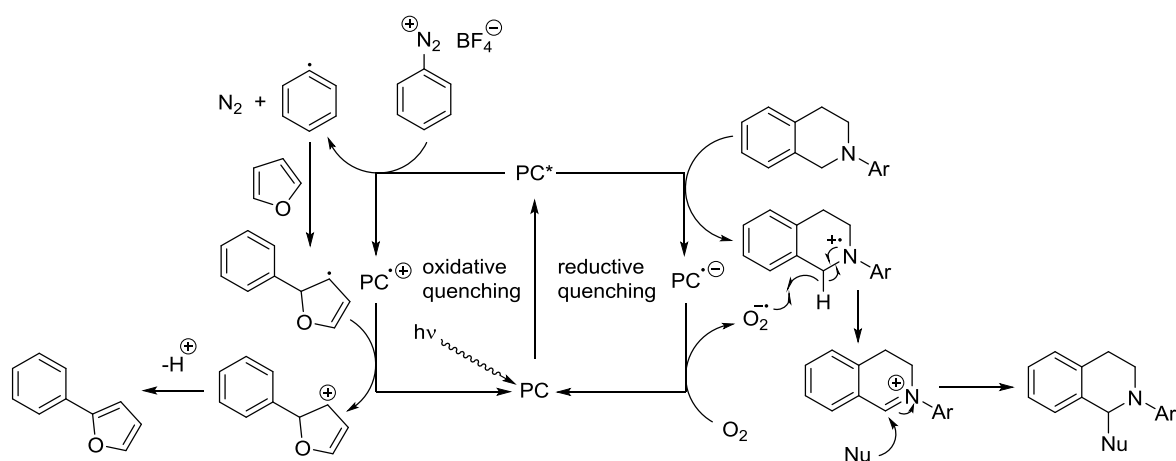
Scheme 9: Light mediated dehydrogenative coupling of tetrahydroisoquinoline with nitromethane.

In the same publication the arylation of heteroarenes with diazonium salts using a structurally simple iodinated BODIPY derivative as photoredoxcatalyst was also reported. The reaction with furane is shown in Scheme 10.



Scheme 10: Example of the arylation of furan by diazonium salts using an iodinated BODIPY derivative as photoredoxcatalyst.

Considering that diazonium salts are electron acceptors and amines such as the ones used in the dehydrogenative coupling of tetrahydroisoquinoline with nitromethane are relatively easily oxidised, the photoredoxcatalyst can be expected to be able to act as both oxidant and reductant. The proposed mechanisms are summarised in Scheme 11: Upon excitation of the photoredoxcatalyst (PC) electron transfer takes place in both reactions. If an electron donor is present (*e.g.* an amine) the excited state can be reduced to give the corresponding radical anion of the catalyst (reductive quenching) and the oxidised amine. Under presence of oxygen the radical anion of the catalyst is thought to be converted to its resting state by electron transfer to oxygen to give a superoxide radical anion ( $\text{O}_2^{\cdot-}$ ). Upon hydrogen atom transfer the iminium ion of the substrate is generated which can be attacked by a nucleophile to deliver the product.



Scheme 11: Summary of the proposed mechanisms for the arylation using diazonium salts (left) and for the dehydrogenative coupling of tetrahydroisoquinoline with nitromethane.

Alternatively, diazonium salts are expected to accept an electron from the excited state of the photocatalyst (PC\*) so that an aryl radical is generated along with the radical cation of the photocatalyst. Addition to furan is thought to give an intermediate radical which can then regenerate the photocatalyst by electron transfer. The resulting carbocation can subsequently be deprotonated to the product.

It is interesting to see that the excited state of the catalyst can act as both an oxidant and a reductant. A simplified explanation for this observation is shown in Figure 6: Upon excitation of the catalyst an electron is transferred from the HOMO to the LUMO generating two singly occupied molecular orbitals (SOMOs). Due to the high energy of the electron in the upper orbital it can be expected to be easily removed and therefore the compound is a stronger reductant in the excited state than in the ground state. Similarly, if an electron has to be accepted by the system it can be placed into the lower lying SOMO of the excited state which was not possible in the ground state. The ability of stabilising the incoming electron explains the fact that excited states are also stronger oxidants than their corresponding ground states.

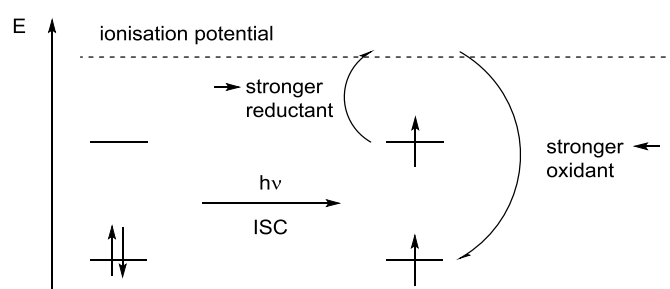


Figure 6: Schematic representation of the altered redox behaviour of excited states compared to their ground state.

It can be concluded that fluorination of organocatalysts can have a tremendous effect on the reaction outcome due to influence on the conformation of the catalyst's ground state, an intermediate or a transition state. This is due to fluorine's high electronegativity that allows for hyperconjugative effects and electrostatic interactions to be induced with a minimal steric footprint owing to the element's small van der Waals radius.<sup>[46]</sup>

Additionally, by introducing halogens like bromine and iodine, the photophysical characteristics of organic compounds can be influenced which may lead to interesting effects in light induced reactions. This is attributed to the heavy atom effect that enhances the probability of intersystem crossings of electronically excited states.

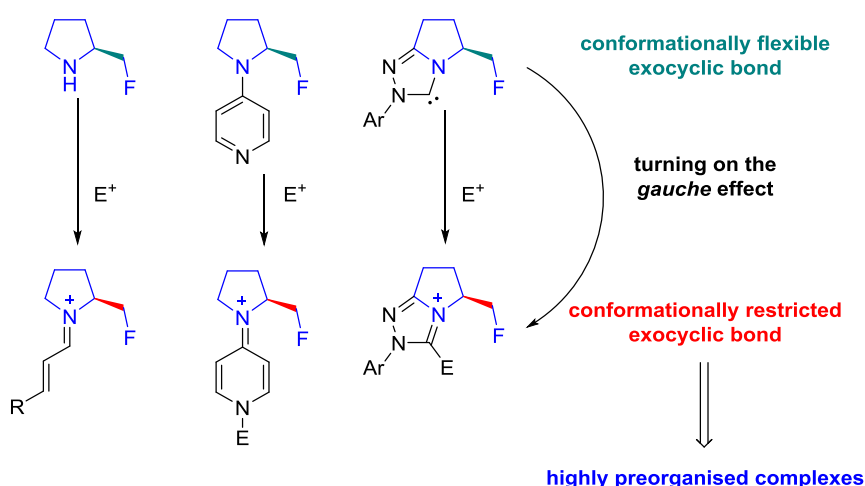
In general, halogen effects in organocatalysis constitute an exciting field of research to which we hope to contribute.

## 4 Fluorinated *N*-Heterocyclic Carbenes

### Application in the Asymmetric Steglich Rearrangement of Carbonates

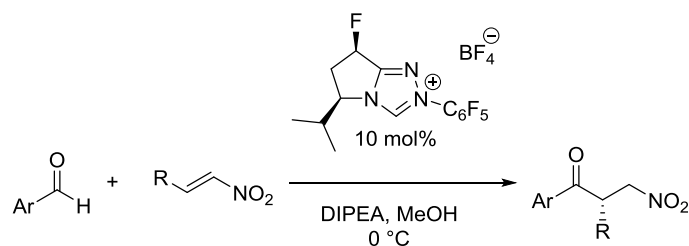
#### 4.1 Introduction

In nucleophilic organo-catalysis mediated by *N*-heterocyclic carbenes, reaction with an electrophile generates a positive charge in the catalyst scaffold, similar to iminium ion or DMAP catalysis. Moreover, in this type of transformation the shielding group is commonly placed in a vicinal relationship to the nitrogen atom that donates electron density. Consequently, this system is pre-disposed to allow for conformational control around the exocyclic bond by means of the fluorine-iminium ion *gauche* effect (Scheme 12). Therefore, introduction of a fluorine atom  $\beta$  to this nitrogen provides a useful platform to study the NHC-fluorine *gauche* effect.<sup>[47][48]</sup> This not only allows for control around the exocyclic C-C bond, but demonstrates the value of this design approach in the three most common nucleophilic catalyst classes.



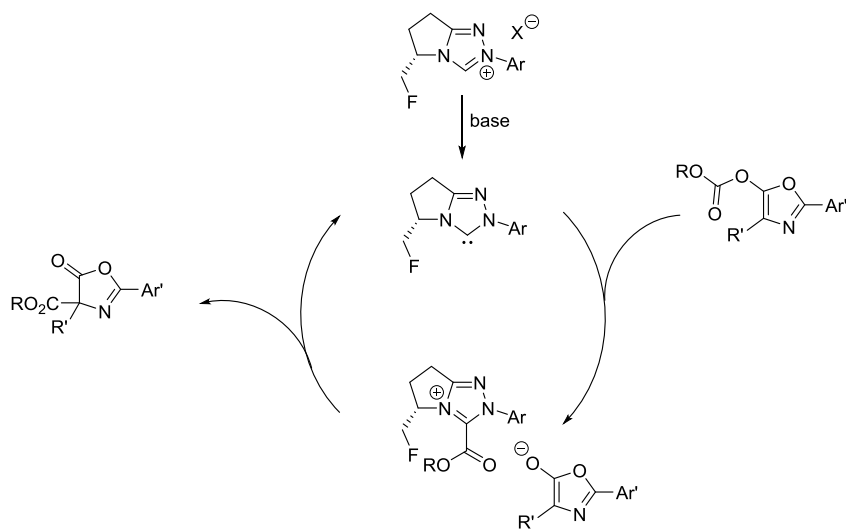
Scheme 12: Conformational restriction upon reaction of nucleophilic catalysts with an electrophile.

It has been reported by Rovis *et al.* that fluorination of the pyrrolidine ring of certain NHCs can have a positive effect on enantioselectivity in the Stetter reactions of aromatic aldehydes and nitroolefins (Scheme 13).<sup>[29]</sup> It is interesting to note that the fluorine atom is also placed in the  $\beta$ -position to the nitrogen atom which likely increases the preference of the fluorine substituent to be axial. This may affect the ring conformation by virtue of the *gauche* effect.<sup>[30][32]</sup>



Scheme 13: Rovis' fluorinated NHC precursor for the enantioselective Stetter reaction.

Motivated by this study the performance of doubly fluorinated NHCs was investigated to explore the role of fluorine substituents in controlling ring conformation and an exocyclic torsion; ultimately this was evaluated in a model reaction. Due to the proximity of the two fluorine substituents it may be expected that repulsion may override potentially intuitive interactions. Conversely, the substituents may act additively or cooperatively. To study these interactions, a model reaction was selected which was well-studied and known to be catalysed by NHCs in an enantioselective fashion. Additionally, due to the fact that a positive charge on the scaffold is important for preorganisation by virtue of the *gauche* effect, a reaction in which the nucleophile attacks the positively charged NHC-substrate complex was favoured over one proceeding *via* a Breslow intermediate. To that end the enantioselective Steglich rearrangement seemed to be well suited. As shown in Scheme 14, upon deprotonation of the triazolium salt the NHC is generated which can subsequently attack an aromatic carbonate to form an acylated triazolium species. The aromatic nucleophile liberated can then react with the activated acetyl group to furnish the *C*-alkylated product with a quaternary stereocentre.<sup>[49]</sup>



Scheme 14: Generalised mechanism of an NHC catalysed Steglich rearrangement.

## 4.2 Synthesis of Appropriate NHC Precursors

As described in chapter 4.1 the effect of double fluorination of triazole NHC scaffolds was the subject of investigation. Consequently, the synthesis of compound **1** was targeted (Figure 7). To probe the effect of individual fluorine substituents, catalyst precursors with one of the two fluorines deleted were envisaged (*i.e.* ring position versus exocyclic position; compounds **2** and **3**). As a control structure, the non-fluorinated compound **4** was also synthesised.

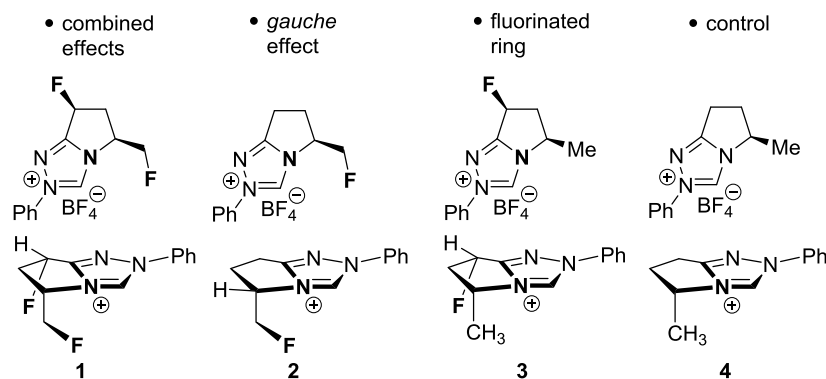
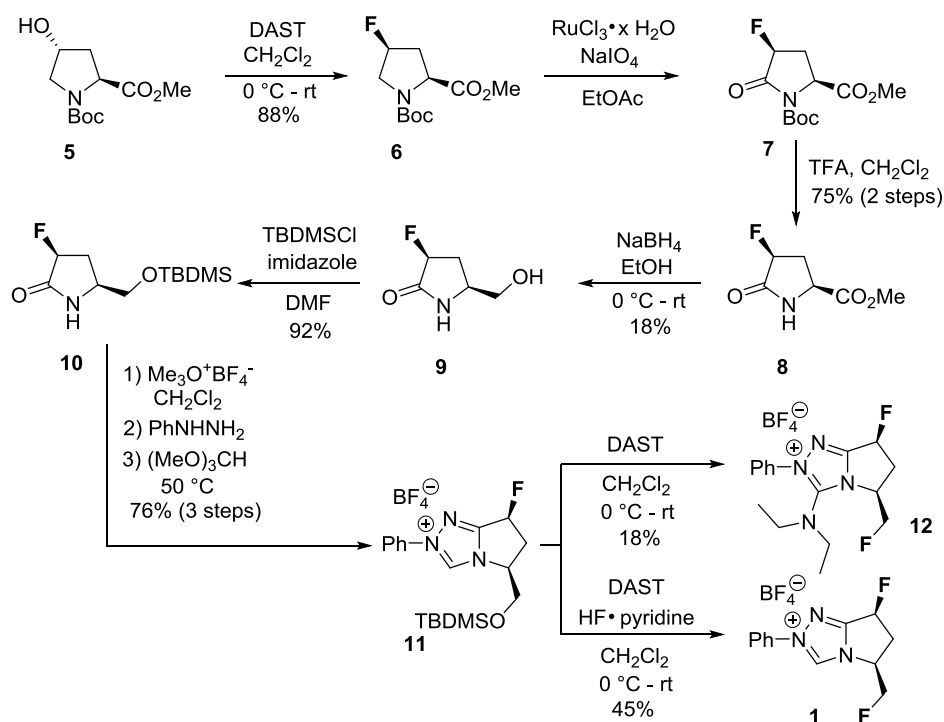


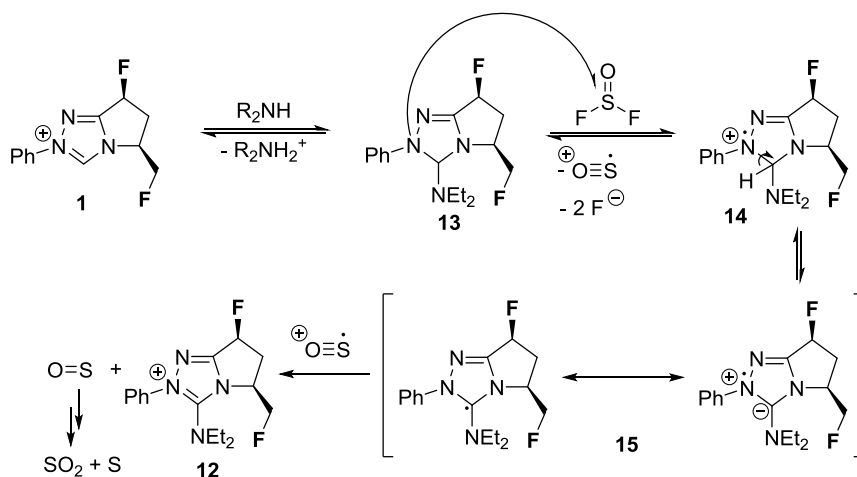
Figure 7: Catalyst precursors for the investigation of fluorine effects in the asymmetric Steglich rearrangement.

Compound **1** was synthesised as shown in Scheme 15: Commercially available, enantiomerically pure proline methylester derivative **5** was treated with DAST in  $\text{CH}_2\text{Cl}_2$  to give fluorinated compound **6** in good yields (88%) with inversion of configuration. Oxidation of the 5-position was achieved by *in situ* generated  $\text{RuO}_4$  in EtOAc to give compound **7** which was directly deprotected using TFA in  $\text{CH}_2\text{Cl}_2$  to furnish lactam **8** (75% over 2 steps). Although the following reduction of the ester functionality proceeded well using  $\text{NaBH}_4$  in EtOH, isolation proved to be difficult due to the hydrophilic nature of the alcohol **9** (18%). Silylation of the primary alcohol using TBDMSCl and imidazole in DMF efficiently gave compound **10** in 92% yield. A one-pot sequence of *O*-alkylation, condensation with phenylhydrazine followed by cyclisation using trimethylorthoformate gave triazolium salt **11** (76% over 3 steps). Interestingly, treatment of this compound with DAST led to incorporation of the reagent's diethylamino moiety into the triazolium structure (compound **12**). However, in order to bypass this problem the conditions were adjusted by addition of Olah's reagent ( $\text{HF}\cdot\text{pyridine}$ , 10 equivalents) which furnished the difluorinated structure **1** in 45% yield without any incorporation of the diethylamine moiety.


 Scheme 15: Synthesis of the difluorinated triazolium salt **1**.

A tentative mechanism to account for the unexpected diethylamine incorporation upon treatment with DAST is proposed in Scheme 16. It can be envisaged that the electron poor triazolium salt is susceptible to attack from diethylamine to form intermediate **13**. As the overall reaction constitutes a formal oxidation of the 2-position of the triazolium salt, an oxidant must be present. Atmospheric oxygen seems unlikely as the reaction was performed under argon at 0.1 M and O<sub>2</sub>-concentration in the solvent can be expected to be around 0.01 M.<sup>[36]</sup> However, thionyl fluoride that is generated upon reaction of the alcohol with DAST may be capable of oxidising intermediate **13**. Single electron transfer would then lead to highly stabilised radical cation **14** and thionyl fluoride derived radical anion which can be expected to decompose to SO<sup>•+</sup> and two fluoride anions (for the electrochemical reduction of thionyl chloride see reference<sup>[50]</sup>). Deprotonation of the 2-position of triazolium derived radical cation may then lead to electron rich radical **15**. A second oxidation step would deliver the observed product **12** along with SO that disproportionates to SO<sub>2</sub> and sulphur.<sup>[50]</sup>

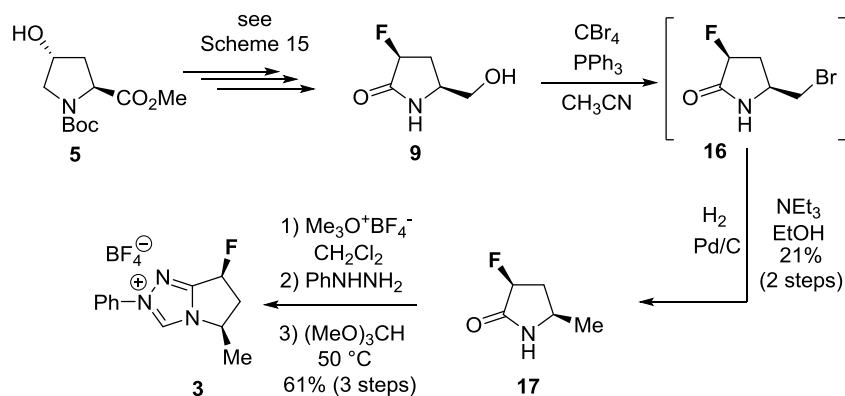




Scheme 16: Proposed mechanism leading to incorporation of the diethylamino moiety; the counterion is omitted for clarity.

Compound **2** had previously been prepared in the group by Dr. Susann Paul during the course of her work on metal-NHC complexes.<sup>[47]</sup> The synthesis involved reduction of L-pyrroglutamic acid followed by silylation of the resulting alcohol. A similar cyclisation procedure gave the triazolium salt which in this case could be fluorinated using DAST, only.

As shown in Scheme 17 compound **16** was prepared from alcohol **9** by an Appel reaction followed by direct reduction of the carbon-bromine bond under hydrogenation conditions to give the desired lactam (**17**) in 21% yield over 2 steps. The target structure (**3**) was obtained in 61% yield by a similar alkylation-condensation-cyclisation sequence as used in the synthesis of the difluorinated triazolium salt **1**.

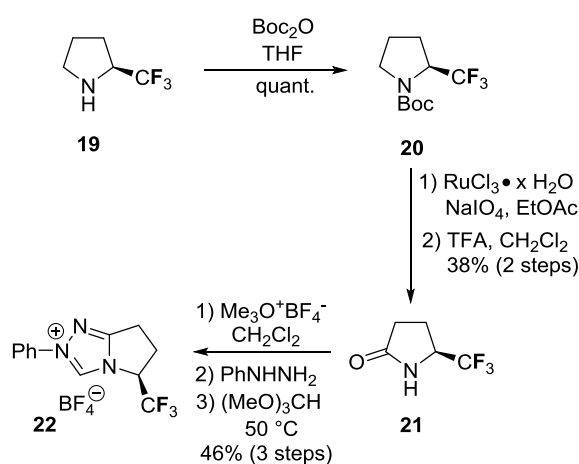


Scheme 17: Synthesis of monofluorinated triazolium salt **3**.

Finally, the non-fluorinated control compound **4** was synthesised starting from commercially available (*S*)-5-(bromomethyl)-2-pyrrolidinone which was submitted to the same conditions as compound **16** (Scheme 17) to give the corresponding methylated lactam (**18**) in 67% yield.

Subsequent cyclisation under the standard conditions, which were also used for the preparation of compounds **1** and **3** gave target structure **4** in 52% yield.

Moreover, in order to increase electronic shielding of one face of the catalyst a trifluoromethylated triazolium salt was prepared. The synthesis shown in Scheme 18 involved Boc-protection of commercially available (*S*)-(+)-2-(trifluoromethyl)-pyrrolidine **19** (quant.) followed by oxidation to the lactam using *in situ* generated RuO<sub>4</sub> and deprotection by TFA to give compound **21** in 38% yield over 2 steps. This was then submitted to the standard alkylation-condensation-cyclisation sequence to give the desired trifluoromethylated triazolium salt **22** (46% over 3 steps).



Scheme 18: Synthesis of trifluoromethylated triazolium salt **22**.

### 4.3 X-ray Structure of Compound **1**

The crystal structure of compound **1** (Figure 8) clearly reveals that the exocyclic fluorine substituent and the nitrogen in vicinal position show a *synclinal-exo* conformation ( $\Phi_{\text{F11CCN4}} = +63.7^\circ$ ) which allows for a stabilising  $\sigma_{\text{CC}} \rightarrow \sigma_{\text{CF}}^*$  interaction. The preference for the *synclinal-exo* over the *synclinal-endo* conformation in the solid state was also observed for the monofluorinated triazolium salt **2** ( $\Phi_{\text{FCCN}} = +67.9^\circ$ ).<sup>[47]</sup> However, the influence of the fluorine atom F10 on the conformation of the exocyclic group can be more accurately investigated by NMR population analysis (see chapter 4.4). The bicyclic system is completely flat with the exception of the carbon atom C7 which is puckered below the plane of the ring. This was also observed for the monofluorinated system, however to a lesser extent: The dihedral angle ( $\Phi_{\text{C5N4C8C7}}$ ) was found to be  $-14.0^\circ$  for the difluorinated triazolium salt while the corresponding angle was measured to be almost  $6^\circ$  smaller in the monofluorinated system

( $\Phi_{C_5N_4C_8C_7} = -8.3^\circ$ ). This translates to a difference of the dihedral angles along the C6-C7 axis: In the monofluorinated system an angle of  $-138.6^\circ$  ( $\Phi_{FC_6C_7H}$ ) was found whereas the corresponding dihedral angle in the difluorinated triazolium salt was measured to be almost  $10^\circ$  larger ( $\Phi_{FC_6C_7H} = -148.0$ ). In general, the closer this angle is to  $180^\circ$  the stronger a hyperconjugative interaction of the type  $\sigma_{CH} \rightarrow \sigma^*_{CF}$  can be expected. Interestingly, in the triazolium ring the two bonds to carbon atom C3 (N2-C3 and N4-C3) are equally long ( $d_{N_2-C_3} = 1.329 \text{ \AA}$  and  $d_{N_4-C_3} = 1.330 \text{ \AA}$ ), indicating that they have very similar amount of  $\pi$ -bond character and thus that the positive charge is equally distributed to both sides. Furthermore, the phenyl substituent is only slightly rotated out of the main plane ( $\Phi_{C_{12}C_{11}N_2C_3} = -8.9^\circ$ ) indicating a good overlap of the  $\pi$ -systems.

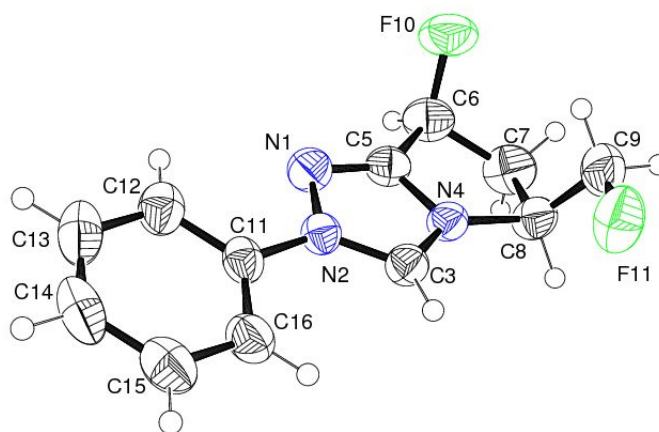


Figure 8: Crystal structure of compound **1**, the counterion is omitted for clarity.

## 4.4 Analysis of the Solution Phase Conformation of the Triazolium Salts.

### 4.4.1 Introduction

The large scalar coupling of fluorine atoms to both hydrogen and carbon atoms allows for facile elucidation of the solution phase conformation as they are often well resolved. It is especially useful to determine the population of different rotamers due to the dependence of the vicinal coupling constants ( $^3J$ ) on the dihedral angle referred to as the Karplus relation.<sup>[51]</sup> In general, two vicinal coupling constants have to be resolved in order to be able to obtain the conformer populations. For both couplings the coupling constants are calculated for a dihedral angle of  $60^\circ$  ( $J_g$ ) and  $180^\circ$  ( $J_a$ ). These calculated coupling constants can be obtained on the basis of the modified Karplus relation for the H-F coupling<sup>[52]</sup> and the well known relation for

H-H coupling<sup>[51]</sup> using group electronegativities that have been tabulated in the literature.<sup>[53][54]</sup> The modified Karplus relation is refined by taking into account the “intramolecular angles” (e.g.  $\angle$ FCC and  $\angle$ HCC) which are typically determined by X-ray analysis. The molar fraction of the conformer in which the coupling partners are in an *anti* relationship ( $x_a$ ) can then be calculated using equation (1) where  $\langle J \rangle$  denotes the measured coupling constant and  $J_g$  and  $J_a$  are the calculated coupling constants for the *gauche* and the *anti* arrangement of the coupling partners, respectively.<sup>[55]</sup>

$$x_a = \frac{\langle J \rangle - J_g}{J_a - J_g} \quad (1)$$

Of particular interest to this study of fluorinated NHC precursors was the population of the staggered rotamers of triazolium salt **1** shown in Figure 9. The conformer populations are calculated in chapter 4.4.2.

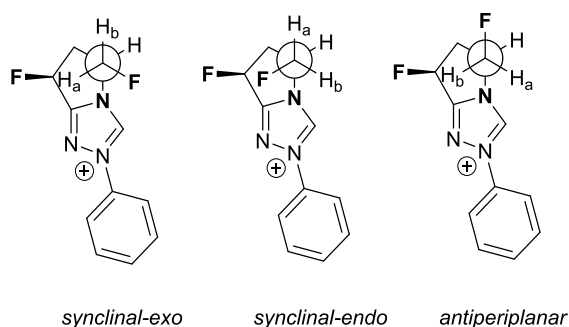


Figure 9: The three staggered rotamers of the difluorinated triazolium salt **1**.

#### 4.4.2 Analysis of the Solution Phase Conformations of Compounds **1** and **2**.

As described in the previous chapter for conformer population analysis of the rotamers of the fluorinated exocyclic moiety, at least two vicinal coupling constants as well as the two angles ( $\angle$ FCC and  $\angle$ HCC) are required. These angles were obtained from the crystal structure and were found to be  $\angle$ FCC = 108.6° and  $\angle$ HCC = 110.8°. The relevant measured and calculated coupling constants, together with the corresponding molar fractions  $x_a$ , are summarised in Table 1.

Table 1: Relevant vicinal coupling constants of the difluorinated triazolium salt **1**.

<b>coupling</b>	<b><i>FCCH</i></b>	<b><i>FCCC</i></b>
<b><math>\langle J \rangle</math> (Hz)</b>	20.3	6.3
<b><math>J_a</math> (Hz)</b>	40.2	11.2 <sup>a)</sup>
<b><math>J_g</math> (Hz)</b>	9.8	1.2 <sup>a)</sup>
<b><math>x_a</math></b>	0.35	0.51

<sup>a)</sup> literature values<sup>[56]</sup>

The conformer population obtained is: *synclinal-endo*: 35%, *synclinal-exo*: 51% and consequently, *antiperiplanar*: 14% (assuming that only three rotamers are populated). This is in good agreement with the expected predominance of the two *gauche*-conformers (86%) and the solid state conformation where the *synclinal-exo* rotamer was also observed.

Analogous calculations were also performed for the monofluorinated triazolium salt **2** based on coupling constants and the corresponding crystal structure obtained by Dr. Susann Paul (Table 2).<sup>[47]</sup>

Table 2: Relevant vicinal coupling constants of the monofluorinated triazolium salt **2**.

<b>coupling</b>	<b><i>FCCH</i></b>	<b><i>FCCC</i></b>
<b><math>\langle J \rangle</math> (Hz)</b>	19.9	6.8
<b><math>J_a</math> (Hz)</b>	39.8	11.2 <sup>a)</sup>
<b><math>J_g</math> (Hz)</b>	9.7	1.2 <sup>a)</sup>
<b><math>x_a</math></b>	0.34	0.56

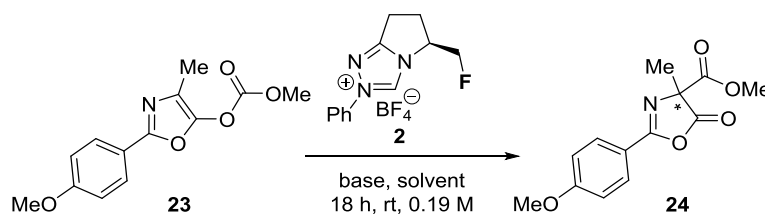
<sup>a)</sup> literature values<sup>[56]</sup>

Comparing the populations of the mono- and the difluorinated triazolium salt it becomes clear that the relative order is conserved (*synclinal-exo* > *synclinal-endo* > *antiperiplanar*). In absolute terms the *synclinal-endo* conformer is similarly populated in both structures (34% vs. 35%). In the monofluorinated structure *synclinal-exo* is slightly more favoured (56% vs. 51%) while the *antiperiplanar* conformer is slightly less populated (10% vs. 14%). However, these differences are extremely small and therefore it can be concluded that although there might be a small interaction between the two fluorine atoms ( ${}^5J_{FF}$  4.9 Hz), the population of the three rotamers discussed above is not significantly influenced.

## 4.5 Asymmetric Steglich Rearrangement Catalysed by Fluorinated NHCs

### 4.5.1 Optimisation of Reaction Conditions

To explore the effect of fluorination on catalysis, the asymmetric Steglich rearrangement was chosen due to the positively charged substrate-catalyst intermediate. The reaction is shown in Scheme 19: Triazolium salt **2** was deprotonated with various bases (equimolar amounts to the catalyst precursor) in various solvents. Under these conditions carbonate **23** rearranged to ester **24**. All reactions were run at a concentration of 0.19 M at rt for 18 h on a 20 mg scale.



Scheme 19: Model reaction of the NHC catalysed Steglich rearrangement.

The conversions and enantiomeric ratios obtained are summarised in Table 3: When the reaction was run in toluene with KHMDS (0.5 M solution in toluene) as base with a catalyst precursor loading of 10 mol%, full conversion to the expected product was observed with an *e.r.* of 80.5:19.5 (entry 1). First, solvents were varied (entries 2-8): The use of chlorinated solvents led to a decrease in both conversion and enantioselectivity (entries 2 and 3). Surprisingly, although Et<sub>2</sub>O and 1,4-dioxane gave good conversions, changing to THF was not tolerated (entries 4-6). In *n*-hexane selectivities comparable to those in toluene were observed (*e.r.* = 79.0:21.0, entry 7) albeit with lower conversions. Chlorobenzene led to decreased selectivity and conversion (entry 8). Next, the influence of the base on the reaction outcome with toluene as solvent was analysed (entries 9-12). Only a marginal effect on the selectivity was observed as the *e.r.* ranged from 78.5:21.5 (KO<sup>t</sup>Bu, entry 10) to 80.5:19.5 (Cs<sub>2</sub>CO<sub>3</sub>, entry 12). The use of DBU (entry 9) and solid KHMDS (entry 11) led to decreased conversion but only to a small drop in selectivity. As Cs<sub>2</sub>CO<sub>3</sub> led to full conversion and the same selectivity as KHMDS these two bases were concluded to be equally competent in this transformation. Variation of the concentration to 0.02 M and to 0.50 M did not significantly affect the conversion or the *e.r.* (entries 13 and 14). Similar observations were made when using Cs<sub>2</sub>CO<sub>3</sub> instead of KHMDS (entries 18 and 19). Interestingly, augmenting catalyst precursor loading to 30 mol% with KHMDS led to significantly decreased selectivities

(*e.r.* = 66.5:33.5, entry 15). However, this was not observed when Cs<sub>2</sub>CO<sub>3</sub> was used (entry 20, *e.r.* = 80.0:20.0, entry 20). Decreasing catalyst precursor loading led to reduced conversion with both bases but did not alter the selectivities (entries 16 and 21). Finally, the use of 1 mol% triazolium salt with KHMDS was not tolerated (no conversion, entry 17).

Table 3: Screening of base, solvent and catalyst loading for the NHC catalysed Steglich rearrangement.

entry	solvent	base	conc. (mol•L <sup>-1</sup> )	loading (mol%)	conversion (%) <sup>a)</sup>	<i>e.r.</i> <sup>a)</sup>
1	toluene	KHMDS	0.19	10	>99	80.5:19.5
2	CH <sub>2</sub> Cl <sub>2</sub>	KHMDS	0.19	10	85	59.0:41.0
3	CDCl <sub>3</sub>	KHMDS	0.19	10	31	70.0:30.0
4	THF	KHMDS	0.19	10	<1	--
5	Et <sub>2</sub> O	KHMDS	0.19	10	>99	74.0:26.0
6	1,4-dioxane	KHMDS	0.19	10	93	74.5:25.5
7	<i>n</i> -hexane	KHMDS	0.19	10	30	79.0:21.0
8	PhCl	KHMDS	0.19	10	57	71.5:28.5
9	toluene	DBU	0.19	10	59	79.5:20.5
10	toluene	KO <sup>t</sup> Bu	0.19	10	10	78.5:21.5
11	toluene	KHMDS (solid)	0.19	10	58	79.0:21.0
12	toluene	Cs <sub>2</sub> CO <sub>3</sub>	0.19	10	>99	80.5:19.5
13	toluene	KHMDS	0.02	10	96	80.5:19.5
14	toluene	KHMDS	0.50	10	>99	79.0:21.0
15	toluene	KHMDS	0.19	30	>99	66.5:33.5
16	toluene	KHMDS	0.19	5	54	80.5:19.5
17	toluene	KHMDS	0.19	1	<1	--
18	toluene	Cs <sub>2</sub> CO <sub>3</sub>	0.02	10	89	81.0:19.0
19	toluene	Cs <sub>2</sub> CO <sub>3</sub>	0.50	10	99	80.0:20.0
20	toluene	Cs <sub>2</sub> CO <sub>3</sub>	0.19	30	99	80.0:20.0
21	toluene	Cs <sub>2</sub> CO <sub>3</sub>	0.19	5	95	80.0:20.0

<sup>a)</sup> The conversion and enantiomeric ratio of the product was determined by HPLC on an Agilent 1260 series system using a reprocil chiral-OM 4.6 mm column. Conversions were corrected for response factors.

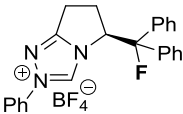
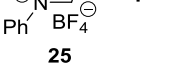
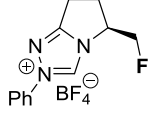

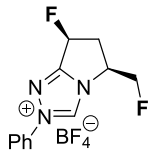

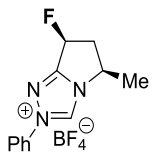
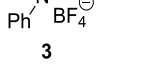

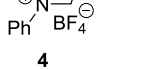
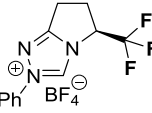

#### 4.5.2 Effect of Differently Substituted NHC Precursors on the Model Reaction

As mentioned previously, KHMDS and Cs<sub>2</sub>CO<sub>3</sub> gave very similar results. For this reason the model reaction was carried out with each catalyst precursor using both bases. In addition to the structures shown in chapter 4.2 a triazolium salt (synthesised by Dr. Susann Paul<sup>[48][47]</sup>) bearing a diphenylfluoromethyl group rather than a fluoromethyl exocyclic substituent was tested. As shown in Table 4 precursor **25** gave essentially no selectivity when deprotonated with Cs<sub>2</sub>CO<sub>3</sub> (entry 1, *e.r.* = 54.5:45.5) and the other enantiomer as with triazolium salt **2** was obtained. The use of KHMDS as base did not lead to any conversion (entry 2). As expected, improvement in selectivity was noted when the reaction was performed in the presence of the difluorinated NHC: An enantiomeric ration of 87.0:13.0 and 86.0:14.0 was obtained when Cs<sub>2</sub>CO<sub>3</sub> and KHMDS were used, respectively. Again, in terms of conversion Cs<sub>2</sub>CO<sub>3</sub> outperformed KHMDS (98% vs. 10% conversion, entries 5 and 6). Upon removal of the fluorine atom on the exocyclic position significantly lower selectivity with both bases (entries 7 and 8) was observed. Once more, the use of KHMDS led to decreased conversion. This was also observed for the reaction catalysed by the nonfluorinated NHC where the rearrangement proceeded with 97% and 75% conversion (entries 9 and 10). In both cases an *e.r.* of 62.5:37.5 was measured which underlines the importance of catalyst fluorination in the NHC catalysed Steglich rearrangement. Trifluoromethylated triazolium salt did not lead to any conversion (entries 11 and 12). This is possibly due to decreased nucleophilicity of the resulting carbene.



*Fluorinated N-Heterocyclic Carbenes*

Table 4: Variation of catalyst precursor in the Steglich rearrangement.

entry	catalyst	base	conversion (%) <sup>a)</sup>	<i>e.r.</i> <sup>a)</sup>
1		Cs <sub>2</sub> CO <sub>3</sub>	77	54.5:45.5 <sup>b)</sup>
2		KHMDS	0	n.d.
3		Cs <sub>2</sub> CO <sub>3</sub>	99	80.5:19.5
4		KHMDS	99	80.5:19.5
5		Cs <sub>2</sub> CO <sub>3</sub>	98	87.0:13.0
6		KHMDS	10	86.0:14.0
7		Cs <sub>2</sub> CO <sub>3</sub>	96	77.5:22.5
8		KHMDS	45	76.0:24.0
9		Cs <sub>2</sub> CO <sub>3</sub>	97	62.5:37.5
10		KHMDS	75	62.5:37.5
11		Cs <sub>2</sub> CO <sub>3</sub>	0	n.d.
12		KHMDS	0	n.d.

<sup>a)</sup> The conversion and enantiomeric ratio of the product was determined by HPLC on an Agilent 1260 series system using a reproil chiral-OM 4.6 mm column. Conversions were corrected for response factors. <sup>b)</sup> Other enantiomer was observed.

### 4.5.3 Conclusion

In conclusion the effect of multiple fluorination of triazolium derived *N*-heterocyclic carbenes was showcased on the example of the asymmetric Steglich rearrangement. By molecular editing it was found that introduction of fluorine atoms in the  $\beta$ -position of the nitrogen at the 4-position of the NHC-precursor has a large effect on the selectivity: While nonfluorinated compound **4** led to the desired product with an *e.r.* of 62.5:37.5, the Steglich rearrangement catalysed by the difluorinated NHC derived from compound **1** delivered the rearrangement product with an *e.r.* of 87:13. To the best of our knowledge, this constitutes the highest selectivity for the NHC catalysed Steglich rearrangement to date.<sup>[49]</sup> Furthermore it was observed that monofluorination also led to significantly improved selectivities (*e.r.* = 80.5:19.5 and 77.5:22.5). Using a trifluoromethylated triazolium salt did not lead to any formation of the product in the model reaction.

## 5 Fluorinated 4-Aminopyridine Derivatives

### 5.1 Introduction

Dimethylaminopyridine (DMAP) and derivatives thereof have long been known to be highly active nucleophilic catalysts.<sup>[57][58]</sup> They are most commonly used in acyl transfer processes such as acylation of alcohols with anhydrides. Over the last two decades, various chiral DMAP analogues have been developed and successfully applied in reactions including kinetic resolution or desymmetrisation of *meso* compounds.<sup>[59][60]</sup> A selection of the most prominent examples are shown in Figure 10.

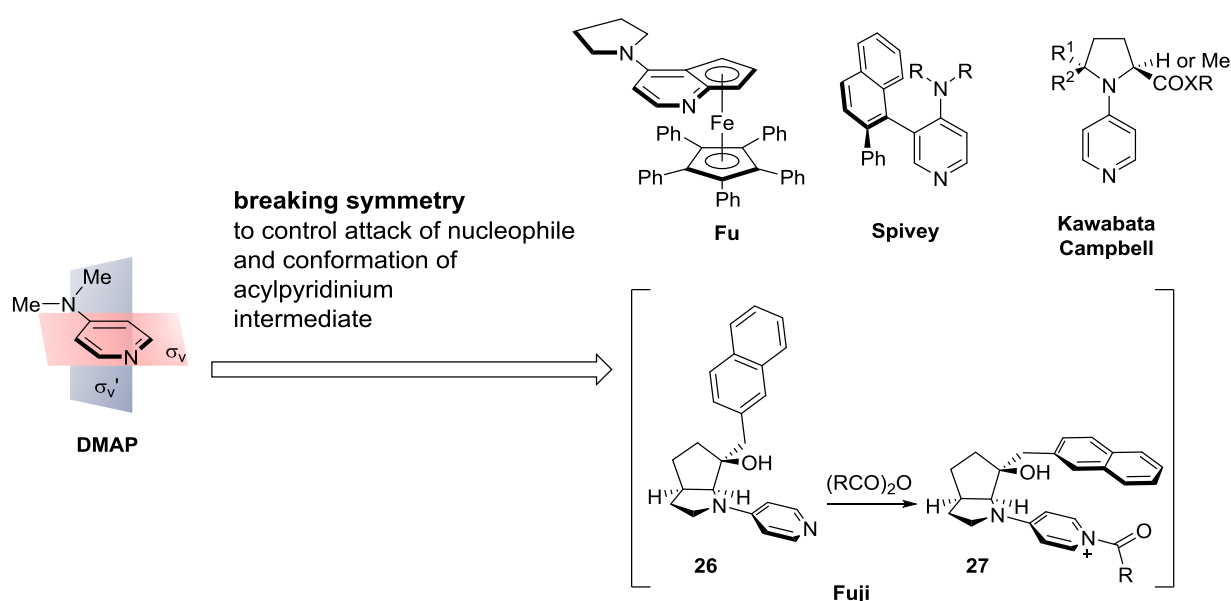
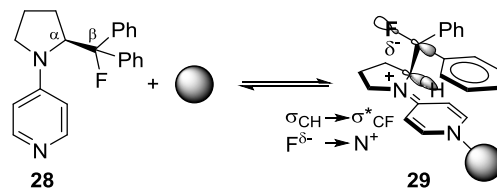


Figure 10: Selected examples of chiral DMAP analogues.

In order to render the catalyst chiral and simultaneously control both the attack of a nucleophile and the conformation of the acylpyridinium intermediate, the two internal symmetry planes ( $\sigma_v$  and  $\sigma_v'$ ) of DMAP must be broken. This has elegantly been achieved by the groups of Fu (planar chirality),<sup>[61]</sup> Spivey (axial chirality),<sup>[62]</sup> Kawabata<sup>[63]</sup> and Campbell<sup>[64]</sup> (stereogenic centres of the amino moiety). Of particular interest in the context of this work is the catalyst designed by Fuji,<sup>[63]</sup> which has been shown to undergo a conformational change upon reaction with the substrate: Starting from an open form (**26**) the system undergoes a conformational change to the closed form (**27**). This efficiently shields one face of the complex and is thought to be favoured by a cation- $\pi$  interaction in the acylpyridinium ion. It can be imagined that a structure containing a  $\beta$ -fluoroamino moiety on the 4-position of the pyridine ring might behave in a similar way: As shown in Scheme 20,

generation of an acylpyridinium cation (**29**) may also allow for a cation- $\pi$  interaction, but charge transmission would create a  $\beta$ -fluoroiminium moiety where a *gauche* effect would be operational. Both effects may be cooperative.



Scheme 20: Possible stabilising effects in a fluorinated DMAP analogue.

## 5.2 Diarylfluoromethyl Derivatives

### 5.2.1 Computational Studies

In a collaboration with Dr. Hans Martin Senn (University of Glasgow) a theoretical conformational analysis of the parent scaffold was performed. The relative energies of the three rotamers partitioned by  $120^\circ$  (shown in Figure 11) were analysed at the DFT level of theory for both cases, the neutral and the acetylated compounds.

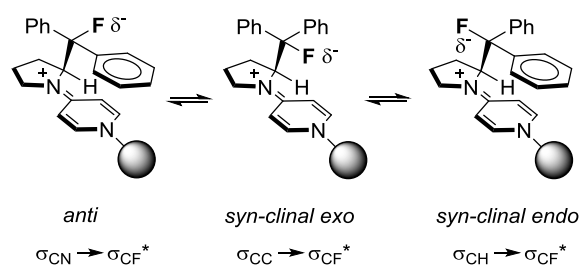
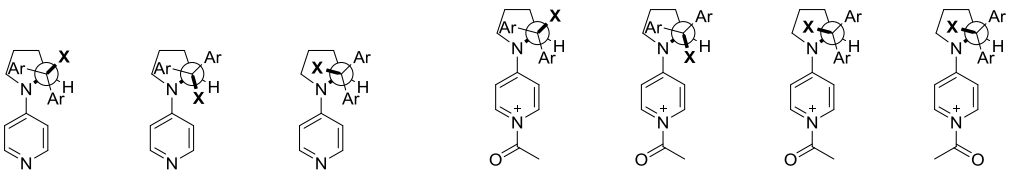


Figure 11: Three rotamers of the acetylated fluorinated DMAP derivative.

It was expected that, due to stabilising hyperconjugative interactions of the form  $\sigma_{\text{CH}} \rightarrow \sigma_{\text{CF}}^*$  and  $\sigma_{\text{CC}} \rightarrow \sigma_{\text{CF}}^*$ , a general preference for the *synclinal* conformers would be observed. Upon acetylation, additional stabilisation due to coulombic interactions ( $\text{F}^{\delta-} \cdots \text{N}^+$ ) was anticipated along with a possible further stabilisation of the *synclinal-endo* conformation owing to a possible cation- $\pi$  interaction. The computational results are summarised in Figure 12: For the neutral systems the *synclinal-endo* conformer was arbitrarily set as the reference ( $0 \text{ kJ}\cdot\text{mol}^{-1}$ ). For the fluorinated compound **28**, the *antiperiplanar* conformer was destabilised compared to the two *synclinal* rotamers by  $6 \text{ kJ}\cdot\text{mol}^{-1}$  and  $13 \text{ kJ}\cdot\text{mol}^{-1}$ . The stabilisation of the *synclinal-*

*exo*-conformer was attributed to a possible C-H- $\pi$  interaction between the aromatic shielding group and the 4-position of the pyrrolidine moiety. The same relative energetic order of rotamers was also calculated for the nonfluorinated compound **30** although with a smaller difference between the *endo* and *anti* conformers and a larger difference between the two *synclinal* rotamers.



	<i>antiperiplanar</i>	<i>synclinal-exo</i>	<i>synclinal-endo</i>	<i>s-trans-ap</i>	<i>s-trans-sc-exo</i>	<i>s-trans-sc-endo</i>	<i>s-cis-sc-endo</i>
X=H (30) <sup>a</sup> Ar=Ph	2	-19	0	8	8	0	1.2
X=F (28) <sup>a</sup> Ar=Ph	6	-7	0	18	6	0	0.4
X=F (31) <sup>b</sup> Ar=4- <sup>t</sup> BuPh	-	-	-	11	6	0	-1
X=F (32) <sup>b</sup> Ar=BiPh	-	-	-	-	-	0	6

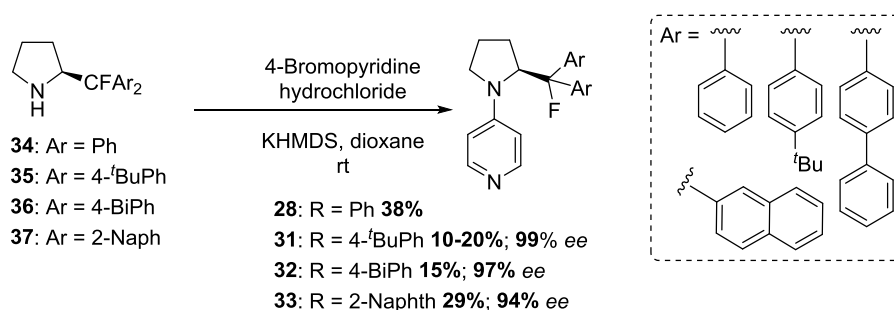
Figure 12: Relative energies of the rotamers for the neutral and the acetylated systems, <sup>a</sup> M05-2X/6-311+G(2df,p), <sup>b</sup> BLYP-D/def2-TZVPP. All energies are in kJ•mol<sup>-1</sup>.

Upon acetylation, rotation about the single bond between the pyridine ring and the carbonyl group had to be taken into account (*s-trans* and *s-cis*). For the fluorinated, acetylated systems the rotamer highest in energy was still calculated to be the one with an *antiperiplanar* alignment of the C-F bond and the vicinal C-N bond. Importantly, for the compound bearing Ph groups (**28**) the *synclinal-exo* rotamer was now calculated to be 6 kJ•mol<sup>-1</sup> higher in energy, a finding that was consistent with a possible cation- $\pi$  interaction. However, for the nonfluorinated compound (**30**) no difference in energy was found for the *synclinal-exo* and the *antiperiplanar* conformers. This can be explained by the absence of a *gauche* effect. The same relative energies (*sc-endo* < *sc-exo* < *anti*) were calculated for the compound with 4-<sup>t</sup>BuPh shielding groups (**31**), however with an energetically slightly lower lying *antiperiplanar* rotamer. In general, rotation of the acetyl group was found to have a minimal effect on the energy, except for the system with biphenyl shielding groups (**32**) for which the *s-trans-synclinal-endo* conformer was found to be 6 kJ•mol<sup>-1</sup> more stable than the *s-cis-synclinal-endo* conformer. This can be rationalised by invoking an interaction between the methyl group of the acetyl moiety with one phenyl ring of the biphenyl substituent (CH- $\pi$ ). From these calculations it can be concluded that the *gauche* effect can also be triggered in

fluorinated DMAP derivatives and leads to a conformational change upon reaction with the substrate.

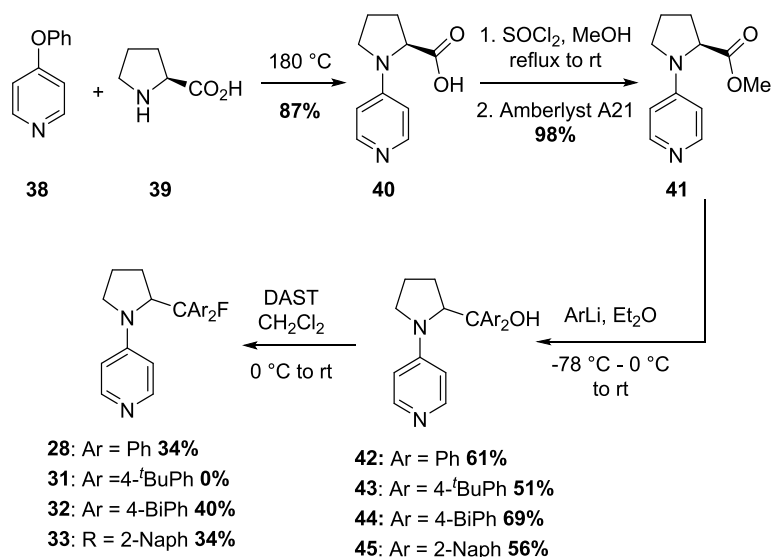
## 5.2.2 Synthesis of Fluorinated DMAP Derivatives Part I

The syntheses of compounds **28** and **31-33** were carried out by Dr. C. Sparr (ETH Thesis No. 19894) and Dr. E.-M. Tanzer (ETH Thesis No. 20919). Two general approaches were adopted to prepare these compounds: Base-mediated coupling of the  $\beta$ -fluoroamines<sup>[65]</sup> (**34-37**) with 4-bromopyridine hydrochloride (Scheme 21)<sup>[66]</sup> or by starting with the coupling step as described in Scheme 22.



Scheme 21: Base mediated coupling of  $\beta$ -fluoroamines with 4-bromopyridine hydrochloride.

The desired fluorinated DMAP derivatives could be accessed by reacting phenoxyproline (**38**) with (L)-proline (**39**) followed by esterification of the carboxylic acid **40** to give compound **41**. Addition of the aryllithium species gave the corresponding carbinols in racemic form which could then be fluorinated to the target compounds (with the exception of 4-<sup>t</sup>BuPh derivative **43**) (Scheme 22).



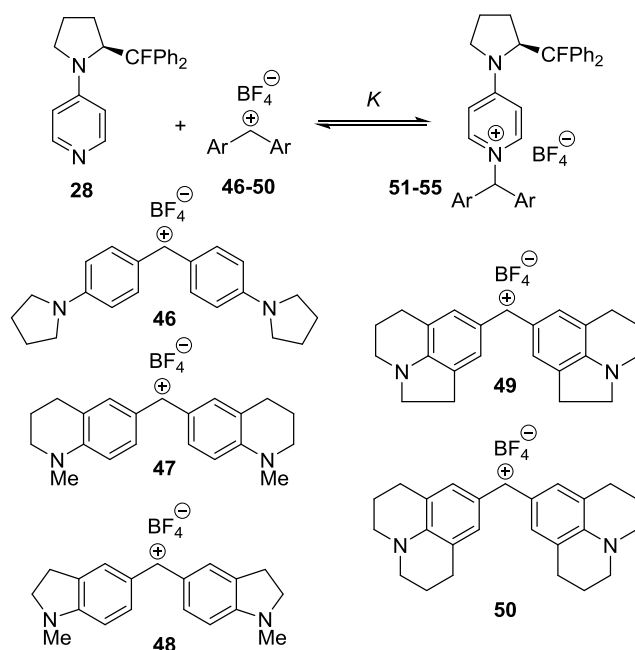
Scheme 22: Alternative synthesis of fluorinated DMAP derivatives.

### 5.2.3 Kinetic Studies by Means of Reaction with Benzhydrylium Ions

In order to quantitatively evaluate the nucleophilicity parameters of fluorinated DMAP derivatives a kinetic study was performed by Dr. Sami Lakhdar (LMU Munich, Germany and ENSICAEN, Caen, France). The relationship (equation 2) was used where  $N$  and  $E$  denote the nucleophilicity and electrophilicity parameters, respectively.  $s_N$  is a measure of the sensitivity of the nucleophile on the change of the electrophile and  $k_2$  is the second order rate constant.<sup>[67]</sup>

$$\log(k_2) = s_N(E + N) \quad (2)$$

To that end fluorinated DMAP derivative **28** was reacted with various benzhydrylium ions (**46-50**, Scheme 23). This procedure was convenient as benzhydrylium ions are intensely coloured and their concentration can thus be followed photometrically. Moreover, their electrophilicity parameters ( $E$ ) had previously been reported in the literature.<sup>[67]</sup>

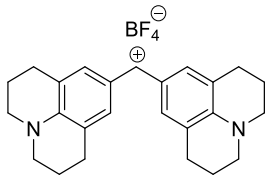
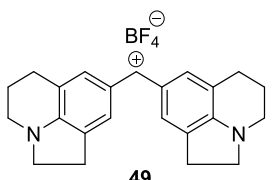


Scheme 23: Reaction of fluorinated DMAP analogue **28** with various benzhydrylium ions.

As a consequence of using a large excess of the DMAP analogue ( $> 10$  eq.) the reactions showed *pseudo* first order kinetics and the corresponding rate constants ( $k_{obs}$ ) were determined by following the decay of the benzhydrylium ion absorbance. By varying the concentration of the nucleophile different first order rate constants  $k_{obs}$  were obtained which were plotted against the initial nucleophile concentration. From the resulting linear relationship the second order rate constant ( $k_2$ ) could be derived: As can be seen from equation (2) when  $\log(k_2)$  is plotted against the electrophilicity parameters ( $E$ ) of the various benzhydrylium ions a linear relationship with a slope corresponding to  $s_N$  and an abscissa corresponding to  $s_N \cdot N$  is obtained. By this procedure a nucleophilicity parameter of  $N = 14.57$  and a sensitivity factor of  $s_N = 0.75$  was found. By comparing these values with the corresponding ones for the parent compound DMAP ( $N = 15.80$ ;  $s_N = 0.66$ )<sup>[68]</sup> or 4-pyrrolidinopyridine ( $N = 15.90$ ;  $s_N = 0.67$ )<sup>[68]</sup> it can be concluded that the nucleophilicity is only slightly diminished. Compound **28** can therefore be expected to show similar kinetic behaviour as DMAP. Additionally, as the reactions with benzhydrylium ions **49** and **50** did not reach completion, equilibrium constants ( $K$ ) for these systems could be derived and again be compared to DMAP. As shown in Table 5, the obtained equilibrium constants were of the same order of magnitude as for DMAP.

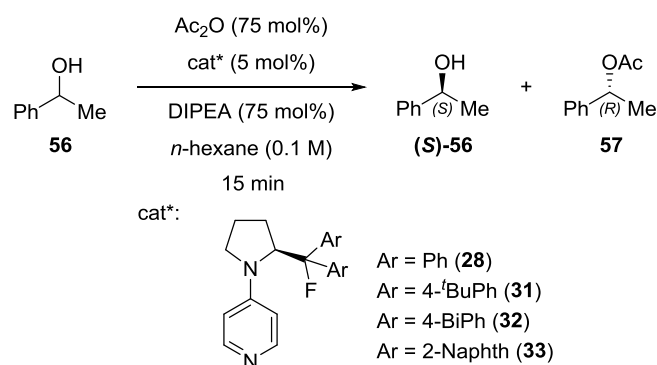


Table 5: Equilibrium constants for the reaction of DMAP and **28** with two benzhydrylium ions.

<i>electrophile</i>	$K(\text{DMAP})^{[68]}$	$K(\mathbf{28})$
 <p><b>50</b></p>	$5.85 \cdot 10^3$	$3.60 \cdot 10^3$
 <p><b>49</b></p>	$5.70 \cdot 10^3$	$4.37 \cdot 10^3$

### 5.2.4 Catalysis Studies Part I

In order to validate the fact that these fluorinated DMAP analogues are competent structures for nucleophilic catalysis they were applied in the kinetic resolution of secondary alcohols. Previous studies by Dr. C. Sparr, Dr. E.-M. Tanzer and Dr. L. Zimmer had shown that structures **28** and **31-33** were effective in catalysing the acetylation of ( $\pm$ )-1-phenylethanol using acetic anhydride and DIPEA in *n*-hexane (see Scheme 24). Under these conditions, short reaction times of only 15 min were sufficient to give conversions between 64% and 80%.



Scheme 24: Initial investigation of catalyst structures **28** and **31-33** in the kinetic resolution of ( $\pm$ )-1-phenylethanol.

This reaction was repeated with catalyst structures **28** and **31-33** on a 100  $\mu\text{mol}$  scale with respect to ( $\pm$ )-1-phenylethanol. The obtained enantiomeric ratios and selectivity factors (*s*) are shown in Table 6. The selectivity factors were calculated according to equation (3) where *c* is the conversion and *ee* is the enantiomeric excess of the starting material (1-phenylethanol).

$$S = \frac{\ln[(1-c)(1-ee)]}{\ln[(1-c)(1+ee)]} \quad (3)^{[69]}$$

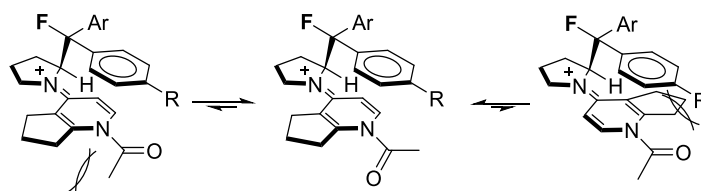
The reaction's selectivities ranged from completely unselective for compound **28** (entry 1, Ar = Ph) to low selectivities with an *s*-factor of 1.56 being the highest (entry 2, Ar = 4-*t*BuPh, **31**). A possible reason for these low selectivities was thought to be the low difference in energy between the *s-cis* and the *s-trans* conformers of the acylpyridinium salts (see chapter 5.2.1).

Table 6: Kinetic resolution of (±)-1-phenylethanol using catalyst structures **28** and **31-33**.

entry	catalyst	conversion (%) <sup>a)</sup>	<i>e.r.</i> (56)	<i>e.r.</i> (57)	<i>s</i>
1	<b>28</b>	80 <sup>b)</sup>	50.0:50.0	50.0:50.0	1.00
2	<b>31</b>	72	64.0:36.0	55.5:44.5	1.56
3	<b>32</b>	57	56.0:44.0	54.5:45.5	1.33
4	<b>33</b>	64	55.0:45.0	52.5:47.5	1.21

<sup>a)</sup> Conversion was determined from the *ee* of the alcohol and the *ee* of the acetate. <sup>b)</sup> Conversion was determined by integration of the GC signals of the alcohol and the acetate (correcting for response factors).

It was envisaged that higher selectivities could be obtained by modifying the catalyst structure to favour formation of only one of the two conformations of the acylpyridinium ion. A possible approach is shown in Scheme 20: Introducing a substituent at the 2- and 3- position of the pyridine moiety would probably lead to unfavourable steric interactions (*A*<sup>1,3</sup>-strain) with both the methyl group of the acetyl group and the aromatic shielding group.

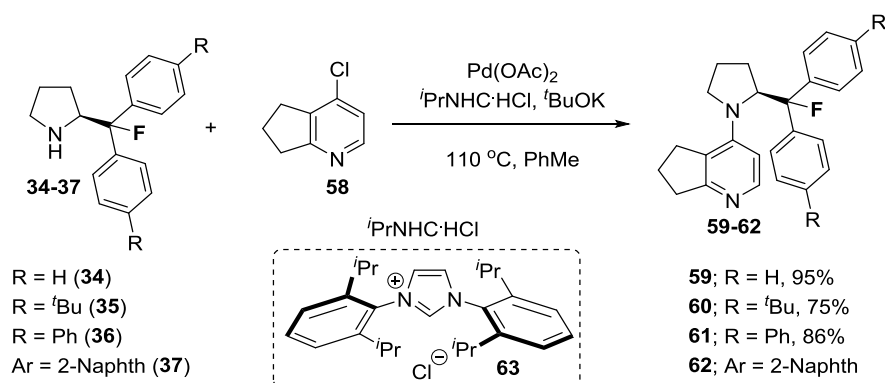


Scheme 25: Favouring one rotamer by introducing *A*<sup>1,3</sup> strain.

### 5.2.5 Synthesis of Fluorinated DMAP Derivatives Part II

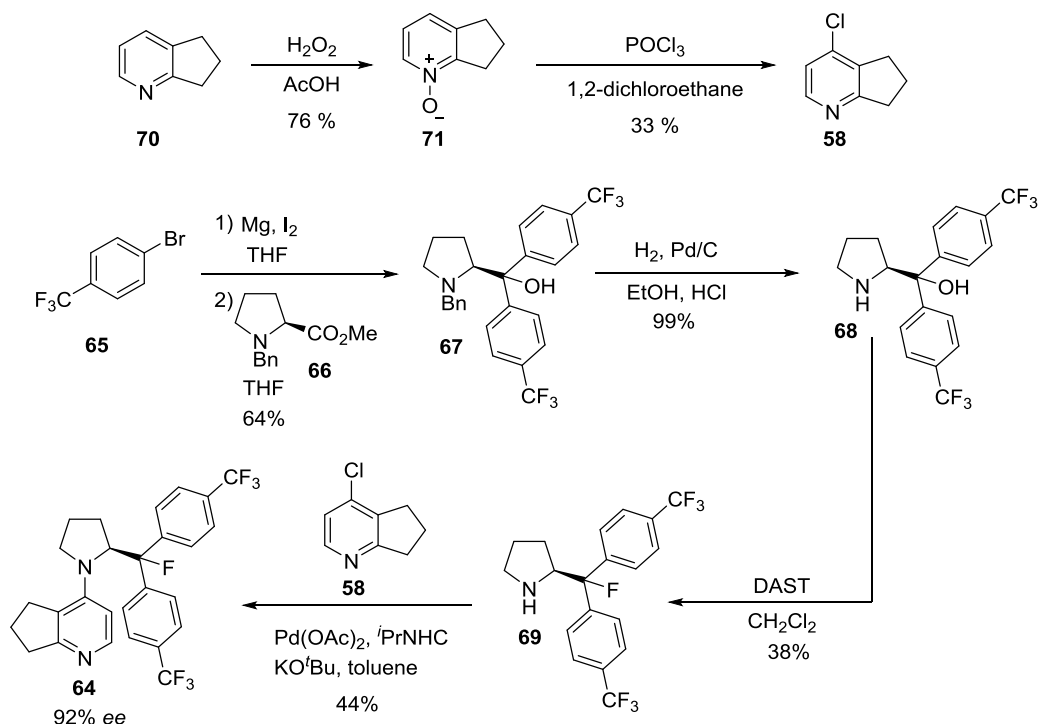
These second generation catalysts were synthesised by Buchwald-Hartwig coupling of 4-chlorocyclopentenopyridine<sup>[70]</sup> and the appropriate β-fluoroamine. It was found that the choice of ligand was of paramount importance for this transformation and that carbene

“*i*PrNHC”<sup>[71]</sup> led to good yields (up to 95%) with only minor loss of optical purity (80% *ee*) (see Scheme 26).



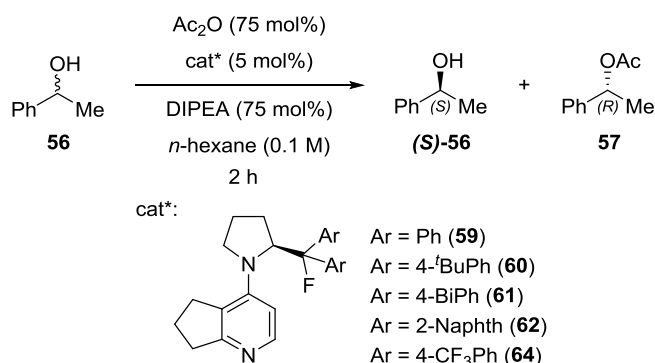
Scheme 26: Buchwald-Hartwig coupling of 4-chlorocyclopentenopyridine with  $\beta$ -fluoroamines.

In addition to catalyst structures **59-62**, a trifluoromethylated catalyst (**64**) was constructed in a similar manner. The synthesis is shown in Scheme 27. Commercially available 1-bromo-4-(trifluoromethyl)-benzene (**65**) was converted to the corresponding Grignard reagent. To this was added benzyl protected (L)-proline-methylester **66** to give carbinol **67** in 64% yield. The product was deprotected under hydrogenative conditions (99%) and fluorinated using DAST to give  $\beta$ -fluoroamine **69** in 38% yield. Pyridine derivative **58** was synthesised according to a literature procedure<sup>[70]</sup> by oxidising commercial cyclopentenopyridine **70** to its *N*-oxide (**71**) using hydrogen peroxide in acetic acid (76%): This was subsequently converted to the 4-chloropyridine derivative **58** with POCl<sub>3</sub> in 1,2-dichloroethane (33%). These two compounds were then coupled using palladium catalysis as described above to give the target compound (**64**) in 44% yield with 92% *ee*.


 Scheme 27: Synthesis of trifluoromethylated DMAP analogue **64**.

## 5.2.6 Catalysis Studies Part II

These second generation catalysts were then again tested in the kinetic resolution of ( $\pm$ )-1-phenylethanol **56** using acetic anhydride and DIPEA in *n*-hexane (see Scheme 28). Slower conversion was observed compared to the reactions catalysed by compounds **28** and **31-33**, and therefore these reactions were stirred for 2 h (cf. 15 min).


 Scheme 28: Investigation of 2<sup>nd</sup> generation catalyst structures **59-62** and **64** in the kinetic resolution of ( $\pm$ )-1-phenylethanol.

The results of the kinetic resolution of ( $\pm$ )-1-phenylethanol catalysed by compounds **59-62** and **64** (Table 7) clearly show that by changing the pyridine component to a

cyclopentenopyridine moiety, the selectivity factors increase. Most remarkably, for the phenyl derivative the unselective reaction previously observed now showed moderate selectivity (entry 1,  $s = 0 \rightarrow s = 2.71$ ). As described in chapter 5.2.4 the highest selectivity was obtained for 4-*t*BuPh derivative **31**. This also holds true for the modified structure **60** which catalysed the kinetic resolution with an  $s$ -factor of 3.17 (entry 2). Interestingly, biphenyl and naphthyl derived catalysts **61** and **62** led to lower selectivities compared to the ones for the non-modified catalysts (entries 3 and 4,  $s = 2.08$  and  $s = 2.47$ , respectively). Trifluoromethylated structure **64** proved to be poorly soluble in *n*-hexane. However, in a more diluted reaction (0.02 M) it catalysed the kinetic resolution with a similar selectivity as 4-*t*BuPh derived structure **60** (entry 5;  $s = 2.90$ ).

Table 7: Kinetic resolution of ( $\pm$ )-1-phenylethanol using catalyst structures **59-62** and **64**.

entry	catalyst	conversion (%)	<i>e.r.</i> ( <b>55</b> )	<i>e.r.</i> ( <b>56</b> )	$s$
1	<b>59</b>	26	57.0:43.0	70.5:29.5	2.71
2	<b>60</b>	29	59.0:41.0	72.5:27.5	3.17
3	<b>61</b>	29	56.0:44.0	65.0:35.0	2.08
4	<b>62</b>	32	58.5:41.5	68.0:32.0	2.47
5 <sup>a)</sup>	<b>64</b>	6	51.5:48.5	73.5:26.5	2.90

<sup>a)</sup> performed at a concentration of 0.02 M.

## 5.2.7 Towards a $C_2$ -Symmetric, Difluorinated DMAP Analogue

### 5.2.7.1 Introduction

A possible alternative to controlling the conformation of the acetyl group in the acylpyridinium salt would be to construct a  $C_2$ -symmetric, difluorinated DMAP analogue as shown in Figure 13. Assuming an attack of the nucleophile in a Bürgi-Dunitz trajectory, a favoured approach to the *Si*-face of the carbonyl centre can be expected due to shielding of the *Re*-face by a phenyl group. This is thought to lead to a preference for the reaction with one of the two enantiomers of the secondary alcohol.

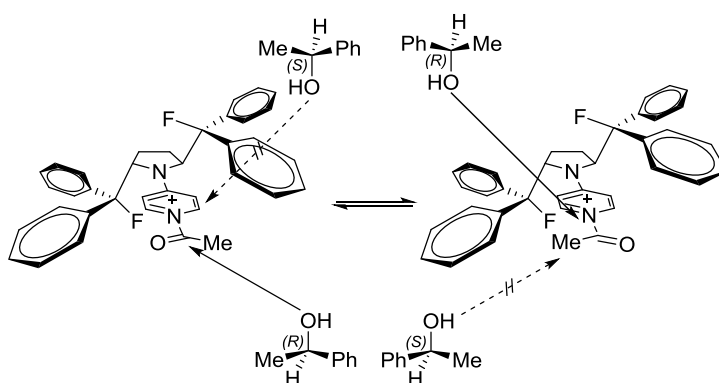
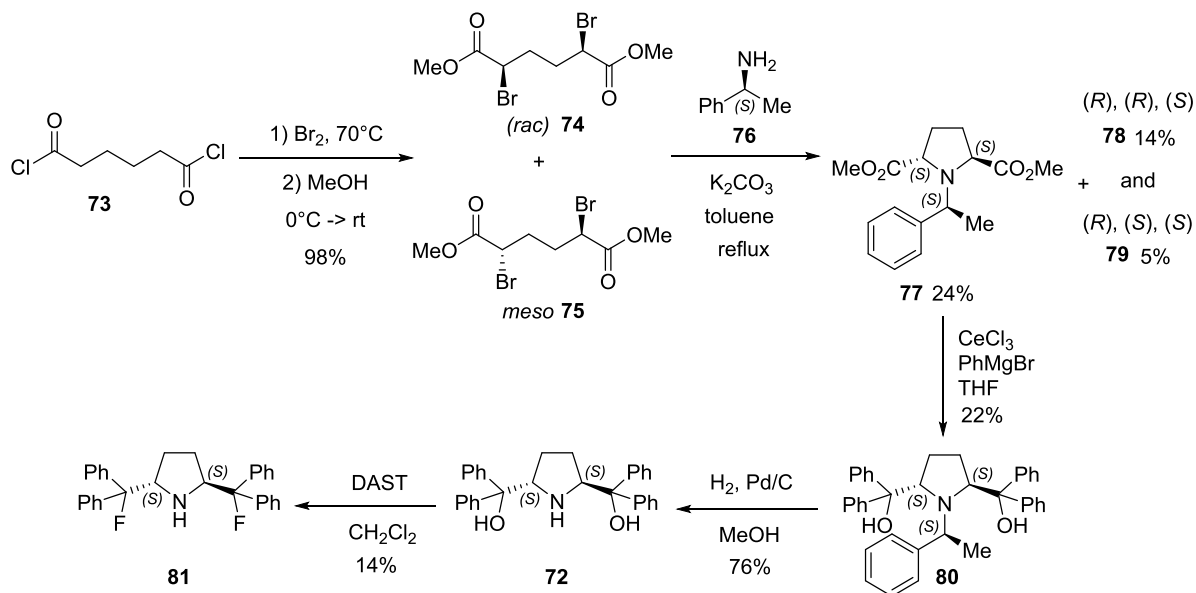


Figure 13: A  $C_2$ -symmetric catalyst and possible trajectories for the attack of the nucleophile.

### 5.2.7.2 Synthesis of $C_2$ -Symmetric, Difluorinated Secondary Amine **81**

Preparation of the requisite difluoride is outlined in Scheme 29. Conveniently, the synthesis of optically pure diol **72** had previously been published by the group of Aggarwal.<sup>[72]</sup> First, commercially available diacid chloride **73** was exposed to refluxing bromine and then esterified by the addition of MeOH to give a mixture of diastereomers (racemic **74** and *meso* **75**).<sup>[73]</sup> Cyclisation with enantiomerically pure (*S*)-phenylethylamine (**76**) gave the three diastereomers which were separated by column chromatography: (*S*),(*S*),(*S*) (**77**) in 24% yield, (*R*),(*R*),(*S*) (**78**) in 14% yield and (*R*),(*S*),(*S*) (**79**) in 5% yield. The major diastereomer was converted to diol **80** in 22% yield using phenylmagnesiumbromide and cerium(III)chloride in THF. Deprotection under a hydrogen atmosphere with palladium on carbon in MeOH gave enantiomerically pure,  $C_2$ -symmetric aminoalcohol **72** (76%). Double fluorination with DAST in  $\text{CH}_2\text{Cl}_2$  delivered target compound **81** in 14% yield. However, extensive attempts to couple this secondary amine to a pyridine moiety were not successful neither did it catalyse the Weitz-Scheffer epoxidation of cinnamaldehyde. This might be

explained by the increased steric hindrance of the amine and the negative inductive effect of the two fluorine atoms. Nevertheless, it constitutes an interesting structure, where rotation of two exocyclic bonds can be restricted by virtue of the fluorine-*gauche* effect. Subsequently, the conformation was investigated by X-ray analysis and NMR spectroscopy.



Scheme 29: Synthesis of a  $C_2$ -symmetric, difluorinated secondary amine.

### 5.2.7.3 X-ray Analysis of $C_2$ -Symmetric, Difluorinated Secondary Amine 81.

The crystal structure of compound **81** was obtained for the corresponding HCl salt and showed three distinct molecules in the unit cell. A representative structure is shown in Figure 14, which clearly confirmed the relative stereochemistry. Moreover, it can be seen that both fluorine atoms are placed *synclinal-endo* to the nitrogen ( $\Phi_{\text{FCCN}} = -53.0^\circ$  and  $-65.0^\circ$ ). The pyrrolidine ring does not adopt an envelope conformation but a half-chair which allows for both diphenylfluoromethyl substituents to be in a *pseudo-equatorial* position. Furthermore, the two phenyl groups that are placed *synclinal-exo* to the nitrogen are close to being parallel most likely to minimise steric repulsion. The angles needed for conformer population analysis ( $\angle\text{FCC(N)}$  and  $\angle\text{HCC(F)}$  for each side) are summarised in Table 8.

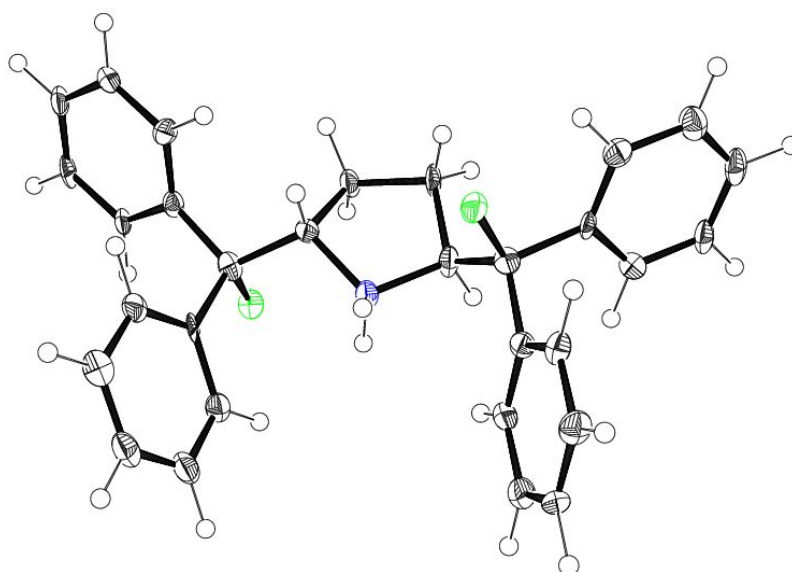


Figure 14: Crystal structure of  $C_2$ -symmetric, difluorinated ammonium salt **81·HCl**, the counterion is omitted for clarity.

Table 8: Relevant angles for conformer population analysis of  $C_2$ -symmetric, difluorinated ammonium salt **81·HCl**.

$\sphericalangle$ FCC(N)	$\sphericalangle$ HCC(F)	$\sphericalangle$ F'C'C'(N)	$\sphericalangle$ H'C'C'(F')
105.8°	109.4°	104.6°	109.5°

#### 5.2.7.4 Analysis of the Solution Phase Conformation of $C_2$ -Symmetric, Difluorinated Amine **81**.

The crystal structure of difluorinated ammonium salt **81·HCl** is not perfectly  $C_2$ -symmetric (hence the different angles for the left and the right side of the molecules in Table 8). The relevant “intramolecular angles” ( $\sphericalangle$ FCC(N) and  $\sphericalangle$ HCC(F), see chapter 5.2.7.3, Table 8) were averaged to be used in the refinement of the Karplus relation.<sup>[52]</sup> The coupling constants for the vicinal coupling of fluorine to carbon for a dihedral angle of 60° and 180° ( $J_g = 1.2$  Hz and  $J_a = 11.2$  Hz) were taken from the literature.<sup>[56]</sup> A summary of the measured as well as the corresponding calculated coupling constants and the resulting conformer population is shown in Table 9: It can be seen that the substituents preferentially adopt a *synclinal-endo* conformation (61%), followed by *synclinal-exo* (25%) and as a consequence the *antiperiplanar* conformer is calculated to be populated by 14%.



Table 9: Conformer population analysis for  $C_2$ -symmetric, difluorinated secondary amine **81**.

coupling	FCCH	FCCC
$\langle J \rangle$ (Hz)	27.5 <sup>a)</sup>	3.7
$J_a$ (Hz)	39.8	11.2 <sup>b)</sup>
$J_g$ (Hz)	8.5	1.2 <sup>b)</sup>
$x_a$	61%	25%

<sup>a)</sup> obtained from  $^{19}\text{F}$ -NMR; <sup>b)</sup> literature values<sup>[56]</sup>

This can be compared to the well known corresponding monosubstituted  $\beta$ -fluoroammonium ion (**82**) which was synthesised and crystallised as the perchlorate salt.<sup>[16]</sup> It becomes evident that conformational preference in solution of the monosubstituted  $\beta$ -fluoroammonium ion and the corresponding  $C_2$ -symmetric analogue is essentially the same for both compounds (*synclinal-endo*: 61% and 62% respectively, *synclinal-exo*: 25% for both and therefore *antiperiplanar*: 14% and 13% respectively).

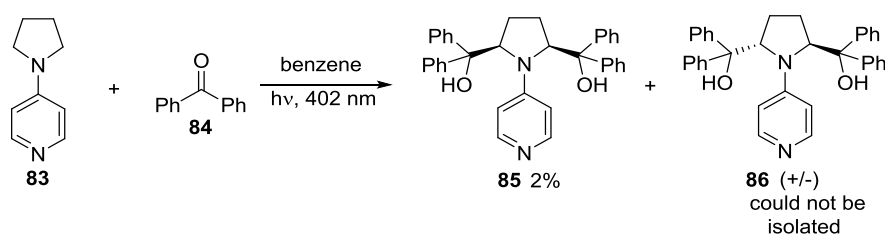
 Table 10: Conformer population analysis of monosubstituted  $\beta$ -fluoroammonium ion **82**.

coupling	FCCH	FCCC
$\langle J \rangle$ (Hz)	29.4 <sup>a)</sup>	3.7
$J_a$ (Hz)	42.0	11.2 <sup>b)</sup>
$J_g$ (Hz)	9.1	1.2 <sup>b)</sup>
$x_a$	62%	25%

<sup>a)</sup> obtained from  $^{19}\text{F}$ -NMR; <sup>b)</sup> literature values<sup>[56]</sup>

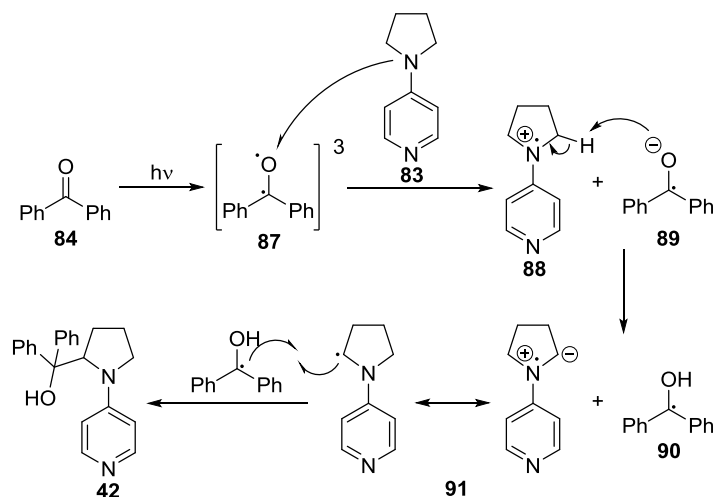
### 5.2.8 Attempted Photochemical Route to a $C_2$ -Symmetric DMAP Analogue

In an attempt to synthesise target compound **86** in a simple two-step procedure, a mixture of 4-pyrrolidinopyridine (**83**) and benzophenone (**84**) was irradiated with visible light (402 nm) in benzene (Scheme 30).



Scheme 30: Reaction of 4-pyrrolidinopyridine with benzophenone under irradiation.

The postulated mechanism is shown in Scheme 31. Irradiation of benzophenone (**84**) is known to generate an excited triplet state (**87**) which can oxidise aromatic amines by single electron transfer.<sup>[74]</sup> The resulting stabilised radical cation (**88**) may then be deprotonated on the 2-position leading to radicals **90** and **91**. Recombination would then lead to monosubstituted carbinol **42** which could undergo a second alkylation on the 5-position in a similar way.



Scheme 31: Possible mechanism for direct substitution of 4-pyrrolidinopyridine with benzophenone.

Although a variety of products were observed, the *meso* diastereomer could be isolated albeit in low yields (2%). Unfortunately, none of the desired compound **86** was isolated. However, single crystals of **85** suitable for X-ray analysis were obtained. The crystal structure is shown in Figure 15. Clearly, both hydroxy groups are oriented in a *synclinal-endo* position ( $\Phi_{\text{OCCN}} = 61.8^\circ$  and  $-49.3^\circ$ ; an example of two oxygen-*gauche* effects) which places a phenyl group on each side above the pyridine moiety. As a consequence, a pyramidalisation of the pyrrolidine nitrogen centre is observed. Moreover, the structure suggests an intramolecular hydrogen bond between the two hydroxyl groups ( $d_{\text{OH}\cdots\text{O}} = 1.816 \text{ \AA}$ ).

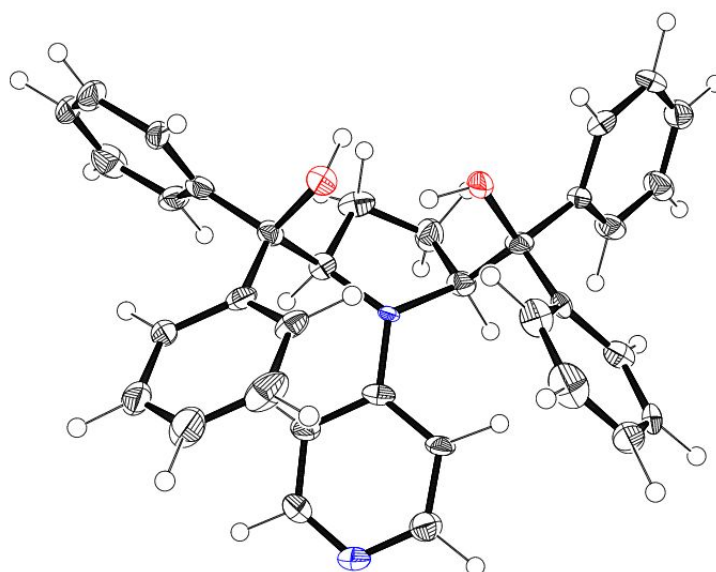
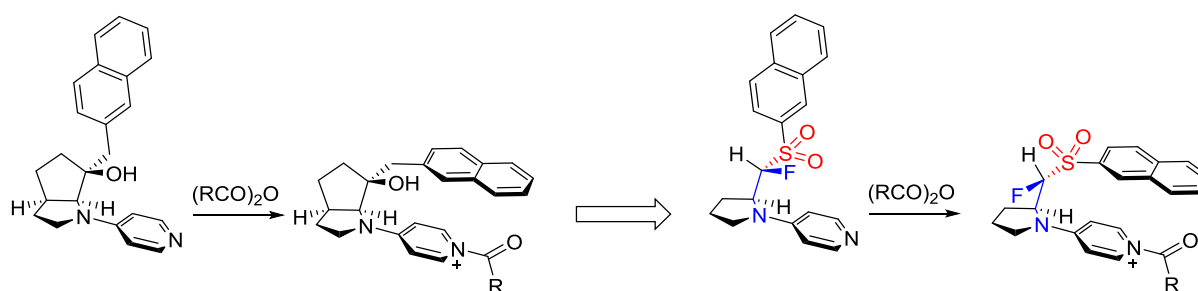


Figure 15: Crystal structure of DMAP derived diol **85**.

### 5.3 $\alpha$ -Fluorosulfones

#### 5.3.1 Introduction

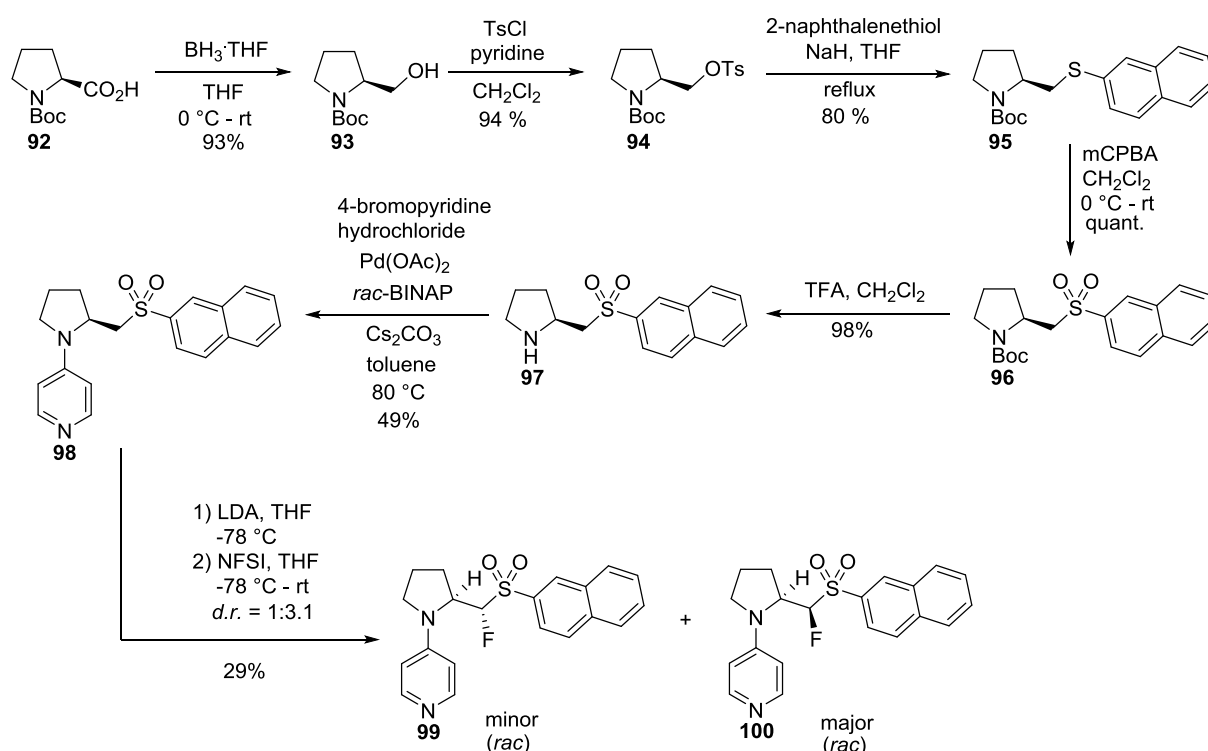
Inspired by the elegant catalyst design by the group of Fuji<sup>[63]</sup> (see chapter 5.1) it was envisaged that a simplified scaffold might constitute a suitable platform for the investigation of an additional stereoelectronic effect: An  $\alpha$ -fluorosulfone can be expected to preferentially align in such a way that the fluorine atom lies *antiperiplanar* to one of the S=O double bonds rather than bisecting the sulfonyl group, thus restricting the rotation between the sulfone (red) and the fluoroamino motif (blue, Scheme 32). In combination with a  $\beta$ -fluoroammonium ion moiety introduction of this motif may allow for the creation of a simplified analogue of Fuji's bicyclic system bearing an  $\alpha$ -fluorosulfonyl sidechain.



Scheme 32: Introducing additional stereoelectronic effects into a DMAP analogue.

5.3.2 Synthesis of DMAP Derived  $\alpha$ -Fluorosulfones

The synthesis of DMAP derived  $\alpha$ -fluorosulfones *via* known compound **97**<sup>[75]</sup> is shown in Scheme 33: Boc-protected (L)-proline (**92**) was reduced using borane in THF (93%) and the resulting alcohol (**93**) was treated with tosylchloride in pyridine and CH<sub>2</sub>Cl<sub>2</sub> (94%). Substitution of the tosylate by 2-naphthalenethiolate in THF gave thioether **95** in 80% yield. Oxidation to the sulfone was achieved with *m*CPBA in CH<sub>2</sub>Cl<sub>2</sub> (quant.) and deprotection with TFA in CH<sub>2</sub>Cl<sub>2</sub> gave  $\beta$ -aminosulfone **97** in 98% yield. Coupling to the pyridine moiety was performed under Buchwald-Hartwig conditions using 4-bromopyridine hydrochloride, Pd(OAc)<sub>2</sub>, BINAP and cesium carbonate in toluene at 80 °C for 24 h to give DMAP analogue **98** in 49% yield. It should be noted that under the same conditions as used for the coupling of  $\beta$ -fluoroamines with 4-chlorocyclopentenopyridine (see chapter 5.2.4) the product was obtained as a racemate. Deprotonation  $\alpha$  to the sulfone using LDA in THF at -78°C followed by fluorination with NFSI gave the desired fluorosulfones **99** and **100** with a *d.r.* of 1:3.1 in 29% yield. The products were obtained in racemic form most likely due to opening of the pyrrolidine ring upon deprotonation.

Scheme 33: Synthesis of DMAP derived  $\alpha$ -fluorosulfones **99** and **100**.

### 5.3.3 Crystal Structures of Fluorinated and Non-Fluorinated Compounds 98-100.

The crystal structures of both diastereomers of DMAP derived  $\alpha$ -fluorosulfones **99** and **100**, as well as the corresponding non-fluorinated compound **98** are shown in Figure 16. The values of the dihedral angles of the sidechain are summarised in Table 10.

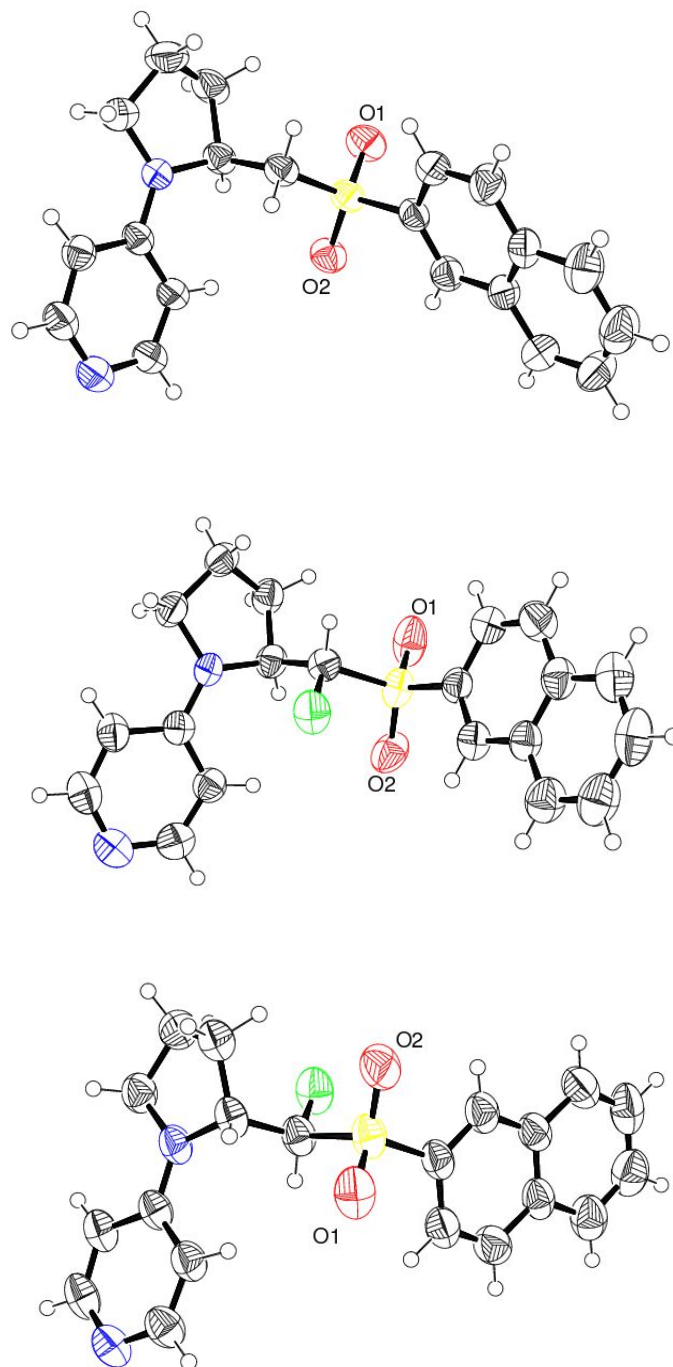


Figure 16: Crystal structures of fluorinated and non-fluorinated compounds **98-100**.

Table 11: Selected dihedral angles of sulfones **98-100**.

compound	$\Phi_{\text{NCCS}}$	$\Phi_{\text{NCCF}}$	$\Phi_{(\text{N})\text{CCSC}}$	$\Phi_{\text{O1SCCarom}}$	$\Phi_{\text{O2SCCarom}}$
non-fluorinated <b>98</b>	147.2° ( <i>anticlinal</i> )	--	-175.2° ( <i>antiperiplanar</i> )	68.4° ( <i>synclinal</i> )	16.8° ( <i>synperiplanar</i> )
fluorinated, major <b>100</b> <sup>a)</sup>	-155.7° ( <i>antiperiplanar</i> )	84.8° ( <i>synclinal-endo</i> )	178.8° ( <i>antiperiplanar</i> )	36.1° ( <i>synclinal</i> )	-12.2° ( <i>synperiplanar</i> )
fluorinated, minor <b>99</b>	156.1 ( <i>antiperiplanar</i> )	39.1° ( <i>synclinal-exo</i> )	176.2° ( <i>antiperiplanar</i> )	29.1° ( <i>synclinal</i> )	-19.7° ( <i>synperiplanar</i> )

<sup>a)</sup> crystal structure solved for other enantiomer (isomerised at C2 compared to **98** and **99**)

It can be seen that for both fluorinated structures the fluorine atom is placed in a *synclinal* position relative to the C-N bond (*endo* for the major diastereomer, *exo* for the minor diastereomer). As a consequence, the relative orientation of the C-N bond to the C-S bond is *antiperiplanar* for both diastereomers. Interestingly, in the nonfluorinated structure this angle is slightly smaller ( $\Phi_{\text{NCCS}} = 147.2^\circ$ , *anticlinal*). The sidechain [(N)CCSC] displays a zig-zag conformation for all compounds with torsion angles ( $\Phi_{(\text{N})\text{CCSC}}$ ) close to  $180^\circ$ . The orientation of the naphthyl group to the sulfonyl group suggests that for the fluorinated compounds the  $\pi$ -system is bisecting the  $\text{SO}_2$  group (represented by opposite signs of torsion angles  $\Phi_{\text{O1SCCarom}}$  and  $\Phi_{\text{O2SCCarom}}$ ). This is likely due to a hyperconjugative effect of the type  $\pi \rightarrow \pi_{\text{SO}_2}^*$ . In the nonfluorinated structure however, the naphthyl group is slightly rotated so that it is bisecting the sulfonyl group. This surprising observation can possibly be attributed to crystal packing forces. In conclusion, these results suggest that for DMAP derived fluorosulfones **98-100** in the neutral form the solid state conformation is not largely influenced by fluorination of the position  $\beta$  to the amine.

## 5.4 Conclusion and Outlook

In summary, the set of nucleophilic organocatalysts containing a  $\beta$ -fluoroamino motif was extended to include the class of DMAP derivatives. Using computational methods the expected conformational switch upon activation of the system (acetylation or protonation) was validated for the parent structure. Kinetic studies revealed a nucleophilicity parameter ( $N$ ) of 14.57 which is similar to the reported value for 4-pyrrolidinopyridine ( $N = 15.90$ )<sup>[68]</sup> showing that incorporation of a diphenylfluoromethyl substituent on the 2-position of the pyrrolidine moiety does not significantly lower the nucleophilicity. This was confirmed by the fact that all of the fluorinated compounds tested were capable of catalysing the acetylation of ( $\pm$ )-1-phenylethanol by acetic anhydride. The low selectivities in this kinetic resolution of the 1<sup>st</sup> generation catalysts (unsubstituted pyridine moiety) were attributed to insufficient control over the orientation of the acetyl group in the transient acylpyridinium salt. Therefore, a 2<sup>nd</sup> generation of fluorinated DMAP analogues were prepared which contained a cyclopentenopyridine entity for the introduction of conformational control by means of  $A^{1,3}$ -strain. These compounds proved to be competent acylation catalysts and led to increased selectivities in the kinetic resolution of ( $\pm$ )-1-phenylethanol (up to  $s = 3.17$ ).

Further studies of these systems may include the investigation of the somewhat surprising observation that for both catalyst generations the same enantiomer is favoured. Additionally, the system could be further refined by modifications of the cyclopentenopyridine moiety.

In addition, attempts to synthesise a  $C_2$ -symmetric difluorinated DMAP analogue were made including the synthesis of a corresponding secondary amine precursor and a direct photochemical approach.

Furthermore, DMAP derivatives containing an  $\alpha$ -fluorosulfone sidechain were synthesised in order to investigate the combination of two consecutive stereoelectronic effects. To that end, crystal structures of the non-fluorinated and the two diastereomers of the fluorinated analogues were obtained. The expected conformational preference of the fluorine atom to be in a *synclinal* position relative to the C-N bond was observed as well as an antiperiplanar arrangement of the C-F bond and one of the S=O double bonds of the sulfonyl group.

## 6 Halogenated Borondipyrromethenes (BODIPY)

### 6.1 Introduction

The characteristic  $C_2$ -symmetry of borondipyrromethene (BODIPY) derivatives, which includes two equivalent electron rich aromatic positions (C2 and C6) allows for simple derivatisation of the core structure.<sup>[76]</sup> A general structure of these compounds is shown in Figure 17.

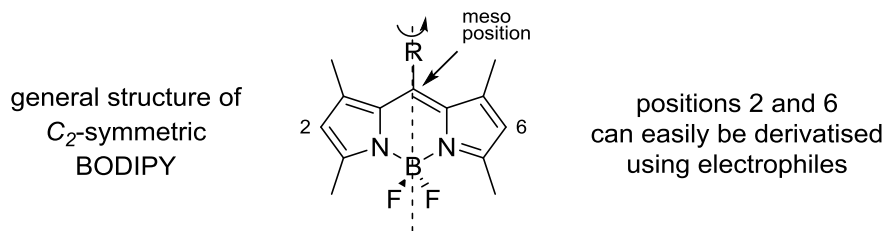
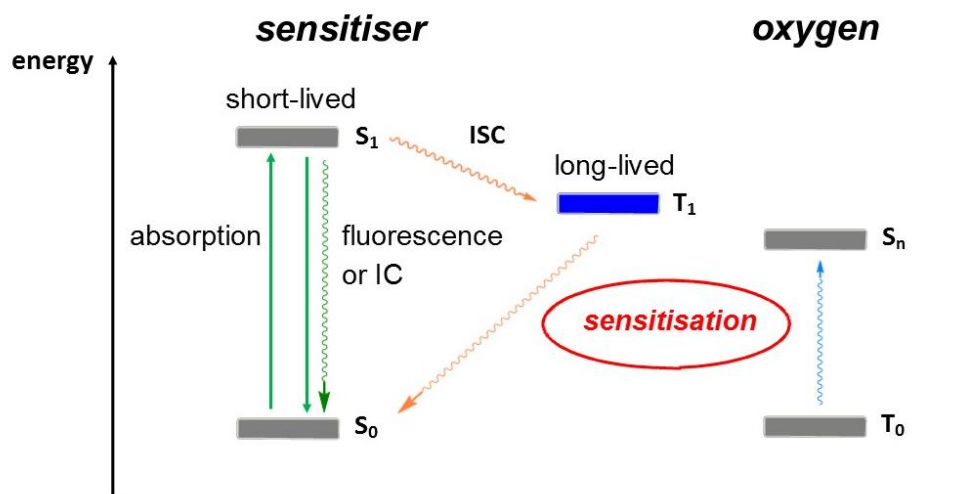


Figure 17: General BODIPY structure.

Halogenation by electrophilic aromatic substitution is facile allowing for the rapid generation of structures that can be further functionalised for example by transition metal catalysed coupling reactions.<sup>[77]</sup> Importantly, halogenated BODIPY structures are themselves highly interesting materials as they exhibit drastically altered photophysical behaviour in comparison to their non-halogenated parent structures: This is commonly referred to as the heavy atom effect.<sup>[37]</sup> Photophysical and photochemical processes are usually described by a Jablonski diagram, which schematically shows the different electronic (and vibrational) states of the compound of interest as well as the possible transitions between these states. As can be seen in Scheme 34 BODIPY structures, as most organic compounds, possess a singlet ground state ( $S_0$ ). Upon irradiation with light of suitable wavelength the molecule can undergo an electronic transition to the first excited singlet state ( $S_1$ ). The probability in doing so is reflected in the absorption coefficient ( $\epsilon$ ). From the  $S_1$  state there are multiple deactivation pathways: The system can reemit a photon (fluorescence) or be converted to a vibrationally excited state of  $S_0$  (internal conversion, IC) which then quickly dissipates its energy by interaction with solvent molecules. These two processes do not involve a change in spin state (singlet-singlet). However, a radiationless transition to the lowest excited triplet state ( $T_1$ ) is also possible which is denoted as Intersystem Crossing (ISC). At first sight such a transition violates the law of conservation of momentum and is therefore a forbidden process. However, in cases where the spin magnetic moment ( $\mu_s$ ) of the electron that undergoes spin inversion is



strongly coupled with its orbital magnetic moment ( $\mu_L$ ), the flip of the spin can be compensated by a change in orbital magnetic momentum.



Scheme 34: Jablonski diagram describing the photosensitised generation of singlet oxygen ( $^1O_2$ ).

Thus, when spin-orbit coupling is strong the total momentum can be conserved even during processes such as ISC. The magnitude of spin-orbit coupling can be calculated by eq. (4):<sup>[36]</sup>

$$E_{SO} = \langle \psi_{S_1} | \hat{H}_{SO} | \psi_{T_1} \rangle \propto \langle \psi_{S_1} | \xi_{SO} \mu_S \mu_L | \psi_{T_1} \rangle \quad (4)$$

From this equation it can be deduced that spin-orbit coupling depends on the magnetic momenta  $\mu_s$  and  $\mu_L$  as well as on the spin-orbit coupling constant  $\xi_{SO}$ , which increases with the atomic number. Consequently, it can be concluded that when heavy atoms are present, spin-orbit coupling will be larger and therefore ISC is expected to be faster. Therefore, the ability of elements with high atomic numbers to promote ISC has been termed the ‘‘heavy atom effect’’.<sup>[36]</sup> This phenomenon can occur when the heavy atom is covalently bound to the chromophore (internal heavy atom effect) but also, albeit in weaker form, when the heavy atom is simply in proximity to the excited molecule (external heavy atom effect). Both effects have been applied in organic photochemistry.<sup>[37]</sup> The efficient population of a chromophore’s triplet state is of high importance for photochemistry as it generally has a comparatively high lifetime that allows for slow processes such as energy- and electron transfer to occur. A common energy acceptor is ground state oxygen ( $^3O_2$ ) which can be excited to its singlet state ( $^1O_2$ ) by energy transfer, a process known as photosensitisation of oxygen. Molecular orbital

diagrams for ground state oxygen together with the two lowest lying electronically excited states is shown in Figure 18.

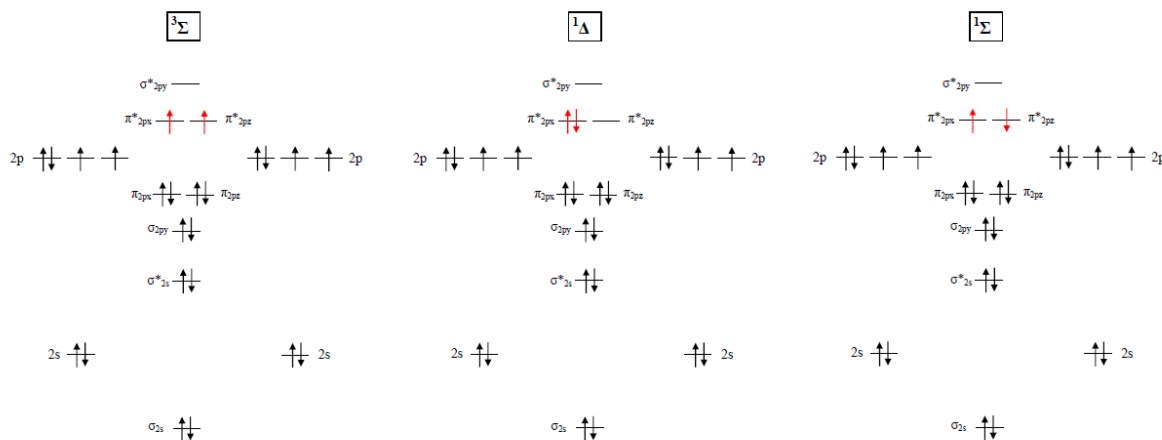
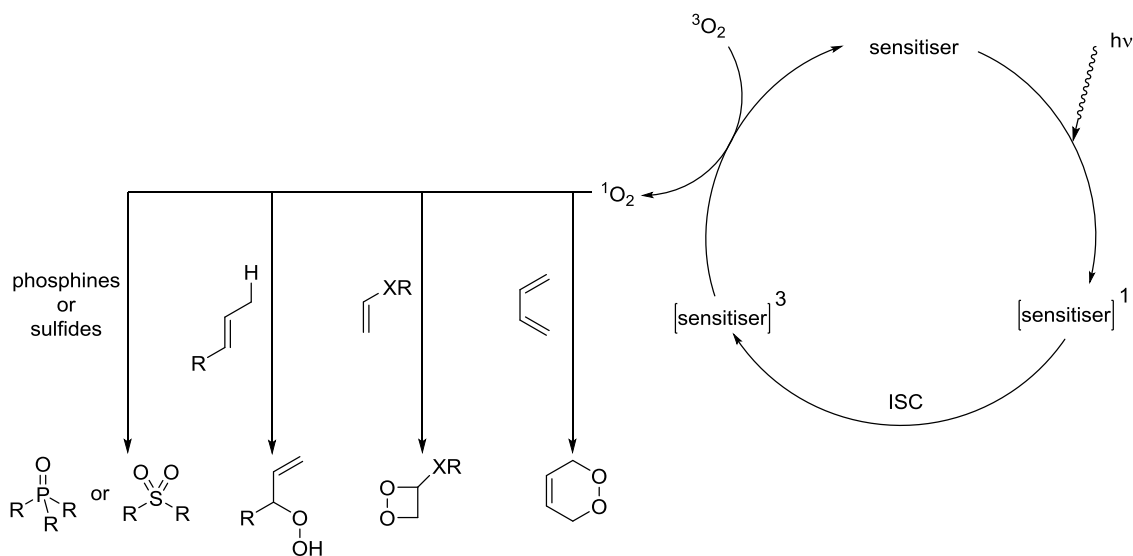


Figure 18: MO diagrams for oxygen in the ground state (left,  $^3\Sigma$ ) and its two lowest lying electronically excited singlet states (centre, right,  $^1\Delta$ ,  $^1\Sigma$ ).

From Figure 18 it is evident that the ground state is a triplet, and the two first excited states are singlet states. These two states are denoted  $^1\Delta$  and  $^1\Sigma$  and have been reported to lie  $22.4 \text{ kcal}\cdot\text{mol}^{-1}$  and  $37.5 \text{ kcal}\cdot\text{mol}^{-1}$ , respectively above the ground state.<sup>[36]</sup> According to Hund's second rule (maximisation of orbital angular momentum) the  $^1\Delta$ -state is energetically favoured compared to the  $^1\Sigma$ -state. Considering that sensitizers are known with triplet energies of more than  $37.5 \text{ kcal}\cdot\text{mol}^{-1}$ <sup>[78]</sup> population of the  $^1\Sigma$ -state is feasible. However, according to Kasha's rule<sup>[36]</sup> internal conversion from high lying excited states to the lowest excited state is usually extremely fast and therefore the photochemically relevant singlet state of oxygen is the  $^1\Delta$ -state. Singlet oxygen as a highly reactive species has found wide application in synthetic organic chemistry.

As shown in Scheme 35 common reactions are [4+2]- and [2+2]-cycloadditions as well as oxidations of heteroatoms and ene-reactions (known as the Schenck-Ene reaction).<sup>[79][80]</sup>



Scheme 35: Generalised, photosensitised singlet oxygen ( $^1\text{O}_2$ ) generation and selected application in synthetic organic chemistry.

Unsurprisingly, a variety of sensitizer structures that efficiently generate singlet oxygen have been discovered and applied in organic chemistry. The most prominent examples, namely tetraphenylporphyrine (TPP), methylene blue and rose bengal are shown in Figure 19.<sup>[79]</sup> It is interesting to note that iodinated BODIPY structures make use of the heavy atom effect in the same way as rose bengal does. Moreover BODIPY and TPP bear a close structural resemblance, suggesting that the pyrromethane moiety is privileged in sensitizer design.

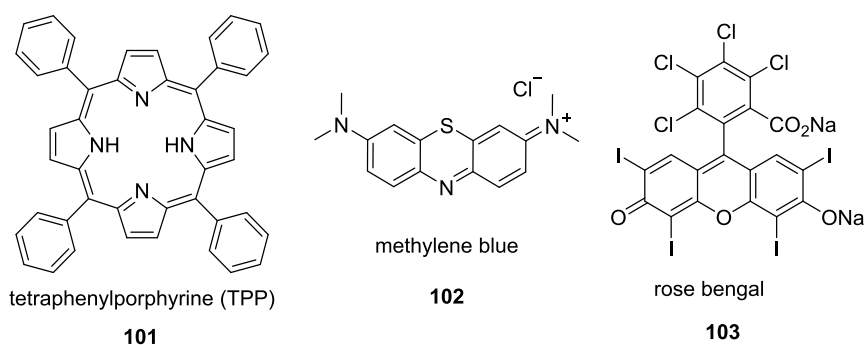
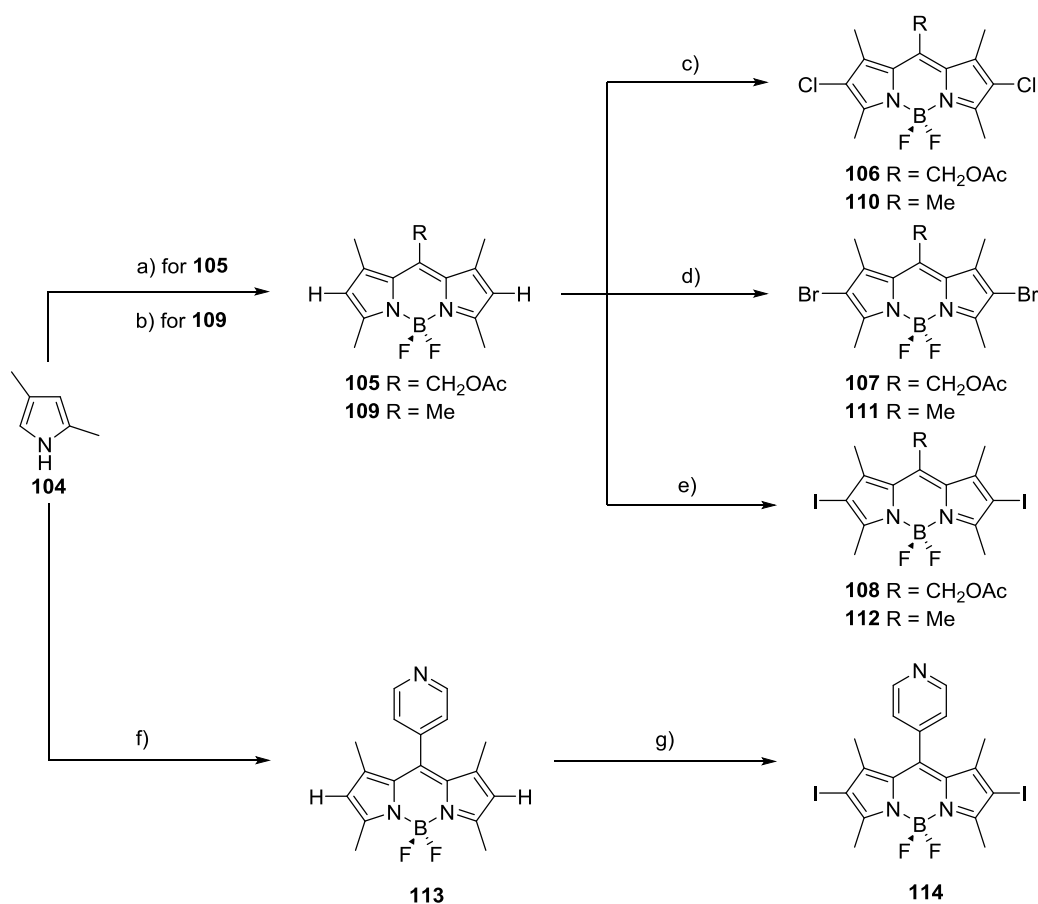


Figure 19: Structure of commonly used photosensitizers for the generation of singlet oxygen.

## 6.2 Investigation of The Internal Heavy Atom Effect in Singlet Oxygen Generation

### 6.2.1 Synthesis of BODIPY Derived Sensitisers

In order to investigate the internal heavy atom effect in the photosensitised singlet oxygen generation, three different BODIPY structures were synthesised following known one step procedures from 2,4-dimethylpyrrole (**104**) and the corresponding carbonyl compound. Subsequent halogenation of the 2- and 6- position was carried out using either iodic acid and iodine in EtOH (for iodination on large scale of compounds **108** and **112**) or NCS, NBS and NIS in 1,1,1,3,3,3-hexafluoroisopropanol for the chloro, bromo or iodo systems, respectively (Scheme 36).<sup>[76][81][82]</sup>

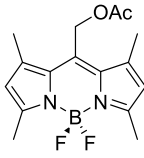
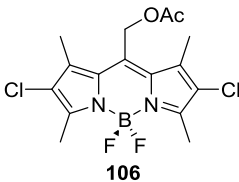
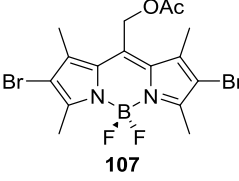
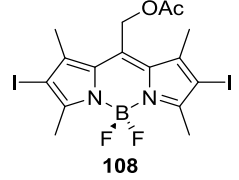
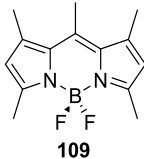
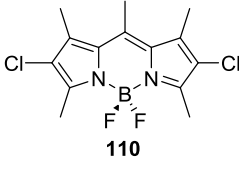


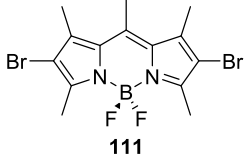
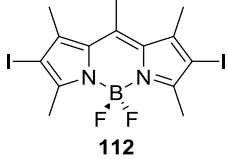
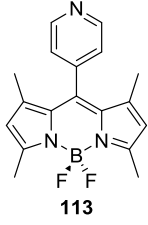
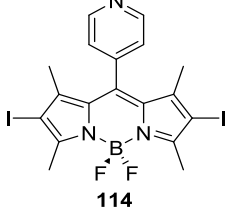
Scheme 36: Synthesis of the BODIPY derived sensitizers: a) i) acetoxyacetyl chloride, CH<sub>2</sub>Cl<sub>2</sub> ii) DIPEA iii) BF<sub>3</sub>•OEt<sub>2</sub>, 10%; b) i) acetyl chloride, CH<sub>2</sub>Cl<sub>2</sub> ii) DIPEA iii) BF<sub>3</sub>•OEt<sub>2</sub>, 26%; c) NCS, HFIP, 71% for R = OAc, 55% for R = Me; d) NBS, HFIP, 51% for R = OAc, 42% for R = Me; e) HIO<sub>3</sub>, I<sub>2</sub>, EtOH, 74% for R = OAc, 84% for R = Me; f) i) 4-pyridinecarboxaldehyde, TFA, CH<sub>2</sub>Cl<sub>2</sub> ii) DDQ, iii) NEt<sub>3</sub>, iv) BF<sub>3</sub>•OEt<sub>2</sub>, 13%; e) NIS, HFIP, 94%.

### 6.2.2 UV-visible Spectra of the Synthesised Compounds 105-114

In order to compare the absorption properties of the chromophores **105-114**, UV-vis spectra of all the synthesised compounds were recorded at a concentration of 10  $\mu\text{M}$  in chloroform. In particular, the absorption maximum ( $\lambda_{\text{max}}$ ), the absorption coefficient at  $\lambda_{\text{max}}$  ( $\epsilon_{\text{max}}$ ) and the area between 390 nm and 700 nm ( $A_{390-700\text{nm}}$ ) were determined. The latter two are baseline corrected. The results are summarised in Table 12:

Table 12: Absorption characteristics of the synthesised BODIPY derivatives.

entry	compound	$\lambda_{\text{max}}$ (nm)	$\epsilon_{\text{max}}(\text{M}^{-1}\cdot\text{cm}^{-1})$	$A_{390-700\text{nm}}(\text{nm})$
1	 <b>105</b>	522	94000	29.1
2	 <b>106</b>	553	95000	43.6
3	 <b>107</b>	554	106000	47.6
4	 <b>108</b>	561	103000	49.8
5	 <b>109</b>	498	98000	25.5
6	 <b>110</b>	525	81000	29.1

7	 <b>111</b>	525	94000	33.3
8	 <b>112</b>	530	96000	36.3
9	 <b>113</b>	506	101000	28.8
10	 <b>114</b>	542	78000	32.6

In general, by changing the substituents at the 2- and 6- positions from H to Cl to Br to I, a bathochromic shift of  $\lambda_{\max}$  was observed. This trend, as well as the small difference between the chlorinated and the brominated species, is in good agreement with the  $\pi$ -donor strength of halogens (Hammett-parameters:  $\sigma_{\text{p,Cl}} = \sigma_{\text{p,Br}} = 0.32 > \sigma_{\text{p,I}} = 0.18$ ).<sup>[83]</sup> The largest effect upon iodination can be seen for the acetoxyated compounds **105** and **108** where a shift of 39 nm was found (entries 1 and 4), followed by the pyridine derivatives **113** and **114** ( $\Delta\lambda_{\max} = 36$  nm, entries 9 and 10) and the methylated compounds **109** and **112** ( $\Delta\lambda_{\max} = 32$  nm, entries 5 and 8). The absorption coefficients ( $\epsilon_{\max}$ ) ranged from 78000  $\text{M}^{-1}\cdot\text{cm}^{-1}$  for compound **114** (entry 10) to 106000  $\text{M}^{-1}\cdot\text{cm}^{-1}$  for compound **107** (entry 3). The fact that the absorption maxima for the pyridine substituted derivatives lie between those of the corresponding methylated and acetoxyated analogues suggests that the aromatic substituent is twisted out of conjugation due to steric interaction with the methyl groups on position 1 and 7. By comparing the absorption coefficients with the areas between 390 nm and 700 nm it becomes clear that no correlation can be drawn. Therefore, the relative total absorption of the compounds can not be deduced from  $\epsilon_{\max}$  even though the spectra are very similar. The UV-vis spectra are shown in Figure 20, Figure 21 and Figure 22.

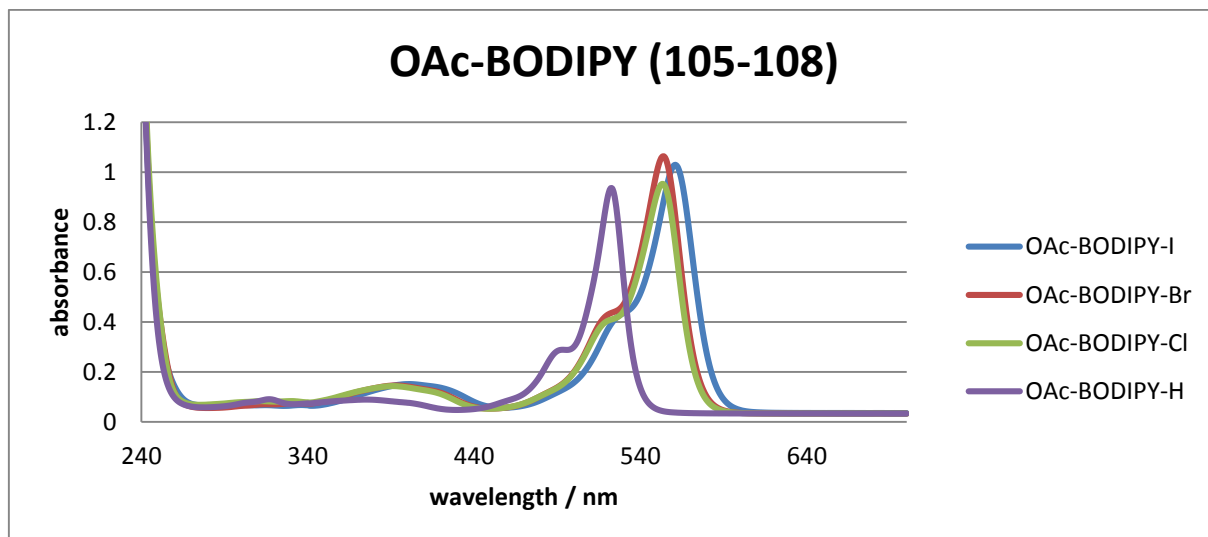


Figure 20: Overlaid UV-vis spectra of compounds **105-108**.

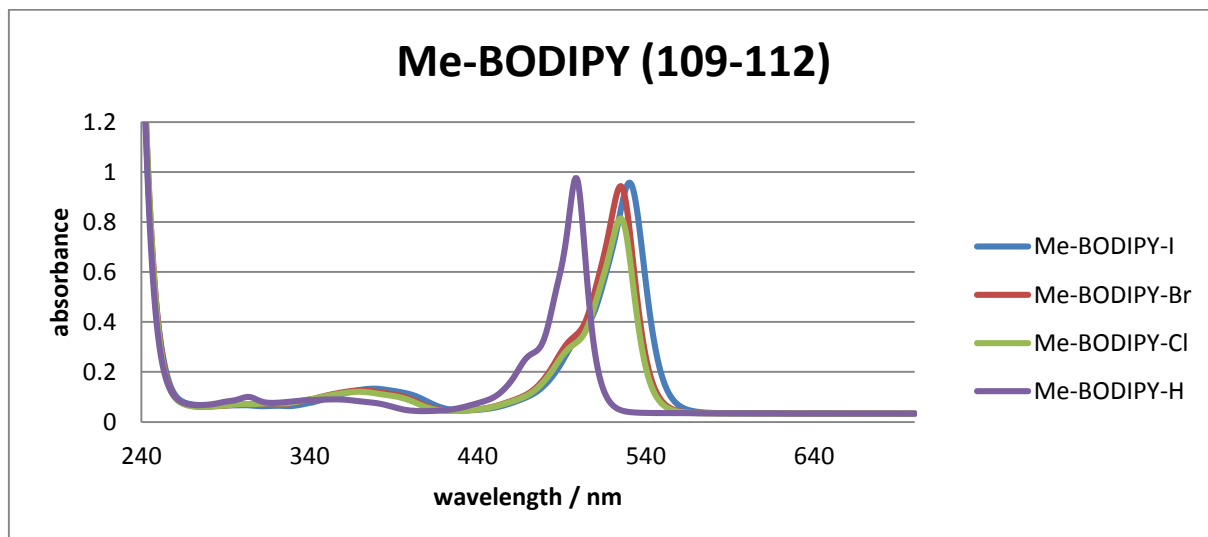


Figure 21: Overlaid UV-vis spectra of compounds **109-112**.

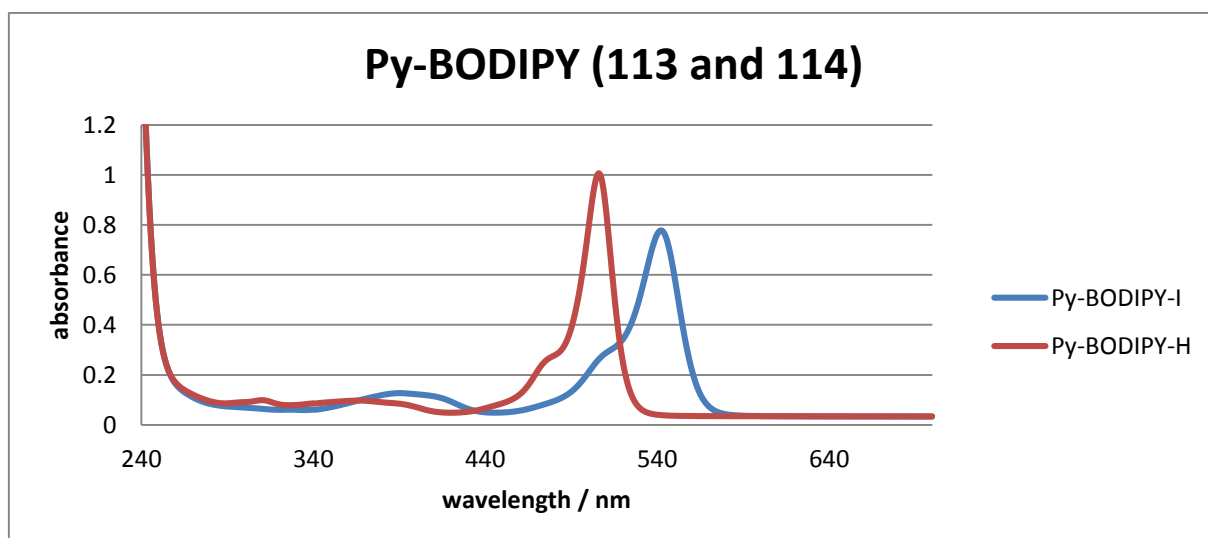


Figure 22: Overlaid UV-vis spectra of compounds **113 and 114**.

The main absorbance in the visible region (~ 430 nm – 800 nm) is attributed to the transition to the first excited singlet state ( $S_0 \rightarrow S_1$ ;  $\pi \rightarrow \pi^*$ ) and the broad peak around 400 nm corresponds to a transition to the second excited singlet state ( $S_0 \rightarrow S_2$ ).<sup>[84][85]</sup> The shoulder on the main absorption band is due to an excitation to a higher vibrational level of  $S_1$  (out of plane vibration).

### 6.2.3 Application of Compound **108** in the Schenck-Ene Reaction

Initially, in order to test the potential of compound **108** as sensitizers in the Schenck-Ene reaction, cyclopentene (**115**) was chosen as substrate as it was known to efficiently react with singlet oxygen.<sup>[86]</sup> The resulting allylic hydroperoxide (**116**) was subsequently reduced to the allylic alcohol (**117**) by washing the solution with an aqueous solution of  $\text{Na}_2\text{S}_2\text{O}_3$ . The reaction sequence is shown in Figure 23. All reactions were performed on a 3.00 mmol scale (204 mg of cyclopentene).

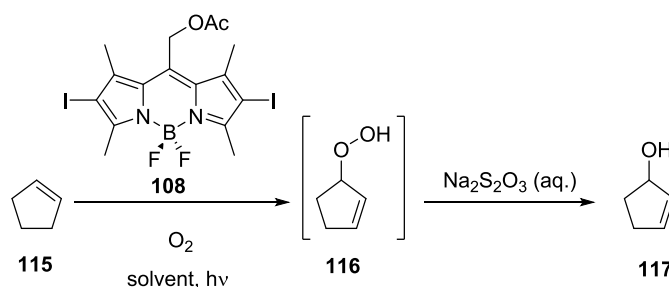


Figure 23: Schenck-Ene reaction of cyclopentene followed by reduction to the allylic alcohol.

Due to very sluggish conversion under an air atmosphere, various methods of running the reaction under a pure oxygen atmosphere were investigated: Method A involved the formation of oxygen by dropwise addition of  $\text{H}_2\text{O}_2$  (aq., 30% w/w) to an aqueous suspension of  $\text{MnO}_2$  to generate oxygen *in situ* which was introduced into the reaction solution by means of a cannula (Figure 24, left).

This constitutes an operationally simple method for generating an oxygen atmosphere without the need for compressed oxygen. As can be seen from Table 13 this method delivered the desired product after 45 h with a catalyst loading of 1 mol% and at a concentration of 1.0 M in  $\text{CDCl}_3$  (entry 1). Unsatisfied with this rather long reaction time, a more conventional method in which oxygen was bubbled through the reaction from a compressed oxygen bottle directly was investigated (Figure 24, middle). This led to significantly reduced reaction times (13 h, entry 2). Gratifyingly, only 0.1 mol% catalyst loading led to quantitative conversion (entry 3).



However, it should be noted that the oxygen flow is difficult to adjust, and that this protocol resulted in the loss of solvent and the volatile starting material. Changing to a solvent with a lower vapour pressure, such as deuterated toluene led to a slower reaction (76% conversion after 13 h, entry 4). When the transformation was simply carried out without bubbling oxygen through the solution (method C, Figure 24, right) the reaction time increased significantly (compare entry 5 with entry 3). The concentration was therefore increased to 10 M in order to reach similar reaction times as with method C. Due to potential hazards of concentrated solutions of hydroperoxides and the general difficulties of isolation of the product due to its volatility a substrate with a higher boiling point was investigated.

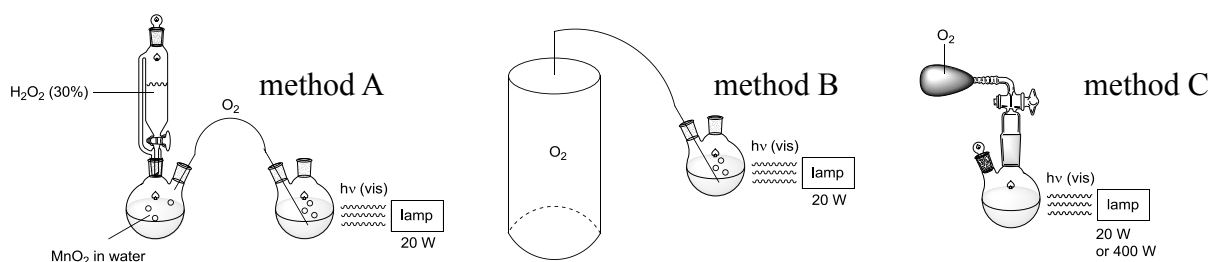


Figure 24: The experimental setups for the Schenk-Ene reaction with cyclopentene.

Table 13: Schenk-Ene reaction with cyclopentene.

entry	method	cat. loading	solvent	conc.	time to full conv. (oxidation)
1	A	1.0 mol%	$\text{CDCl}_3$	1.0 M	45 h
2	B	1.0 mol%	$\text{CDCl}_3$	1.0 M	13 h
3	B	0.1 mol%	$\text{CDCl}_3$	1.0 M	13 h
4	B	0.1 mol%	toluene- $\text{D}_8$	1.0 M	> 13 h <sup>a)</sup>
5	C (20W)	0.1 mol%	$\text{CDCl}_3$	1.0 M	66 h
6	C (20W)	0.1 mol%	$\text{CDCl}_3$	10 M	13.5 h

<sup>a)</sup> 76% conversion after 13 h.

### 6.2.4 Investigating (-)- $\beta$ -Pinene as a Substrate in the Schenck-Ene Reaction

As a less volatile substrate, (-)- $\beta$ -pinene (**118**) seemed well suited to this investigation. Not only is its vapour pressure low (3.35 mmHg at 299.97 K)<sup>[87]</sup> but only one regioisomer is formed on account of Bredt's Rule. Moreover, no diastereomers are formed in this transformation.<sup>[88]</sup> The reaction conditions are shown in Figure 25.

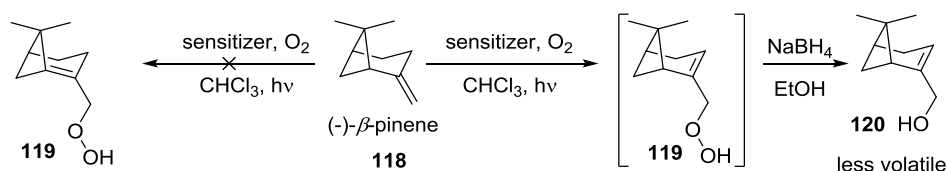
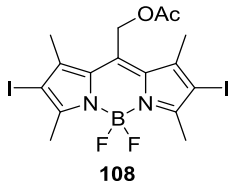
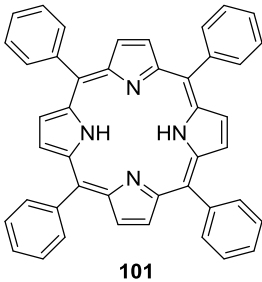
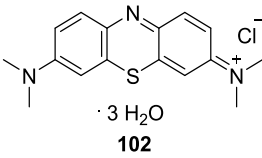
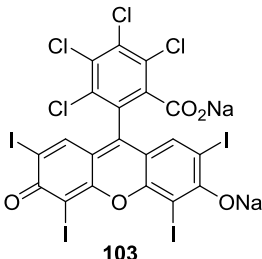
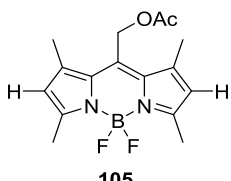


Figure 25: Schenck-Ene reaction of (-)- $\beta$ -pinene.

The reactions were carried out using method C (see chapter 6.2.3) with a 400 W halogen lamp (at a distance of 20 cm) in  $\text{CHCl}_3$ . As a consequence of the higher power of the light source the reaction mixtures were heated to  $36^\circ\text{C}$ . As is shown in Table 14, when using 1.0 mol% of sensitizer at a concentration of 2.1 M full conversion was reached after 8 h (Table 14, entry 1). Upon reduction with  $\text{NaBH}_4$  in  $\text{EtOH}$  the desired allylic alcohol **120** could be isolated in 64% yield with minor impurities. This result was then compared with the reaction promoted by the well established sensitizers tetraphenylporphyrin (TPP), methylene blue and rose bengal. GC analysis showed 98% conversion after 8 h when using TPP (entry 2) which showcased the high efficiency of sensitizer **108** in the generation of singlet oxygen. A significant decrease in conversion after 8 h was observed in the methylene blue sensitised reaction (24%, entry 3). The low conversion when using rose bengal (3% after 6 h, entry 4) can probably be attributed to the low solubility of the sensitizer in  $\text{CHCl}_3$ . As expected, when sensitizer **105** was employed (which lacks the iodine atoms on the 2- and 6-position), low conversion was observed after 6 h (2%, entry 5) which is likely due to inefficient ISC (see chapter 6.1). Although these initial results were promising, the low yield (which may be due to further oxidation of the allylic hydroperoxide **119**) required a second reaction to be explored in order to validate this first data set and to compare the efficiency of the different sensitizers more accurately. To that end the well documented [4+2] addition of singlet oxygen with anthracene (**121**) was investigated.<sup>[89]</sup>

## Halogenated Borondipyrromethenes (BODIPY)

Table 14: The Schenck-Ene reaction with (-)- $\beta$ -pinene using different sensitisers.

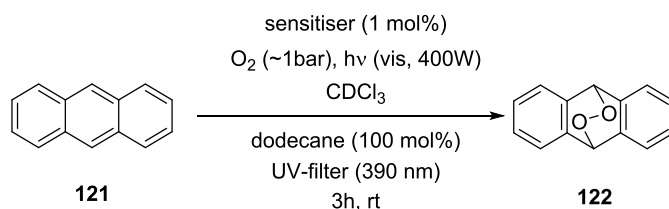
entry	sensitiser	method	sensitiser loading	concentration	conversion <sup>b)</sup>
1	 <p style="text-align: center;"><b>108</b></p>	C (400 W) <sup>a)</sup>	1.0 mol%	2.1 M	full (8 h) <sup>c)</sup>
2	 <p style="text-align: center;"><b>101</b> tetraphenylporphyrin (TPP)</p>	C (400 W) <sup>a)</sup>	1.0 mol%	2.1 M	98% (8 h)
3	 <p style="text-align: center;"><b>102</b> methylene blue</p>	C (400 W) <sup>a)</sup>	1.0 mol%	2.1 M	24% (8 h)
4	 <p style="text-align: center;"><b>103</b> rose bengal</p>	C (400 W) <sup>a)</sup>	1.0 mol%	2.1 M	3% (6 h)
5	 <p style="text-align: center;"><b>105</b></p>	C (400 W) <sup>a)</sup>	1.0 mol%	2.1 M	2% (6 h)

<sup>a)</sup> see chapter 6.2.3; <sup>b)</sup> conversion to the hydroperoxide determined by GC, non-corrected;

<sup>c)</sup> myrtenol isolated in 64% yield.

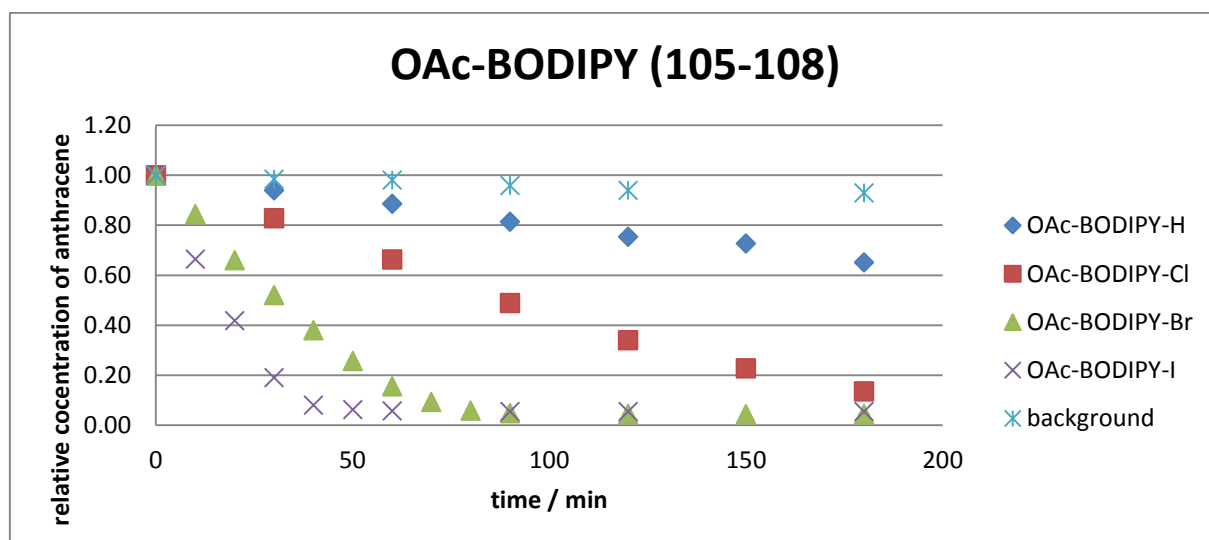
### 6.2.5 Application of the Acetoxyated BODIPY Sensitisers in the Photosensitised Oxidation of Anthracene

In order to compare the efficiency of the various BODIPY structures in the generation of singlet oxygen, a method to follow the reactions using a simple setup which ideally could be performed without any special equipment or UV-vis spectrometer was desirable. To that end, the well known [4+2]-cycloaddition of singlet oxygen and anthracene was chosen due to the high efficiency, the formation of a single product, only and the possibility of analysis by gas chromatography.<sup>[89]</sup> Deuterated chloroform was the solvent of choice as it does not contain any C-H bonds which deactivate singlet oxygen<sup>[36]</sup> anthracene (**121**) and all of the BODIPY sensitiser display solubility. Irradiation was conducted using a 400 W halogen lamp at a distance of 30 cm to prevent heating of the reaction mixture and a UV-filter (cut-off at 390 nm) was placed in front of the solution in order to minimise sensitisation of oxygen by the substrate.<sup>[90]</sup> All reactions were irradiated for 3 h under an oxygen atmosphere and at a concentration of 0.1 M with respect to anthracene (100  $\mu\text{mol}$  scale using 1 mol% of sensitiser). Dodecane (100  $\mu\text{mol}$ ) was added as an internal standard prior to irradiation for accurate determination of the conversion by GC. Aliquots were taken in regular time intervals and the conversion was determined by gas chromatography. The conditions are summarised in Scheme 37.



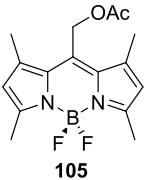
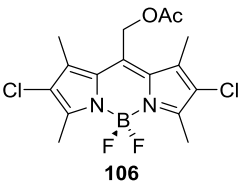
Scheme 37: Conditions of the model reaction: oxidation of anthracene to its endoperoxide **122** with singlet oxygen.

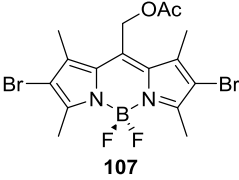
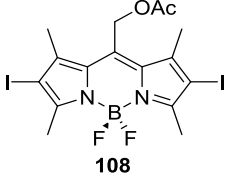
Interestingly, in all reactions a linear dependence of the conversion and reaction time was observed, up to well over 50% conversion. This allowed for facile determination and comparison of the initial reaction rate constant ( $k^{\text{ini}}$ ) for all transformations. The consumption of anthracene over time under these conditions with structures **105-108** is shown in Figure 26.

Figure 26: Consumption of anthracene over time with structures **105-108** as sensitisers.

A clear dependence of the initial rates on the substituents on the 2- and 6-positions is observed: As expected the heavier the substituent the faster the reaction. The conversion in the absence of any sensitiser was also measured as a control (background). In order to compare the reaction rates quantitatively the initial rates (over the linear part) of each reaction was determined as well as the conversion after 30 min of irradiation. The results are summarised in Table 15.

Table 15: Dependence of the initial rate, conversion after 30 min and isolated yield of the product using OAc-derived sensitisers **105-108**.

entry	sensitiser	initial rate ( $\mu\text{M}\cdot\text{s}^{-1}$ )	conversion after 30 min	isolated yield
1	none	0.7	1%	n.d.
2		3.2	6%	20%
3		9.2	17%	84%

4	 107	26.0	48%	79%
5	 108	44.6	81%	82%

The background reaction (entry 1) shows only minimal conversion with an initial rate of  $0.7 \mu\text{M}\cdot\text{s}^{-1}$ . The fact that it still derives from zero could be due to some absorbance of anthracene above 390 nm that would allow for autoxidation; it is known that anthracene can generate singlet oxygen when irradiated with UV-light.<sup>[90]</sup> By comparing the background reaction with the one catalysed by parent compound **105** (entries 1 and 2) it is clear that even without any heavy atoms on the 2- and 6- position this BODIPY structure is able to generate singlet oxygen. Upon addition of catalyst structure **105**, a clear increase in the initial rate ( $3.2 \mu\text{M}\cdot\text{s}^{-1}$  vs.  $0.7 \mu\text{M}\cdot\text{s}^{-1}$ ) was observed. As expected, upon halogenation the reaction rates increased in the order  $\text{Cl} < \text{Br} < \text{I}$ , consistent with an internal heavy atom effect (entries 3-5;  $9.2 \mu\text{M}\cdot\text{s}^{-1}$ ,  $26.0 \mu\text{M}\cdot\text{s}^{-1}$  and  $44.6 \mu\text{M}\cdot\text{s}^{-1}$ , respectively). Overall, upon iodination an increase of the initial rate from  $3.2 \mu\text{M}\cdot\text{s}^{-1}$  to  $44.6 \mu\text{M}\cdot\text{s}^{-1}$  ( $\Delta k_{\text{H-I}}^{\text{ini}} = 41.4 \mu\text{M}\cdot\text{s}^{-1}$ ) was observed.

### 6.2.6 Application of the Methylated BODIPY Sensitisers in the Photosensitised Oxidation of Anthracene

In order to investigate the effect of the OAc-group on the *meso*-position of the sensitizer on the performance in the anthracene oxidation, the title reaction was performed using compounds **109-112** under identical conditions to those described in chapter 6.2.5. The decay of the anthracene signal over time for the reactions with the structures **109-112** is illustrated in Figure 27 and the obtained initial rate constants, conversions after 30 min and isolated yields are summarised in Table 16.

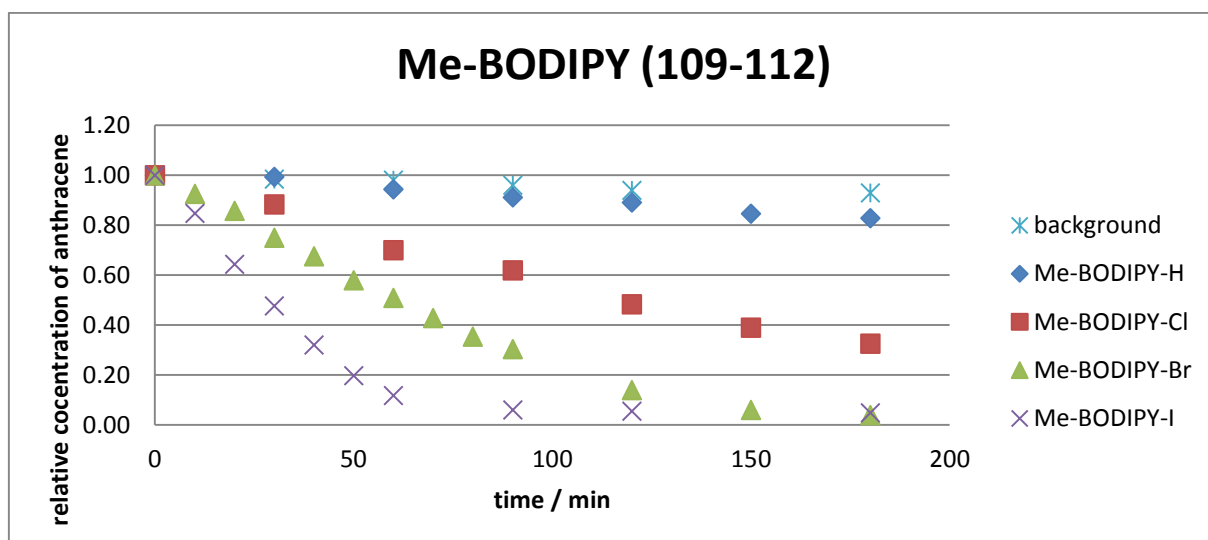

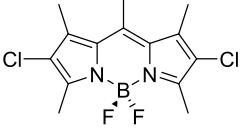
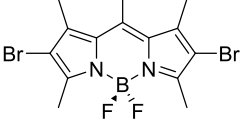
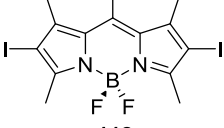

 Figure 27: Consumption of anthracene over time with structures **109-112** as sensitisers.

Table 16: Dependence of the initial rate, conversion after 30 min and isolated yield using the methylated sensitisers.

entry	sensitiser	initial rate ( $\mu\text{M}\cdot\text{s}^{-1}$ )	conversion after 30 min	isolated yield
1	none	0.7	1%	n.d.
2	 <b>109</b>	1.7	1%	14%
3	 <b>110</b>	7.2	12%	53%
4	 <b>111</b>	13.7	25%	71%
5	 <b>112</b>	28.8	52%	77%

Clearly, the expected dependence of the initial rate constants on the halogen substituents ( $\text{Cl} < \text{Br} < \text{I}$ ) is also observed with the methyl-derived sensitisers (entries 3-5,  $7.2 \mu\text{M}\cdot\text{s}^{-1}$ ,

13.7  $\mu\text{M}\cdot\text{s}^{-1}$  and 28.8  $\mu\text{M}\cdot\text{s}^{-1}$ , respectively). Importantly, the nonhalogenated sensitizer **109** accelerated the reaction compared to the background reaction by a factor of about 2.5 (entries 1 and 2, 0.7  $\mu\text{M}\cdot\text{s}^{-1}$  vs. 1.7  $\mu\text{M}\cdot\text{s}^{-1}$ ). In this case a smaller rate enhancement was observed upon iodination of the parent structure **109** ( $\Delta k_{\text{H-I}}^{\text{ini}} = 27.1 \mu\text{M}\cdot\text{s}^{-1}$  (compared to 41.4  $\mu\text{M}\cdot\text{s}^{-1}$  for the acetylated structures). In general, a poorer performance of the sensitizers **109-112** compared to their acetoxyated analogues **105-108** was observed.

### 6.2.7 Application of the Pyridine Derived BODIPY Sensitizers in the Photosensitized Oxidation of Anthracene

According to the report of Caruso et al.<sup>[91]</sup> BODIPY structure **114** with a 4-pyridyl substituent on the *meso*-position is a highly efficient singlet oxygen generator. For this reason compounds **113** and **114** were also prepared and evaluated in the title reaction. A graph of the conversion against time for compounds **113** and **114** as well as for **108** and **112** for comparison are shown in Figure 28.

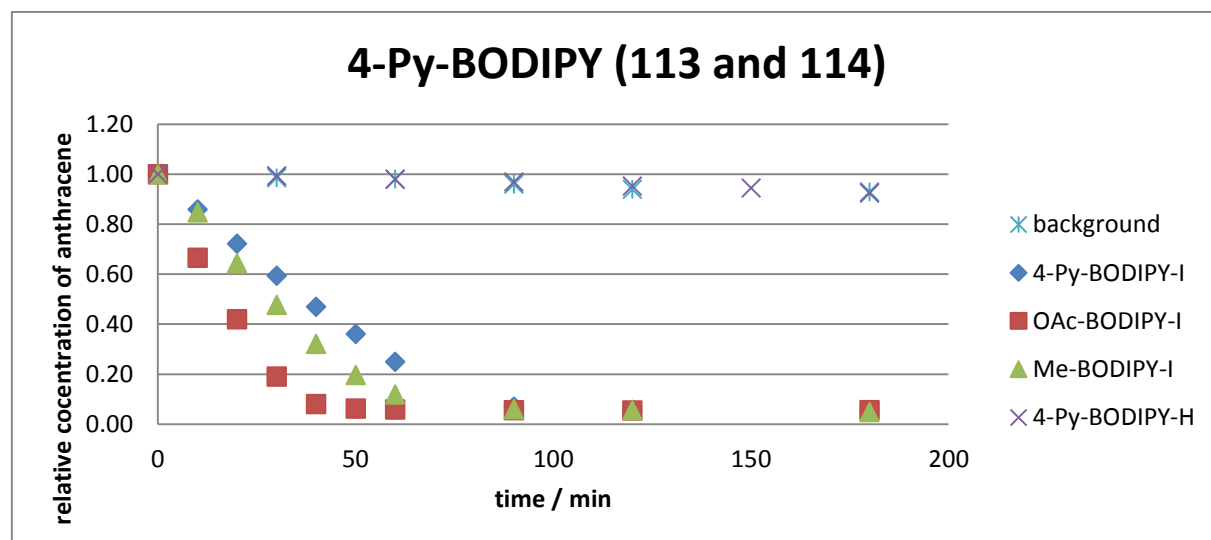


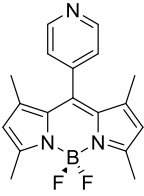
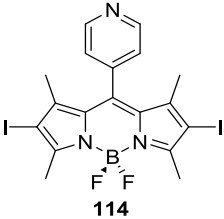
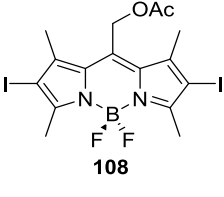
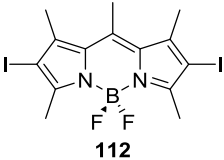
Figure 28: Consumption of anthracene over time with structures **108** and **112-114** as sensitizers.

Surprisingly, the non-halogenated derivative **113** closely mirrored the initial rate behaviour as the background reaction and can therefore be assumed to be unable to generate singlet oxygen. Although this clearly changes upon iodination, compound **114** led to the lowest initial rate of the investigated iodinated sensitizers. The results for compounds **108** and **112-114** are shown in Table 17.



*Halogenated Borondipyrromethenes (BODIPY)*

Table 17: Dependence of the initial rate, conversion after 30 min and isolated yield of the product using the 4-Py-derived sensitiser **113** and **114** along with compounds **108** and **112**.

entry	sensitiser	initial rate ( $\mu\text{M}\cdot\text{s}^{-1}$ )	conversion after 30 min	isolated yield
1	none	0.7	1%	n.d.
2	 <b>113</b>	0.7	1%	6%
3	 <b>114</b>	22.1	41%	80%
4	 <b>108</b>	44.6	81%	82%
5	 <b>112</b>	28.8	52%	77%

By comparing entries 2 and 3 it can be seen that in the case of the 4-pyridine derived sensitiser iodination leads to an increase of the initial rate from  $0.7 \mu\text{M}\cdot\text{s}^{-1}$  to  $22.1 \mu\text{M}\cdot\text{s}^{-1}$  ( $\Delta k_{\text{H-I}}^{\text{ini}} = 21.4 \mu\text{M}\cdot\text{s}^{-1}$ ) which is the smallest increase of this study.

### 6.2.8 Correlation of the Initial Rates with the Spin Orbit Coupling Constants

As mentioned in chapter 6.1 the heavy atom effect can be quantified by the spin orbit coupling constants ( $\xi$ ). The values for hydrogen, chlorine, bromine and iodine are given in Table 18.<sup>[36]</sup>

Table 18: Spin orbit coupling constants for hydrogen, chlorine, bromine and iodine.<sup>[36]</sup>

element	atomic number	spin orbit coupling constant $\xi$ (kcal•mol <sup>-1</sup> )
Hydrogen	1	<0.1
Chlorine	17	2
Bromine	35	7
Iodine	53	14

As the initial rates do not only depend on the rate of intersystem crossing but also on the efficiency of absorption in the region of irradiation (i.e. 390 nm-700 nm) they were divided by the integrated absorption spectrum  $A_{390-700\text{ nm}}$  in order to obtain a more accurate parameter for the effect of the substituents. The obtained values were then plotted against the spin orbit coupling constants  $\xi$ . The resulting graphs are shown in Figure 29.

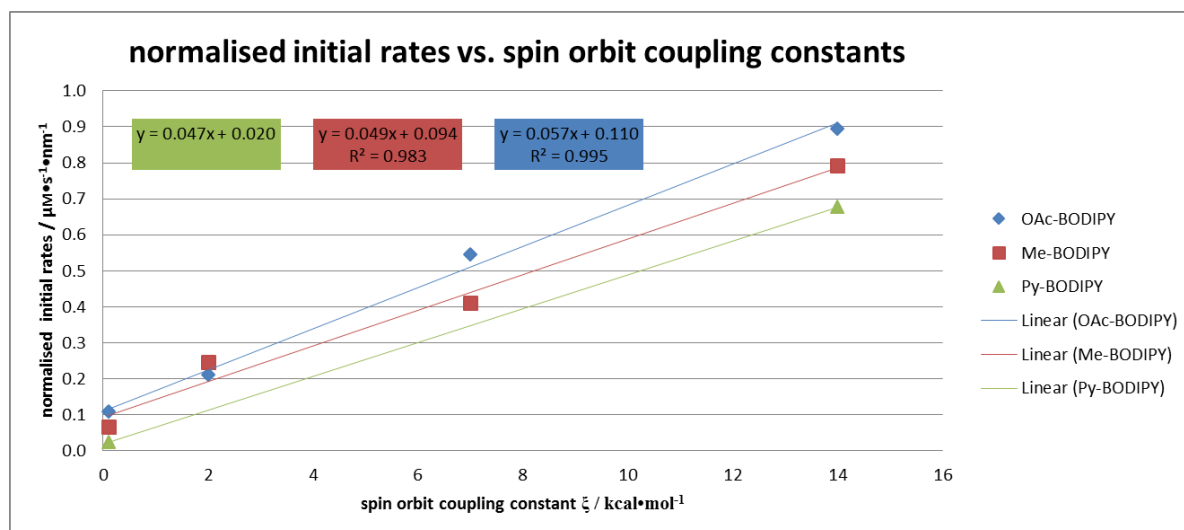


Figure 29: Normalised initial rates vs. spin orbit coupling constants.

Approximately linear relationships were observed. In all the cases the slopes are very similar, indicating that the sensitivity of the systems on the incorporation of heavy atoms does not depend on the *meso* substituent.

### **6.3 Conclusion and Outlook**

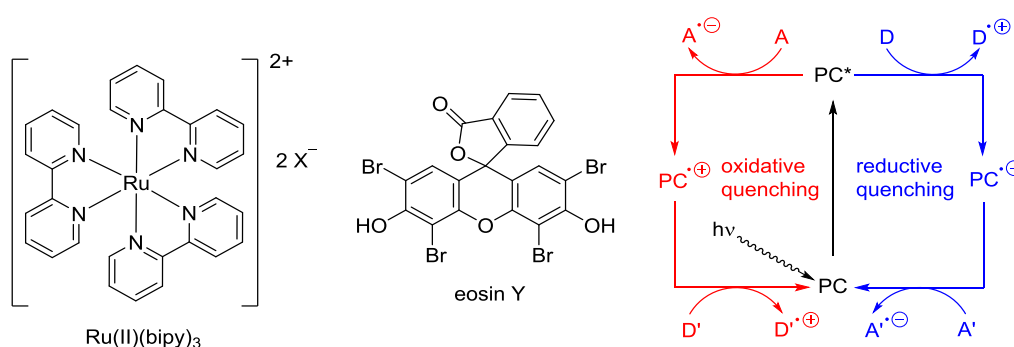
In summary, the effect of halogenation on the performance of BODIPY structures in singlet oxygen generation was investigated. For this, well studied reactions such as the Schenck-Ene reaction and the oxidation of anthracene to the corresponding endoperoxide were performed. Additionally, a simple, GC based method for the determination of the initial rate constants for the formation of the endoperoxide was developed. This allowed the comparison of ten different BODIPY derived sensitizers. Increased initial rates were observed when going from the non halogenated compound to the chlorinated, brominated and iodinated analogues. This was attributed to an increased heavy atom effect which was shown by correlation of the initial rates with the corresponding spin orbit coupling constants.

It is envisaged that this procedure can be applied to investigate the external heavy atom effect, in which a heavy atom additive is used to enhance the probability of intersystem crossing.

## 7 Imidazolidinones as Photoredoxcatalysts

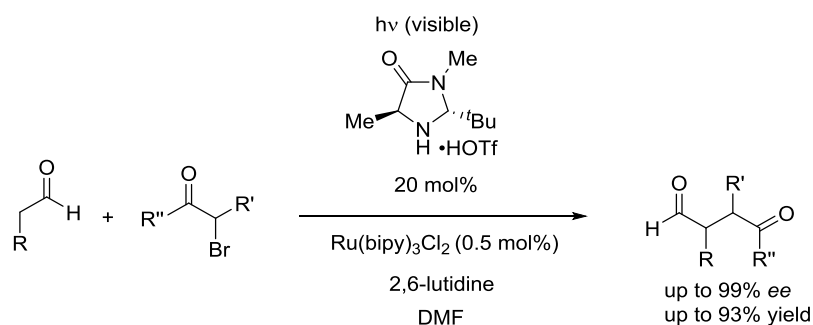
### 7.1 Introduction

Molecules that are excited by light can undergo intersystem crossing (ISC) to the first excited triplet state ( $T_1$ ), which may have a sufficiently long lifetime to transfer energy to a ground state molecule in a process known as sensitisation (see chapter 6.1). However, energy transfer is not the only possible relaxation pathway. Electron transfer can also occur and this process has been the focus of increased attention over the past decade, particularly when visible light can be used. If the photoactive compound is regenerated, the process is often referred to as “photoredox catalysis”.<sup>[41][42]</sup> Organometallic compounds such as Ru(II)(bipy)<sub>3</sub> (Scheme 38, left) are widely employed as catalysts in such processes.<sup>[43]</sup> However, organic chromophores such as eosin Y (Scheme 38, centre) have also been successfully applied in this field.<sup>[39][45]</sup> In general, upon excitation of the chromophore (photocatalyst) to an electronically excited state it can act as both an oxidant (reductive quenching of the excited state) or as a reductant (oxidative quenching of the excited state). The resulting intermediates (radical anion or radical cation) are then converted back to the original catalyst structure by a second electron transfer (Scheme 38, right).



Scheme 38: Structure of two photocatalysts (PC) and a general mechanism for photoredox catalysis.

An elegant application of this type of chemistry can be found in dual catalysis,<sup>[92]</sup> where a photocatalyst is used in combination with another organocatalyst, for example a secondary amine. One of the first examples thereof is the  $\alpha$ -alkylation of aldehydes developed by the group of MacMillan.<sup>[44]</sup> The generalised reaction is shown in Scheme 39.

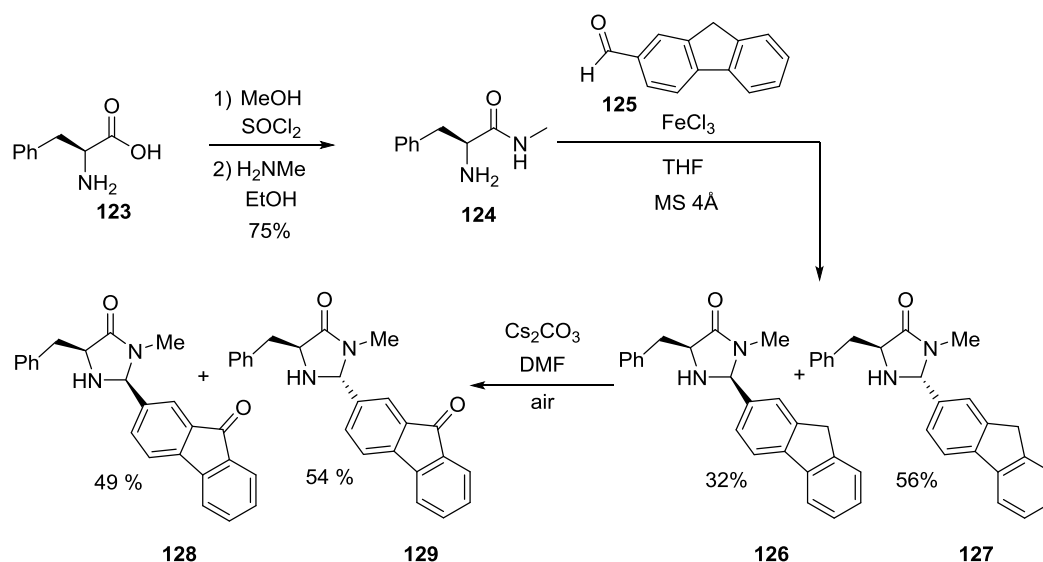


Scheme 39: MacMillan's  $\alpha$ -alkylation of aldehydes.

We were therefore interested whether it would be possible to find a small organic chromophore that could be integrated into a secondary amine to give a catalyst structure that would fulfill both tasks: enamine activation as well as photoredox catalysis. A structure capable of activating a substrate and simultaneously inducing a photochemical reaction has been reported by the group of Bach.<sup>[93]</sup> However, to the best of our knowledge no example of secondary amines bearing a photochemically active substituent is known. Although preliminary studies had already been conducted during the Master's Thesis, for this dissertation imidazolidinones as general scaffolds were investigated instead of pyrrolidines. From this earlier work it was known that fluorenone is capable of catalysing the  $\alpha$ -alkylation of aldehydes in combination with secondary amines.

## 7.2 Synthesis of a Phenylalanine Derived Photoredoxcatalyst

It was envisaged that a simple strategy to incorporate the fluorenone moiety into a secondary amine scaffold would be to build up imidazolidinones by cyclisation of amino acid derived  $\alpha$ -amino amides with commercially available 2-fluorencarboxaldehyde (**125**). The synthesis of the corresponding phenylalanine derivatives is shown in Scheme 40.



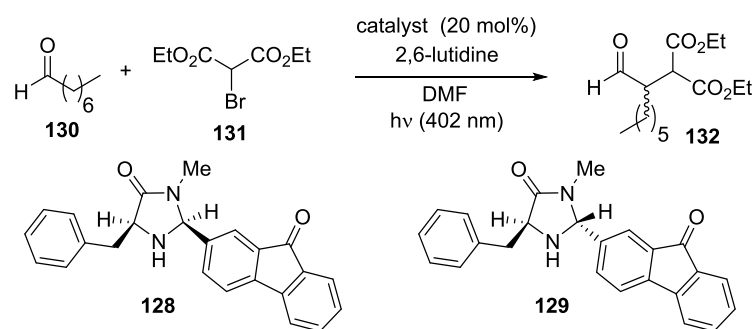
Scheme 40: Synthesis of a phenylalanine derived photoredoxcatalyst.

(L)-Phenylalanine (**123**) was esterified with thionylchloride in MeOH to give the corresponding ester as the hydrochloride salt. Conversion to the amide with methylamine in MeOH gave the desired amide **124** (75% over 2 steps). This was then cyclised with 2-fluorencarboxaldehyde (**125**) in THF with FeCl<sub>3</sub> and molecular sieves (4 Å) to the imidazolidinones **126** and **127** in 88% combined yield. Oxidation of the fluorene moiety to fluorenone was achieved by stirring each of the diastereomers with Cs<sub>2</sub>CO<sub>3</sub> in DMF under air which gave the target compounds in 49% and 54% yield for the *syn*- (**128**) and the *anti* (**129**) diastereomers, respectively. The relative configuration of the compounds was assigned by NOE analysis.

### 7.3 Application of the Phenylalanine Derived Catalysts in the $\alpha$ -Alkylation of Octanal

The  $\alpha$ -alkylation of octanal (**130**) with bromomalonate (**131**) was selected as model reaction to evaluate the two diastereomers of the phenylalanine derived photoredoxcatalyst. As a convenient light source LEDs (1 W, 402 nm) were used, and the reactions were irradiated from the bottom at a distance of 1 cm which resulted in a slight temperature increase to approximately 30 °C. The performance of the two catalysts in the model reaction is shown in Table 19.

Table 19:  $\alpha$ -Alkylation of octanal using phenylalanine derived photoredox catalysts **128** and **129**.



catalyst system	temperature	conversion <sup>a)</sup>	<i>e.r.</i> <sup>b)</sup>
<b>129</b>	30 °C	n.d. <sup>c)</sup>	81.5:18.5
<b>129</b>	0 °C	64%	86.5:13.5
<b>128</b>	30 °C	70%	44.5:55.5

<sup>a)</sup> determined by GC after 2 h; <sup>b)</sup> determined by GC after reduction to the corresponding alcohol; <sup>c)</sup> not determined.

Gratifyingly, it was found that both diastereomers of this catalyst led to conversion to the desired product (**132**). However, the *anti* diastereomer (**129**) delivered the product with notably higher enantioselectivity than the *syn* diastereomer (**128**) (*e.r.* = 81.5:18.5 vs. 44.5:55.5). By lowering the temperature to 0 °C, the selectivity could be increased to *e.r.* = 86.5:13.5. However, it was not possible to drive any of the reactions to completeness. In order to investigate the possibility of degradation of the catalyst the reaction was followed by GC. A plot of conversion versus time is shown in Figure 30.

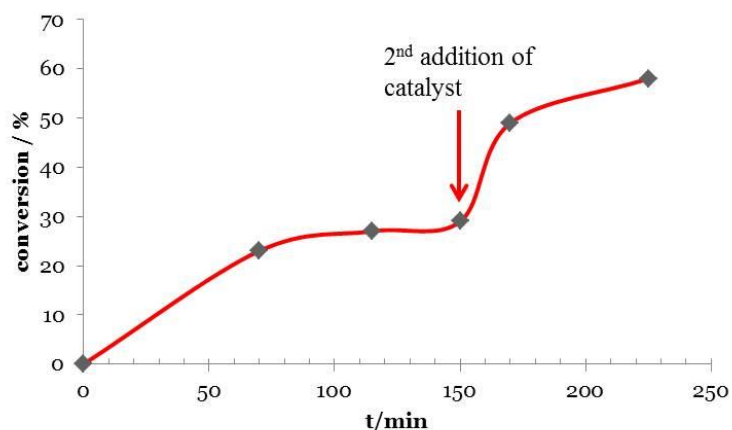
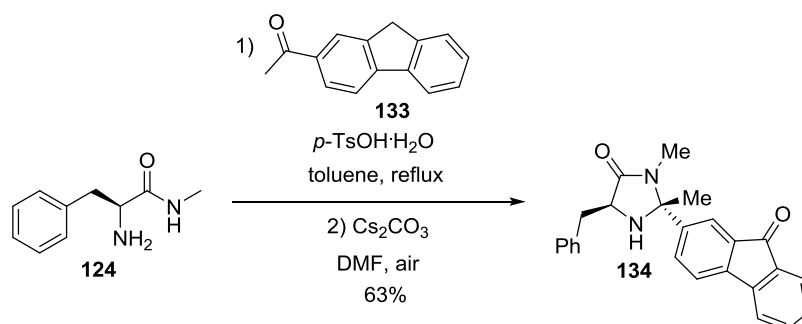


Figure 30: A plot of the conversion versus time using catalyst **129**.

After 60 min the reaction had already almost reached maximum conversion. At  $t = 150$  min additional catalyst (20 mol%) was added which led to further conversion. Moreover, a solution of compound **129** in deuterated DMF was irradiated for 3.5 h in the absence of substrate to explore the possibility of degradation further.  $^1\text{H}$  NMR spectra were recorded before and after irradiation and compared. It was clearly seen that the signal for the proton at the 2-position of the imidazolidinone (4.7 ppm) had almost completely disappeared. Considering the potential stability of a radical at this position (benzylic and stabilised by two nitrogen atoms) an alternative catalyst structure containing a methyl group at the 2-position was envisaged to be more stable under these reaction conditions. To that end, an analogous procedure as for compound **127** using 2-acetylfluorene (**133**) in place of 2-fluorencarboxaldehyde (**125**) was employed to give the desired compound (**134**) in 63% yield over two steps (Scheme 41).



Scheme 41: Synthesis of a methylated phenylalanine derived catalyst.



The relative stereochemistry was assigned by X-ray analysis of the hydrochloride salt (Figure 31). Unfortunately, this compound proved to be entirely inactive in catalysing the  $\alpha$ -alkylation of octanal. This is likely due steric hindrance preventing enamine formation.

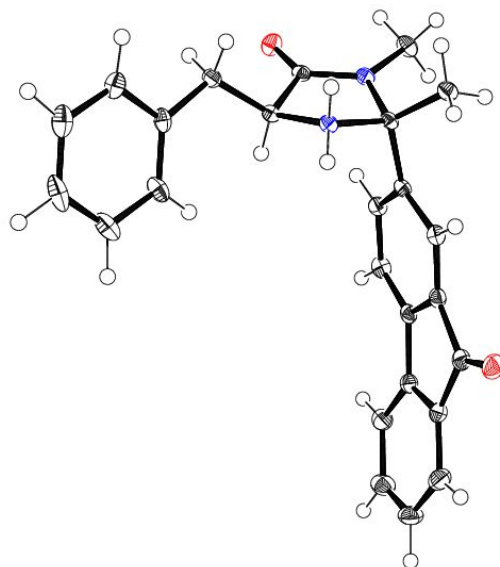


Figure 31: X-ray structure of the hydrochloride salt of compound **134**, the counterion is omitted for clarity.

#### 7.4 Conclusion and Outlook

In conclusion, imidazolidinone derivatives bearing a fluorenone group on the 2-position were synthesised and applied in the  $\alpha$ -alkylation of octanal. It is thought that the secondary amine is responsible for activation of the aldehyde *via* enamine catalysis and that the fluorenone moiety acts as a photoredox catalyst. To the best of our knowledge these structures constitute the first examples of catalysts that comprise both a secondary amine and a photochemically active component. The synthesised structures were applied in the known  $\alpha$ -alkylation of octanal and delivered the desired product with an *e.r.* of up to 86.5:13.5.

Attempts to construct a more robust catalyst by introducing an additional methyl group at the 2-position of the imidazolidinone scaffold led to a structure that was inefficient in catalysis. Possible future work would include the synthesis of sterically less demanding structures such as the corresponding alanine derived catalyst which can be expected to generate the enamine more efficiently.

## 8 Conclusion and Outlook

In summary, the effect of fluorination of organocatalysts was investigated using dimethylaminopyridine (DMAP) derivatives and triazolium salt derived *N*-heterocyclic carbenes (NHCs) as suitable platforms. These structures were used as nucleophilic catalysts in model reactions such as the kinetic resolution of ( $\pm$ )-1-phenylethanol for the DMAP derived systems and the asymmetric Steglich rearrangement for the NHCs. The observed results were rationalised by conformational effects triggered by a combination of hyperconjugative interactions of the energetically low-lying antibonding orbitals of the C-F bonds ( $\sigma^*_{CF}$ ) with bonding molecular orbitals ( $\sigma_{CH}$  or  $\sigma_{CC}$ ) and electrostatic effects ( $F^{\delta-}\cdots N^+$ ). It can be concluded that this type of strategy represents a valuable tool for conformational control in organocatalysis.

Learning from the effects of fluorine introduction in NHC catalysis it might be interesting to synthesise DMAP derivatives which contain a fluorine atom on the pyrrolidine part of the structure. For example the study of both diastereomers of the 4-fluoro derivatives may be of interest.

The effects introduced by chlorination, bromination and iodination of organic compounds were investigated using halogenated borondipyrromethene (BODIPY) structures. The difference in their ability to generate singlet oxygen ( $^1O_2$ ) was attributed to an unequally pronounced heavy atom effect.

In future, the introduction of heavy halogen atoms into various chromophores followed by evaluation of their ability to generate singlet oxygen using the method described in this thesis may be used to develop novel sensitisers and photoredox catalysts.

Furthermore, a catalyst structure which contains a secondary amine for enamine activation as well as a fluorenone moiety as a photoactive sidechain was synthesised and applied in the  $\alpha$ -alkylation of octanal. The catalyst was found to lead to the desired product with an e.r. of 86.5:13.5.

It would be interesting to investigate the pathway of decomposition of the catalyst which is observed under the reaction conditions. Insights thereof may lead to a more robust and possibly more active catalyst.

## 9 Abbreviations

Ac	acetyl
aq.	aqueous
Ar	aryl
b	broad
Bn	benzyl
<sup>t</sup> Bu	<i>tert</i> -butyl
<i>c</i>	cyclo
cat	catalyst
conc.	concentrated
conv.	conversion
$\delta$	chemical shift
d	doublet
DAST	diethylaminosulfur trifluoride
<i>d.r.</i>	diastereomeric ratio
DFT	density functional theory
DIPEA	<i>N,N</i> -diisopropylethylamine
DMAP	4-(dimethylamino) pyridine
DMF	<i>N,N</i> -dimethylformamide
DMSO	dimethylsulfoxide
<i>e.r.</i>	enantiomeric ratio
eq.	equivalents
Et	ethyl
Et <sub>2</sub> O	diethyl ether
EtOAc	ethylacetate
EtOH	ethanol
EWG	electronwithdrawing group
GC	gas chromatography
HOMO	highest occupied molecular orbital
HPLC	high pressure liquid chromatography
Hz	Hertz
<sup>i</sup> Pr	<i>iso</i> -propyl
IR	infrared Spectroscopy
KHMDS	potassium hexamethyl-disilazane

## Abbreviations

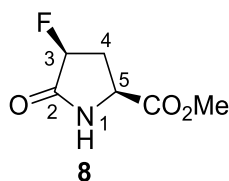
---

LUMO	lowest occupied molecular orbital
m	multiplet, medium
M	molar
<i>m</i> CPBA	<i>m</i> -chloroperbenzoic acid
Me	methyl
MeOH	methanol
MS	molecular sieves, mass spectrometry
n.d.	not determined
NBS	<i>N</i> -bromosuccinimide
NCS	<i>N</i> -chlorosuccinimide
NHC	<i>N</i> -heterocyclic carbene
NIS	<i>N</i> -iodosuccinimide
NMR	nuclear magnetic resonance
Ph	phenyl
ppm	parts per million
Py	pyridine
quant	quantitative
rac	racemic
rt	room temperature
s	singlet, strong
<i>t</i>	<i>tert</i>
t	triplet
TFA	trifluoroacetic acid
THF	tetrahydrofuran
TLC	thin layer chromatography
TBDMS	<i>tert</i> -butyldimethylsilyl
q	quartet
w	weak

## 10 Experimental Part

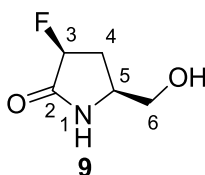
### General Methods

All reactions were performed under an atmosphere of argon. All chemicals were reagent grade and used as supplied unless stated otherwise. All reactions were magnetically stirred. Solvents for extractions and chromatography were technical grade. Extracts were dried over technical grade  $\text{Na}_2\text{SO}_4$  or  $\text{MgSO}_4$ . Analytical thin layer chromatography (TLC) was performed on pre-coated *Merck* silica gel 60 F<sub>254</sub> plates (0.25 mm) and visualised by UV, CAM, ninhydrine or  $\text{KMnO}_4$  stain. Flash column chromatography was carried out on *Fluka* silica gel 60 (230-400 mesh). Concentration *in vacuo* was performed at ~10 mbar and 40 °C, drying at  $\sim 10^{-2}$  mbar and room temperature.  $^1\text{H}$  NMR,  $^{13}\text{C}$  NMR and  $^{19}\text{F}$  NMR spectra were recorded on a *Bruker AVANCE 300 MHz*, *Bruker AV 400 MHz*, *DRX 400 MHz*, and an *Agilent DD2 600* spectrometer. Chemical shifts ( $\delta$ ) are reported in ppm relative to the solvent residual peak. The multiplicities are reported as: s = singlet, d = doublet, t = triplet, q = quartet, sext = sextet, m = multiplet, br = broad. Melting points were measured on a *Büchi B540* melting point apparatus and are uncorrected. IR spectra were measured on a Perkin-Elmer Spectrum 100 FTIR spectrometer and reported in  $\text{cm}^{-1}$ . The intensities of the bands are reported as: w = weak, m = medium, s = strong. Optical rotations were obtained using a JASCO P-2000 polarimeter in a 10 cm long cell. High-resolution mass spectra (HR ESI and EI MS) were performed by the MS service at the Laboratory of Organic Chemistry of the ETH Zürich and the Organic Chemistry Institute of the WWU Münster. HPLC analyses were performed on an Agilent 1260 system.

**N-Heterocyclic Carbene Precursors****(2S,4S)-Methyl-4-fluoro-5-oxopyrrolidine-2-carboxylate (8)**

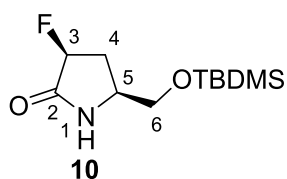
To a black suspension of ruthenium(III)chloride hydrate (158 mg, ~704  $\mu\text{mol}$ ) in a solution of **6** (870 mg, 3.52 mmol) in EtOAc (15 mL) was added an aqueous solution of  $\text{NaIO}_4$  (10%, 100 mL) to give a dark red, biphasic solution, which turned into a bright yellow solution overnight. After 3.5 days the solution was cooled to 0 °C and *i*-PrOH (50 mL) was added to give a dark brown suspension. This was allowed to warm to rt and stirred for 7 h. Water (100 mL) was added and the mixture was extracted with EtOAc (6 x 200 mL). The combined organic layers were dried over  $\text{MgSO}_4$  and concentrated *in vacuo* to give a white solid (664 mg).  $^1\text{H}$ - and  $^{19}\text{F}$  NMR showed clean conversion with partial deprotection (protected : unprotected = 1 : 1.2). This mixture was dissolved in  $\text{CH}_2\text{Cl}_2$  (35 mL) and treated with TFA (3.5 mL) dropwise. The colourless solution was stirred for 2.5 h to give a light red solution which was cooled to 0 °C.  $\text{NaHCO}_3$  (sat., 50 mL) was added slowly until pH 8 was reached. The organic layer was washed and the aqueous layer was extracted with EtOAc (3 x 50 mL). The combined organic layers were dried over  $\text{MgSO}_4$  and concentrated to give a light yellow oil (424 mg, 75% over two steps);  $R_f$  0.54 (MeOH :  $\text{CH}_2\text{Cl}_2$  / 1 : 10);  $[\alpha]_D^{20}$  -40.7 (*c* 1.00 in MeOH);  $\nu_{\text{max}}$  (neat)/ $\text{cm}^{-1}$  3252w, 2960w, 2076w, 1708s, 1440m, 1332m, 1204s, 1136s, 1094m, 1056s, 1029m, 998m, 949m, 889m, 801m, 741m, 721s;  $^1\text{H}$  NMR (300 MHz,  $\text{CDCl}_3$ ):  $\delta$  = 7.29 (1H, s, NH), 5.06 (1H, ddd,  $^2J_{\text{HF}}$  52.2,  $^3J$  7.8,  $^3J$  6.3,  $\text{C}^3\text{H}$ ), 4.21 (1H, ddd,  $^3J$  8.4,  $^3J$  6.6,  $^3J$  2.4,  $\text{C}^5\text{H}$ ), 3.80 (3H, s,  $\text{CH}_3$ ), 2.89 (1H, ddt,  $^3J_{\text{HF}}$  14.8,  $^2J$  14.2,  $^3J$  7.9,  $\text{C}^4\text{HH}$ ), 2.36 (1H, ddt,  $^3J_{\text{HF}}$  25.8,  $^2J$  14.1,  $^3J$  6.4,  $\text{C}^4\text{HH}$ );  $^{13}\text{C}$  NMR (75 MHz,  $\text{CDCl}_3$ ):  $\delta$  = 171.9 (d,  $^2J_{\text{CF}}$  20.5,  $\text{C}^2$ ), 171.0 ( $\text{CO}_2\text{Me}$ ), 87.2 (d,  $^1J_{\text{CF}}$  185.8,  $\text{C}^3$ ), 53.1 ( $\text{CH}_3$ ), 52.0 (d,  $^3J_{\text{CF}}$  3.5,  $\text{C}^5$ ), 31.9 (d,  $^2J_{\text{CF}}$  21.1,  $\text{C}^4$ );  $^{19}\text{F}$  NMR (282 MHz,  $\text{CDCl}_3$ ):  $\delta$  = -189.7 (dddd,  $^2J$  52.1,  $^3J$  25.6,  $^3J$  14.3,  $^4J$  1.1);  $[m/z$  (ESI) found: 184.0386 ( $\text{M}+\text{Na}$ ) $^+$ ,  $\text{C}_6\text{H}_8\text{FNO}_3\text{Na}^+$  requires 184.0386].

(3*S*,5*S*)-3-Fluoro-5-(hydroxymethyl)-pyrrolidin-2-one (**9**)



A light yellow solution of **8** (966 mg, 6.00 mmol) in EtOH (60 mL) was cooled to 0 °C and treated with NaBH<sub>4</sub> (454 mg, 12.0 mmol) to give a white suspension. This was stirred for 15 min and allowed to warm to rt to give a clear, colourless solution. After 90 min the solution was cooled to 0 °C and an aqueous solution of citric acid (10%, 60 mL) was added carefully. This gave a white suspension which turned back into a clear solution when the addition was complete. The solution was concentrated *in vacuo* to give a colourless oil, which was coevaporated with EtOH (4 x 20 mL) to give a white solid. This was purified by column chromatography (dry loading, MeOH : CH<sub>2</sub>Cl<sub>2</sub> / 1 : 15) to give a white, crystalline solid (140 mg, 18%); *R<sub>f</sub>* 0.21 (MeOH : CH<sub>2</sub>Cl<sub>2</sub> / 1 : 10); m.p. 107-108 °C; [ $\alpha$ ]<sub>D</sub><sup>20</sup> -34.8 (*c* 1.00 in MeOH);  $\nu_{\text{max}}$  (neat)/cm<sup>-1</sup> 3348m, 3228m, 2964w, 2945w, 2884w, 2508w, 2340w, 1980w, 1705s, 1451m, 1408m, 1330m, 1299s, 1280m, 1258w, 1233m, 1183w, 1111m, 1095s, 1075s, 1053s, 1005s, 967m, 928w, 869m, 815m, 727s, 615s; <sup>1</sup>H NMR (400 MHz, CD<sub>3</sub>OD):  $\delta$  = 5.10 (1H, ddd, <sup>2</sup>*J*<sub>HF</sub> 53.0, <sup>3</sup>*J* 8.3, <sup>3</sup>*J* 6.7, C<sup>3</sup>H), 3.75-3.55 (2H, m, C<sup>5</sup>H and C<sup>6</sup>HH), 3.48 (1H, dd, <sup>2</sup>*J* 11.0, <sup>3</sup>*J* 5.5, C<sup>6</sup>HH), 2.61 (1H, dddd, <sup>3</sup>*J*<sub>HF</sub> 13.7, <sup>2</sup>*J* 12.8, <sup>3</sup>*J* 8.3, <sup>3</sup>*J* 6.7, C<sup>4</sup>HH), 1.96 (1H, ddt, <sup>3</sup>*J*<sub>HF</sub> 28.2, <sup>2</sup>*J* 13.1, <sup>3</sup>*J* 6.5, C<sup>4</sup>HH); <sup>13</sup>C NMR (100 MHz, CD<sub>3</sub>OD):  $\delta$  = 174.7 (d, <sup>2</sup>*J*<sub>CF</sub> 20.6, C<sup>2</sup>), 90.2 (d, <sup>1</sup>*J*<sub>CF</sub> 182.6, C<sup>3</sup>), 65.4 (C<sup>6</sup>), 53.9 (d, <sup>3</sup>*J*<sub>CF</sub> 3.6, C<sup>5</sup>), 31.3 (d, <sup>2</sup>*J*<sub>CF</sub> 19.5, C<sup>4</sup>); <sup>19</sup>F NMR (282 MHz, CD<sub>3</sub>OD):  $\delta$  = -189.4 (dddd, <sup>2</sup>*J* 53.0, <sup>3</sup>*J* 28.8, <sup>3</sup>*J* 13.1, <sup>4</sup>*J* 4.3); [*m/z* (ESI) found: 156.0414 (M+Na)<sup>+</sup>, C<sub>5</sub>H<sub>8</sub>FNO<sub>2</sub>Na<sup>+</sup> requires 156.0431].

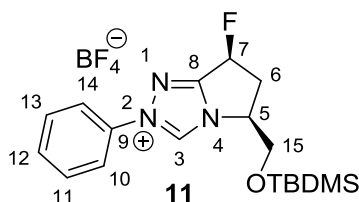
**(3*S*,5*S*)-5-(((*tert*-Butyldimethylsilyl)-oxy)-methyl)-3-fluoropyrrolidin-2-one (10)**



A colourless solution of **9** (103 mg, 774  $\mu\text{mol}$ ) in DMF (7.7 mL) was treated with TBDMSCl (140 mg, 929  $\mu\text{mol}$ ) and imidazole (79.0 mg, 1.16 mmol). The light yellow solution was stirred for 72 h and water (30 mL) was added. The mixture was extracted with  $\text{CH}_2\text{Cl}_2$  (3 x 30 mL). The combined organic layers were washed with water (3 x 100 mL), dried over  $\text{MgSO}_4$  and concentrated. The residue was taken up in  $\text{CH}_2\text{Cl}_2$  (30 mL) and washed with water (2 x 30 mL), dried over  $\text{MgSO}_4$  and concentrated to give a white solid (176 mg, 92%);  $R_f$  0.57 (MeOH :  $\text{CH}_2\text{Cl}_2$  / 1 : 10); m.p. 78-79  $^\circ\text{C}$ ;  $[\alpha]_D^{20}$  +11.8 ( $c$  0.32 in  $\text{CHCl}_3$ );  $\nu_{\text{max}}$  (neat)/ $\text{cm}^{-1}$  3085w, 2954m, 2930m, 2885w, 2857m, 2162w, 2051w, 1980w, 1705s, 1471w, 1462m, 1407w, 1389w, 1361w, 1337w, 1316w, 1298w, 1253m, 1183w, 1141m, 1123s, 1101s, 1084s, 1063m, 1033m, 1006m, 991m, 940w, 888w, 833s, 812s, 773s, 714s, 681m, 636m;  $^1\text{H}$  NMR (400 MHz,  $\text{CDCl}_3$ ):  $\delta$  = 6.54 (1H, br s, NH), 5.05 (1H, ddd,  $^2J_{\text{HF}}$  52.5,  $^3J$  8.2,  $^3J$  6.5,  $\text{C}^3\text{H}$ ), 3.73-3.63 (2H, m,  $\text{C}^5\text{HH}$  and  $\text{C}^6\text{HH}$ ), 3.53-3.46 (1H, m,  $\text{C}^6\text{HH}$ ), 2.57 (1H, tdd,  $^3J_{\text{HF}}$  and  $^2J$  14.0,  $^3J$  8.2,  $^3J$  6.7,  $\text{C}^4\text{HH}$ ), 1.91 (1H, ddt,  $^3J_{\text{HF}}$  27.1,  $^2J$  14.0,  $^3J$  6.2,  $\text{C}^4\text{HH}$ ), 0.88 (9H, s,  $^t\text{Bu}$ ), 0.062 (3H, s,  $\text{SiCH}_3$ ), 0.059 (3H, s,  $\text{SiCH}_3$ );  $^{13}\text{C}$  NMR (100 MHz,  $\text{CDCl}_3$ ):  $\delta$  = 171.7 (d,  $^2J_{\text{CF}}$  20.7,  $\text{C}^2$ ), 88.0 (d,  $^1J_{\text{CF}}$  185.0,  $\text{C}^3$ ), 66.7 ( $\text{C}^6$ ), 52.5 (d,  $^3J_{\text{CF}}$  3.2,  $\text{C}^5$ ), 30.4 (d,  $^2J_{\text{CF}}$  19.9,  $\text{C}^4$ ), 25.9 (3C,  $\text{SiC}(\text{CH}_3)_3$ ), 18.3 ( $\text{SiC}(\text{CH}_3)_3$ ), -5.32 ( $\text{SiCH}_3$ ), -5.33 ( $\text{SiCH}_3$ );  $^{19}\text{F}$  NMR (376 MHz,  $\text{CDCl}_3$ ):  $\delta$  = -187.8 (dddd,  $^2J$  52.4,  $^3J$  27.4,  $^3J$  13.8,  $^4J$  3.4); [ $m/z$  (ESI) found: 270.1291 ( $\text{M}+\text{Na}$ ) $^+$ ,  $\text{C}_{11}\text{H}_{22}\text{FNO}_2\text{SiNa}^+$  requires 270.1302].

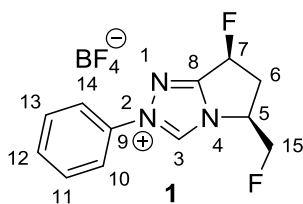


**(5*S*,7*S*)-5-(*tert*-Butyl-dimethylsilyloxy)-7-fluoro-2-phenyl-6,7-dihydro-5*H*-pyrrolo-[2,1-*c*][1,2,4]-triazol-2-ium tetrafluoroborate (**11**)**



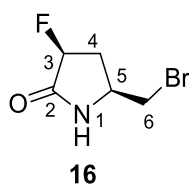
A colourless solution of **10** (207 mg, 838  $\mu\text{mol}$ ) in  $\text{CH}_2\text{Cl}_2$  (6.0 mL) was treated with trimethyloxonium tetrafluoroborate (149 mg, 1.01 mmol) to give a suspension. After 2 h 45 min phenylhydrazine (99.3  $\mu\text{L}$ , 1.01 mmol) was added to give a yellow solution. This was stirred for 15 min to give a bright orange solution which was concentrated and dried on high-vacuum (30 min) to give a sticky solid. This material was dissolved in trimethylorthoformate (6.0 mL) and the orange solution was stirred for 29 h. The mixture was concentrated and dried on high-vacuum to give an orange solid, which was purified by column chromatography (MeOH :  $\text{CH}_2\text{Cl}_2$  / 1 : 20) to give a brown solid. This was then washed with  $\text{Et}_2\text{O}$  (2 x 5 mL) to give a beige solid (277 mg, 76%);  $R_f$  0.61 (MeOH :  $\text{CH}_2\text{Cl}_2$  / 1 : 5); m.p. 119-122  $^\circ\text{C}$ ;  $[\alpha]_D^{20}$  -34.8 ( $c$  0.45 in  $\text{CHCl}_3$ );  $\nu_{\text{max}}$  (neat)/ $\text{cm}^{-1}$  3127w, 2956w, 2931w, 2887w, 2858w, 2168w, 2052w, 1982w, 1683w, 1596w, 1525m, 1499w, 1471m, 1434w, 1412w, 1399w, 1361w, 1335w, 1320w, 1288w, 1254m, 1220m, 1208m, 1152w, 1050s, 1036s, 1005s, 976s, 940m, 915m, 836s, 776s, 759s, 723m, 712m, 685s, 667m, 611w;  $^1\text{H}$  NMR (300 MHz,  $\text{CDCl}_3$ ):  $\delta$  = 10.05 (1H, s, NCHN), 7.83-7.73 (2H, m,  $\text{C}^{11}\text{H}$  and  $\text{C}^{13}\text{H}$ ), 7.55-7.46 (3H, m,  $\text{C}^{10}\text{H}$ ,  $\text{C}^{14}\text{H}$  and  $\text{C}^{12}\text{H}$ ), 6.15 (1H, ddd,  $^2J_{\text{HF}}$  55.4,  $^3J$  7.6,  $^3J$  1.8,  $\text{C}^7\text{H}$ ), 5.15-5.02 (1H, m,  $\text{C}^5\text{H}$ ), 4.26 (1H, dd,  $^2J$  11.6,  $^3J$  3.2,  $\text{C}^{15}\text{HH}$ ), 3.77 (1H, dd,  $^2J$  11.7,  $^3J$  3.6,  $\text{C}^{15}\text{HH}$ ), 3.46 (1H, ddd,  $^3J_{\text{HF}}$  32.0,  $^2J$  15.6,  $^3J$  8.1,  $\text{C}^6\text{HH}$ ), 2.76 (1H, ddt,  $^3J_{\text{HF}}$  27.8,  $^2J$  15.1,  $^3J$  2.4,  $\text{C}^6\text{HH}$ ), 0.77 (9H, s,  $^t\text{Bu}$ ), 0.04 (3H, s,  $\text{SiCH}_3$ ), 0.01 (3H, s,  $\text{SiCH}_3$ );  $^{13}\text{C}$  NMR (75 MHz,  $\text{CDCl}_3$ ):  $\delta$  = 159.4 (d,  $^2J_{\text{CF}}$  23.5,  $\text{C}^8$ ), 137.1 (NCHN), 135.5 ( $\text{C}^9$ ), 131.2 ( $\text{C}^{12}$ ), 130.4 (2C,  $\text{C}^{10}$  and  $\text{C}^{14}$ ), 121.1 (2C,  $\text{C}^{11}$  and  $\text{C}^{13}$ ), 83.1 (d,  $^1J_{\text{CF}}$  187.7,  $\text{C}^7$ ), 62.9 ( $\text{C}^{15}$ ), 61.9 ( $\text{C}^5$ ), 37.5 (d,  $^2J_{\text{CF}}$  22.4,  $\text{C}^6$ ), 25.7 (3C,  $\text{SiC}(\text{CH}_3)_3$ ), 18.2 ( $\text{SiC}(\text{CH}_3)_3$ ), -5.5 ( $\text{SiCH}_3$ ), -5.6 ( $\text{SiCH}_3$ );  $^{19}\text{F}$  NMR (282 MHz,  $\text{CDCl}_3$ ):  $\delta$  = -151.7 ( $^{10}\text{BF}_4^-$ ), -151.8 ( $^{11}\text{BF}_4^-$ ), -173.4 (dtd,  $^2J$  54.4,  $^3J$  27.2,  $^4J$  2.5); [ $m/z$  (ESI) found: 348.1913 ( $\text{M-BF}_4$ ) $^+$ ,  $\text{C}_{18}\text{H}_{27}\text{FN}_3\text{OSi}^+$  requires 348.1902].

**(5*S*,7*S*)-5-Fluoro-7-fluoro-2-phenyl-6,7-dihydro-5*H*-pyrrolo-[2,1-*c*][1,2,4]-triazol-2-ium tetrafluoroborate (1)**



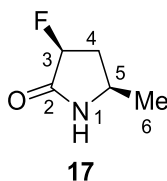
A light orange solution of **11** (250 mg, 575  $\mu\text{mol}$ ) in  $\text{CH}_2\text{Cl}_2$  (5.8 mL) in a polypropylene flask was cooled to 0 °C and treated with hydrogen fluoride pyridine (70%, 149  $\mu\text{L}$ , 5.75 mmol) dropwise to give a deep blue solution. DAST (152  $\mu\text{L}$ , 1.15 mmol) was added dropwise to give a brown solution which was allowed to warm to rt and stirred for 21 h. The dark brown solution was cooled to 0 °C and carefully treated with  $\text{NaHCO}_3$  (sat., 10 mL) and allowed to warm to rt. The mixture was extracted with  $\text{CH}_2\text{Cl}_2$  (6 x 10 mL), the combined organic layers were dried over  $\text{Na}_2\text{SO}_4$  and concentrated to give a brown solid. This was purified by column chromatography (MeOH :  $\text{CH}_2\text{Cl}_2$  / 1 : 20) and washed with  $\text{CHCl}_3$  to give a light brown solid (83.0 mg, 45%). Crystals which were suitable for X-ray analysis were obtained by vapor diffusion ( $\text{Et}_2\text{O}$  / MeOH).  $R_f$  0.27 (MeOH :  $\text{CH}_2\text{Cl}_2$  / 1 : 10); m.p. 143-145 °C;  $[\alpha]_D^{20}$  -9.4 ( $c$  0.52 in acetone);  $\nu_{\text{max}}$  (neat)/ $\text{cm}^{-1}$  3110w, 3036w, 2926w, 2855w, 2331w, 2162w, 1974w, 1706w, 1595w, 1524m, 1470w, 1433w, 1407w, 1332w, 1290w, 1258w, 1222m, 1165w, 1005s, 973s, 949s, 920m, 890m, 874m, 836w, 768s, 746m, 688s, 656m, 633w, 613w;  $^1\text{H}$  NMR (400 MHz,  $(\text{CD}_3)_2\text{CO}$ ):  $\delta$  = 10.67 (1H, s, NCHN), 8.07-7.97 (2H, m,  $\text{C}^{11}\text{H}$  and  $\text{C}^{13}\text{H}$ ), 7.78-7.67 (3H, m,  $\text{C}^{10}\text{H}$ ,  $\text{C}^{14}\text{H}$  and  $\text{C}^{12}\text{H}$ ), 6.51 (1H, dddd,  $^2J_{\text{HF}}$  54.6,  $^3J$  7.3,  $^3J$  2.3,  $^4J$  1.1,  $\text{C}^7\text{H}$ ), 5.52-5.39 (1H, m,  $\text{C}^5\text{H}$ ), 5.18 (1H, ddd,  $^3J_{\text{HF}}$  46.2,  $^2J$  10.6,  $^3J$  3.0, FCHH), 4.90 (1H, ddd,  $^3J_{\text{HF}}$  46.7,  $^2J$  10.6,  $^3J$  6.6, FCHH), 3.71 (1H, ddddd,  $^3J_{\text{HF}}$  25.7,  $^2J$  16.0,  $^3J$  8.9,  $^3J$  7.3,  $^4J_{\text{HF}}$  1.6,  $\text{C}^6\text{HH}$ ), 2.94 (1H, dddd,  $^3J_{\text{HF}}$  26.9,  $^2J$  15.5,  $^3J$  3.8,  $^3J$  2.4,  $\text{C}^6\text{HH}$ );  $^{13}\text{C}$  NMR (100 MHz,  $(\text{CD}_3)_2\text{CO}$ ):  $\delta$  = 159.9 (d,  $^2J_{\text{CF}}$  23.4,  $\text{C}^8$ ), 139.9 (NCHN), 136.8 ( $\text{C}^9$ ), 132.1 ( $\text{C}^{12}$ ), 131.1 (2C,  $\text{C}^{10}$  and  $\text{C}^{14}$ ), 122.5 (2C,  $\text{C}^{11}$  and  $\text{C}^{13}$ ), 84.1 (d,  $^1J_{\text{CF}}$  184.4,  $\text{C}^7$ ), 83.0 (d,  $^1J_{\text{CF}}$  173.3,  $\text{C}^{15}$ ), 60.8 (d,  $^2J_{\text{CF}}$  19.2,  $\text{C}^5$ ), 37.5 (dd,  $^2J_{\text{CF}}$  22.6,  $^3J_{\text{CF}}$  6.3,  $\text{C}^6$ );  $^{19}\text{F}$  NMR (282 MHz,  $(\text{CD}_3)_2\text{CO}$ ):  $\delta$  = -151.8 ( $^{10}\text{BF}_4^-$ ), -151.9 ( $^{11}\text{BF}_4^-$ ), -174.9 (dddd,  $^2J$  54.8,  $^3J$  26.8,  $^3J$  25.7,  $^5J_{\text{FF}}$  5.1,  $J$  4.1,  $\text{C}^7\text{F}$ ), -226.0 (tdt,  $^2J$  46.7,  $^3J$  20.3,  $^5J_{\text{FF}}$  4.6,  $\text{C}^{15}\text{F}$ ); [ $m/z$  (ESI) found: 236.0990 ( $\text{M-BF}_4^-$ ) $^+$ ,  $\text{C}_{12}\text{H}_{12}\text{F}_2\text{N}_3^+$  requires 236.0994].

**(3*S*,5*S*)-5-(Bromomethyl)-3-fluoropyrrolidin-2-one (16)**



A white suspension of **9** (207 mg, 1.56 mmol) and triphenylphosphine (568 mg, 1.71 mmol) in acetonitrile (2.5 mL) was cooled to 0 °C and treated with a solution of tetrabromomethane (568 mg, 1.71 mmol) in acetonitrile (5.0 mL). The mixture was allowed to warm to rt to give a clear, light yellow solution. This was stirred for 5 d, concentrated *in vacuo* and dried on high vacuum. *n*-Hexane (5.0 mL) and water (5.0 mL) was added and the resulting suspension was vigorously stirred for 1 h and filtered. *n*-Hexane (5.0 mL) and water (5.0 mL) was added to the residue, the mixture was stirred for 30 min and filtered. The aqueous layer of the combined solutions was extracted with CHCl<sub>3</sub> (6 x 10 mL). The combined organic layers (only CHCl<sub>3</sub>) were dried over Na<sub>2</sub>SO<sub>4</sub> and concentrated *in vacuo* to give a white solid (117 mg) which was directly used in the next step. *R<sub>f</sub>* 0.43 (MeOH : CH<sub>2</sub>Cl<sub>2</sub> / 1 : 10); <sup>1</sup>H NMR (300 MHz, CDCl<sub>3</sub>): δ = 6.51 (1H, s, NH), 5.06 (1H, ddd, <sup>2</sup>*J*<sub>HF</sub> 52.1, <sup>3</sup>*J* 7.8, <sup>3</sup>*J* 5.7, C<sup>3</sup>H), 3.96-3.84 (1H, m, C<sup>5</sup>H), 3.49 (1H, dd, <sup>2</sup>*J* 10.4, <sup>3</sup>*J* 5.0, C<sup>6</sup>HH), 3.38 (1H, dd, <sup>2</sup>*J* 10.4, <sup>3</sup>*J* 8.0, C<sup>6</sup>HH), 2.68 (1H, ddt, <sup>3</sup>*J*<sub>HF</sub> 17.4, <sup>2</sup>*J* 14.6, <sup>3</sup>*J* 7.4, C<sup>4</sup>HH), 2.08 (1H, ddt, <sup>3</sup>*J*<sub>HF</sub> 25.8, <sup>2</sup>*J* 14.4, <sup>3</sup>*J* 5.5, C<sup>4</sup>HH); <sup>19</sup>F NMR (282 MHz, CDCl<sub>3</sub>): δ = -186.2 (dddd, <sup>2</sup>*J* 51.9, <sup>3</sup>*J* 26.0, <sup>3</sup>*J* 17.5, <sup>4</sup>*J* 3.4).

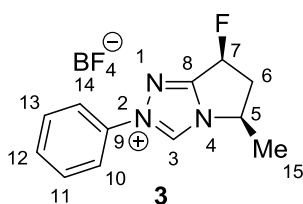
**(3*S*,5*R*)-3-Fluoro-5-methylpyrrolidin-2-one (17)**



To a solution of **16** (102 mg, 520 μmol) and triethylamine (72 μL, 520 μmol) in EtOH (1.5 mL) was added palladium on carbon (5%, 30 mg) to give a black suspension, which was placed under an atmosphere of hydrogen (~ 1 bar). This was stirred for 46 h and filtered over celite. The solution was concentrated *in vacuo* to give a white solid which was purified by column chromatography (MeOH : CH<sub>2</sub>Cl<sub>2</sub> / 1 : 20) to give a white solid (33.6 mg, 21% over 2 steps). *R<sub>f</sub>* 0.42 (MeOH : CH<sub>2</sub>Cl<sub>2</sub> / 1 : 10); m.p. 104-105 °C; [α]<sub>D</sub><sup>20</sup> -0.5 (*c* 1.00 in CHCl<sub>3</sub>); ν<sub>max</sub> (neat)/cm<sup>-1</sup> 3414w, 3002w, 2976m, 2937m, 2879m, 2802w, 2755m, 2738m, 2676s, 2603m, 2529w, 2492m, 2347w, 2239w, 1981w, 1707w, 1475s, 1434s, 1397s, 1384m, 1365m, 1332w,

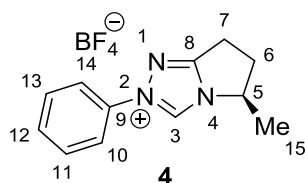
1288w, 1170s, 1117m, 1069m, 1035s, 904w, 849m, 804s, 750m, 719m, 690m, 622w;  $^1\text{H}$  NMR (300 MHz,  $\text{CDCl}_3$ ):  $\delta$  = 7.69 (1H, br s, NH), 5.05 (1H, dt,  $^2J_{\text{HF}}$  52.6,  $^3J$  7.8,  $\text{C}^3\text{H}$ ), 3.66 (1H, sextd,  $^3J$  6.4,  $^4J_{\text{HF}}$  3.6,  $\text{C}^5\text{H}$ ), 2.68 (1H, dddd,  $^2J$  13.5,  $^3J_{\text{HF}}$  10.1,  $^3J$  8.1,  $^3J$  6.3,  $\text{C}^4\text{HH}$ ), 1.82 (1H, ddt,  $^3J_{\text{HF}}$  26.5,  $^2J$  13.4,  $^3J$  7.4,  $\text{C}^4\text{HH}$ ), 1.30 (3H, d,  $^3J$  6.2,  $\text{CH}_3$ );  $^{13}\text{C}$  NMR (75 MHz,  $\text{CDCl}_3$ ):  $\delta$  = 172.7 (d,  $^2J_{\text{CF}}$  20.2,  $\text{C}^2$ ), 89.0 (d,  $^1J_{\text{CF}}$  185.3,  $\text{C}^3$ ), 46.5 (d,  $^3J_{\text{CF}}$  4.9,  $\text{C}^5$ ), 36.6 (d,  $^2J_{\text{CF}}$  18.3,  $\text{C}^4$ ), 22.4 ( $\text{CH}_3$ );  $^{19}\text{F}$  NMR (282 MHz,  $\text{CDCl}_3$ ):  $\delta$  = -189.2 (dddd,  $^2J$  52.6,  $^3J$  26.5,  $^3J$  10.1,  $^4J$  3.4).

**(5*R*,7*S*)-7-Fluoro-5-methyl-2-phenyl-6,7-dihydro-5*H*-pyrrolo-[2,1-*c*][1,2,4]-triazol-2-ium tetrafluoroborate (3)**



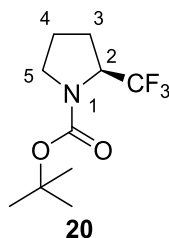
To a colourless solution of **17** (25.3 mg, 216  $\mu\text{mol}$ ) in  $\text{CH}_2\text{Cl}_2$  (2.0 mL) was added  $\text{Me}_3\text{O}^+\cdot\text{BF}_4^-$  (38.4 mg, 259  $\mu\text{mol}$ ) to give a suspension which turned into a light yellow solution over 3.5 h. Phenylhydrazine (26  $\mu\text{L}$ , 259  $\mu\text{mol}$ ) was added to give an orange solution which was stirred for 15 min and concentrated. The resulting red solid was dissolved in trimethyl orthoformate (2.0 mL), heated to 50  $^\circ\text{C}$  and stirred for 14 h. The yellow solution was cooled to rt and concentrated to give an orange solid which was purified by column chromatography ( $\text{MeOH} : \text{CH}_2\text{Cl}_2 / 1 : 20$ ) to give an orange solid (40.4 mg, 61%).  $R_f$  0.16 ( $\text{MeOH} : \text{CH}_2\text{Cl}_2 / 1 : 10$ ); m.p. 186-189  $^\circ\text{C}$ ;  $[\alpha]_D^{20}$  -18.2 ( $c$  1.00 in acetone);  $\nu_{\text{max}}$  (neat)/ $\text{cm}^{-1}$  3133w, 2925w, 2355w, 2162w, 1980w, 1705w, 1593m, 1523m, 1497w, 1471w, 1433m, 1404m, 1395m, 1344m, 1293w, 1228s, 1184w, 1157w, 1051s, 1032s, 974s, 919s, 899m, 869m, 843w, 786w, 764s, 739s, 686s, 634m, 612m;  $^1\text{H}$  NMR (300 MHz,  $(\text{CD}_3)_2\text{CO}$ ):  $\delta$  = 10.59 (1H, s, NCHN), 8.01-7.95 (2H, m,  $\text{C}^{11}\text{H}$  and  $\text{C}^{13}\text{H}$ ), 7.75-7.65 (3H, m,  $\text{C}^{10}\text{H}$ ,  $\text{C}^{14}\text{H}$  and  $\text{C}^{12}\text{H}$ ), 6.47 (1H, ddd,  $^2J_{\text{HF}}$  54.6,  $^3J$  7.1,  $^3J$  3.3,  $\text{C}^7\text{H}$ ), 5.23-5.09 (1H, m,  $\text{C}^5\text{H}$ ), 3.64 (1H, dddd,  $^3J_{\text{HF}}$  23.1,  $^2J$  14.9,  $^3J$  7.6,  $^3J$  7.2,  $\text{C}^6\text{HH}$ ), 2.74 (1H, dddd,  $^3J_{\text{HF}}$  26.6,  $^2J$  14.9,  $^3J$  4.5,  $^3J$  3.4,  $\text{C}^6\text{HH}$ ), 1.84 (3H, d,  $^3J$  6.7,  $\text{CH}_3$ );  $^{13}\text{C}$  NMR (75 MHz,  $(\text{CD}_3)_2\text{CO}$ ):  $\delta$  = 159.5 (d,  $^2J_{\text{CF}}$  23.4,  $\text{C}^8$ ), 139.4 (NCHN), 136.9 ( $\text{C}^9$ ), 131.9 ( $\text{C}^{12}$ ), 131.1 (2C,  $\text{C}^{10}$  and  $\text{C}^{14}$ ), 122.2 (2C,  $\text{C}^{11}$  and  $\text{C}^{13}$ ), 85.0 (d,  $^1J_{\text{CF}}$  183.5,  $\text{C}^7$ ), 57.6 ( $\text{C}^5$ ), 43.5 (d,  $^2J_{\text{CF}}$  21.0,  $\text{C}^6$ ), 21.1 ( $\text{CH}_3$ );  $^{19}\text{F}$  NMR (282 MHz,  $(\text{CD}_3)_2\text{CO}$ ):  $\delta$  = -151.5 ( $^{10}\text{BF}_4^-$ ), -151.6 ( $^{11}\text{BF}_4^-$ ), -176.5 (dddd,  $^2J_{\text{HF}}$  54.2,  $^3J$  27.0,  $^3J$  23.2,  $^4J_{\text{HF}}$  4.1);  $[m/z$  (ESI) found: 218.1091 ( $\text{M}-\text{BF}_4^-$ ) $^+$ ,  $\text{C}_{12}\text{H}_{13}\text{FN}_3\text{O}^+$  requires 218.1088].

**(R)-5-Methyl-2-phenyl-6,7-dihydro-5H-pyrrolo-[2,1-c][1,2,4]-triazol-2-ium tetrafluoroborate (4)**



To a yellow solution of **18** (54.8 mg, 55.3  $\mu\text{mol}$ ) in  $\text{CH}_2\text{Cl}_2$  (5.5 mL) was added  $\text{Me}_3\text{O}^+\cdot\text{BF}_4^-$  (98.3 mg, 664  $\mu\text{mol}$ ) to give a suspension which turned into a colourless solution over 1 h. Phenylhydrazine was added to give a yellow solution. This was stirred for 3 h to give a bright red solution, which was concentrated *in vacuo*. The residue was dissolved in trimethyl orthoformate (5.5 mL) and heated to 50 °C. After 12 h the mixture was cooled to rt and concentrated *in vacuo* to give a brown oil. This was purified by column chromatography (MeOH :  $\text{CH}_2\text{Cl}_2$  / 1 : 20) to give a beige solid (82.0 mg, 52%).  $R_f$  0.21 (MeOH :  $\text{CH}_2\text{Cl}_2$  / 1 : 10); m.p. 120-124 °C;  $[\alpha]_D^{20}$  -23.1 (*c* 1.00 in acetone);  $\nu_{\text{max}}$  (neat)/ $\text{cm}^{-1}$  3133w, 2927w, 2265w, 2116w, 1981w, 1659w, 1591m, 1521m, 1497w, 1469m, 1438m, 1385m, 1318w, 1287w, 1223m, 1056s, 978m, 914s, 764s, 733s, 689m, 649m;  $^1\text{H}$  NMR (400 MHz,  $(\text{CD}_3)_2\text{CO}$ ):  $\delta$  = 10.44 (1H, s, NCHN), 8.01-7.90 (2H, m,  $\text{C}^{11}\text{H}$  and  $\text{C}^{13}\text{H}$ ), 7.74-7.59 (3H, m,  $\text{C}^{10}\text{H}$ ,  $\text{C}^{14}\text{H}$  and  $\text{C}^{12}\text{H}$ ), 5.08 (1H, sext,  $^3J$  6.8,  $\text{C}^5\text{H}$ ), 3.47-3.28 (2H, m,  $\text{C}^7\text{H}_2$ ), 3.14 (1H, dtd,  $^2J$  12.9,  $^3J$  7.6,  $^3J$  5.2,  $\text{C}^6\text{HH}$ ), 2.60 (1H, dddd,  $^2J$  13.1,  $^3J$  9.1,  $^3J$  8.2,  $^3J$  7.5,  $\text{C}^6\text{HH}$ ), 1.77 (3H, d,  $^3J$  6.5);  $^{13}\text{C}$  NMR (100 MHz,  $(\text{CD}_3)_2\text{CO}$ ):  $\delta$  = 163.6 ( $\text{C}^8$ ), 138.2 (NCHN), 137.0 ( $\text{C}^9$ ), 131.4 ( $\text{C}^{12}$ ), 131.1 (2C,  $\text{C}^{10}$  and  $\text{C}^{14}$ ), 121.8 (2C,  $\text{C}^{11}$  and  $\text{C}^{13}$ ), 58.5 ( $\text{C}^5$ ), 36.1 ( $\text{C}^6$ ), 22.5 ( $\text{C}^7$ ), 19.7 ( $\text{CH}_3$ );  $^{19}\text{F}$  NMR (282 MHz,  $(\text{CD}_3)_2\text{CO}$ ):  $\delta$  = -151.4 ( $^{10}\text{BF}_4^-$ ), -151.5 ( $^{11}\text{BF}_4^-$ ); [ $m/z$  (ESI) found: 200.1185 ( $\text{M-BF}_4^-$ ) $^+$ ,  $\text{C}_{12}\text{H}_{14}\text{N}_3^+$  requires 200.1183].

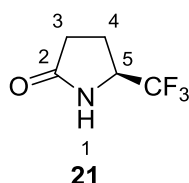
**(S)-tert-Butyl-2-(trifluoromethyl)-pyrrolidine-1-carboxylate (20)**



To a solution of **19** (178 mg, 1.28 mmol) in THF (13 mL) was added a solution of  $\text{Boc}_2\text{O}$  (279 mg, 1.28 mmol) in THF (2.0 mL) to give a colourless solution which was stirred for 15 h.  $\text{CH}_2\text{Cl}_2$  (50 mL) was added and the mixture was washed with water (50 mL). The organic layer was dried over  $\text{Na}_2\text{SO}_4$  and concentrated *in vacuo* to give a light yellow liquid

(306 mg; quant.) as a mixture of rotamers.  $R_f$  0.57 ( $\text{CH}_2\text{Cl}_2$ );  $[\alpha]_D^{20} +7.4$  ( $c$  0.75 in  $\text{CHCl}_3$ );  $\nu_{\text{max}}$  (neat)/ $\text{cm}^{-1}$  2980w, 2894w, 2289w, 2113w, 1982w, 1810w, 1774w, 1705s, 1480w, 1457w, 1393s, 1367s, 1310m, 1288m, 1270s, 1235m, 1208m, 1163s, 1137s, 1115s, 1068s, 982m, 922m, 905m, 882m, 847m, 808m, 774m, 682m, 608w;  $^1\text{H}$  NMR (600 MHz,  $\text{CDCl}_3$ ):  $\delta = 4.51$ - $4.25$  (1H, br m,  $\text{C}^2\text{H}$ ),  $3.61$ - $3.36$  (2H, br m,  $\text{C}^5\text{H}_2$ ),  $2.12$ - $1.85$  (4H, br m,  $\text{C}^3\text{H}_2$  and  $\text{C}^4\text{H}_2$ ),  $1.46$  (9H, s,  $t\text{Bu}$ );  $^{13}\text{C}$  NMR (150 MHz,  $\text{CDCl}_3$ ):  $\delta = 154.5$  (NCO),  $126.0$  (br q,  $^1J_{\text{CF}} 282$ ,  $\text{CF}_3$ ),  $80.7$  ( $\text{OC}(\text{CH}_3)_3$ ),  $57.9$  ( $\text{C}^2$ ),  $47.2$  and  $46.7$  ( $\text{C}^5$ ),  $28.4$  (3C,  $\text{C}(\text{CH}_3)_3$ ),  $26.6$ ,  $25.8$ ,  $23.9$  and  $23.0$  ( $\text{C}^3$  and  $\text{C}^4$ );  $^{19}\text{F}$  NMR (564 MHz,  $\text{CDCl}_3$ ):  $\delta = -75.1$  and  $-75.2$ ;  $[m/z$  (ESI) found:  $262.1028$  ( $\text{M}+\text{Na}$ ) $^+$ ,  $\text{C}_{10}\text{H}_{16}\text{F}_3\text{NO}_2\text{Na}^+$  requires  $262.1031$ ].

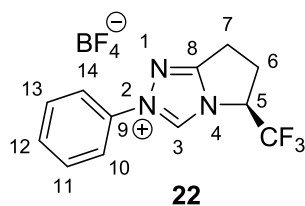
**(S)-5-(Trifluoromethyl)-pyrrolidin-2-one (21)**



To a solution of **20** (247 mg, 1.03 mmol) in EtOAc (5.0 mL) was added an aqueous solution of  $\text{NaIO}_4$  (10%, 30 mL) to give a biphasic mixture which was vigorously stirred. Ruthenium(III)chloride hydrate was added (47.0 mg,  $\sim 207$   $\mu\text{mol}$ ) to give a brown solution. After 14.5 h *i*-PrOH (15 mL) was added to the now yellow solution to give a black suspension, which was stirred for 3 h. Water (100 mL) was added and the mixture was extracted with EtOAc (200 mL). The organic layer was dried over  $\text{Na}_2\text{SO}_4$  and concentrated to give a brown oil (241 mg). This was dissolved in  $\text{CH}_2\text{Cl}_2$  (10 mL) and treated with TFA (1.0 mL). The solution was stirred for 45 min and poured into  $\text{NaHCO}_3$  (sat., 50 mL). The mixture was extracted with EtOAc (50 mL), the organic layer was dried over  $\text{Na}_2\text{SO}_4$  and concentrated *in vacuo* to give a yellow solid. This was purified by column chromatography ( $\text{MeOH} : \text{CH}_2\text{Cl}_2 / 1 : 10$ ) to give a light yellow solid (60.0 mg, 38% over 2 steps).  $R_f$  0.57 ( $\text{MeOH} : \text{CH}_2\text{Cl}_2 / 1 : 10$ ); m.p.  $104$ - $105$   $^\circ\text{C}$  (lit.<sup>[11]</sup>  $107$ - $108$   $^\circ\text{C}$ );  $[\alpha]_D^{20} +2.2$  ( $c$  0.66 in MeOH) (lit.<sup>[11]</sup>  $-5.5$  ( $c$  1.20 in MeOH));  $^1\text{H}$  NMR (300 MHz,  $\text{CDCl}_3$ ):  $\delta = 6.80$  (1H, br s,  $\text{NH}$ ),  $4.14$ - $4.00$  (1H, m,  $\text{NCH}$ ),  $2.60$ - $2.15$  (4H, m,  $\text{C}^3\text{H}_2$  and  $\text{C}^4\text{H}_2$ );  $^{13}\text{C}$  NMR (75 MHz,  $\text{CDCl}_3$ ):  $\delta = 178.5$  ( $\text{C}^2$ ),  $125.3$  (q,  $^1J_{\text{CF}} 280.5$ ,  $\text{CF}_3$ ),  $55.1$  (q,  $^2J_{\text{CF}} 32.5$ ,  $\text{NCH}$ ),  $28.5$  ( $\text{C}^3$ ),  $20.8$  (q,  $^3J_{\text{CF}} 1.8$ ,  $\text{C}^4$ );  $^{19}\text{F}$  NMR (282 MHz,  $\text{CDCl}_3$ ):  $\delta = -78.8$  (d,  $^3J 7.0$ ).

Data in agreement with the literature values<sup>[94]</sup>

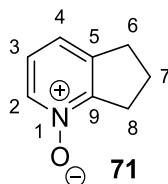
**(S)-2-Phenyl-5-(trifluoromethyl)-6,7-dihydro-5H-pyrrolo-[2,1-c][1,2,4]-triazol-2-ium tetrafluoroborate (22)**



To a light yellow solution of **21** (50.0 mg, 327  $\mu\text{mol}$ ) in  $\text{CH}_2\text{Cl}_2$  (3.0 mL) was added  $\text{Me}_3\text{O}^+\text{BF}_4^-$  (58.0 mg, 392  $\mu\text{mol}$ ) to give a suspension. This was stirred for 75 min, treated with phenylhydrazine (39  $\mu\text{L}$ , 392  $\mu\text{mol}$ ) and stirred for 13.5 h. The solution was concentrated *in vacuo* and the residue was dissolved in trimethyl orthoformate (3.0 mL). The solution was stirred at rt for 2.5 h, heated to 50  $^\circ\text{C}$  and stirred for 4.5 h. The yellow solution was cooled to rt and concentrated *in vacuo* to give a dark yellow oil. This material was purified by column chromatography ( $\text{MeOH} : \text{CH}_2\text{Cl}_2 / 1 : 15$ ) to give a brown solid which was washed with  $\text{CHCl}_3$  to give a beige solid (52.0 mg, 46%).  $R_f$  0.32 ( $\text{MeOH} : \text{CH}_2\text{Cl}_2 / 1 : 10$ ); m.p. 139-142  $^\circ\text{C}$ ;  $[\alpha]_D^{20} +117.9$  ( $c$  0.67 in acetone);  $\nu_{\text{max}}$  (neat)/ $\text{cm}^{-1}$  3109w, 3048w, 2981w, 2325w, 2164w, 1994w, 1760w, 1608m, 1595m, 1530m, 1514w, 1471w, 1443w, 1425w, 1383m, 1330w, 1291s, 1232w, 1179s, 1164m, 1137s, 1060s, 1048s, 1018s, 972s, 919m, 905m, 887m, 843s, 765s, 735m, 699m, 687s, 675s, 638m, 614w;  $^1\text{H}$  NMR (400 MHz,  $\text{CDCl}_3$ ):  $\delta$  = 10.7 (1H, s, NCHN), 8.03-7.96 (2H, m,  $\text{C}^{11}\text{H}$  and  $\text{C}^{13}\text{H}$ ), 7.75-7.65 (3H, m,  $\text{C}^{10}\text{H}$ ,  $\text{C}^{14}\text{H}$  and  $\text{C}^{12}\text{H}$ ), 5.92-5.82 (1H, m,  $\text{C}^5\text{H}$ ), 3.65-3.38 (3H, m,  $\text{C}^6\text{HH}$  and  $\text{C}^7\text{H}_2$ ), 3.18-3.08 (1H, m,  $\text{C}^6\text{HH}$ );  $^{13}\text{C}$  NMR (100 MHz,  $\text{CDCl}_3$ ):  $\delta$  = 164.4 ( $\text{C}^8$ ), 139.7 (NCHN), 136.8 ( $\text{C}^9$ ), 132.0 ( $\text{C}^{12}$ ), 131.0 (2C,  $\text{C}^{10}$  and  $\text{C}^{14}$ ), 124.4 (q,  $^1J_{\text{CF}}$  279.9,  $\text{CF}_3$ ), 122.5 (2C,  $\text{C}^{11}$  and  $\text{C}^{13}$ ), 60.6 (q,  $^2J_{\text{CF}}$  34.7,  $\text{C}^5$ ), 29.0 (q,  $^3J_{\text{CF}}$  1.5,  $\text{C}^6$ ), 21.7 ( $\text{C}^7$ );  $^{19}\text{F}$  NMR (282 MHz,  $\text{CDCl}_3$ ):  $\delta$  = -76.0 (d,  $^3J$  7.0,  $\text{CF}_3$ ), -152.0 ( $^{10}\text{BF}_4^-$ ), -152.1 ( $^{11}\text{BF}_4^-$ ); [ $m/z$  (ESI) found: 254.0905 ( $\text{M-BF}_4^-$ ) $^+$ ,  $\text{C}_{12}\text{H}_{11}\text{F}_3\text{N}_3\text{O}^+$  requires 254.0900].

## Dimethylaminopyridine Derivatives

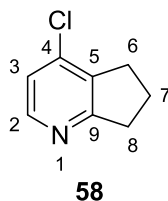
### 6,7-Dihydro-5H-cyclopenta[b]pyridine-1-oxide (71)



To **70** (2.00 g, 16.8 mmol) was added acetic acid (10 mL) and hydrogen peroxide (30%, 1.80 mL, 17.5 mmol) to give an orange solution which was stirred at 80 °C for 13 h to give a slightly yellow solution. Another portion of hydrogen peroxide (30%, 1.80 mL, 17.5 mmol) was added and the solution stirred for two more hours at 80 °C. The solution was cooled to 0 °C, carefully neutralised with NaHCO<sub>3</sub> (sat., 150 mL) and extracted with CH<sub>2</sub>Cl<sub>2</sub> (3 x 150 mL). The combined organic layers were dried (Na<sub>2</sub>SO<sub>4</sub>) and concentrated *in vacuo* to give a beige solid (1.73 g, 76%); R<sub>f</sub> 0.32 (MeOH : CH<sub>2</sub>Cl<sub>2</sub> / 1 : 25); m.p. 109-113 °C; <sup>1</sup>H NMR (300 MHz, CDCl<sub>3</sub>): δ = 8.06-8.01 (1H, m, C2H), 7.14-6.97 (2H, m, C3H and C4H), 3.17 (2H, t, <sup>3</sup>J 7.7, C8H<sub>2</sub>), 3.06-2.97 (2H, m, C6H<sub>2</sub>) and 2.24-2.10 (2H, m, C7H<sub>2</sub>).

Data in agreement with the literature values<sup>[70]</sup>

### 4-Chloro-6,7-dihydro-5H-cyclopenta[b]pyridine (58)

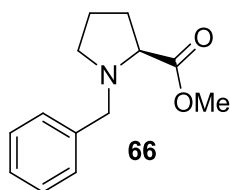


To a solution of **71** (1.50 g, 11.1 mmol) in 1,2-dichloroethane (50 mL) at 0 °C in a dry flask was added POCl<sub>3</sub> (2.03 mL, 22.2 mmol) over a period of 10 min to give a yellow solution. This was stirred at rt for 30 min during that time a change of colour to brown was observed. The solution was heated to 80 °C, stirred for 2 h and cooled to rt. Ice was added, the mixture was neutralised by means of NaOH (6 M) and extracted with CHCl<sub>3</sub> (3 x 50 mL). The combined organic layers were dried (Na<sub>2</sub>SO<sub>4</sub>) and concentrated *in vacuo* to give a red liquid. This was purified by column chromatography (EtOAc : cyclohexane / 1 : 1) to give a light red oil (553 mg, 33%); R<sub>f</sub> 0.33 (EtOAc : *c*-Hex : NEt<sub>3</sub> / 1 : 1 : 0.02); <sup>1</sup>H NMR (300 MHz, CDCl<sub>3</sub>): δ = 8.22 (1H, d, <sup>3</sup>J 5.5, C2H), 7.05 (1H, d, <sup>3</sup>J 5.5, C3H), 3.09 and 3.00 (4H, t, <sup>3</sup>J 7.7, C6H<sub>2</sub> and C8H<sub>2</sub>) and 2.22-2.09 (2H, m, C7H<sub>2</sub>).

Data in agreement with the literature values<sup>[70]</sup>



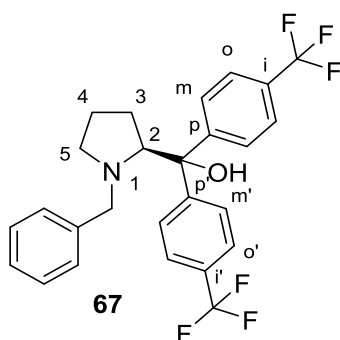
**(S)-Methyl-1-benzylpyrrolidine-2-carboxylate (66)**



To a colourless solution of L-Proline (5.76 g, 50.0 mmol) in MeOH (100 mL) at 0 °C, SOCl<sub>2</sub> (4.38 mL, 60.0 mmol) was added over a period of 10 min. The solution was warmed to rt and stirred at reflux for 2 h. The solution was cooled to rt and the solvent was removed *in vacuo*. The residue was co-evaporated with toluene (3 x 20 mL) to give a colourless oil, which was dissolved in toluene (50 mL). DIPEA (42.7 mL, 247 mmol) was added and the solution was cooled to 0 °C for the addition of BnBr (6.54 mL, 55.0 mmol) over a period of 10 min. The resulting white suspension was stirred at reflux for 14 h, then cooled to rt., NaHCO<sub>3</sub> (sat., 50 mL) was added and the mixture was extracted with EtOAc (2 x 50 mL). The combined organic layers were washed with brine (2 x 50 mL), dried (Na<sub>2</sub>SO<sub>4</sub>) and concentrated *in vacuo* to give a brown oil, which was purified by distillation (75 °C, 0.3 mbar) to give a colourless oil (9.41 g, 86%). <sup>1</sup>H NMR (300 MHz, CDCl<sub>3</sub>): δ = 7.21-7.36 (5H, m, C<sub>6</sub>H<sub>5</sub>), 3.89 (1H, d, <sup>2</sup>J 12.8, C<sub>6</sub>H<sub>5</sub>), 3.65 (3H, s, CH<sub>3</sub>), 3.57 (1H, d, <sup>2</sup>J 12.8, NCHHPh), 3.25 (1H, dd, <sup>3</sup>J 8.8, <sup>3</sup>J 6.2, NCH), 3.01-3.09 (1H, m, NCHHCH<sub>2</sub>), 2.34-2.44 (1H, m, NCHHCH<sub>2</sub>), 2.04-2.21 (1H, m, NCHCHH), 1.68-2.03 (3H, m, NCHCHH and NCH<sub>2</sub>CH<sub>2</sub>), R<sub>f</sub> = 0.47 (MeOH / CH<sub>2</sub>Cl<sub>2</sub> 1:70, UV254 nm).

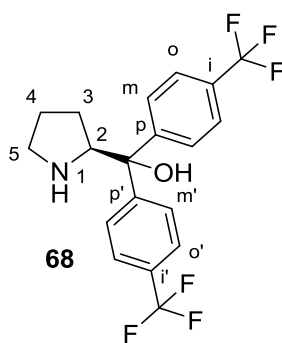
Data in agreement with literature values<sup>[95]</sup>

(S)-(1-Benzylpyrrolidin-2-yl)-bis-(4-(trifluoromethyl)-phenyl)-methanol (67)



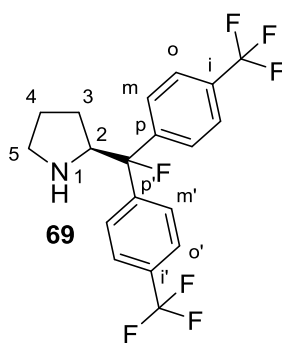
To a suspension of activated magnesium (173 mg, 7.11 mmol) in a yellow solution of iodine (2.00 mg, 7.88  $\mu\text{mol}$ ), in THF (500  $\mu\text{L}$ ) in a dry flask was added **65** (1.00 mL, 7.11 mmol) while heating to reflux. As soon as a change of colour to dark red was observed more THF (5.0 mL) was added while the mixture was still maintained at reflux. After 15 min the solution was cooled to 0  $^{\circ}\text{C}$  and a solution of (S)-methyl-1-benzylpyrrolidine-2-carboxylate (625 mg, 2.84 mmol) in THF (1.0 mL) was added over a period of 5 min. The mixture was stirred at rt for 23 h, cooled to 0  $^{\circ}\text{C}$  and HCl (conc., 5.0 mL) was added. The mixture was stirred for 2 h, THF was evaporated *in vacuo*, the mixture cooled to 0  $^{\circ}\text{C}$  and set basic (pH 10) with NaOH (3 M). A change of colour from red to yellow was observed. Water (40 mL) was added and the mixture was extracted with  $\text{CH}_2\text{Cl}_2$  (80 mL). The organic layer was dried over  $\text{Na}_2\text{SO}_4$  and concentrated *in vacuo* to give a brown oil. This was purified by column chromatography (EtOAc :  $^{\circ}\text{Hex}$  / 1 : 20) to give a colourless oil (64%);  $R_f$  0.50 (EtOAc :  $^{\circ}\text{Hex}$  / 1 : 10);  $[\alpha]_D^{25} +4.3$  ( $c$  1.00 in  $\text{CHCl}_3$ );  $\nu_{\text{max}}$  (neat)/ $\text{cm}^{-1}$  3029w, 2951w, 2878w, 2810w, 1616m, 1496w, 1455w, 1416m, 1373m, 1323s, 1163s, 1122s, 1069s, 1017s, 909m, 852m, 824m, 734m, 700m, 652m;  $^1\text{H}$  NMR (400 MHz,  $\text{CDCl}_3$ ):  $\delta$  = 7.88 (2H, d,  $^3J$  8.2,  $C^m$ ), 7.72 (2H, d,  $^3J$  8.2,  $C^{m'}$ ), 7.59 (2H, d,  $^3J$  8.2,  $C^{o'}$ ), 7.57 (2H, d,  $^3J$  8.2,  $C^o$ ), 7.30 – 7.19 (3H, m, Bn ortho and Bn para), 7.06 – 7.00 (2H, m, Bn meta), 5.25 (1H, br s, OH), 4.06 (1H, dd,  $^3J$  9.1,  $^3J$  4.5,  $C^2H$ ), 3.29 (1H, d,  $^2J$  12.8, NCHHPh), 3.13 (1H, d,  $^2J$  12.8, NCHHPh), 3.02 – 2.94 (1H, m,  $C^5HH$ ), 2.50 – 2.40 (1H, m,  $C^5HH$ ), 2.04 – 1.90 (1H, m,  $C^3HH$ ), 1.73 – 1.62 (3H, m,  $C^3HH$  and  $C^4H_2$ );  $^{13}\text{C}$  NMR (100 MHz,  $\text{CDCl}_3$ ):  $\delta$  = 151.5 ( $C^p$ ), 149.9 ( $C^{p'}$ ), 139.0 (Bn ipso), 129.1 (q,  $^2J_{\text{CF}}$  32.5,  $C^i$ ), 128.9 (q,  $^2J_{\text{CF}}$  32.4,  $C^{i'}$ ), 128.4 (2C, Bn meta), 128.3 (2C, Bn ortho), 127.2 (Bn para), 126.0 ( $C^m$ ), 125.9 ( $C^{m'}$ ), 125.4 (q,  $^3J_{\text{CF}}$  3.9,  $C^o$ ), 125.3 (q,  $^3J_{\text{CF}}$  3.8,  $C^{o'}$ ), 124.1 (q,  $^1J_{\text{CF}}$  272.0,  $\text{CF}_3$ ), 124.0 (q,  $^1J_{\text{CF}}$  272.2,  $\text{CF}_3'$ ), 77.6 ( $\text{CAr}_2\text{OH}$ ), 70.4 ( $C^2$ ), 60.5 (NCH<sub>2</sub>Ph), 55.5 ( $C^5$ ), 29.9 ( $C^3$ ), 24.0 ( $C^4$ );  $^{19}\text{F}$  NMR (376 MHz,  $\text{CDCl}_3$ ):  $\delta$  = -62.4 and -62.5 (two s, 2 x 3F,  $\text{CF}_3$  and  $\text{CF}_3'$ );  $[m/z]$  (ESI) found: 480.1772  $[\text{M}+\text{H}]^+$ ,  $\text{C}_{26}\text{H}_{24}\text{F}_6\text{NO}$  requires 480.1757].

(S)-Pyrrolidin-2-ylbis-(4-(trifluoromethyl)-phenyl)-methanol (**68**)



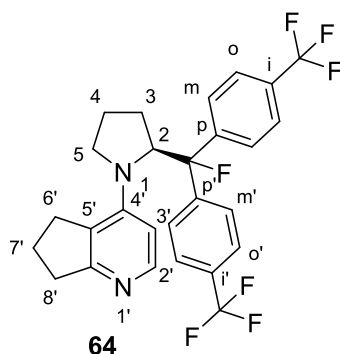
A black suspension of palladium on carbon (10%, 1.14 g) in a solution of **67** (3.65 g, 7.62 mmol) and HCl (conc. 926  $\mu$ L) in EtOH (70 mL) was evacuated and set under an atmosphere of hydrogen. This was repeated twice and the mixture was stirred for 4 h. The mixture was filtered over celite, which was flushed with EtOH. The solvent was removed *in vacuo* to give a white solid. EtOAc (250 mL) and NaOH (1 M, 250 mL) was added to give a biphasic mixture of pH 9. The layers were separated and the aqueous layer was extracted with EtOAc (250 mL). The combined organic layers were dried over Na<sub>2</sub>SO<sub>4</sub> and concentrated *in vacuo* to give a slightly orange oil (2.92 g, 99%);  $R_f$  0.19 (EtOAc);  $[\alpha]_D^{25}$  -2.8 (*c* 1.00 in CDCl<sub>3</sub>);  $\nu_{\max}$  (neat)/cm<sup>-1</sup> 3356w, 2949w, 2878w, 1616m, 1415m, 1322s, 1161s, 1120s, 1097s, 1068s, 1017s, 995m, 909m, 831s, 770m, 734m; <sup>1</sup>H NMR (400 MHz, CDCl<sub>3</sub>):  $\delta$  = 7.70 (2H, d, <sup>3</sup>*J* 8.2, *C<sup>m</sup>*), 7.63 (2H, d, <sup>3</sup>*J* 8.3, *C<sup>m'</sup>*), 7.57 (2H, d, <sup>3</sup>*J* 8.3, *C<sup>o'</sup>*), 7.44 (2H, d, <sup>3</sup>*J* 8.2, *C<sup>o</sup>*), 4.79 (1H, br s, OH), 4.30 (1H, t, <sup>3</sup>*J* 7.7, *C<sup>2H</sup>*), 3.11 – 2.93 (2H, m, *C<sup>5H2</sup>*), 1.82 – 1.71 (2H, m, *C<sup>4H2</sup>*), 1.63 – 1.54 (2H, m, *C<sup>3H2</sup>*); <sup>13</sup>C NMR (100 MHz, CDCl<sub>3</sub>):  $\delta$  = 151.5 (*C<sup>p</sup>*), 148.6 (*C<sup>p'</sup>*), 129.3 (q, <sup>2</sup>*J*<sub>CF</sub> 32.5, *C<sup>i</sup>*), 129.1 (q, <sup>2</sup>*J*<sub>CF</sub> 32.4, *C<sup>i'</sup>*), 126.4 (*C<sup>m</sup>*), 126.0 (*C<sup>m'</sup>*), 125.5 (q, <sup>3</sup>*J*<sub>CF</sub> 3.8, *C<sup>o</sup>*), 125.3 (q, <sup>3</sup>*J*<sub>CF</sub> 3.8, *C<sup>o'</sup>*), 122.92 (q, <sup>1</sup>*J*<sub>CF</sub> 271.9, CF<sub>3</sub>), 122.87 (q, <sup>1</sup>*J*<sub>CF</sub> 272.1, CF<sub>3</sub>'), 77.1 (CAr<sub>2</sub>OH, partially covered by solvent peak), 64.3 (*C<sup>2</sup>*), 47.0 (*C<sup>5</sup>*), 26.6 (*C<sup>3</sup>*), 26.6 (*C<sup>4</sup>*); <sup>19</sup>F NMR (376 MHz, CDCl<sub>3</sub>):  $\delta$  = -62.50 and -62.54 (two s, 2 x 3F, CF<sub>3</sub> and CF<sub>3</sub>'); [*m/z* (ESI) found: 390.1297 [M+H]<sup>+</sup>, C<sub>19</sub>H<sub>18</sub>F<sub>6</sub>NO requires 390.1287].

(S)-2-(Fluorobis-(4-(trifluoromethyl)-phenyl)-methyl)-pyrrolidine (**69**)



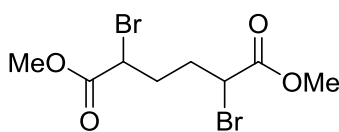
To a colourless solution of **68** (320 mg, 823  $\mu\text{mol}$ ) in  $\text{CH}_2\text{Cl}_2$  (9.0 mL) in a centrifuge tube at 0 °C was added DAST (202  $\mu\text{L}$ , 1.65 mmol) over a period of 2 min. The solution was stirred at 0 °C, a change of colour from slightly yellow to red was observed. After 14 h the mixture was slowly allowed to warm to rt (4.5 h) and cooled to 0 °C again.  $\text{NaHCO}_3$  (sat., 10 mL) was slowly added and an evolution of gas was observed. The layers were separated and the aqueous layer was extracted with  $\text{CH}_2\text{Cl}_2$  (3 x 10 mL). The combined organic layers were dried over  $\text{Na}_2\text{SO}_4$  and concentrated *in vacuo* to give a brown oil. This was purified by column chromatography ( $\text{MeOH} : \text{CH}_2\text{Cl}_2 : \text{NH}_3(\text{aq}) / 1 : 100 : 0.1$ ) to give a yellow oil (76 mg). This was further purified by protonation ( $\text{HCl}$  in  $\text{MeOH}$ ) and crystallisation from  $\text{MeOH} / \text{Et}_2\text{O}$  to give a white solid (34.6 mg, 10%);  $R_f$  0.67 ( $\text{MeOH} : \text{CH}_2\text{Cl}_2 : \text{NH}_3(\text{aq}) / 1 : 50 : 0.1$ ); m.p.  $\geq 210$  °C (decomp.);  $[\alpha]_D^{25}$  -2.4 ( $c$  1.00 in  $\text{CDCl}_3$ );  $\nu_{\text{max}}$  (neat)/ $\text{cm}^{-1}$  3287w, 2950w 2872w, 1618w, 1416m, 1322s, 1160s, 1119s, 1065s, 1019s, 992m, 910w, 826s, 770m, 733m, 710m, 669m, 639w, 605m;  $^1\text{H}$  NMR (400 MHz,  $\text{CDCl}_3$ ):  $\delta$  = 7.69 (2H, d,  $^3J$  8.4,  $C^m$ ), 7.63 (2H, d,  $^3J$  8.3,  $C^o$ ), 7.61 (2H, d,  $^3J$  8.3,  $C^{o'}$ ), 7.55 (2H, d,  $^3J$  8.4,  $C^{m'}$ ), 4.26 (1H, dt,  $^3J_{\text{HF}}$  27.3,  $^3J$  7.3,  $C^2\text{H}$ ), 3.07 – 2.98 (1H, m,  $C^5\text{H}_a$ ), 2.93 – 2.84 (1H, m,  $C^5\text{H}_b$ ), 1.88 – 1.68 (4H, m,  $C^3\text{H}_2$  and  $C^4\text{H}_2$ );  $^{13}\text{C}$  NMR (100 MHz,  $\text{CDCl}_3$ ):  $\delta$  = 145.8 (d,  $^2J_{\text{CF}}$  23.7,  $C^p$ ), 145.3 (d,  $^2J_{\text{CF}}$  24.5,  $C^{p'}$ ), 130.4 (q,  $^2J_{\text{CF}}$  32.6,  $C^i$ ), 130.3 (q,  $^2J_{\text{CF}}$  32.6,  $C^{i'}$ ), 126.2 (d,  $^3J_{\text{CF}}$  9.5,  $C^m$ ), 125.9 – 125.6 (2C, m,  $C^o$  and  $C^{o'}$ ), 125.4 (d,  $^3J_{\text{CF}}$  9.6,  $C^{m'}$ ), 124.0 and 123.9 (two q,  $^1J_{\text{CF}}$  272.7 and 272.2,  $\text{CF}_3$  and  $\text{CF}_3'$ ), 99.3 (d,  $^1J_{\text{CF}}$  184.7,  $\text{C}_{\text{Ar}_2\text{F}}$ ), 64.5 (d,  $^2J_{\text{CF}}$  22.4,  $C^2$ ), 47.7 ( $C^5$ ), 26.8 (d,  $^3J_{\text{CF}}$  3.3,  $C^3$ ), 26.0 ( $C^4$ );  $^{19}\text{F}$  NMR (376 MHz,  $\text{CDCl}_3$ ):  $\delta$  = -63.3 and -63.4 (two s, 2 x 3F,  $\text{CF}_3$  and  $\text{CF}_3'$ ), -169.8 (d, 1F,  $^3J$  31.3,  $\text{C}_{\text{Ar}_2\text{F}}$ );  $[m/z]$  (ESI) found: 392.1250  $[\text{M}+\text{H}]^+$ ,  $\text{C}_{19}\text{H}_{17}\text{F}_7\text{N}^+$  requires 392.1244].

(S)-4-(2-(Fluorobis-(4-(trifluoromethyl)-phenyl)-methyl)-pyrrolidin-1-yl)-6,7-dihydro-5H-cyclopenta[*b*]pyridine (**64**)



To a mixture of **69** (78.2 mg, 200  $\mu\text{mol}$ ), palladium(II)acetate (4.50 mg, 20.0  $\mu\text{mol}$ ), **58** (17.1 mg, 40.0  $\mu\text{mol}$ ) and KO<sup>t</sup>Bu (89.6 mg, 800  $\mu\text{mol}$ ) in a dry flask was added a solution of 4-chloro-6,7-dihydro-5H-cyclopenta[*b*]pyridine (30.8 mg, 200  $\mu\text{mol}$ ) in toluene (2.00 mL). The brown suspension was heated to 110 °C, stirred at that temperature for 14 h, cooled to rt and filtered over celite, which was washed with EtOAc. The solution was concentrated *in vacuo* to give a dark red oil. This was purified by column chromatography (MeOH : CH<sub>2</sub>Cl<sub>2</sub> : NH<sub>3(aq)</sub> / 1 : 50 : 0.1) to give a yellow solid (45.0 mg, 44%);  $R_f$  = 0.31 (MeOH : CH<sub>2</sub>Cl<sub>2</sub> / 1 : 50, UV (254 nm)); m.p. 61-63 °C;  $[\alpha]_D^{25}$  +9.1 (*c* 1.00 in CDCl<sub>3</sub>);  $\nu_{\text{max}}$  (neat)/cm<sup>-1</sup> 2961w, 1619w, 1579m, 1480m, 1412m, 1372m, 1321s, 1163s, 1118s, 1068s, 1017s, 900w, 833s, 804m, 772m, 713m, 670m; <sup>1</sup>H NMR (400 MHz, CDCl<sub>3</sub>):  $\delta$  = 7.80 (1H, d, <sup>3</sup>*J* 5.8 Hz, C<sup>2</sup>*H*), 7.69 (2H, d, <sup>3</sup>*J* 8.5 Hz, 2 x C<sup>o</sup>*H*), 7.58 (2H, d, <sup>3</sup>*J* 8.4 Hz, 2 x C<sup>m</sup>*H*), 7.41 (2H, d, <sup>3</sup>*J* 8.9 Hz, 2 x C<sup>m'</sup>*H*), 7.38 (2H, d, <sup>3</sup>*J* 8.9 Hz, 2 x C<sup>o'</sup>*H*), 6.15 (1H, d, <sup>3</sup>*J* 5.9 Hz, C<sup>3'</sup>*H*), 5.17 (1H, ddd, <sup>3</sup>*J*<sub>HF</sub> 24.4 Hz, <sup>3</sup>*J* 8.6 Hz, <sup>3</sup>*J* 2.5 Hz, C<sup>2</sup>*H*), 3.71 - 3.79 (1H, m, C<sup>5</sup>*HH*), 3.28 - 3.37 (1H, m, C<sup>5</sup>*HH*), 2.69 - 3.97 (4H, m, C<sup>6'</sup>*H*<sub>2</sub> and C<sup>8'</sup>*H*<sub>2</sub>), 2.14 - 2.27 (1H, m, C<sup>3</sup>*HH*), 1.75 - 2.07 (5H, m, C<sup>3</sup>*HH*, C<sup>3</sup>*H*<sub>2</sub> and C<sup>7'</sup>*H*<sub>2</sub>); <sup>13</sup>C NMR (100 MHz, CDCl<sub>3</sub>):  $\delta$  = 166.3 (C<sup>9'</sup>), 152.3 (C<sup>4'</sup>), 147.4 (C<sup>2'</sup>), 144.6 (d, <sup>2</sup>*J*<sub>CF</sub> 22.9, C<sup>p</sup>), 144.0 (d, <sup>2</sup>*J*<sub>CF</sub> 24.0, C<sup>p'</sup>), 130.9 (q, <sup>2</sup>*J*<sub>CF</sub> 32.8, C<sup>i</sup>), 130.7 (q, <sup>2</sup>*J*<sub>CF</sub> 32.5, C<sup>i'</sup>), 127.0 (2C, d, <sup>3</sup>*J*<sub>CF</sub> 6.2, C<sup>m'</sup>), 126.9 (2C, d, <sup>3</sup>*J*<sub>CF</sub> 6.4, C<sup>m</sup>), 125.6 (q, <sup>3</sup>*J*<sub>CF</sub> 3.8, C<sup>o</sup>), 124.7 (q, <sup>3</sup>*J*<sub>CF</sub> 3.7, C<sup>o'</sup>), 123.9 (q, <sup>1</sup>*J*<sub>CF</sub> 272.8, CF<sub>3</sub>), 123.8 (q, <sup>1</sup>*J*<sub>CF</sub> 272.5, CF<sub>3</sub>'), 122.0 (C<sup>5'</sup>), 108.3 (C<sup>3'</sup>), 101.6 (d, <sup>1</sup>*J*<sub>CF</sub> 185.0, CAr<sub>2</sub>F), 63.4 (d, <sup>2</sup>*J*<sub>CF</sub> 21.8, C<sup>2</sup>), 52.3 (C<sup>5</sup>), 34.4 and 32.4 (C<sup>6'</sup> and C<sup>8'</sup>), 28.5 (d, <sup>3</sup>*J*<sub>CF</sub> 3.0, C<sup>3</sup>), 24.0 (d, <sup>4</sup>*J*<sub>CF</sub> 2.6, C<sup>4</sup>), 23.0 (C<sup>7'</sup>); <sup>19</sup>F NMR (376 MHz, CDCl<sub>3</sub>):  $\delta$  = -62.7 and -62.9 (two s, 2 x 3F, CF<sub>3</sub> and CF<sub>3</sub>'), -155.3 (br s, 1F, CAr<sub>2</sub>F); [HR-MS (ESI): Found 509.1815 [M+H]<sup>+</sup>. C<sub>27</sub>H<sub>24</sub>F<sub>7</sub>N<sub>2</sub><sup>+</sup>: requires 509.1823].

**Dimethyl-2,5-dibromohexanedioate (74 and 75)**

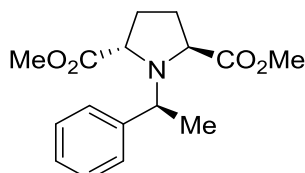


**74 and 75**

A dry flask was loaded with **73** (20.0 mL, 138 mmol) and heated to 70 °C. Bromine (16.4 mL, 319 mmol) was added in portions over a period of 8.5 h and stirred for 13 h. The mixture was cooled to rt and nitrogen was bubbled through it for 5 min. The gases were passed into Na<sub>2</sub>S<sub>2</sub>O<sub>3</sub> (sat.) followed by NaOH (1 M). The mixture was transferred via cannula into a flask loaded with MeOH (100 mL) at 0 °C, allowed to warm to rt and stirred for 3 h. The solution was concentrated *in vacuo*, dissolved in EtOAc (1 L), washed with Na<sub>2</sub>S<sub>2</sub>O<sub>3</sub> (sat., 500 mL), dried (Na<sub>2</sub>SO<sub>4</sub>) and concentrated *in vacuo* to give a pale yellow oil and a brown solid (mixture of diastereomers, 45.0 g, 98%); *R<sub>f</sub>* = 0.23 (EtOAc : cyclohexane / 1 : 10, KMnO<sub>4</sub>); <sup>1</sup>H NMR (300 MHz, CDCl<sub>3</sub>): δ = 4.21 – 4.29 (2H, m, CHBr), 3.79 (6H, two s, CO<sub>2</sub>CH<sub>3</sub>), 1.99 – 2.40 (4H, m, CHCH<sub>2</sub>CH<sub>2</sub>).

Data in agreement with the literature values<sup>[73]</sup>

**(2*S*,5*S*)-Dimethyl-1-((*S*)-1-phenylethyl)-pyrrolidine-2,5-dicarboxylate (77)**



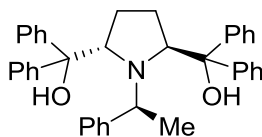
**77**

A biphasic solution of a mixture of **74** and **75** (10.4 g, 31.3 mmol), (*S*)-1-phenylethylamine (4.00 mL, 31.3 mmol) and K<sub>2</sub>CO<sub>3</sub> (5.19 g, 37.6 mmol) in a mixture of toluene (20 mL) and water (10 mL) was stirred at reflux for 22 h. The mixture was cooled to rt, the two layers were separated and the aqueous layer was extracted with cyclohexane (2 x 100 mL). The combined organic layers were washed with brine (200 mL), dried (Na<sub>2</sub>SO<sub>4</sub>) and concentrated *in vacuo* to give an orange oil (10 g). This was separated into the three diastereomers to give a slightly yellow oil ((*S*),(*S*),(*S*), 2.2 g, 24%), [a white solid ((*R*),(*R*),(*S*), 1.3 g, 14%) and a yellow oil (meso, 470 mg, 5.2%)]. (*S*),(*S*),(*S*): *R<sub>f</sub>* = 0.46 (EtOAc : cyclohexane / 1 : 5, KMnO<sub>4</sub>); [*α*]<sub>D</sub><sup>25</sup> = -84.6 (*c* 1.50, CHCl<sub>3</sub>, Lit.<sup>[73]</sup> -107.0); <sup>1</sup>H NMR (300 MHz, CDCl<sub>3</sub>): δ = 7.17 – 7.35 (5H, m, C<sub>6</sub>H<sub>5</sub>), 4.00 (1H, q, <sup>3</sup>*J* 6.6 Hz, PhCH), 3.75 – 3.81 (2H, m, NCHCH<sub>2</sub>), 3.65 (6H, s,

2 x CO<sub>2</sub>CH<sub>3</sub>), 2.24 – 2.42 (2H, m, 2 x NCHCHH), 1.74 – 1.91 (2H, m, 2 x NCHCHH), 1.29 (3H, d, <sup>3</sup>J 6.7 Hz, NCHCH<sub>3</sub>).

Data in agreement with the literature values<sup>[72]</sup>

**((2*S*,5*S*)-1-((*S*)-1-Phenylethyl)-pyrrolidine-2,5-diyl)-bis-(diphenylmethanol) (80)**

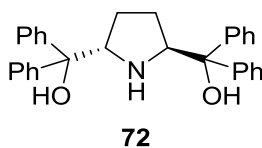


**80**

CeCl<sub>3</sub>·H<sub>2</sub>O (5.47 g, 20.6 mmol) was stirred at 135 °C under vacuum for 16 h. Argon was introduced and white powder was cooled to rt. THF (70 mL, dry) was added and the resulting suspension was stirred for 2 h and cooled to 0 °C. PhMgBr (2.8 M in Et<sub>2</sub>O, 7.36 mL, 20.6 mmol) was added over a period of 3 min to give a brown suspension, which was stirred at 0 °C for 1.5 h. A solution of **77** (1.00 g, 3.44 mmol) in THF (5.0 mL, dry) was added to give a yellow suspension, which was stirred for 1 h, warmed to rt and stirred for 18.5 h. Acetic acid in water (5 mL in 100 mL) was added to the brown suspension at 0 °C to give a green solution. The layers were separated and the aqueous layer was extracted with EtOAc (4 x 100 mL). The combined organic layers were washed with brine (3 x 35 mL), NaHCO<sub>3</sub> (sat., 2 x 35 mL) and brine again (35 mL), dried (Na<sub>2</sub>SO<sub>4</sub>) and concentrated *in vacuo* to give a brown solid. This was purified by column chromatography (EtOAc : cyclohexane / 1 : 10 → 1 : 6) to give a white solid (881 mg, 47%, m.p. 207 – 209 °C, Lit.<sup>[72]</sup> 210 - 211 °C); R<sub>f</sub> = 0.17 (EtOAc : cyclohexane / 1 : 10, Ninhydrin); [α]<sub>D</sub><sup>25</sup> = - 106.0 (c 1.00, CHCl<sub>3</sub>, Lit.<sup>[72]</sup> - 105.3); <sup>1</sup>H NMR (300 MHz, CDCl<sub>3</sub>): δ = 7.02 – 7.50 (23H, m, aromatic H), 6.57 – 6.67 (2H, m, aromatic H), 4.44 (1H, q, <sup>3</sup>J 6.7 Hz, PhCH), 3.73 – 3.90 (2H, m, 2 x NCH), 2.95 (2H, br s, 2 x OH), 1.92 – 2.10 (2H, m, 2 x NCHCHH), 1.62 – 1.84 (2H, m, 2 x NCHCHH), 1.50 (3H, d, <sup>3</sup>J 6.6 Hz, NCHCH<sub>3</sub>).

Data in agreement with the literature values<sup>[72]</sup>

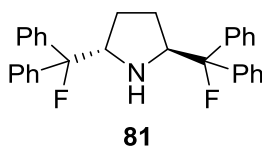
**(2*S*,5*S*)-Pyrrolidine-2,5-diylbis-(diphenylmethanol) (72)**



A black suspension of **80** (844 mg, 1.56 mmol), palladium on carbon (10%, 220 mg) in MeOH (20 mL) was set under an atmosphere of hydrogen and stirred at rt for 61 h. It was filtered over celite, which was washed with MeOH (100 mL) and EtOAc (250 mL). The solution was concentrated *in vacuo* to give a white solid, which was recrystallised from EtOAc to give a white solid (515 mg, 76%, m.p. 229 – 231 °C, Lit.<sup>[72]</sup> 234 - 235 °C);  $R_f = 0.53$  (EtOAc : cyclohexane / 1 : 5, UV(254 nm), Ninhydrin);  $[\alpha]_D^{25} = -102.6$  ( $c$  1.50, CHCl<sub>3</sub>, Lit.<sup>[72]</sup> -106.6); <sup>1</sup>H NMR (300 MHz, CDCl<sub>3</sub>):  $\delta = 7.11 - 7.50$  (20H, m, aromatic H), 4.30 – 4.39 (2H, m, 2 x NCH), 3.48 (2H, br s, OH), 1.44 – 1.76 (5H, m, NH and NCHCH<sub>2</sub>CH<sub>2</sub>).

Data in agreement with the literature values<sup>[72]</sup>

**(2*S*,5*S*)-2,5-Bis-(fluorodiphenylmethyl)-pyrrolidine (81)**

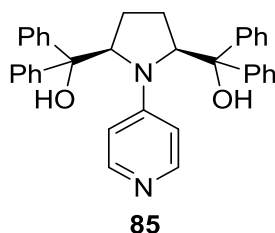


A centrifuge vial was loaded with **72** (400 mg, 917  $\mu$ mol), which was stirred under vacuum for 30 min before argon was introduced and CH<sub>2</sub>Cl<sub>2</sub> (10 mL) was added to give a white suspension. This was cooled to 0 °C and DAST (448  $\mu$ L, 3.66 mmol) was added over a period of 5 min to give a bright red solution which was allowed to warm to rt over a period of 8 h. NaHCO<sub>3</sub> (sat., 25 mL) was added slowly at 0 °C which caused a evolution of gas. CH<sub>2</sub>Cl<sub>2</sub> (15 mL) was added and the layers were separated. The aqueous layer was extracted with CH<sub>2</sub>Cl<sub>2</sub> (3 x 15 mL) and the combined organic layers were dried (Na<sub>2</sub>SO<sub>4</sub>) and concentrated *in vacuo* to give a brown oil. This was purified by column chromatography (MeOH : CH<sub>2</sub>Cl<sub>2</sub> : NH<sub>3(aq)</sub> / 1 : 200 : 0.1) to give an orange solid, which was recrystallised from EtOAc to give a white solid (55.9 mg, 14%);  $R_f$  0.30 (EtOAc : *c*-Hex / 1 : 10); m.p. 133-134 °C;  $[\alpha]_D^{25} = -43.6$  ( $c$  1.00 in CHCl<sub>3</sub>);  $\nu_{\max}$  (neat)/cm<sup>-1</sup> 3365w, 3060w, 3030w, 2962w, 2927w, 1738w, 1600w, 1494m, 1448m, 1317w, 1300w, 1237m, 1209w, 1136m, 1094w, 1061m, 1033m, 976m, 946m, 913m, 900m, 808w, 754s, 741s, 696s, 662m; <sup>1</sup>H NMR (400 MHz, CDCl<sub>3</sub>):  $\delta = 7.50-7.16$  (20H, m, Ar-*H*), 4.36 (2H, dm, <sup>3</sup>*J*<sub>HF</sub> 28.1, 2 x NCH) and



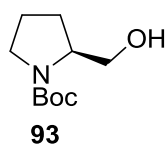
1.88-1.69 (4H, m, NCHCH<sub>2</sub>CH<sub>2</sub>); <sup>13</sup>C NMR (100 MHz, CDCl<sub>3</sub>): δ = 142.8 (2C, d, <sup>2</sup>J<sub>CF</sub> 23.4, 2 x C<sup>ipso</sup>), 142.4 (2C, d, <sup>2</sup>J<sub>CF</sub> 24.1, 2 x C<sup>ipso</sup>'), 128.4 (2C, d, <sup>4</sup>J<sub>CF</sub> 0.7, 2 x C<sup>meta</sup>), 128.3 (2C, d, <sup>4</sup>J<sub>CF</sub> 1.1, 2 x C<sup>meta</sup>'), 127.7 (2C, d, <sup>5</sup>J<sub>CF</sub> 1.3, 2 x C<sup>para</sup>), 127.5 (2C, d, <sup>5</sup>J<sub>CF</sub> 1.1, 2 x C<sup>para</sup>'), 125.7 (2C, d, <sup>3</sup>J<sub>CF</sub> 9.1, 2 x C<sup>ortho</sup>), 125.2 (2C, d, <sup>3</sup>J<sub>CF</sub> 9.3, 2 x C<sup>ortho</sup>'), 100.7 (2C, d, <sup>1</sup>J<sub>CF</sub> 183.4, 2 x NCHCF), 64.1 (2C, d, <sup>2</sup>J<sub>CF</sub> 21.6, 2 x NCH) and 26.3 (2C, d, <sup>3</sup>J<sub>CF</sub> 3.7, 2 x NCHCH<sub>2</sub>); <sup>19</sup>F NMR (376 MHz, CDCl<sub>3</sub>): δ = -168.5 (2F, d, <sup>3</sup>J<sub>HF</sub> 27.5); [*m/z* (ESI) found: 440.2179 (M+H)<sup>+</sup>, C<sub>30</sub>H<sub>28</sub>F<sub>2</sub>N requires 440.2184].

**((2*R*,5*S*)-1-(Pyridin-4-yl)-pyrrolidine-2,5-diyl)-bis-(diphenylmethanol) (85)**



A slightly yellow solution of 4-pyrrolidinopyridine (259 mg, 1.75 mmol) and benzophenone (1.27 g, 7.00 mmol) in benzene (7.0 mL) was degassed by bubbling argon through it (15 min). The vial was placed above a LED at a distance of 1 cm. The mixture was irradiated (402 nm, 300 mA) for 14 h. The mixture was concentrated *in vacuo* to give a yellow oil, which was purified by column chromatography (MeOH : CH<sub>2</sub>Cl<sub>2</sub> / 1 : 40 → 1 : 20) to give a light yellow solid (17.0 mg, 2%); R<sub>f</sub> 0.47 (MeOH : CH<sub>2</sub>Cl<sub>2</sub> / 1 : 10); δ = 7.64-7.57 (4H, m, Ar), 7.55-7.46 (6H, m, Ar), 7.42-7.34 (4H, m, Ar), 7.32-7.27 (2H, m, Ar), 7.13-7.05 (6H, m, Ar), 5.65-5.60 (2H, m, C3'-*H* and C5'-*H*), 2.26-2.13 (2H, m, 2 x NCHCHH) and 1.95-1.81 (2H, m, 2 x NCHCHH); [*m/z* (ESI) found: 513.2534 (M+H)<sup>+</sup>, C<sub>35</sub>H<sub>33</sub>N<sub>2</sub>O<sub>2</sub> requires 513.2537].

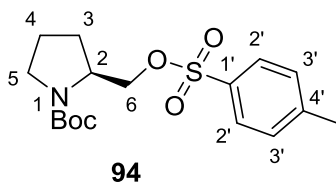
**(S)-tert-Butyl-2-(hydroxymethyl)-pyrrolidine-1-carboxylate (93)**



A colourless solution of **92** (2.00 g, 9.30 mmol) in THF (30 mL) at 0 °C was treated with a borane THF complex solution (1 M, 23.3 mL, 23.3 mmol) over 20 min. The solution was allowed to warm to rt and stirred for 2 h. It was cooled to 0 °C and water (30 mL) followed by Rochelle salt solution (sat., 30 mL) was carefully added. The mixture was extracted with EtOAc (3 x 30 mL). The combined organic layers were washed with 100 mL of a 1 : 1 mixture of water and Rochelle salt solution (sat.), dried over Na<sub>2</sub>SO<sub>4</sub> and concentrated *in vacuo* to give a clear, light yellow oil (1.70 g, 91%); *R<sub>f</sub>* 0.28 (MeOH : CH<sub>2</sub>Cl<sub>2</sub> / 1 : 20);  $[\alpha]_D^{25}$  -43.9 (*c* 1.05 in CHCl<sub>3</sub>); <sup>1</sup>H NMR (300 MHz, CDCl<sub>3</sub>): δ = 4.76 (1H, br. s, OH), 4.02-3.80 (1H, m, NCH), 3.68-3.51 (2H, m, CH<sub>2</sub>OH), 3.50-3.38 (1H, m, NCHH), 3.36-3.23 (1H, m, NCHH), 2.07-1.93 (1H, m, NCHCHH), 1.90-1.69 (3H, m, NCHCHH and NCH<sub>2</sub>CH<sub>2</sub>), 1.46 (9H, s, *t*-Bu).

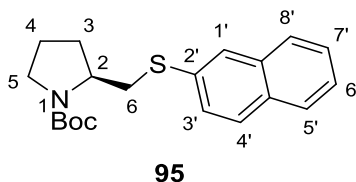
Data in agreement with the literature values<sup>[75]</sup>

**(S)-tert-Butyl-2-((tosyloxy)-methyl)-pyrrolidine-1-carboxylate (94)**



A colourless solution of **93** (8.00 g, 39.8 mmol) and pyridine (24 mL) in CH<sub>2</sub>Cl<sub>2</sub> (80 mL) was cooled to 0 °C and treated with *p*-toluenesulfonyl chloride (9.50 g, 39.8 mmol) portionwise to give a yellow solution. This was stirred at rt for 60 h and CH<sub>2</sub>Cl<sub>2</sub> (80 mL) was added. The solution was washed with water (2 x 80 mL), citric acid (10%, 3 x 80 mL) and brine (80 mL). The organic layer was dried over Na<sub>2</sub>SO<sub>4</sub> and concentrated *in vacuo* to give a yellow oil (14.0 g, 99%); *R<sub>f</sub>* 0.36 (MeOH : CH<sub>2</sub>Cl<sub>2</sub> / 1 : 20);  $[\alpha]_D^{25}$  -36.3 (*c* 1.00 in CHCl<sub>3</sub>); <sup>1</sup>H NMR (300 MHz, CDCl<sub>3</sub>): δ = 7.77 (2H, d, <sup>3</sup>*J* 8.2, C2'H), 7.34 (2H, d, <sup>3</sup>*J* 7.8, C3'H), 4.17-3.80 (3H, m, C2-H and C5-H<sub>2</sub>), 3.40-3.18 (2H, m, C6-H<sub>2</sub>), 2.45 (3H, s, PhCH<sub>3</sub>), 2.02-1.71 (4H, m, C3-H<sub>2</sub> and C4-H<sub>2</sub>), 1.41 (3H, s, <sup>t</sup>Bu-minor), 1.37 (6H, s, <sup>t</sup>Bu-major). Data in agreement with the literature values<sup>[75]</sup>

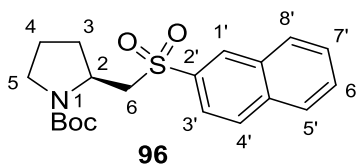
**(S)-tert-Butyl-2-((naphthalen-2-ylthio)-methyl)-pyrrolidine-1-carboxylate (95)**



NaH was washed with *n*-hexane (5 mL). The solvent was removed and replaced by THF (17 mL). The white suspension was cooled to 0 °C and 2-naphthalenethiol (2.50 g, 15.6 mmol) was added portion wise. The yellow solution was stirred for 5 min and treated with a solution of **94** (4.62 g, 13.0 mmol) in THF (26 mL). This was heated to reflux for 5 h and the resulting brown suspension was cooled to 0 °C. Water (200 mL) was added and the solution was extracted with CH<sub>2</sub>Cl<sub>2</sub> (3 x 200 mL). The combined organic layers were dried over MgSO<sub>4</sub> and concentrated *in vacuo* to give a brown oil. This was purified by column chromatography (dry loading, dry loading, EtOAc : <sup>c</sup>Hex / 1 : 20) to give a white solid (3.53 g, 79%); R<sub>f</sub> 0.36 (EtOAc : <sup>c</sup>Hex / 1 : 10); m.p. 98-100 °C; [α]<sub>D</sub><sup>20</sup> +9.7 (*c* 1.00 in CHCl<sub>3</sub>); <sup>1</sup>H NMR (300 MHz, CDCl<sub>3</sub>): δ = 7.97 (0.6H, s, naphthyl), 7.83 (0.4H, s, naphthyl), 7.81-7.68 (3H, m, naphthyl), 7.56-7.37 (3H, m, naphthyl), 4.12 (0.5H, br s), 3.97 (0.5H, br s), 3.71-3.25 (3H, m), 2.98-2.72 (1H, m), 2.14-1.73 (4H, m, C3-*H*<sub>2</sub> and C4-*H*<sub>2</sub>), 1.45 (3.5H, s, <sup>t</sup>Bu), 1.43 (5.5H, s, <sup>t</sup>Bu).

Data in agreement with the literature values<sup>[75]</sup>

**(S)-tert-Butyl-2-((naphthalen-2-ylsulfonyl)-methyl)-pyrrolidine-1-carboxylate (96)**

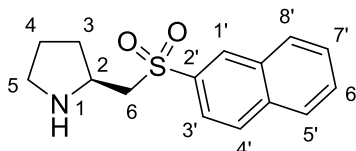


A slightly yellow solution of **95** (3.52 g, 10.3 mmol) in CH<sub>2</sub>Cl<sub>2</sub> (100 mL) was cooled to 0 °C and treated with 3-chloroperbenzoic acid (70%, 6.34 g, 25.7 mmol) to give a white suspension. The suspension was allowed to warm to rt and stirred for 15.5 h. Na<sub>2</sub>S<sub>2</sub>O<sub>3</sub> (sat., 60 mL) was added followed by NaHCO<sub>3</sub> (sat., 120 mL) and the mixture was vigorously stirred for 15 min. This was extracted with CH<sub>2</sub>Cl<sub>2</sub> (1 x 100 mL and 2 x 200 mL). The combined organic layers were dried over MgSO<sub>4</sub> and concentrated *in vacuo* to give a white solid (3.86 g, quant.); R<sub>f</sub> 0.40 (EtOAc : <sup>c</sup>Hex / 1 : 2); m.p. 105-108 °C; [α]<sub>D</sub><sup>20</sup> -17.8 (*c* 1.00 in CHCl<sub>3</sub>); <sup>1</sup>H NMR (300 MHz, CDCl<sub>3</sub>): δ = 8.49 (1H, s, naphthyl), 8.07-7.96 (2H, m, naphthyl), 7.96-7.82 (2H, m, naphthyl), 7.74-7.56 (2H, m, naphthyl), 4.25-4.07 (1H, m), 3.96

(0.4H, d,  $J$  13.8), 3.63 (0.6H, d,  $J$  13.8), 3.39-3.20 (2H, m), 3.11 (1H, dd,  $J$  13.7,  $J$  10.6), 2.41-2.19 (1H, m), 2.19-2.01 (1H, m), 1.99-1.74 (2H, m), 1.37 (4H, s, <sup>t</sup>Bu), 1.29 (5H, s, <sup>t</sup>Bu).

Data in agreement with the literature values<sup>[75]</sup>

**(S)-2-((Naphthalen-2-ylsulfonyl)-methyl)-pyrrolidine (97)**

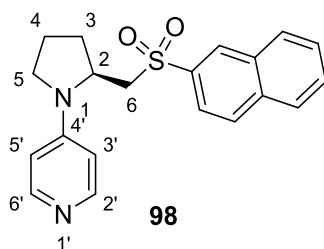


**97**

A colourless solution of **96** (529 mg, 1.41 mmol) in CH<sub>2</sub>Cl<sub>2</sub> (5 mL) was treated with TFA (1.08 mL, 14.1 mmol) drop wise. The solution was stirred for 1.5 h and concentrated *in vacuo*. The residue was taken up in CH<sub>2</sub>Cl<sub>2</sub> (25 mL) and water (20 mL) followed by KOH (1 M, 40 mL) was added. The mixture was extracted with CH<sub>2</sub>Cl<sub>2</sub> (1 x 20 mL, 1 x 50 mL) and the combined organic layers were dried over Na<sub>2</sub>SO<sub>4</sub> and concentrated *in vacuo* to give a yellow solid (380 mg, 98%);  $R_f$  0.43 (MeOH : CH<sub>2</sub>Cl<sub>2</sub> / 1 : 5); m.p. 46-49 °C;  $[\alpha]_D^{25}$  +5.9 ( $c$  1.00 in CHCl<sub>3</sub>); <sup>1</sup>H NMR (300 MHz, CDCl<sub>3</sub>):  $\delta$  = 8.51 (1H, s, naphth), 7.84-8.08 (4H, m, naphth), 7.58-7.73 (2H, m, naphth), 3.57 (1H, p,  $J$  6.7, C2-*H*), 3.32 (2H, d,  $J$  6.2, SO<sub>2</sub>CH<sub>2</sub>), 3.06-2.84 (2H, m, C5-*H*<sub>2</sub>), 2.05-1.87 (1H, m, C4-*H*/C3-*H*), 1.85-1.63 (2H, m, C4-*H*/C3-*H*), 1.52-1.38 (1H, m, C4-*H*/C3-*H*).

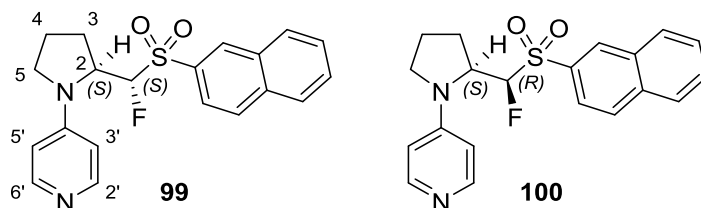
Data in agreement with the literature values<sup>[75]</sup>

(S)-4-(2-((Naphthalen-2-ylsulfonyl)-methyl)-pyrrolidin-1-yl)-pyridine (**98**)



A brown suspension of **97** (440 mg, 1.60 mmol), 4-bromopyridine hydrochloride (621 mg, 3.20 mmol), Pd(dba)<sub>2</sub> (46.0 mg, 80.0 μmol), cesium carbonate (2.09 g, 6.40 mmol) and (±)-BINAP (199 mg, 320 μmol) in toluene (16 mL) was vigorously stirred for 15 min then heated to 80 °C for 24 h. As TLC showed no conversion palladium(II)acetate (18.0 mg, 80.2 μmol) and the mixture was heated to 80 °C and stirred at that temperature for a total of 26 h. After cooling to rt water (300 mL) was added and the mixture was extracted with CH<sub>2</sub>Cl<sub>2</sub> (3 x 300 mL). The combined organic layers were dried over Na<sub>2</sub>SO<sub>4</sub> and concentrated to give a brown resin which was purified by column chromatography (MeOH : CH<sub>2</sub>Cl<sub>2</sub> / 1 : 20) and further by using (MeOH : CH<sub>2</sub>Cl<sub>2</sub> : NH<sub>3(aq)</sub> / 100 : 2.5 : 5) to give a colourless oil. This was coevaporated with EtOH to give a white solid (275 mg, 49%); *R<sub>f</sub>* 0.26 (MeOH : CH<sub>2</sub>Cl<sub>2</sub> / 1 : 10); m.p. 125-128 °C;  $[\alpha]_D^{25} +45.0$  (*c* 1.00 in CHCl<sub>3</sub>);  $\nu_{\max}$  (neat)/cm<sup>-1</sup> 3048w, 2971w, 2924w, 2848w, 2497w, 1929w, 1818w, 1720w, 1624w, 1592m, 1544m, 1512m, 1461w, 1432w, 1388m, 1352m, 1314m, 1291s, 1267m, 1229s, 1204s, 1161m, 1144s, 1123s, 1104s, 1069s, 1019w, 1002m, 987s, 954m, 922m, 909m, 860m, 844m, 820m, 800s, 756s, 741s, 668s, 660m; <sup>1</sup>H NMR (600 MHz, CDCl<sub>3</sub>): δ = 8.54 (1H, d, *J* 1.3, naphth), 8.08-8.02 (2H, m, C2'-H and C6'-H), 8.06 (1H, d, *J* 8.8, naphth), 8.02 (1H, d, *J* 8.0, naphth), 7.96 (1H, d, *J* 8.2, naphth), 7.91 (1H, dd, *J* 8.6, *J* 1.9, naphth), 7.73-7.69 (1H, m, naphth), 7.68-7.64 (1H, m, naphth), 6.23-6.19 (2H, m, C3'-H and C5'-H), 4.33 (1H, dd, <sup>2</sup>*J* 10.0, <sup>3</sup>*J* 7.0, C2-H), 3.38-3.33 (2H, m, SO<sub>2</sub>CHH and), 3.15 (1H, td, <sup>2</sup>*J* 9.8, <sup>3</sup>*J* 6.7, C5-H), 3.07 (1H, dd, <sup>2</sup>*J* 14.3, <sup>3</sup>*J* 10.2, SO<sub>2</sub>CHH), 2.30-2.23 (1H, m, C3-HH), 2.16-2.07 (2H, m, C3-HH and C4-HH) and 2.06-1.96 (1H, C4-HH); <sup>13</sup>C NMR (150 MHz, CDCl<sub>3</sub>): δ = 150.2 (C4'), 150.0 (2C, C2' and C6'), 136.3 (C<sup>quat</sup>), 135.6 (C<sup>quat</sup>), 132.3 (C<sup>quat</sup>), 130.10 (C<sup>naphth</sup>), 130.05 (C<sup>naphth</sup>), 129.8 (C<sup>naphth</sup>), 129.6 (C<sup>naphth</sup>), 128.19 (C<sup>naphth</sup>), 128.18 (C<sup>naphth</sup>), 122.6 (C<sup>naphth</sup>), 107.2 (2C, C3' and C5'), 57.1 (SO<sub>2</sub>CH), 52.8 (C2) and 47.0 (C5), 31.2 (C3) and 22.8 (C4); [*m/z* (ESI) found: 353.1323 (M+H)<sup>+</sup>, C<sub>20</sub>H<sub>21</sub>N<sub>2</sub>O<sub>2</sub>S requires 353.1318].

**4-((S)-2-((S)-Fluoro-(naphthalen-2-ylsulfonyl)-methyl)-pyrrolidin-1-yl)-pyridine (99)**  
**and**  
**4-((S)-2-((R)-Fluoro-(naphthalen-2-ylsulfonyl)-methyl)-pyrrolidin-1-yl)-pyridine (100)**



A colourless solution of **98** (144 mg, 409  $\mu\text{mol}$ ) in THF (4.0 mL) was cooled to  $-78\text{ }^\circ\text{C}$ . LDA in THF, *n*-heptane and ethylbenzene (2.0 M, 246  $\mu\text{L}$ , 491  $\mu\text{mol}$ ) was added drop wise to give a bright yellow solution. This was stirred for 15 min and treated with NFSI (129 mg, 409  $\mu\text{mol}$ ) in THF (500  $\mu\text{L}$ ) drop wise to give a pale yellow solution. This was stirred for 15 min, allowed to warm to rt and stirred for another 60 min.  $\text{NH}_4\text{Cl}$  (aq., sat., 10 mL) was added followed by water (10 mL) and the mixture was extracted with  $\text{CH}_2\text{Cl}_2$  (3 x 20 mL). The combined organic layers were dried over  $\text{Na}_2\text{SO}_4$  and concentrated *in vacuo* to give a yellow solid. Purification by column chromatography (MeOH :  $\text{CH}_2\text{Cl}_2$  :  $\text{NH}_3(\text{aq.})$  / 1 : 40 : 0.1  $\rightarrow$  1 : 10 : 0.1) gave two yellow solids as racemates (major: 22.3 mg, 15%; minor: 5.1 mg, 3%; and mixed fractions 16.1 mg, 11%):

**(S),(S)/(R),(R); minor:**  $R_f$  0.33 (MeOH :  $\text{CH}_2\text{Cl}_2$  / 1 : 10),  $\nu_{\text{max}}$  (neat)/ $\text{cm}^{-1}$  3056w, 2925w, 2652w, 2162w, 1985w, 1715w, 1644s, 1594s, 1537s, 1458m, 1385m, 1349m, 1301s, 1280m, 1212m, 1148s, 1126s, 1083s, 1070s, 1021m, 993s, 953m, 923w, 857m, 807s, 754s, 721s, 691m, 662s;  $^1\text{H}$  NMR (300 MHz,  $\text{CDCl}_3$ ):  $\delta$  = 8.58 (1H, br. s, naphth), 8.17-8.10 (2H, m, C2'-H and C6'-H), 8.09-7.90 (4H, m, naphth), 7.77-7.64 (2H, m, naphth), 6.48-6.42 (2H, m, C3'-H and C5'-H), 4.91 (1H, dd,  $^2J_{\text{HF}}$  48.7,  $^3J$  9.5), 4.64-4.54 (1H, m, NCH), 3.58-3.49 (1H, m, NCHH), 3.33-3.20 (1H, m, NCHH), 2.67-2.58 (1H, m, NCHCHH), 2.30-2.08 and (3H, m, NCHCHH and  $\text{NCH}_2\text{CH}_2$ );  $^{19}\text{F}$  NMR (282 MHz,  $\text{CDCl}_3$ ):  $\delta$  = -177.4 (d,  $^2J_{\text{HF}}$  49.1); [ $m/z$  (ESI) found: 371.1219 ( $\text{M}+\text{H}$ ) $^+$ ,  $\text{C}_{20}\text{H}_{20}\text{FN}_2\text{O}_2\text{S}$  requires 371.1224].

**(S),(R)/(R),(S); major:**  $R_f$  0.47 (MeOH :  $\text{CH}_2\text{Cl}_2$  / 1 : 10); m.p. 85-89  $^\circ\text{C}$ ;  $\nu_{\text{max}}$  (neat)/ $\text{cm}^{-1}$  3032w, 2971w, 2869w, 2288w, 2162w, 1980w, 1921w, 1645w, 1592s, 1545m, 1510s, 1485m, 1461w, 1429w, 1388s, 1361m, 1323s, 1282m, 1238m, 1216m, 1151s, 1131s, 1114s, 1072s, 1040m, 1003s, 992s, 929w, 906m, 854m, 808s, 749s, 722m, 696m, 659s;  $^1\text{H}$  NMR (300 MHz,  $\text{CDCl}_3$ ):  $\delta$  = 8.56 (1H, br. s, naphth), 8.33-8.26 (2H, m, C2'-H and C6'-H), 8.09-7.99 (2H, m, naphth), 7.99-7.86 (2H, m, naphth), 7.77-7.59 (2H, m, naphth), 6.66-6.51 (2H, m, C3'-H and C5'-H), 5.40 (1H, d,  $^2J_{\text{HF}}$  48.5, FCH), 4.78 (1H, dd,  $^3J_{\text{HF}}$  30.1,  $^3J$  7.0, NCH), 3.56-3.42 (1H, m, NCHH), 3.29-3.16 (1H, m, NCHH), 2.60-2.42 (1H, m, NCHCHH), 2.21-

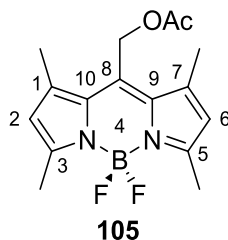
### Experimental Part

---

1.97 (3H, m, NCHCHH and NCH<sub>2</sub>CH<sub>2</sub>); <sup>13</sup>C NMR (75 MHz, CDCl<sub>3</sub>): δ = 150.6 (C4'), 150.3 (2C, C2' and C6'), 135.9 (C<sup>naphth</sup>), 132.6 (C<sup>naphth</sup>), 132.2 (C<sup>naphth</sup>), 131.8 (C<sup>naphth</sup>), 130.1 (C<sup>naphth</sup>), 130.0 (C<sup>naphth</sup>), 129.7 (C<sup>naphth</sup>), 128.2 (C<sup>naphth</sup>), 128.1 (C<sup>naphth</sup>), 123.3 (C<sup>naphth</sup>), 107.6 (2C, C3' and C5'), 100.7 (d, <sup>1</sup>J<sub>CF</sub> 228.3, FC), 55.6 (d, <sup>2</sup>J<sub>CF</sub> 19.4, C2), 47.5 (C5), 26.6 (d, <sup>3</sup>J<sub>CF</sub> 6.7, C3) and 24.4 (d, <sup>4</sup>J<sub>CF</sub> 3.4, C4) ; <sup>19</sup>F NMR (282 MHz, CDCl<sub>3</sub>): δ = -194.8 (dd, <sup>2</sup>J<sub>HF</sub> 48.7, <sup>3</sup>J<sub>HF</sub> 29.8); [*m/z* (ESI) found: 371.1216 (M+H)<sup>+</sup>, C<sub>20</sub>H<sub>20</sub>FN<sub>2</sub>O<sub>2</sub>S requires 371.1224].

## Borondipyrromethene (BODIPY) derivatives

## 8-Acetoxyethyl-1,3,5,7-tetramethyl pyrromethene difluoroborate (105)

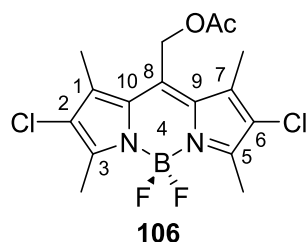


To a light yellow solution of 2,4-dimethylpyrrole (2.16 mmol, 21.0 mmol) in dry CH<sub>2</sub>Cl<sub>2</sub> (100 mL) was added 2-chloro-2-oxoethyl acetate (1.40 mL, 13.0 mmol) dropwise to give an orange solution which was stirred for 4 h. To the resulting dark red solution was added DIPEA (7.30 mL, 43.0 mmol) to give a dark green solution which was stirred for 15 min and then treated with BF<sub>3</sub>•OEt<sub>2</sub> (5.30 mL, 43.0 mmol) to give a dark red solution. After stirring for 30 min the mixture was washed with water (300 mL). The aqueous layer was extracted with CH<sub>2</sub>Cl<sub>2</sub> (2 x 300 mL) and the combined organic layers were dried over Na<sub>2</sub>SO<sub>4</sub> and concentrated *in vacuo* to give a dark red oil. This was purified by column chromatography (CH<sub>2</sub>Cl<sub>2</sub> : *c*-hex / 1 : 1 → 1 : 2) to give an orange, green fluorescent solid (322 mg, 10%). R<sub>f</sub> 0.63 (CH<sub>2</sub>Cl<sub>2</sub>); m.p. 191-193 °C; ν<sub>max</sub> (neat)/cm<sup>-1</sup> 2925w, 1753m, 1740m, 1551m, 1508s, 1469m, 1409m, 1389m, 1369m, 1306m, 1189s, 1158s, 1138s, 1072s, 1021s, 969s, 915s, 835s, 810s, 754m, 717s, 662m; <sup>1</sup>H NMR (400 MHz, CDCl<sub>3</sub>): δ = 6.08 (2H, s, C<sup>2</sup>H and C<sup>6</sup>H), 5.29 (2H, s, CH<sub>2</sub>), 2.53 (6H, s, C<sup>3</sup>CH<sub>3</sub> and C<sup>5</sup>CH<sub>3</sub>), 2.35 (6H, s, C<sup>1</sup>CH<sub>3</sub> and C<sup>7</sup>CH<sub>3</sub>) and 2.13 (3H, s, CH<sub>3</sub>CO<sub>2</sub>R); <sup>13</sup>C NMR (100 MHz, CDCl<sub>3</sub>): δ = 170.7 (CH<sub>3</sub>CO<sub>2</sub>R), 156.8 (2C, C<sup>3</sup> and C<sup>5</sup>), 141.6 (2C, C<sup>1</sup> and C<sup>7</sup>), 133.4 (C<sup>8</sup>), 132.8 (2C, C<sup>9</sup> and C<sup>10</sup>), 122.5 (2C, C<sup>2</sup> and C<sup>6</sup>), 58.0 (CH<sub>2</sub>), 20.7 (CH<sub>3</sub>CO<sub>2</sub>R), 15.8 (2C, C<sup>1</sup>CH<sub>3</sub> and C<sup>7</sup>CH<sub>3</sub>) and 14.8 (2C, t, <sup>4</sup>J<sub>CF</sub> 2.4, C<sup>3</sup>CH<sub>3</sub> and C<sup>5</sup>CH<sub>3</sub>); <sup>19</sup>F NMR (282 MHz, CDCl<sub>3</sub>): δ = -146.4 (Ψ<sub>q</sub>, <sup>1</sup>J<sub>BF</sub> 32.5); [*m/z* (ESI) found: 343.1402 (M+Na)<sup>+</sup>, C<sub>16</sub>H<sub>19</sub>BF<sub>2</sub>N<sub>2</sub>O<sub>2</sub>Na requires 343.1400].

Data in agreement with the literature values<sup>[76]</sup>



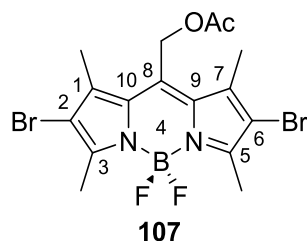
**8-Acetoxyethyl-2,6-dichloro-1,3,5,7-tetramethyl pyrromethene difluoroborate (106)**



To a brown solution of **105** (16.0 mg, 50.0  $\mu\text{mol}$ ) in 1,1,1,3,3,3-hexafluoro-2-propanol (500  $\mu\text{L}$ ) was added NCS (14.7 mg, 1.10 mmol) to give a dark purple solution which was stirred for 75 min. A solution of  $\text{Na}_2\text{S}_2\text{O}_3 \cdot 5\text{H}_2\text{O}$  (aq., 10% w/w, 1.0 mL) was added and the mixture was extracted with  $\text{CH}_2\text{Cl}_2$  (2 x 1.0 mL). The combined organic layers were dried over  $\text{Na}_2\text{SO}_4$  and concentrated *in vacuo* to give a dark purple solid which was purified by column chromatography ( $\text{CH}_2\text{Cl}_2$  : *n*-pent / 1 : 1) to give a red solid (13.9 mg, 71%).  $R_f$  0.69 ( $\text{CH}_2\text{Cl}_2$ ); m.p. 207-210  $^\circ\text{C}$ ;  $\nu_{\text{max}}$  (neat)/ $\text{cm}^{-1}$  2927w, 1733s, 1558s, 1506m, 1470s, 1448m, 1407m, 1391m, 1377m, 1357s, 1319m, 1220s, 1179s, 1128s, 1113s, 1082s, 1067s, 1055s, 1030s, 991s, 917s, 895s, 883s, 839m, 720s, 678m, 662m, 656m;  $^1\text{H}$  NMR (600 MHz,  $\text{CDCl}_3$ ):  $\delta$  = 5.30 (2H, s,  $\text{CH}_2$ ), 2.57 (6H, s,  $\text{C}^3\text{CH}_3$  and  $\text{C}^5\text{CH}_3$ ), 2.36 (6H, s,  $\text{C}^1\text{CH}_3$  and  $\text{C}^7\text{CH}_3$ ) and 2.14 (3H, s,  $\text{CH}_3\text{CO}_2\text{R}$ );  $^{13}\text{C}$  NMR (150 MHz,  $\text{CDCl}_3$ ):  $\delta$  = 170.5 ( $\text{CH}_3\text{CO}_2\text{R}$ ), 153.9 (2C,  $\text{C}^3$  and  $\text{C}^5$ ), 136.3 (2C,  $\text{C}^1$  and  $\text{C}^7$ ), 134.3 ( $\text{C}^8$ ), 131.4 (2C,  $\text{C}^9$  and  $\text{C}^{10}$ ), 123.7 (2C,  $\text{C}^2$  and  $\text{C}^6$ ), 57.9 ( $\text{CH}_2$ ), 20.7 ( $\text{CH}_3\text{CO}_2\text{R}$ ), 13.1 (2C,  $\text{C}^1\text{CH}_3$  and  $\text{C}^7\text{CH}_3$ ) and 12.8 (2C, t,  $^4J_{\text{CF}}$  2.4,  $\text{C}^3\text{CH}_3$  and  $\text{C}^5\text{CH}_3$ );  $^{19}\text{F}$  NMR (564 MHz,  $\text{CDCl}_3$ ):  $\delta$  = -146.4 ( $\Psi_{\text{q}}$ ,  $^1J_{\text{BF}}$  31.5); [ $m/z$  (ESI) found: 411.0622 ( $\text{M}+\text{Na}$ ) $^+$ ,  $\text{C}_{16}\text{H}_{17}\text{BCl}_2\text{F}_2\text{N}_2\text{O}_2\text{Na}$  requires 411.0626].

Data in agreement with the literature values<sup>[76]</sup>

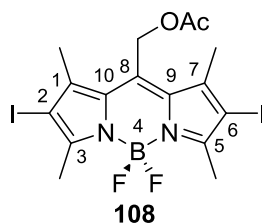
**8-Acetoxyethyl-2,6-dibromo-1,3,5,7-tetramethyl pyrromethene difluoroborate (107)**



To a brown solution of **105** (16.0 mg, 50.0  $\mu\text{mol}$ ) in 1,1,1,3,3,3-hexafluoro-2-propanol (500  $\mu\text{L}$ ) was added NBS (19.6 mg, 1.10 mmol) to give a dark purple solution which was stirred for 15 min. A solution of  $\text{Na}_2\text{S}_2\text{O}_3 \cdot 5\text{H}_2\text{O}$  (aq., 10% w/w, 1.0 mL) was added and the

mixture was extracted with CH<sub>2</sub>Cl<sub>2</sub> (2 x 1.0 mL). The combined organic layers were dried over Na<sub>2</sub>SO<sub>4</sub> and concentrated *in vacuo* to give a dark purple solid which was purified by column chromatography (CH<sub>2</sub>Cl<sub>2</sub> : *n*-pent / 1 : 1) to give a red solid (12.1 mg, 51%). R<sub>f</sub> 0.72 (CH<sub>2</sub>Cl<sub>2</sub>); m.p. 235-238 °C;  $\nu_{\max}$  (neat)/cm<sup>-1</sup> 2925w, 1734m, 1556s, 1501m, 1464m, 1447m, 1404m, 1388m, 1376m, 1352s, 1313m, 1217s, 1173s, 1126s, 1098s, 1081s, 1048s, 1028s, 987s, 917s, 888s, 875s, 838m, 719s, 678m, 658m; <sup>1</sup>H NMR (600 MHz, CDCl<sub>3</sub>):  $\delta$  = 5.31 (2H, s, CH<sub>2</sub>), 2.59 (6H, s, C<sup>3</sup>CH<sub>3</sub> and C<sup>5</sup>CH<sub>3</sub>), 2.38 (6H, s, C<sup>1</sup>CH<sub>3</sub> and C<sup>7</sup>CH<sub>3</sub>) and 2.14 (3H, s, CH<sub>3</sub>CO<sub>2</sub>R); <sup>13</sup>C NMR (150 MHz, CDCl<sub>3</sub>):  $\delta$  = 170.5 (CH<sub>3</sub>CO<sub>2</sub>R), 155.3 (2C, C<sup>3</sup> and C<sup>5</sup>), 138.9 (2C, C<sup>1</sup> and C<sup>7</sup>), 133.9 (C<sup>8</sup>), 131.9 (2C, C<sup>9</sup> and C<sup>10</sup>), 113.1 (2C, C<sup>2</sup> and C<sup>6</sup>), 58.1 (CH<sub>2</sub>), 20.7 (CH<sub>3</sub>CO<sub>2</sub>R), 15.0 (2C, C<sup>1</sup>CH<sub>3</sub> and C<sup>7</sup>CH<sub>3</sub>) and 14.1 (2C, t, <sup>4</sup>J<sub>CF</sub> 2.6, C<sup>3</sup>CH<sub>3</sub> and C<sup>5</sup>CH<sub>3</sub>); <sup>19</sup>F NMR (564 MHz, CDCl<sub>3</sub>):  $\delta$  = -146.1 ( $\Psi$ <sub>q</sub>, <sup>1</sup>J<sub>BF</sub> 31.6); [*m/z* (ESI) found: 500.9591 (M+Na)<sup>+</sup>, C<sub>16</sub>H<sub>17</sub>BBr<sub>2</sub>F<sub>2</sub>N<sub>2</sub>O<sub>2</sub>Na requires 500.9595].

### 8-Acetoxyethyl-2,6-diiodo-1,3,5,7-tetramethyl pyrromethene difluoroborate (108)

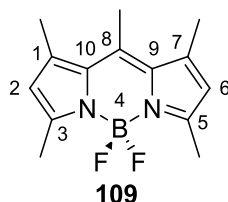


To an orange suspension of **105** (157 mg, 491  $\mu$ mol) in EtOH (50 mL) under air was added iodine (249 mg, 981  $\mu$ mol) and HIO<sub>3</sub> (173 mg, 981  $\mu$ mol) to give a dark red suspension which was stirred for 24 h. Water (50 mL) was added and the mixture was extracted with CH<sub>2</sub>Cl<sub>2</sub> (2 x 50 mL). The combined organic layers were washed with a Na<sub>2</sub>S<sub>2</sub>O<sub>3</sub>•5H<sub>2</sub>O solution (aq., 10% w/w, 100 mL) and the aqueous layer was back-extracted with CH<sub>2</sub>Cl<sub>2</sub> (50 mL). The combined organic layers were dried over Na<sub>2</sub>SO<sub>4</sub> and concentrated *in vacuo*. Purification by column chromatography (CH<sub>2</sub>Cl<sub>2</sub> : *c*-Hex / 1 : 1, dry loading) afforded **108** as a red solid (208 mg, 74%). R<sub>f</sub> 0.83 (CH<sub>2</sub>Cl<sub>2</sub>); m.p. 185-188 °C;  $\nu_{\max}$  (neat)/cm<sup>-1</sup> 3468w, 2921w, 1737s, 1544s, 1489m, 1439m, 1398m, 1374m, 1345s, 1307m, 1217s, 1172s, 1123s, 1077s, 1044s, 1031s, 984s, 917s, 837s, 741m, 719s, 677s, 656s; <sup>1</sup>H NMR (400 MHz, CDCl<sub>3</sub>):  $\delta$  = 5.30 (2H, s, CH<sub>2</sub>), 2.63 (6H, s, C<sup>3</sup>CH<sub>3</sub> and C<sup>5</sup>CH<sub>3</sub>), 2.39 (6H, s, C<sup>1</sup>CH<sub>3</sub> and C<sup>7</sup>CH<sub>3</sub>) and 2.14 (3H, s, CH<sub>3</sub>CO<sub>2</sub>R); <sup>13</sup>C NMR (100 MHz, CDCl<sub>3</sub>):  $\delta$  = 170.5 (CH<sub>3</sub>CO<sub>2</sub>R), 158.1 (2C, C<sup>3</sup> and C<sup>5</sup>), 143.6 (2C, C<sup>1</sup> and C<sup>7</sup>), 132.9 (C<sup>8</sup>), 132.7 (2C, C<sup>9</sup> and C<sup>10</sup>), 87.4 (2C, C<sup>2</sup> and C<sup>6</sup>), 58.4 (CH<sub>2</sub>), 20.7 (CH<sub>3</sub>CO<sub>2</sub>R), 18.3 (2C, C<sup>1</sup>CH<sub>3</sub> and C<sup>7</sup>CH<sub>3</sub>) and 16.5 (2C, t, <sup>4</sup>J<sub>CF</sub> 2.6, C<sup>3</sup>CH<sub>3</sub> and C<sup>5</sup>CH<sub>3</sub>);

$^{19}\text{F}$  NMR (282 MHz,  $\text{CDCl}_3$ ):  $\delta = -145.6$  ( $\Psi_{\text{q}}$ ,  $^1J_{\text{BF}}$  31.8); [ $m/z$  (ESI) found: 594.9329 ( $\text{M}+\text{Na}$ ) $^+$ ,  $\text{C}_{16}\text{H}_{17}\text{BF}_2\text{I}_2\text{N}_2\text{O}_2\text{Na}$  requires 594.9333].

Data in agreement with the literature values<sup>[76]</sup>

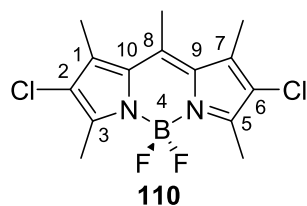
### 1,3,5,7,8-Pentamethyl pyrromethene difluoroborate (109)



A light orange solution of 2,4-dimethylpyrrole (1.90 mL, 18.5 mmol) in dry  $\text{CH}_2\text{Cl}_2$  (100 mL) was cooled to  $0\text{ }^\circ\text{C}$  then acetyl chloride (789  $\mu\text{L}$ , 11.1 mmol) was added dropwise to give a yellow solution which was allowed to warm to rt and stirred for 26 h. To the resulting dark red solution was added DIPEA (6.42 mL, 36.9 mmol) and the solution was stirred for 15 min before the addition of  $\text{BF}_3\cdot\text{OEt}_2$  (4.56 mL, 36.9 mmol). The dark red solution was stirred for 30 min, a saturated  $\text{NaHCO}_3$  solution (aq., 200 mL) was added and the mixture was extracted with  $\text{CH}_2\text{Cl}_2$  (3 x 200 mL). The combined organic layers were dried over  $\text{Na}_2\text{SO}_4$  and concentrated *in vacuo* to give a dark red solid which was purified by column chromatography ( $\text{CH}_2\text{Cl}_2$  : *c*-hex / 1:1) to give a bright orange solid (627 mg, 26%).  $R_f$  0.33 ( $\text{CH}_2\text{Cl}_2$  : *c*-hex / 1 : 1); m.p.  $260\text{--}262\text{ }^\circ\text{C}$ ;  $\nu_{\text{max}}$  (neat)/ $\text{cm}^{-1}$  2985w, 1721w, 1667w, 1554m, 1531m, 1500m, 1435m, 1400s, 1362m, 1303m, 1227w, 1188s, 1159s, 1128m, 1074s, 1056s, 1026s, 996m, 972s, 840m, 806s, 764m, 747m, 723s, 698m, 675m;  $^1\text{H}$  NMR (400 MHz,  $\text{CDCl}_3$ ):  $\delta = 6.04$  (2H, s,  $\text{C}^2\text{H}$  and  $\text{C}^6\text{H}$ ), 2.55 (3H, s,  $\text{C}^8\text{CH}_3$ ), 2.51 (6H, s,  $\text{C}^3\text{CH}_3$  and  $\text{C}^5\text{CH}_3$ ) and 2.40 (6H, s,  $\text{C}^1\text{CH}_3$  and  $\text{C}^7\text{CH}_3$ );  $^{13}\text{C}$  NMR (100 MHz,  $\text{CDCl}_3$ ):  $\delta = 153.7$  (2C,  $\text{C}^3$  and  $\text{C}^5$ ), 141.6 ( $\text{C}^8$ ), 141.1 (2C,  $\text{C}^1\text{CH}_3$  and  $\text{C}^7\text{CH}_3$ ), 132.2 (2C,  $\text{C}^9$  and  $\text{C}^{10}$ ), 121.4 (2C,  $\text{C}^2$  and  $\text{C}^6$ ), 17.4 (2C,  $\text{C}^1\text{CH}_3$  and  $\text{C}^7\text{CH}_3$ ), 16.5 (C,  $\text{C}^8\text{CH}_3$ ) and 14.6 (2C, t,  $^4J_{\text{CF}}$  2.4,  $\text{C}^3\text{CH}_3$  and  $\text{C}^5\text{CH}_3$ );  $^{19}\text{F}$  NMR (282 MHz,  $\text{CDCl}_3$ ):  $\delta = -146.7$  ( $\Psi_{\text{q}}$ ,  $^1J_{\text{BF}}$  32.9); [ $m/z$  (ESI) found: 285.1348 ( $\text{M}+\text{Na}$ ) $^+$ ,  $\text{C}_{14}\text{H}_{17}\text{BF}_2\text{N}_2\text{Na}$  requires 285.1345].

Data in agreement with the literature values<sup>[99]</sup>

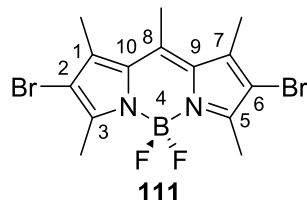
**2,6-Dichloro-1,3,5,7,8-pentamethyl pyrromethene difluoroborate (110)**



To a clear orange solution of **109** (30.0 mg, 115  $\mu\text{mol}$ ) in 1,1,1,3,3,3-hexafluoro-2-propanol (1.2 mL) was added NCS (33.8 mg, 252  $\mu\text{mol}$ ) to give an orange suspension. After 1 h  $\text{CH}_2\text{Cl}_2$  (500  $\mu\text{L}$ ) was added and the mixture was stirred for 30 min before it was diluted with more  $\text{CH}_2\text{Cl}_2$  (5.0 mL) and washed with a solution of  $\text{Na}_2\text{S}_2\text{O}_3 \cdot 5\text{H}_2\text{O}$  (aq., 10% w/w, 5.0 mL). The aqueous layer was extracted with  $\text{CH}_2\text{Cl}_2$  (5.0 mL), the combined organic layers were dried over  $\text{Na}_2\text{SO}_4$  and concentrated *in vacuo* to give a red solid. Purification by column chromatography ( $\text{CH}_2\text{Cl}_2$  : *n*-pent / 1 : 1) gave a red solid (21.1 mg, 55%).  $R_f$  0.53 ( $\text{CH}_2\text{Cl}_2$  : *c*-hex / 1 : 1); m.p. 269-272  $^\circ\text{C}$ ;  $\nu_{\text{max}}$  (neat)/ $\text{cm}^{-1}$  2927w, 1548m, 1501m, 1470m, 1447m, 1404m, 1384m, 1350m, 1313m, 1226m, 1192s, 1131m, 1110s, 1065s, 1052s, 1026m, 997s, 903m, 891m, 829m, 723m, 695m, 677m, 658m;  $^1\text{H}$  NMR (600 MHz,  $\text{CDCl}_3$ ):  $\delta$  = 2.62 (3H, s,  $\text{C}^8\text{CH}_3$ ), 2.55 (6H, s,  $\text{C}^3\text{CH}_3$  and  $\text{C}^5\text{CH}_3$ ) and 2.42 (6H, s,  $\text{C}^1\text{CH}_3$  and  $\text{C}^7\text{CH}_3$ );  $^{13}\text{C}$  NMR (150 MHz,  $\text{CDCl}_3$ ):  $\delta$  = 150.9 (2C,  $\text{C}^3$  and  $\text{C}^5$ ), 142.4 ( $\text{C}^8$ ), 136.0 (2C,  $\text{C}^1$  and  $\text{C}^7$ ), 130.6 (2C,  $\text{C}^9$  and  $\text{C}^{10}$ ), 122.5 (2C,  $\text{C}^2$  and  $\text{C}^6$ ), 17.2 ( $\text{C}^8\text{CH}_3$ ), 14.7 (2C,  $\text{C}^1\text{CH}_3$  and  $\text{C}^7\text{CH}_3$ ) and 12.5 (2C, t,  $^4J_{\text{CF}}$  2.4,  $\text{C}^3\text{CH}_3$  and  $\text{C}^5\text{CH}_3$ );  $^{19}\text{F}$  NMR (564 MHz,  $\text{CDCl}_3$ ):  $\delta$  = -146.7 ( $\Psi\text{q}$ ,  $^1J_{\text{BF}}$  31.3); [ $m/z$  (ESI) found: 353.0567 ( $\text{M}+\text{Na}$ ) $^+$ ,  $\text{C}_{14}\text{H}_{15}\text{BCl}_2\text{F}_2\text{N}_2\text{Na}$  requires 353.0571].

Data in agreement with the literature values<sup>[100]</sup>

**2,6-Dibromo-1,3,5,7,8-pentamethyl pyrromethene difluoroborate (111)**

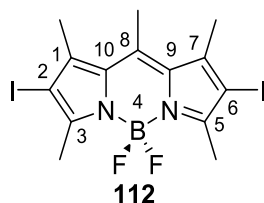


To a clear orange solution of **109** (30.0 mg, 115  $\mu\text{mol}$ ) in 1,1,1,3,3,3-hexafluoro-2-propanol (1.2 mL) was added NBS (44.9 mg, 252  $\mu\text{mol}$ ) to give a dark red suspension. After 20 min it was diluted with  $\text{CH}_2\text{Cl}_2$  (5.0 mL) and washed with a solution of  $\text{Na}_2\text{S}_2\text{O}_3 \cdot 5\text{H}_2\text{O}$  (aq., 10% w/w, 5.0 mL). The aqueous layer was extracted with  $\text{CH}_2\text{Cl}_2$  (5.0 mL), the combined organic layers were dried over  $\text{Na}_2\text{SO}_4$  and concentrated *in vacuo* to give a red solid. Purification by

column chromatography (CH<sub>2</sub>Cl<sub>2</sub> : *n*-pent / 1 : 1) gave a red solid (20.4 mg, 42%). *R<sub>f</sub>* 0.59 (CH<sub>2</sub>Cl<sub>2</sub> : *c*-hex / 1 : 1); m.p. 236-239 °C;  $\nu_{\max}$  (neat)/cm<sup>-1</sup> 2922w, 1543m, 1466m, 1446m, 1400m, 1382m, 1345s, 1309m, 1224m, 1189s, 1130m, 1100s, 1067s, 1046s, 993s, 897m, 827m, 721s; <sup>1</sup>H NMR (600 MHz, CDCl<sub>3</sub>):  $\delta$  = 2.63 (3H, s, C<sup>8</sup>CH<sub>3</sub>), 2.57 (6H, s, C<sup>3</sup>CH<sub>3</sub> and C<sup>5</sup>CH<sub>3</sub>) and 2.44 (6H, s, C<sup>1</sup>CH<sub>3</sub> and C<sup>7</sup>CH<sub>3</sub>); <sup>13</sup>C NMR (150 MHz, CDCl<sub>3</sub>):  $\delta$  = 152.4 (2C, C<sup>3</sup> and C<sup>5</sup>), 142.1 (C<sup>8</sup>), 138.5 (2C, C<sup>1</sup> and C<sup>7</sup>), 131.4 (2C, C<sup>9</sup> and C<sup>10</sup>), 111.8 (2C, C<sup>2</sup> and C<sup>6</sup>), 17.5 (C<sup>8</sup>CH<sub>3</sub>), 16.6 (2C, C<sup>1</sup>CH<sub>3</sub> and C<sup>7</sup>CH<sub>3</sub>) and 13.8 (2C, t, <sup>4</sup>J<sub>CF</sub> 2.6, C<sup>3</sup>CH<sub>3</sub> and C<sup>5</sup>CH<sub>3</sub>); <sup>19</sup>F NMR (564 MHz, CDCl<sub>3</sub>):  $\delta$  = -146.3 (Ψq, <sup>1</sup>J<sub>BF</sub> 31.9); [*m/z* (ESI) found: 442.9524 (M+Na)<sup>+</sup>, C<sub>14</sub>H<sub>15</sub>BBr<sub>2</sub>F<sub>2</sub>N<sub>2</sub>Na requires 442.9540].

Data in agreement with the literature values<sup>[81]</sup>

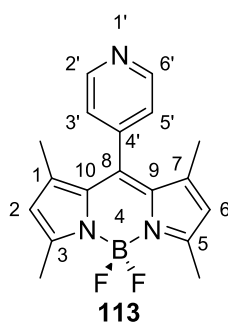
### 2,6-Diiodo-1,3,5,7,8-pentamethyl pyrromethene difluoroborate (**112**)



To a bright orange suspension of **109** in EtOH (50 mL) under air was added iodine (254 mg, 1.00 mmol) and HIO<sub>3</sub> (176 mg, 1.00 mmol) to give a dark orange suspension which was stirred for 16 h. A solution of Na<sub>2</sub>S<sub>2</sub>O<sub>3</sub>•5H<sub>2</sub>O (aq., 10% w/w, 100 mL) was added and the mixture was extracted with CH<sub>2</sub>Cl<sub>2</sub> (2 x 100 mL). The combined organic layers were dried over Na<sub>2</sub>SO<sub>4</sub> and concentrated *in vacuo*. Purification by column chromatography (CH<sub>2</sub>Cl<sub>2</sub> : *c*-Hex / 1 : 1, dry loading) afforded **112** as a bright red solid (217 mg, 84%). *R<sub>f</sub>* 0.67 (CH<sub>2</sub>Cl<sub>2</sub> : *c*-hex / 1 : 1); m.p. 220-222 °C;  $\nu_{\max}$  (neat)/cm<sup>-1</sup> 2965w, 2091w, 1536m, 1442m, 1379m, 1340m, 1305m, 1223w, 1188m, 1092s, 1066s, 988s, 826m, 720s; <sup>1</sup>H NMR (600 MHz, CDCl<sub>3</sub>):  $\delta$  = 2.62 (3H, s, C<sup>8</sup>CH<sub>3</sub>), 2.61 (6H, s, C<sup>3</sup>CH<sub>3</sub> and C<sup>5</sup>CH<sub>3</sub>) and 2.46 (6H, s, C<sup>1</sup>CH<sub>3</sub> and C<sup>7</sup>CH<sub>3</sub>); <sup>13</sup>C NMR (150 MHz, CDCl<sub>3</sub>):  $\delta$  = 155.2 (2C, C<sup>3</sup> and C<sup>5</sup>), 143.1 (2C, C<sup>1</sup> and C<sup>7</sup>), 141.3 (C<sup>8</sup>), 132.3 (2C, C<sup>9</sup> and C<sup>10</sup>), 85.9 (2C, C<sup>2</sup> and C<sup>6</sup>), 20.0 (2C, C<sup>1</sup>CH<sub>3</sub> and C<sup>7</sup>CH<sub>3</sub>), 18.0 (C<sup>8</sup>CH<sub>3</sub>) and 16.2 (2C, t, <sup>4</sup>J<sub>CF</sub> 2.7, C<sup>3</sup>CH<sub>3</sub> and C<sup>5</sup>CH<sub>3</sub>); <sup>19</sup>F NMR (282 MHz, CDCl<sub>3</sub>):  $\delta$  = -145.9 (Ψq, <sup>1</sup>J<sub>BF</sub> 32.0); [*m/z* (ESI) found: 539.9283 (M+Na)<sup>+</sup>, C<sub>14</sub>H<sub>15</sub>BF<sub>2</sub>I<sub>2</sub>N<sub>2</sub>Na requires 539.9278].

Data in agreement with the literature values<sup>[81]</sup>

**8-(4'-Pyridyl)-1,3,5,7-tetramethyl pyrromethene difluoroborate (113)**

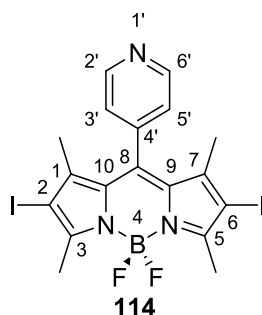


A colourless solution of 2,4-dimethylpyrrole (500  $\mu\text{L}$ , 4.86 mmol) and 4-pyridinecarboxaldehyde (218  $\mu\text{L}$ , 2.31 mmol) in dry  $\text{CH}_2\text{Cl}_2$  (20 mL) was treated with TFA (13  $\mu\text{L}$ ) and stirred for 50 min to give a clear, bright orange solution. A suspension of DDQ (524 mg, 2.31 mmol) in dry  $\text{CH}_2\text{Cl}_2$  (5 mL) was added to give a dark red solution which was stirred for 50 min.  $\text{NEt}_3$  (5 mL) was added and the resulting dark green solution was stirred for 30 min before  $\text{BF}_3 \cdot \text{OEt}_2$  (5 mL) was added. The obtained dark red solution was stirred for 2 h, then water (100 mL) was added. The mixture was extracted with  $\text{CH}_2\text{Cl}_2$  (100 mL), the organic layer was dried over  $\text{Na}_2\text{SO}_4$  and concentrated *in vacuo* to give a dark red oil. This was purified by column chromatography (EtOAc : *c*-hex / 1 : 1) to give a red, green fluorescent solid (94.8 mg, 13%).

$R_f$  0.39 (EtOAc : *c*-hex / 1 : 1); m.p. 218-221  $^\circ\text{C}$ ;  $\nu_{\text{max}}$  (neat)/ $\text{cm}^{-1}$  2924w, 1599w, 1537s, 1505s, 1464m, 1435m, 1404m, 1368m, 1360m, 1303s, 1263m, 1217w, 1180s, 1152s, 1120m, 1073s, 1051s, 963s, 827m, 809s, 766s, 718s, 671;  $^1\text{H}$  NMR (400 MHz,  $\text{CDCl}_3$ ):  $\delta$  = 8.79-8.75 (2H, m,  $\text{C}^{2'}\text{H}$  and  $\text{C}^{6'}\text{H}$ ), 7.32-7.29 (2H, m,  $\text{C}^{3'}\text{H}$  and  $\text{C}^{5'}\text{H}$ ), 6.00 (2H, s,  $\text{C}^2\text{H}$  and  $\text{C}^6\text{H}$ ), 2.55 (6H, s,  $\text{C}^3\text{CH}_3$  and  $\text{C}^5\text{CH}_3$ ) and 1.40 (6H, s,  $\text{C}^1\text{CH}_3$  and  $\text{C}^7\text{CH}_3$ );  $^{13}\text{C}$  NMR (100 MHz,  $\text{CDCl}_3$ ):  $\delta$  = 156.6 (2C,  $\text{C}^3$  and  $\text{C}^5$ ), 150.7 (2C,  $\text{C}^{2'}$  and  $\text{C}^{6'}$ ), 143.8 ( $\text{C}^8$ ), 142.8 (2C,  $\text{C}^1$  and  $\text{C}^7$ ), 137.7 ( $\text{C}^{4'}$ ), 130.5 (2C,  $\text{C}^9$  and  $\text{C}^{10}$ ), 123.5 (2C,  $\text{C}^{3'}$  and  $\text{C}^{5'}$ ), 121.9 (2C,  $\text{C}^2$  and  $\text{C}^6$ ), 14.77 (2C, t,  $^4J_{\text{CF}}$  2.2,  $\text{C}^3\text{CH}_3$  and  $\text{C}^5\text{CH}_3$ ) and 14.75 (2C,  $\text{C}^1\text{CH}_3$  and  $\text{C}^7\text{CH}_3$ );  $^{19}\text{F}$  NMR (282 MHz,  $\text{CDCl}_3$ ):  $\delta$  = -146.3 ( $\Psi_q$ ,  $^1J_{\text{BF}}$  32.5); [ $m/z$  (ESI) found: 326.1633 ( $\text{M}+\text{H}$ ) $^+$ ,  $\text{C}_{18}\text{H}_{19}\text{BF}_2\text{N}_3\text{O}$  requires 326.1635].

Data in agreement with the literature values<sup>[82]</sup>

**2,6-Diiodo-8-(4'-pyridyl)-1,3,5,7-tetramethyl pyrromethene difluoroborate (114)**

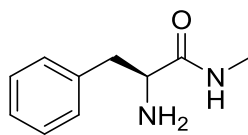


To a dark red solution of **113** (14.0 mg, 43.1  $\mu\text{mol}$ ) in 1,1,1,3,3,3-hexafluoro-2-propanol (370  $\mu\text{L}$ ) was added NIS (20.1 mg, 89.1  $\mu\text{mol}$ ) and the mixture was stirred for 10 min. A solution of  $\text{Na}_2\text{S}_2\text{O}_3 \cdot 5\text{H}_2\text{O}$  (aq., 10% w/w, 10 mL) was added and the mixture was extracted with  $\text{CH}_2\text{Cl}_2$  (3 x 10 mL). The combined organic layers were dried over  $\text{Na}_2\text{SO}_4$  and concentrated *in vacuo* to give a red solid which was purified by column chromatography (EtOAc : *c*-hex / 1 : 4, dry loading) to give a dark red solid (23.4 mg, 94%).  $R_f$  0.65 (EtOAc : *c*-hex / 1 : 1); m.p. 220-223  $^\circ\text{C}$ ;  $\nu_{\text{max}}$  (neat)/ $\text{cm}^{-1}$  2921w, 2852w, 2313w, 2094w, 1888w, 1709w, 1636w, 1602w, 1526s, 1444m, 1397m, 1344m, 1306m, 1270w, 1167s, 1119s, 1060s, 986s, 917s, 867m, 823m, 794m, 761s, 718s, 705s, 659;  $^1\text{H}$  NMR (400 MHz,  $\text{CDCl}_3$ ):  $\delta$  = 8.84 (2H, d,  $^3J$  5.4,  $\text{C}^{2'}\text{H}$  and  $\text{C}^{6'}\text{H}$ ), 7.36 (2H, d,  $^3J$  5.9,  $\text{C}^{3'}\text{H}$  and  $\text{C}^{5'}\text{H}$ ), 2.65 (6H, s,  $\text{C}^3\text{CH}_3$  and  $\text{C}^5\text{CH}_3$ ) and 1.42 (6H, s,  $\text{C}^1\text{CH}_3$  and  $\text{C}^7\text{CH}_3$ );  $^{13}\text{C}$  NMR (100 MHz,  $\text{CDCl}_3$ ):  $\delta$  = 158.2 (2C,  $\text{C}^3$  and  $\text{C}^5$ ), 150.1 (2C,  $\text{C}^{2'}\text{H}$  and  $\text{C}^{6'}\text{H}$ ), 144.9 (2C,  $\text{C}^1$  and  $\text{C}^7$ ), 144.6 ( $\text{C}^4$ ), 136.7 ( $\text{C}^8$ ), 130.3 (2C,  $\text{C}^9$  and  $\text{C}^{10}$ ), 123.7 (2C,  $\text{C}^{3'}\text{H}$  and  $\text{C}^{5'}\text{H}$ ), 86.6 (2C,  $\text{C}^2$  and  $\text{C}^6$ ), 17.5 (2C,  $\text{C}^1\text{CH}_3$  and  $\text{C}^7\text{CH}_3$ ) and 16.3 (2C, t,  $^4J_{\text{CF}}$  2.4,  $\text{C}^3\text{CH}_3$  and  $\text{C}^5\text{CH}_3$ );  $^{19}\text{F}$  NMR (282 MHz,  $\text{CDCl}_3$ ):  $\delta$  = -145.6 ( $\Psi_{\text{q}}$ ,  $^1J_{\text{BF}}$  32.0); [ $m/z$  (ESI) found: 577.9571 ( $\text{M}+\text{H}$ ) $^+$ ,  $\text{C}_{18}\text{H}_{17}\text{BF}_2\text{I}_2\text{N}_3$  requires 577.9567].

Data in agreement with the literature values<sup>[82]</sup>

Photoredoxcatalysts

(*S*)-2-Amino-*N*-methyl-3-phenylpropanamide (**124**)



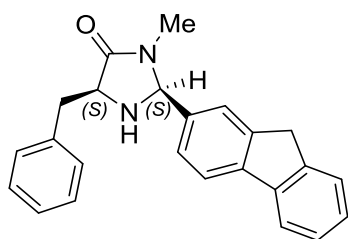
**124**

A suspension of L-Phenylalanine (5.00 g, 30.3 mmol) in MeOH (50 mL) in a dry flask was treated with SOCl<sub>2</sub> (2.65 mL, 36.4 mmol) at 0 °C to give a colourless solution. This was stirred at reflux for 15 h, cooled to rt and concentrated *in vacuo* to give (*S*)-Methyl-2-amino-3-phenylpropanoate hydrochloride as a white solid (quant.). A solution of methylamine in EtOH (15.1 mL, 8 M, 121 mmol) was added to give a white suspension, which was stirred at rt for 24 h and concentrated *in vacuo* to give a light green solid. NaHCO<sub>3</sub> (sat., 20 mL) was added and the mixture was extracted with CH<sub>2</sub>Cl<sub>2</sub> (2 x 20 mL). The combined organic layers were dried (Na<sub>2</sub>SO<sub>4</sub>) and concentrated to give a light green solid (4.04 g, 75 % over two steps); m.p. 66-68 °C; [ $\alpha$ ]<sub>D</sub><sup>25</sup> -79.2 (*c* 1.00 in CHCl<sub>3</sub>); <sup>1</sup>H NMR (300 MHz, CDCl<sub>3</sub>):  $\delta$  = 7.37-7.19 (5H, m, Ph), 3.61 (1H, dd, <sup>3</sup>*J* 9.5, <sup>3</sup>*J* 3.9, NCH), 3.30 (1H, dd, <sup>2</sup>*J* 13.7, <sup>3</sup>*J* 3.9, PhCHH), 2.82 (3H, d, <sup>3</sup>*J* 5.0, NCH<sub>3</sub>) and 2.67 (1H, dd, <sup>2</sup>*J* 13.7, <sup>3</sup>*J* 9.5, PhCHH).

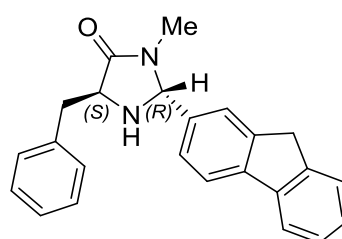
Data in agreement with the literature values<sup>[96]</sup>

(*2S,5S*)- and (*2R,5S*)-5-Benzyl-2-(9*H*-fluoren-2-yl)-3-methylimidazolidin-4-one

(**126** and **127**)



**126**



**127**

A dry flask was loaded with MS (4 Å), **124** (147 mg, 825  $\mu$ mol), 9*H*-fluorene-2-carbaldehyde (**125**) (160 mg, 825  $\mu$ mol) and FeCl<sub>3</sub> (26.7 mg, 165  $\mu$ mol). THF (3.0 mL) was added to give a brown mixture which was stirred at rt for 18 h. The mixture was concentrated *in vacuo*, dissolved in CH<sub>2</sub>Cl<sub>2</sub> (3.0 mL) and washed with water (3 x 3.0 mL). The organic layer was dried (Na<sub>2</sub>SO<sub>4</sub>) and concentrated *in vacuo* to give a yellow oil (*syn* : *anti* = 1 : 1.3). This was purified by column chromatography (EtOAc : <sup>c</sup>Hex / 1 : 1  $\rightarrow$  MeOH : CH<sub>2</sub>Cl<sub>2</sub> / 1 : 10) to give

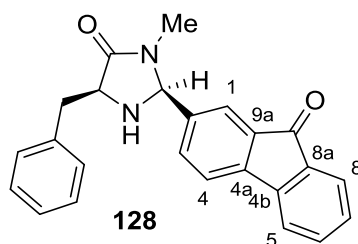


two yellow solids (164 mg, 56 % (*trans*)), (92.4 mg, 32 % (*cis*)). The relative stereochemistry was determined by means of NOE-experiments.

**cis:**  $R_f$  0.14 (EtOAc :  $^o$ Hex / 1 : 1); m.p. 57-60 °C;  $[\alpha]_D^{25}$  -87.0 (*c* 0.10 in CHCl<sub>3</sub>);  $\nu_{\max}$  (neat)/cm<sup>-1</sup> 3330w, 3027w, 2919w, 1948w, 1689s, 1582w, 1496m, 1472m, 1453s, 1430s, 1398s, 1331m, 1302m, 1274m, 1213m, 1178m, 1135m, 1096m, 1029m, 1005m, 953m, 928m, 884w, 829m, 771s, 736s, 699s; <sup>1</sup>H NMR (400 MHz, CDCl<sub>3</sub>):  $\delta$  = 7.76 (1H, d, <sup>3</sup>*J* 7.2 Hz, fluorene), 7.65 (1H, d, <sup>3</sup>*J* 7.8 Hz, fluorene), 7.54 (1H, d, <sup>3</sup>*J* 7.2 Hz, fluorene), 7.23-7.40 (7H, m, Ph and fluorene), 6.90 (1H, dd, <sup>3</sup>*J* 7.8 Hz, <sup>4</sup>*J* 1.4 Hz, fluorene), 6.79 (1H, s, fluorene), 5.19 (1H, d, *J* 1.4 Hz, NCHN), 3.90 (1H, t, <sup>3</sup>*J* 4.5 Hz, C(O)CH), 3.78 (2H, s, ArCH<sub>2</sub>Ar), 3.34 (1H, dd, <sup>2</sup>*J* 14.1 Hz, <sup>3</sup>*J* 5.2 Hz, PhCHH), 3.12 (1H, dd, <sup>2</sup>*J* 14.1 Hz, <sup>3</sup>*J* 4.8 Hz, PhCHH), 2.58 (3H, s, NCH<sub>3</sub>); <sup>13</sup>C NMR (100 MHz, CDCl<sub>3</sub>):  $\delta$  = 174.5 (C=O), 144.2 (C<sup>quat</sup>), 143.6 (C<sup>quat</sup>), 143.3 (C<sup>quat</sup>), 141.0 (C<sup>quat</sup>), 137.1 (C<sup>quat</sup>), 136.8 (C<sup>quat</sup>), 130.2 (2C, C<sup>ortho</sup>), 129.0 (2C, C<sup>meta</sup>), 127.4 (C<sup>arom</sup>), 127.1 (C<sup>arom</sup>), 127.0 (C<sup>arom</sup>), 126.3 (C<sup>arom</sup>), 125.2 (C<sup>arom</sup>), 123.5 (C<sup>arom</sup>), 120.3 (C<sup>arom</sup>), 120.2 (C<sup>arom</sup>), 77.9 (NCHN), 60.5 (C(O)CH), 36.9 (ArCH<sub>2</sub>Ar), 36.8 (PhCH<sub>2</sub>), 27.5 (CH<sub>3</sub>). [*m/z* (EI) found: 354.1722 (M)<sup>+</sup>, C<sub>24</sub>H<sub>22</sub>N<sub>2</sub>O requires 354.1732].

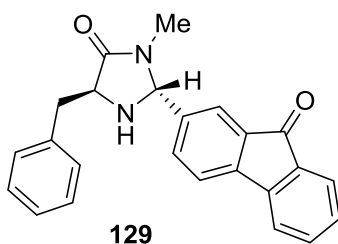
**trans:**  $R_f$  0.44 (EtOAc :  $^o$ Hex / 1 : 1); m.p. 131-134 °C;  $[\alpha]_D^{25}$  +52.0 (*c* 0.10 in CHCl<sub>3</sub>);  $\nu_{\max}$  (neat)/cm<sup>-1</sup> 3375w, 3284w, 3025w, 2921w, 2861w, 1686s, 1667s, 1605w, 1496w, 1470m, 1455m, 1428s, 1395s, 1361m, 1323m, 1300w, 1277m, 1214m, 1156w, 1141w, 1121m, 1094m, 1004m, 950w, 843m, 802m, 767s, 739s, 702s, 692s, 656m; <sup>1</sup>H NMR (400 MHz, CDCl<sub>3</sub>):  $\delta$  = 7.80-7.73 (2H, m, fluorene), 7.54 (1H, d, <sup>3</sup>*J* 7.3, fluorene), 7.41-7.35 (2H, m, fluorene), 7.34-7.20 (7H, m, fluorene and Ph), 4.95 (1H, d, *J* 1.7, NCHN), 4.14-4.09 (1H, m, C(O)CH), 3.88 (2H, s, ArCH<sub>2</sub>Ar), 3.16 (1H, dd, <sup>2</sup>*J* 13.7 Hz, <sup>3</sup>*J* 4.0 Hz, PhCHH), 2.99 (1H, dd, <sup>2</sup>*J* 13.7 Hz, <sup>3</sup>*J* 7.4 Hz, PhCHH), 2.62 (3H, s, NCH<sub>3</sub>); <sup>13</sup>C NMR (100 MHz, CDCl<sub>3</sub>):  $\delta$  = 174.4 (C=O), 144.3 (C<sup>quat</sup>), 143.6 (C<sup>quat</sup>), 143.1 (C<sup>quat</sup>), 141.0 (C<sup>quat</sup>), 137.9 (2C, C<sup>quat</sup>), 129.8 (2C, C<sup>ortho</sup>), 128.6 (2C, C<sup>meta</sup>), 127.4 (C<sup>arom</sup>), 127.1 (C<sup>arom</sup>), 126.9 (C<sup>arom</sup>), 125.7 (C<sup>arom</sup>), 125.3 (C<sup>arom</sup>), 123.4 (C<sup>arom</sup>), 120.5 (C<sup>arom</sup>), 120.3 (C<sup>arom</sup>), 78.1 (NCHN), 60.3 (C(O)CH), 39.0 (ArCH<sub>2</sub>Ar), 37.0 (PhCH<sub>2</sub>), 27.4 (CH<sub>3</sub>).; [*m/z* (EI) found: 354.1726 (M)<sup>+</sup>, C<sub>24</sub>H<sub>22</sub>N<sub>2</sub>O requires 354.1732].

(2*S*,5*S*)-5-Benzyl-3-methyl-2-(9-oxo-9*H*-fluoren-2-yl)-imidazolidin-4-one (**128**)

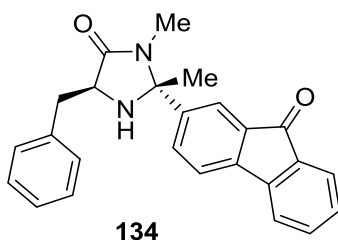


Cs<sub>2</sub>CO<sub>3</sub> (160 mg, 490 μmol) was suspended in a yellow solution of **126** (86.6 mg, 245 μmol) in DMF (2.0 mL). The mixture was stirred at rt under an air atmosphere for 62 h. A change of colour to brown was observed. Rochelle salt solution (sat., 20 mL) was added and the mixture was extracted with CH<sub>2</sub>Cl<sub>2</sub> (2 x 20 mL). The combined organic layers were washed with a Rochelle salt solution (sat.) – water mixture (1 : 3, 2 x 40 mL) and water (3 x 30 mL), dried over Na<sub>2</sub>SO<sub>4</sub> and concentrated *in vacuo* to give a yellow resin. This was purified by column chromatography (MeOH : CH<sub>2</sub>Cl<sub>2</sub> / 1 : 30) to give a yellow resin (44.0 mg, 49 %); R<sub>f</sub> 0.19 (EtOAc); [α]<sub>D</sub><sup>25</sup> -85.6 (*c* 1.00 in CHCl<sub>3</sub>); ν<sub>max</sub> (neat)/cm<sup>-1</sup> 3324w, 3054w, 2921w, 2852w, 2162w, 2047w, 1943w, 1694s (broad), 1616m, 1603m, 1496w, 1477w, 1455w, 1434m, 1399s, 1332m, 1293m, 1265m, 1178m, 1157m, 1135m, 1103s, 1029w, 1002m, 945m, 916m, 841m, 807w, 768m, 734s and 700s; <sup>1</sup>H NMR (600 MHz, CDCl<sub>3</sub>): δ = 7.66 (1H, d, *J* 7.3, C1-*H*), 7.53-7.48 (2H, m, C5-*H* and C6-*H*), 7.40 (1H, d, <sup>3</sup>*J* 7.6, C4-*H*), 7.34-7.30 (4H, m, *Ph*<sup>meta</sup> and C7-*H* and *Ph*<sup>para</sup>), 7.27-7.23 (3H, m, C8-*H* and *Ph*<sup>ortho</sup>), 6.95 (1H, d, <sup>3</sup>*J* 7.7, C3-*H*), 5.20 (1H, br. s, NCHN), 3.91 (1H, br. s, NCHC), 3.24 (1H, dd, <sup>2</sup>*J* 14.0, <sup>3</sup>*J* 5.6, PhCHH), 3.16 (1H, dd, <sup>2</sup>*J* 13.9, <sup>3</sup>*J* 3.9, PhCHH) and 2.59 (3H, s, NCH<sub>3</sub>); <sup>13</sup>C NMR (150 MHz, CDCl<sub>3</sub>): δ = 193.0 (ArC(O)Ar), 174.3 (NC(O)C), 145.8 (C4*b*), 143.8 (C4*a*), 140.0 (C2), 136.7 (C<sup>ipso</sup>), 135.03 (C6), 134.99 (C9*a*), 134.4 (C8*a*), 133.8 (C3), 129.9 (2C, C<sup>ortho</sup>), 129.7 (C7), 129.0 (2C, C<sup>meta</sup>), 127.4 (C<sup>para</sup>), 124.7 (C1), 123.3 (C8), 121.0 (C4), 120.7 (C5), 77.16 (NCHN, under solvent signal, assigned by HSQC), 60.4 (NCHC), 37.3 (PhCH<sub>2</sub>) and 27.5 (NCH<sub>3</sub>); [*m/z* (ESI) found: 391.1418 (M+Na)<sup>+</sup>, C<sub>24</sub>H<sub>20</sub>N<sub>2</sub>O<sub>2</sub>Na requires 391.1422].

(2*R*,5*S*)-5-Benzyl-3-methyl-2-(9-oxo-9*H*-fluoren-2-yl)-imidazolidin-4-one (**129**)



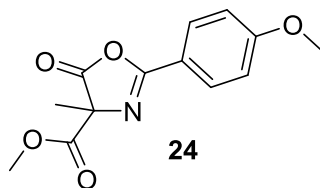
Cs<sub>2</sub>CO<sub>3</sub> (221 mg, 678 μmol) was suspended in a yellow solution of **129** (120 mg, 339 μmol). The mixture was stirred at rt under an air atmosphere for 67 h. A change of colour to brown was observed. Rochelle salt solution (sat., 20 mL) was added and the mixture was extracted with CH<sub>2</sub>Cl<sub>2</sub> (2 x 20 mL). The combined organic layers were washed with a Rochelle salt solution (sat.) – water mixture (1 : 3, 2 x 40 mL) and water (3 x 30 mL), dried (Na<sub>2</sub>SO<sub>4</sub>) and concentrated *in vacuo* to give a yellow resin. This was purified by column chromatography (MeOH : CH<sub>2</sub>Cl<sub>2</sub> / 1 : 30) to give a yellow resin (68.0 mg, 54 %); R<sub>f</sub> 0.33 (EtOAc : <sup>c</sup>Hex / 1 : 1); m.p. 73-76 °C; [α]<sub>D</sub><sup>25</sup> +56.0 (*c* 0.10 in CHCl<sub>3</sub>); ν<sub>max</sub> (neat)/cm<sup>-1</sup> 3318w, 3028w, 2920w, 1688s (broad), 1616s, 1603s, 1496w, 1479w, 1454s, 1432s, 1398s, 1337m, 1292m, 1256m, 1178s, 1157w, 1135w, 1103s, 1029w, 1001w, 965w, 925w, 844m, 768s, 737s, 670s, 651s, 623s; <sup>1</sup>H NMR (400 MHz, CDCl<sub>3</sub>): δ = 7.66 (1H, d, *J* 7.3, fluorenone), 7.54-7.47 (3H, m, fluorenone), 7.39-7.22 (8H, m, fluorenone and Ph), 4.87 (1H, d, <sup>4</sup>*J* 1.4, NCHN), 4.16-4.09 (1H, m, NCHCH<sub>2</sub>), 3.17 (1H, dd, <sup>2</sup>*J* 13.7, <sup>3</sup>*J* 4.1, PhCHH), 3.03 (1H, dd, <sup>2</sup>*J* 13.7, <sup>3</sup>*J* 7.0, PhCHH) and 2.59 (3H, s, NCH<sub>3</sub>); <sup>13</sup>C NMR (75 MHz, CDCl<sub>3</sub>): δ = 193.2 (ArC(O)Ar), 174.3 (NC(O)C), 145.6 (*C*<sup>quat</sup>), 143.9 (*C*<sup>quat</sup>), 141.0 (*C*<sup>quat</sup>), 137.5 (*C*<sup>quat</sup>), 135.2 (*C*<sup>quat</sup>), 135.1 (*C*<sup>fluorenone</sup>), 134.4 (*C*<sup>quat</sup>), 133.3 (*C*<sup>fluorenone</sup>), 129.8 (2*C*, *C*<sup>ortho</sup>), 129.7 (*C*<sup>fluorenone</sup>), 128.7 (2*C*, *C*<sup>meta</sup>), 127.0 (*C*<sup>para</sup>), 124.7 (*C*<sup>fluorenone</sup>), 122.9 (*C*<sup>fluorenone</sup>), 121.0 (*C*<sup>fluorenone</sup>), 120.8 (*C*<sup>fluorenone</sup>), 77.3 (NCHN), 60.1 (NCHCH<sub>2</sub>), 38.9 (PhCH<sub>2</sub>) and 27.3 (NCH<sub>3</sub>); [*m/z* (EI) found: 368.1520 (M)<sup>+</sup>, C<sub>24</sub>H<sub>20</sub>N<sub>2</sub>O requires 368.1525].

**(2*R*,5*S*)-5-Benzyl-2,3-dimethyl-2-(9-oxo-9*H*-fluoren-2-yl)-imidazolidin-4-one (134)**

A brown solution of **133** (3.50 g, 16.8 mmol), **124** (2.99 g, 16.8 mmol) and *p*-TsOH·H<sub>2</sub>O (31.9 mg, 168 μmol) in toluene (180 mL) was stirred at reflux in a flask equipped with a Dean-Stark condenser for 60 h. The mixture was cooled to rt and concentrated *in vacuo* to give a brown oil (cis:trans = 1.1 : 1). This was purified by column chromatography (EtOAc : <sup>c</sup>Hex / 1 : 10 → 1 : 0, dry loading) to give a yellow oil (1.90 g (trans)) and an orange oil (1.90 g (cis)); Cs<sub>2</sub>CO<sub>3</sub> (3.36 g, 10.3 mmol) was suspended in a yellow solution of (2*R*,5*S*)-5-benzyl-2-(9*H*-fluoren-2-yl)-2,3-dimethylimidazolidin-4-one (1.90 g, 5.16 mmol) in DMF (50 mL). The mixture was stirred at rt for 13 h while air was bubbled through it. A change of colour to brown was observed. Water (50 mL) was added and the mixture was extracted with CH<sub>2</sub>Cl<sub>2</sub> (2 x 50 mL). The combined organic layers were washed with water (6 x 50 mL), dried over Na<sub>2</sub>SO<sub>4</sub> and concentrated *in vacuo* to give a yellow oil solid (1.24 g, 63 % over 2 steps); *R*<sub>f</sub> 0.32 (EtOAc : <sup>c</sup>Hex / 1 : 1); m.p. 55-59 °C; [α]<sub>D</sub><sup>25</sup> +32.2 (*c* 1.00 in CHCl<sub>3</sub>); ν<sub>max</sub> (neat)/cm<sup>-1</sup> 3330w, 3060w, 3028w, 2924w, 1674s (broad), 1615m, 1603s, 1496w, 1455m, 1424m, 1393s, 1292m, 1253m, 1181s, 1154m, 1107s, 1087m, 1065m, 1030w, 1001w, 954m, 911w, 841m, 807w, 769m, 767s, 700s, 660m, 649m, 635m and 622m; <sup>1</sup>H NMR (400 MHz, CDCl<sub>3</sub>): δ = 7.66 (1H, d, <sup>3</sup>*J* 7.4, fluorenone), 7.59 (1H, d, *J* 1.6, fluorenone), 7.53-7.46 (3H, m, fluorenone), 7.39 (1H, dd, <sup>3</sup>*J* 7.8, *J* 1.9, fluorenone), 7.33-7.22 (6H, m, fluorenone and Ph), 3.89 (1H, dd, <sup>3</sup>*J* 6.6, <sup>3</sup>*J* 4.5, NCH), 3.17 (1H, <sup>2</sup>*J* 14.0, <sup>3</sup>*J* 4.4, PhCHH), 3.06 (1H, <sup>2</sup>*J* 14.0, <sup>3</sup>*J* 6.8, PhCHH), 2.76 (3H, s, NCH<sub>3</sub>) and 1.55 (3H, s, CCH<sub>3</sub>); <sup>13</sup>C NMR (100 MHz, CDCl<sub>3</sub>): δ = 193.5 (ArC(O)Ar), 173.6 (NC(O)C), 144.40 (C<sup>quat</sup>), 144.37 (C<sup>quat</sup>), 143.9 (C<sup>quat</sup>), 137.3 (C<sup>quat</sup>), 135.04 (C<sup>fluorenone</sup>), 134.98 (C<sup>quat</sup>), 134.5 (C<sup>quat</sup>), 131.6 (C<sup>fluorenone</sup>), 129.8 (2C, C<sup>ortho</sup>), 129.5 (C<sup>fluorenone</sup>), 128.7 (2C, C<sup>meta</sup>), 127.0 (C<sup>para</sup>), 124.7 (C<sup>fluorenone</sup>), 121.5 (C<sup>fluorenone</sup>), 120.8 (C<sup>fluorenone</sup>), 120.7 (C<sup>fluorenone</sup>), 78.5 (NCN), 59.4 (NCH), 38.0 (PhCH<sub>2</sub>), 26.30 (CCH<sub>3</sub>) and 26.26 (NCH<sub>3</sub>); [*m/z* (ESI) found: 405.1573 (M+Na)<sup>+</sup>, C<sub>25</sub>H<sub>22</sub>N<sub>2</sub>O<sub>2</sub>Na requires 405.1579].

General procedures for catalyses

Methyl-2-(4-methoxyphenyl)-4-methyl-5-oxo-4,5-dihydrooxazole-4-carboxylate (**24**)

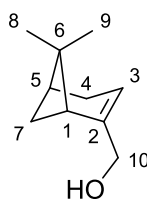


A suspension of the catalyst (7.6  $\mu\text{mol}$ ) in toluene (200  $\mu\text{L}$ ) was treated with  $\text{Cs}_2\text{CO}_3$  (2.5 mg, 7.6  $\mu\text{mol}$ ) and stirred for 15 min. A solution of **23** (20.0 mg, 76.0  $\mu\text{mol}$ ) in toluene (200  $\mu\text{L}$ ) was then added. The mixture was stirred for a further 18 h, after which time the solution was concentrated *in vacuo* and filtered over a plug of silica gel ( $\text{CH}_2\text{Cl}_2$  as eluent). The resulting solution was then concentrated *in vacuo* and the residue was analysed by chiral HPLC: Reprosil chiral-OM (5  $\mu\text{m}$ ; 4.6 mm x 25 cm); eluent: *i*PrOH (with 10% AcOH) : *n*Hex = 1 : 19; flow rate: 1  $\text{mL}\cdot\text{min}^{-1}$ ;  $t_R(\text{minor})$ : 7.7 min,  $t_R(\text{major})$ : 10.6 min.

**Kinetic resolution of ( $\pm$ )-1-phenylethanol:**

To a solution or a suspension of the catalyst (5.00  $\mu\text{mol}$ ) in *n*-hexane (1.0 mL) was added DIPEA (12.7  $\mu\text{L}$ , 75.0  $\mu\text{mol}$ ), ( $\pm$ )-1-phenylethanol (12.1  $\mu\text{L}$ , 100  $\mu\text{mol}$ ) and  $\text{Ac}_2\text{O}$  (7.1  $\mu\text{L}$ , 75.0  $\mu\text{mol}$ ). The mixture was stirred for 15 min (catalysts **28** and **31-33**) (2h for catalysts **59-62** and **64**), filtered over silica gel ( $\text{CH}_2\text{Cl}_2$  as eluent) and concentrated to give a colourless oil. This was dissolved in  $\text{CH}_2\text{Cl}_2$  (1.0 mL) and analysed by GC using a Supelco  $\beta$ -DEX 120 column (100  $^\circ\text{C}$  isotherm): (*S*)-1-phenylethylacetate  $t_R = 27.0$  min, (*R*)-1-phenylethylacetate  $t_R = 29.5$  min, (*R*)-1-phenylethanol  $t_R = 31.5$  min, (*S*)-1-phenylethanol  $t_R = 34.3$  min.

**((1*R*,5*S*)-6,6-Dimethylbicyclo[3.1.1]hept-2-en-2-yl)-methanol (120)**



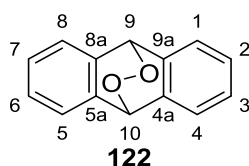
**120**

A 10 mL Schlenk flask was loaded with the appropriate sensitiser (1.0 mol%) and set under an oxygen atmosphere.  $\text{CHCl}_3$  (600  $\mu\text{L}$ ) and (-)- $\beta$ -pinene (200  $\mu\text{L}$ , 1.27 mmol) was added and the mixture was irradiated with a halogen lamp (400 W, as Schwabe (Art.-Nr. 46012)) at 20 cm distance. After the indicated time irradiation was stopped, the solution was cooled to 0 °C and diluted with EtOH (5 mL).  $\text{NaBH}_4$  (94.5 mg, 2.50 mmol) was added portionwise and the mixture was stirred for 10 min, then allowed to warm to rt. After 1 h the solution was treated with citric acid solution (aq., 10%, 5 mL) at 0 °C and allowed to warm to rt, then stirred for 1 h. Water (5 mL) was added and the mixture was extracted with  $\text{CH}_2\text{Cl}_2$  (3 x 10 mL). The combined organic layers were dried over  $\text{Na}_2\text{SO}_4$  and concentrated *in vacuo*. The residue was purified by column chromatography ( $\text{CH}_2\text{Cl}_2$ ) and concentrated *in vacuo* at 100 mbar to give a colourless oil (124 mg, 64%).

$R_f$  0.28 ( $\text{CH}_2\text{Cl}_2$ );  $^1\text{H}$  NMR (300 MHz,  $\text{CDCl}_3$ ):  $\delta$  = 5.46-5.41 (1H, m,  $\text{C}^3\text{H}$ ), 3.95-3.92 (2H,  $\text{C}^{10}\text{H}_2$ ), 2.37 (1H, dt,  $J$  8.6, 5.6,  $\text{C}^7\text{HH}$ ), 2.28-2.20 (2H, m,  $\text{C}^4\text{H}_2$ ), 2.13-2.05 (2H, m,  $\text{C}^5\text{H}$  and  $\text{C}^1\text{H}$ ), 1.26 (3H, s,  $\text{C}^8\text{H}_3$ ), 1.14 (1H, d,  $J$  8.6,  $\text{C}^7\text{HH}$ ) and 0.80 (3H, s,  $\text{C}^9\text{H}_3$ ).

Data in agreement with the literature values<sup>[97]</sup>

**9,10-Dihydro-9,10-epidioxyanthracene (122)**



**122**

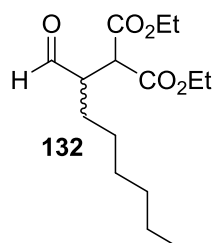
A 10 mL Schlenk flask was set under an oxygen atmosphere and loaded with a solution of anthracene (17.8 mg, 100  $\mu\text{mol}$ ), the appropriate sensitiser (1  $\mu\text{mol}$ ) and *n*-dodecane (22.7  $\mu\text{L}$ , 100  $\mu\text{mol}$ ) in  $\text{CDCl}_3$  (1.0 mL). The solution was irradiated with a halogen lamp (400 W, as Schwabe (Art.-Nr. 46012)) at 30 cm distance through a UV filter (hama, UV 390 Protect Filter, 52 mm) while stirring at 500 rpm. Aliquots (~10  $\mu\text{L}$ ) were taken at the indicated times, diluted with  $\text{CH}_2\text{Cl}_2$  and kept in the dark until analysed by gas chromatography (method: 40 °C to 180 °C at 10 °C per minute, then 180 °C isothermal;  $t_R$ : *n*-

dodecane: 10.6 min; anthracene: 35.3 min; endoperoxide decomposes). Irradiation was stopped after 3 h, the solution was concentrated *in vacuo* at 30 °C and the residue was purified by column chromatography to give a white solid.

$R_f$  0.23 (CH<sub>2</sub>Cl<sub>2</sub> : *n*-pentane / 1 : 2);  $\nu_{\max}$  (neat)/cm<sup>-1</sup> 2968w, 1668w, 1600w, 1461m, 1316m, 1241w, 1172w, 933w, 867m, 808m, 767s, 752s, 714m; <sup>1</sup>H NMR (400 MHz, CDCl<sub>3</sub>):  $\delta$  = 7.45-7.39 (4H, m, C<sup>1</sup>H, C<sup>4</sup>H, C<sup>5</sup>H and C<sup>8</sup>H), 7.32-7.26 (4H, m, C<sup>2</sup>H, C<sup>3</sup>H, C<sup>6</sup>H and C<sup>7</sup>H) and 6.03 (2H, s, C<sup>9</sup>H and C<sup>10</sup>H); <sup>13</sup>C NMR (100 MHz, CDCl<sub>3</sub>):  $\delta$  = 138.2 (4C, C<sup>4a</sup>, C<sup>5a</sup>, C<sup>8a</sup> and C<sup>9a</sup>), 128.1 (4C, C<sup>2</sup>, C<sup>3</sup>, C<sup>6</sup> and C<sup>7</sup>), 123.7 (4C, C<sup>1</sup>, C<sup>4</sup>, C<sup>5</sup> and C<sup>8</sup>), and 79.5 (2C, C<sup>9</sup> and C<sup>10</sup>); [ $m/z$  (ESI) found: 233.0579 (M+Na)<sup>+</sup>, C<sub>14</sub>H<sub>10</sub>O<sub>2</sub>Na requires 233.0578].

Data in agreement with the literature values<sup>[98]</sup>

### Diethyl-2-(1-oxooctan-2-yl)-malonate (132)

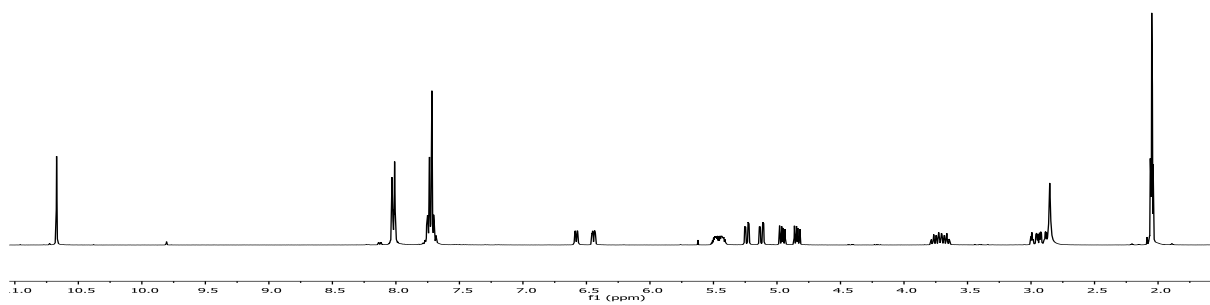
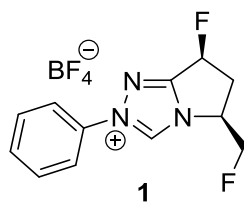


A yellow solution of the appropriate catalyst (31.4  $\mu$ mol), octanal (40.2 mg, 314  $\mu$ mol), diethylbromomalonate (26.8  $\mu$ L, 157  $\mu$ mol) and 2,6-lutidine (15.9  $\mu$ L, 157  $\mu$ mol) in DMF was degassed by passing argon through the solution for 2-3 min and irradiated with LEDs (402 nm, 1 W) at a distance of 1 cm. Conversion was followed by GC (Supelco  $\beta$ -DEX 120 column; 170 °C isotherm,  $t_R$  (bromomalonate): 4.1 min;  $t_R$ (product): 24.7 min). <sup>1</sup>H NMR (300 MHz, CDCl<sub>3</sub>):  $\delta$  = 9.78 (1H, d, <sup>3</sup> $J$  1.2, CHO), 4.16-4.28 (4H, m, <sup>3</sup> $J$  7.1, CO<sub>2</sub>CH<sub>2</sub>CH<sub>3</sub>), 3.74 (1H, d, <sup>3</sup> $J$  8.6, CH(CO<sub>2</sub>Et)<sub>2</sub>), 3.05-3.16 (1H, m, HC(O)CH), 1.58-1.77 (2H, m, CH<sub>2</sub>(CH<sub>2</sub>)<sub>4</sub>CH<sub>3</sub>), 1.23-1.36 (14H, m, CH<sub>2</sub>(CH<sub>2</sub>)<sub>4</sub>CH<sub>3</sub>, CH(CO<sub>2</sub>CH<sub>2</sub>CH<sub>3</sub>)<sub>2</sub>), 0.84-0.93 (3H, m, CH<sub>2</sub>(CH<sub>2</sub>)<sub>4</sub>CH<sub>3</sub>);  $R_f$  = 0.30 (Et<sub>2</sub>O / cyclohexane 1:4). Enantiomeric excess was determined after reduction to the alcohol using NaBH<sub>4</sub> in MeOH by GC: 170 °C isotherm,  $t_R$  (minor): 41.0 min;  $t_R$ (major): 42.3 min).

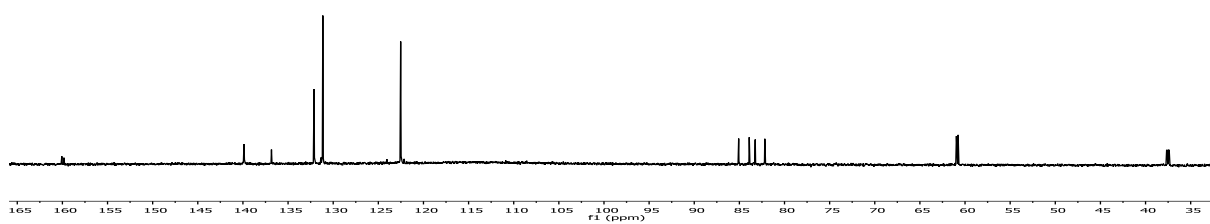
Data in agreement with the literature values<sup>[45]</sup>

Selected NMR Spectra

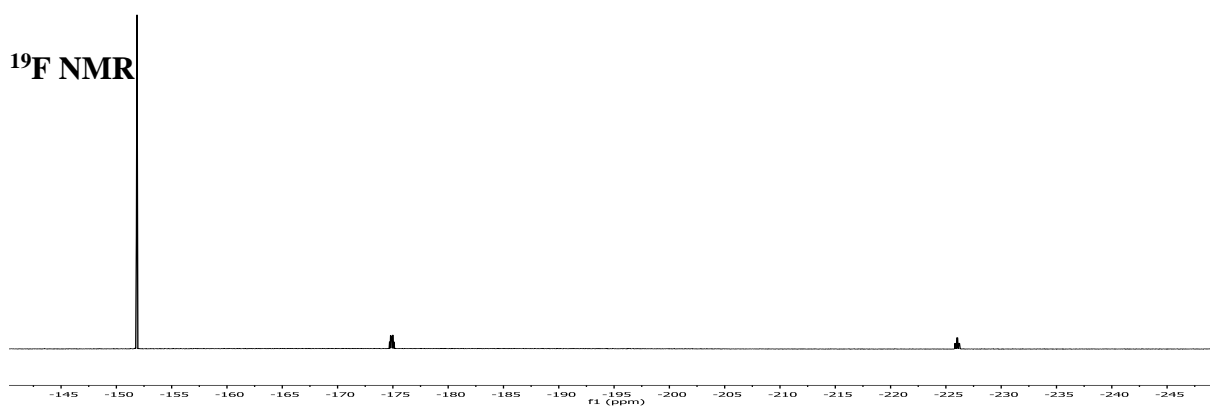
$^1\text{H}$  NMR



$^{13}\text{C}$  NMR

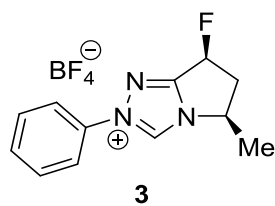


$^{19}\text{F}$  NMR

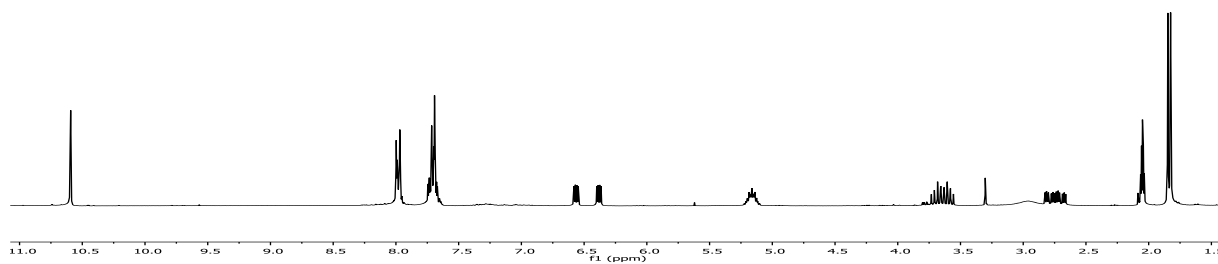




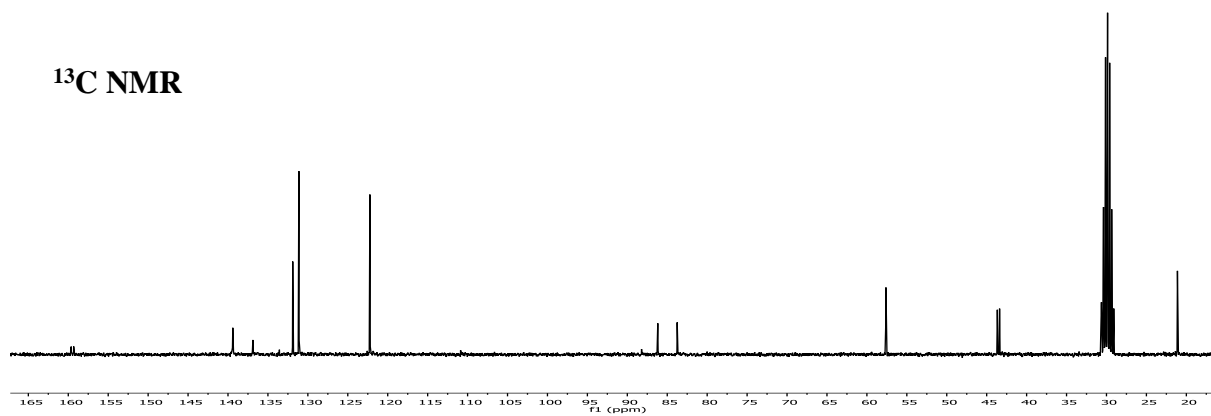
Experimental Part



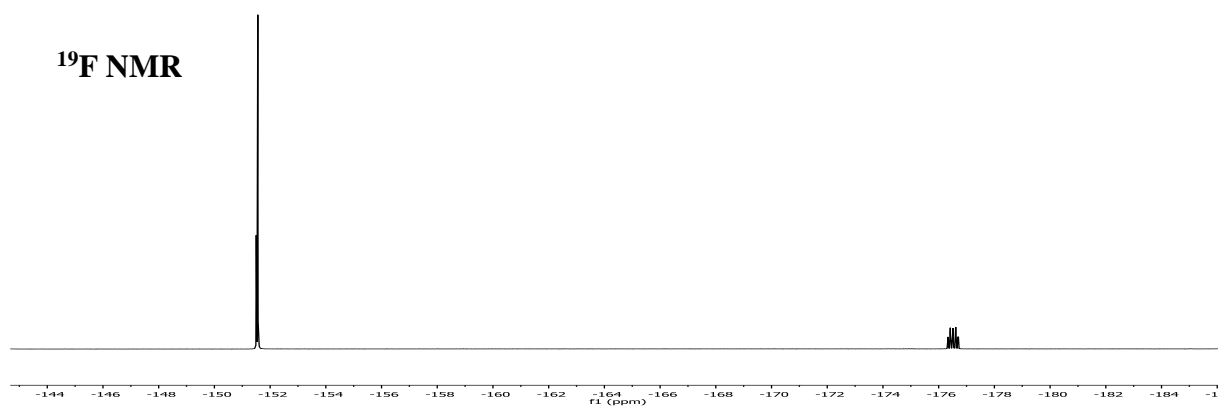
$^1\text{H}$  NMR



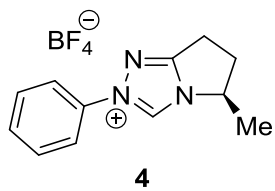
$^{13}\text{C}$  NMR



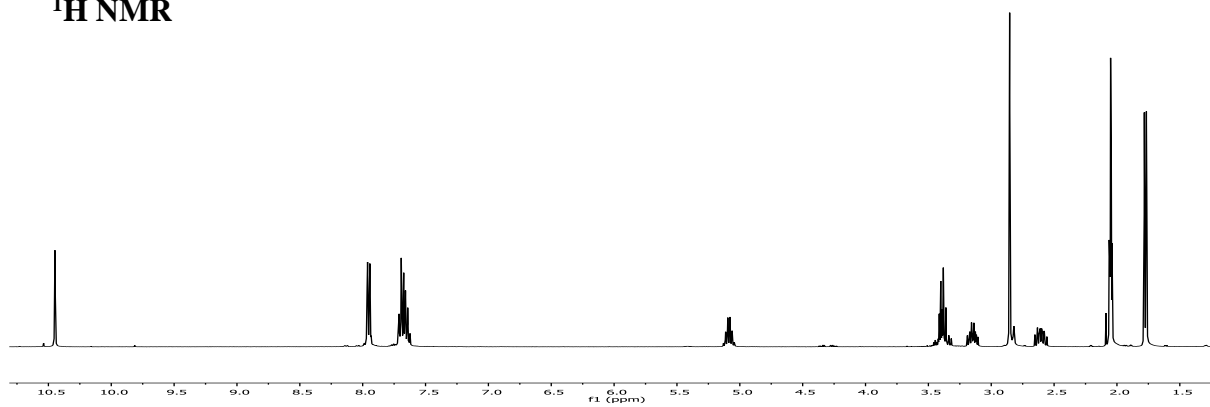
$^{19}\text{F}$  NMR



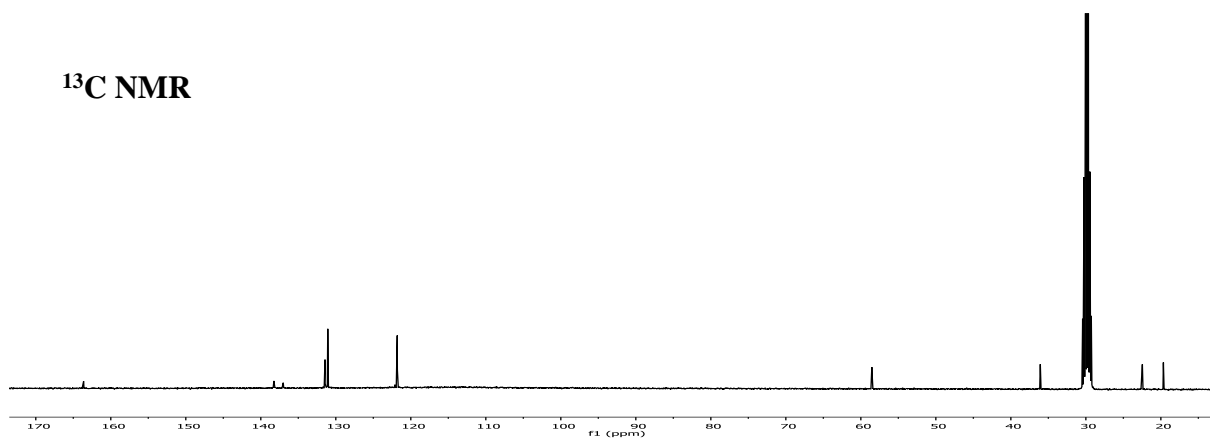
Experimental Part



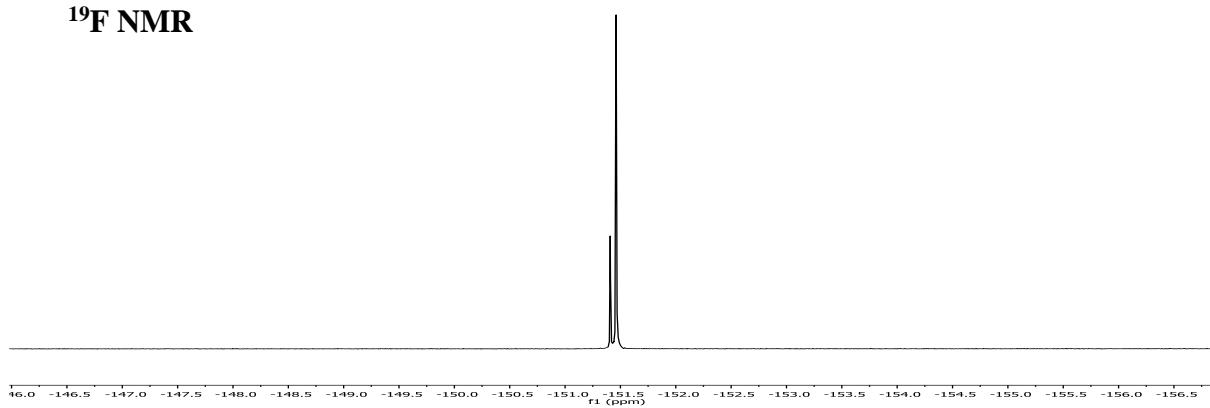
$^1\text{H}$  NMR



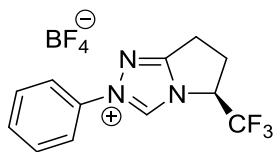
$^{13}\text{C}$  NMR



$^{19}\text{F}$  NMR

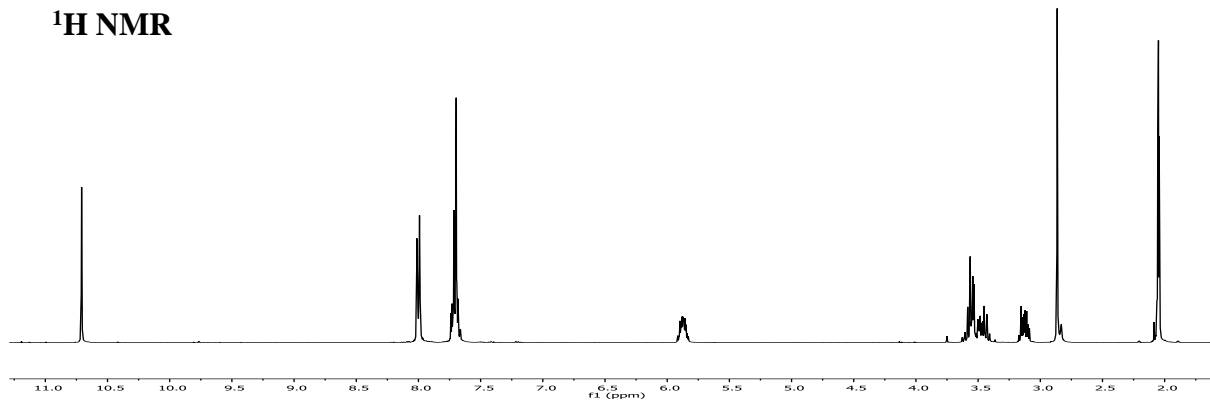


Experimental Part

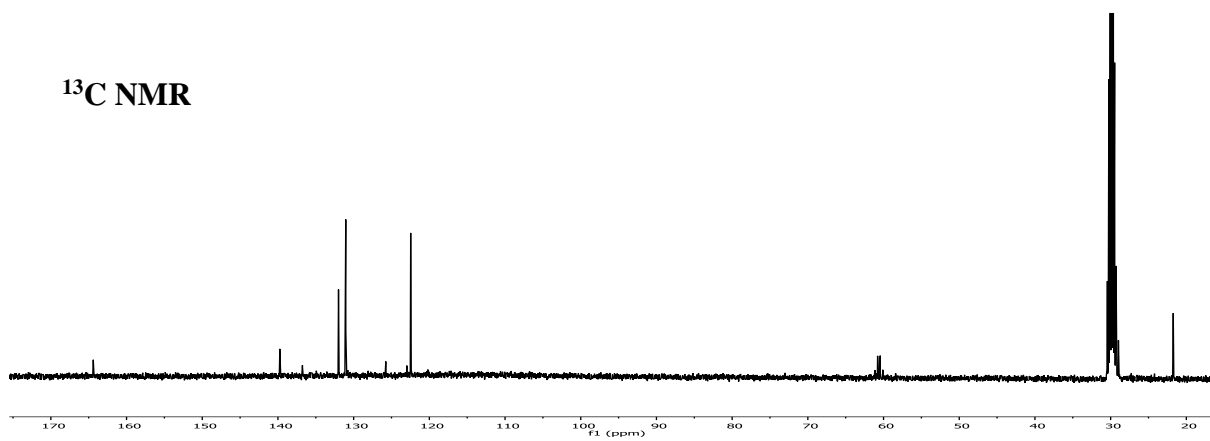


22

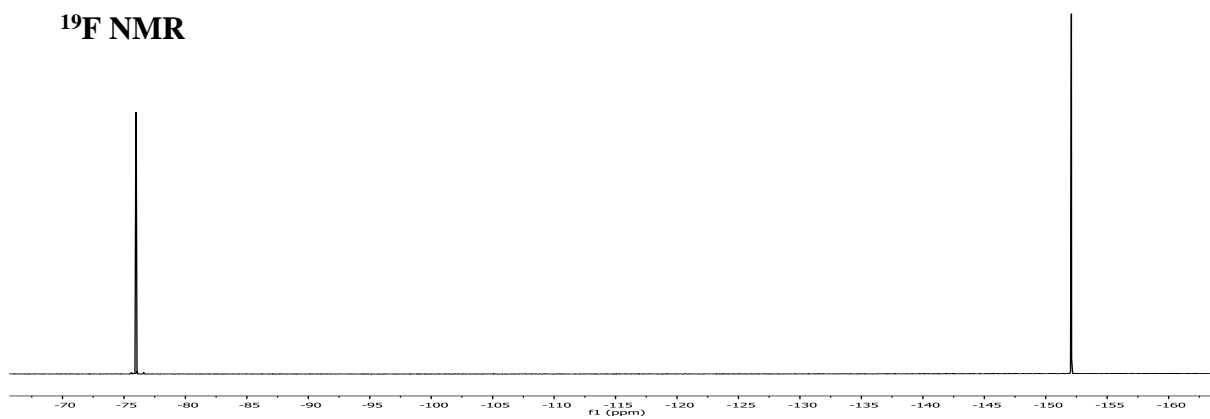
$^1\text{H}$  NMR

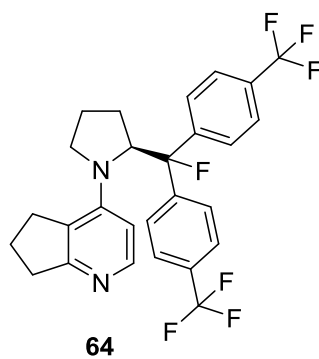


$^{13}\text{C}$  NMR

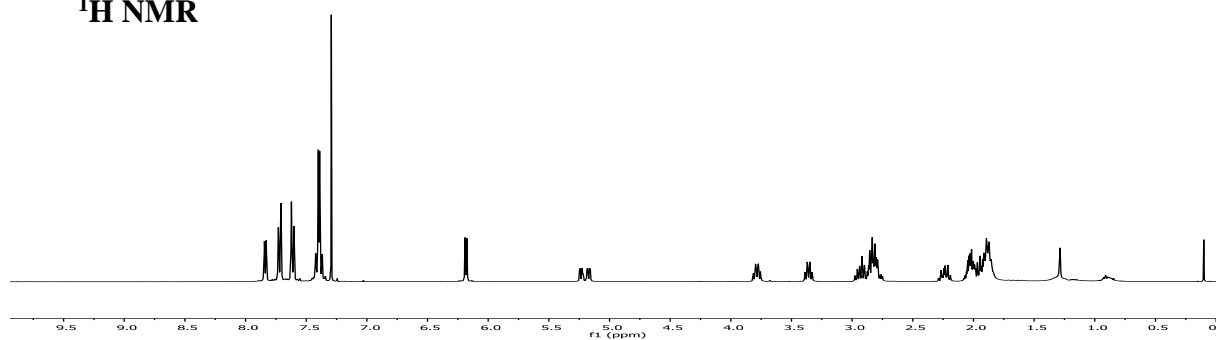


$^{19}\text{F}$  NMR

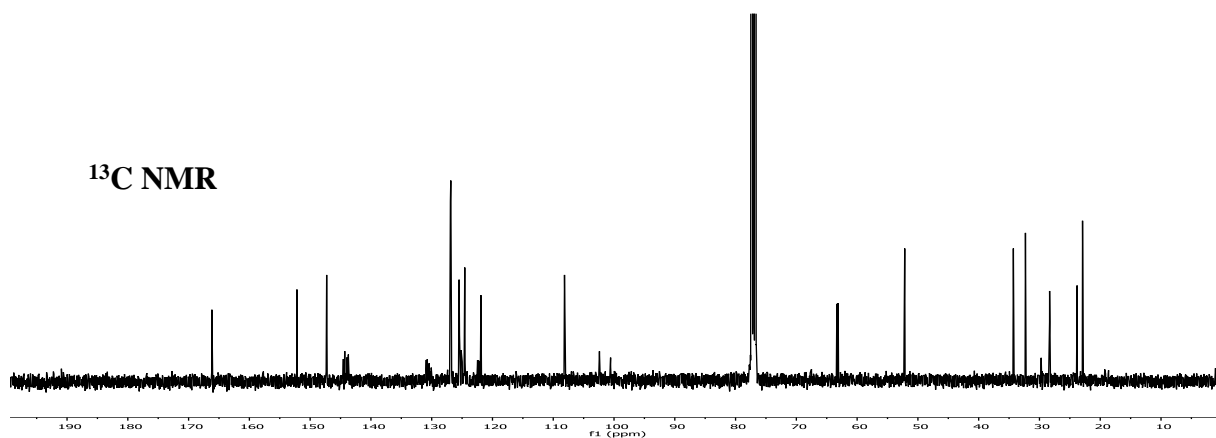




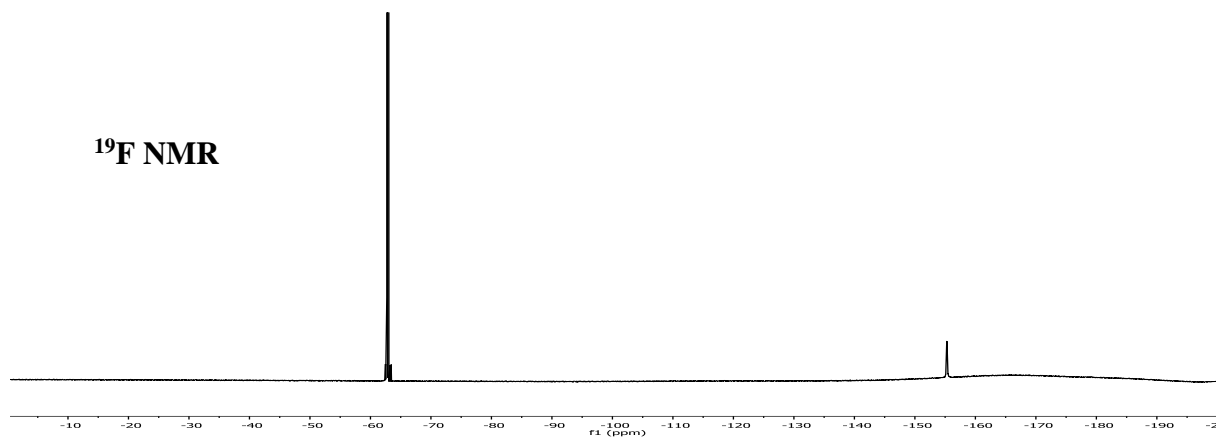
<sup>1</sup>H NMR

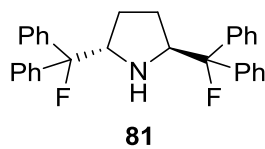


<sup>13</sup>C NMR

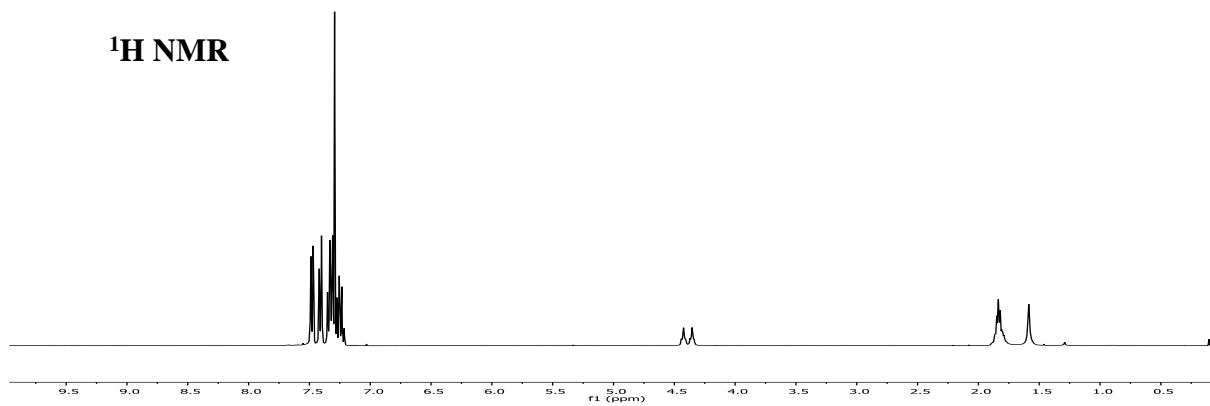


<sup>19</sup>F NMR

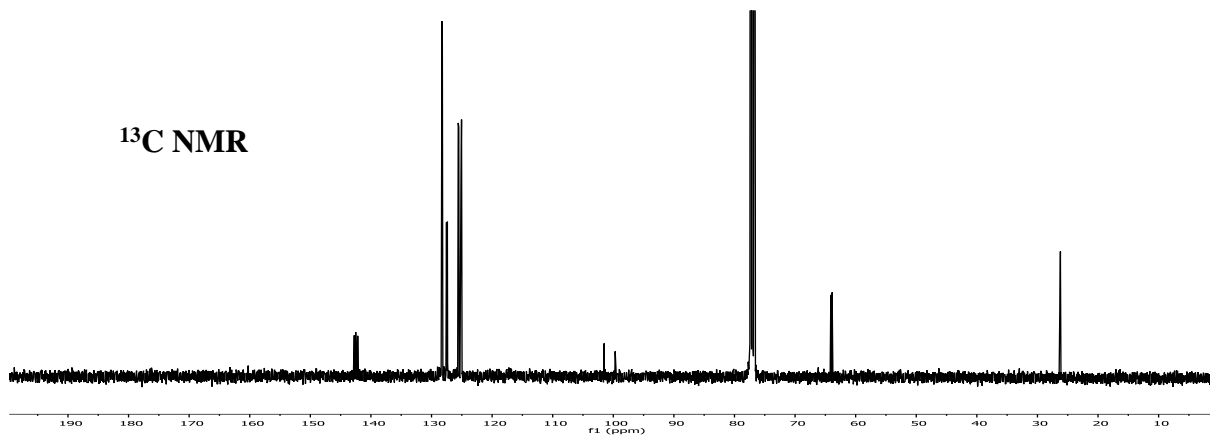




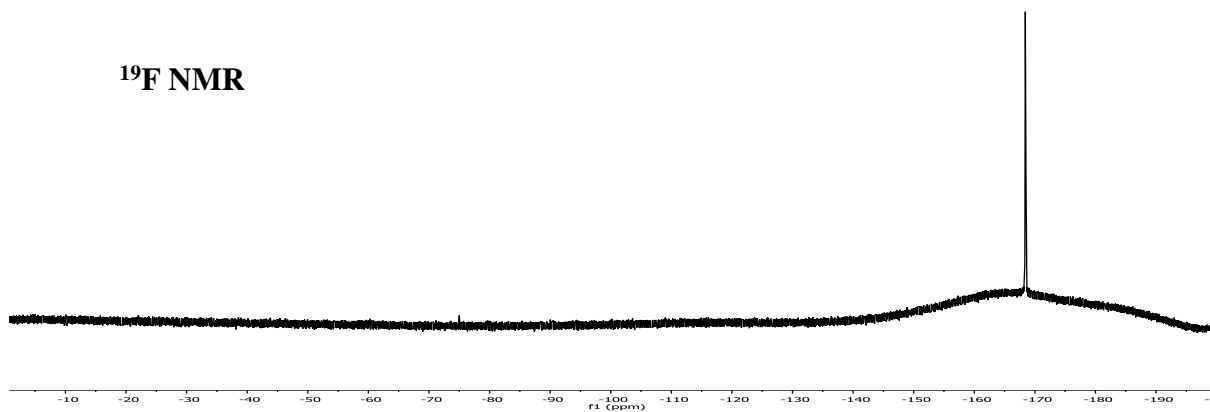
**<sup>1</sup>H NMR**



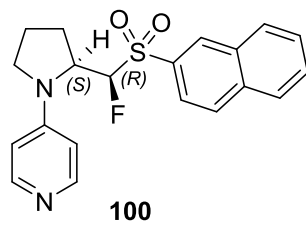
**<sup>13</sup>C NMR**



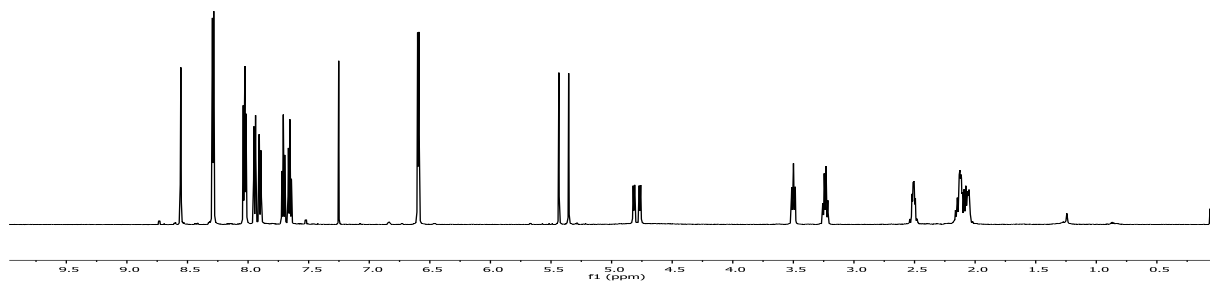
**<sup>19</sup>F NMR**



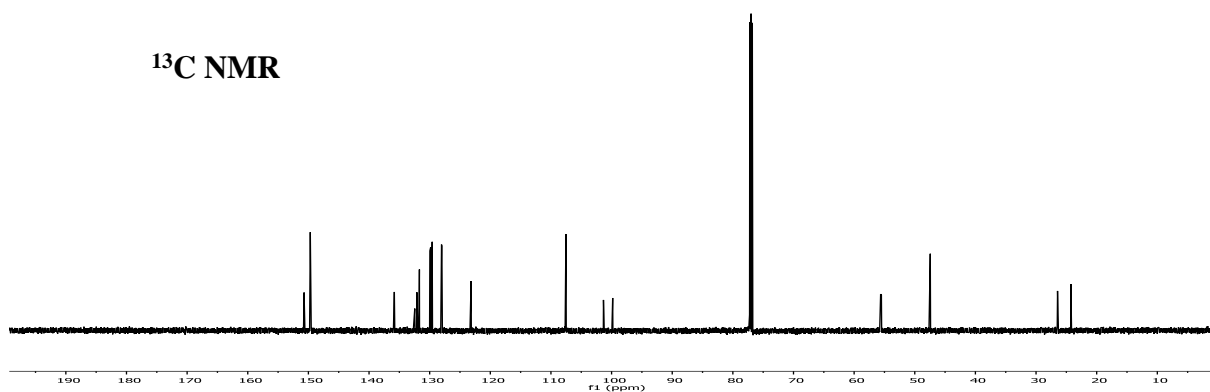
Experimental Part



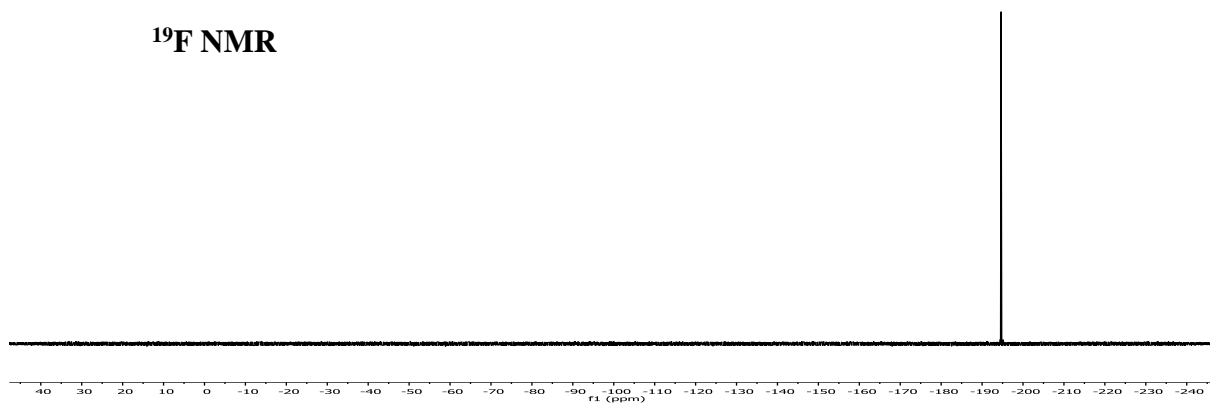
**<sup>1</sup>H NMR**



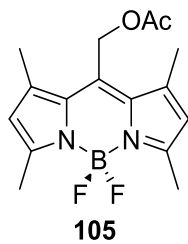
**<sup>13</sup>C NMR**



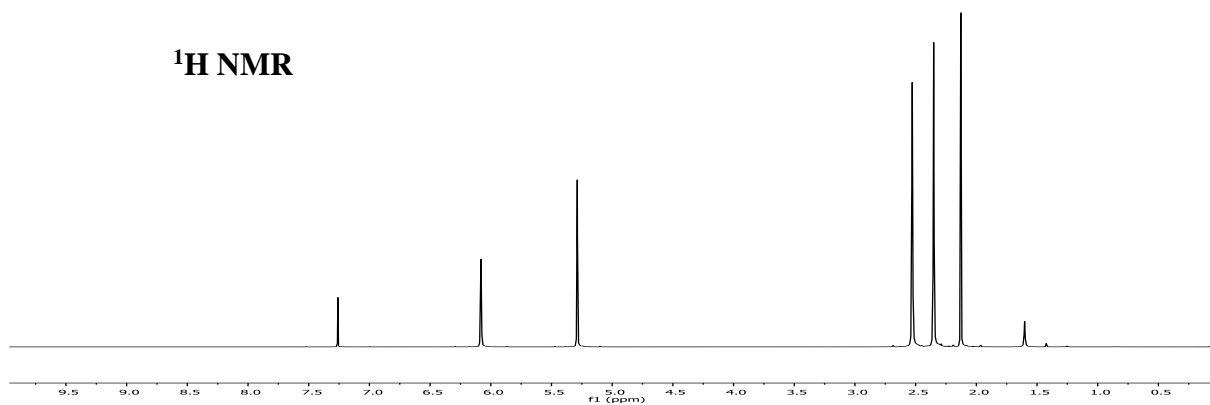
**<sup>19</sup>F NMR**



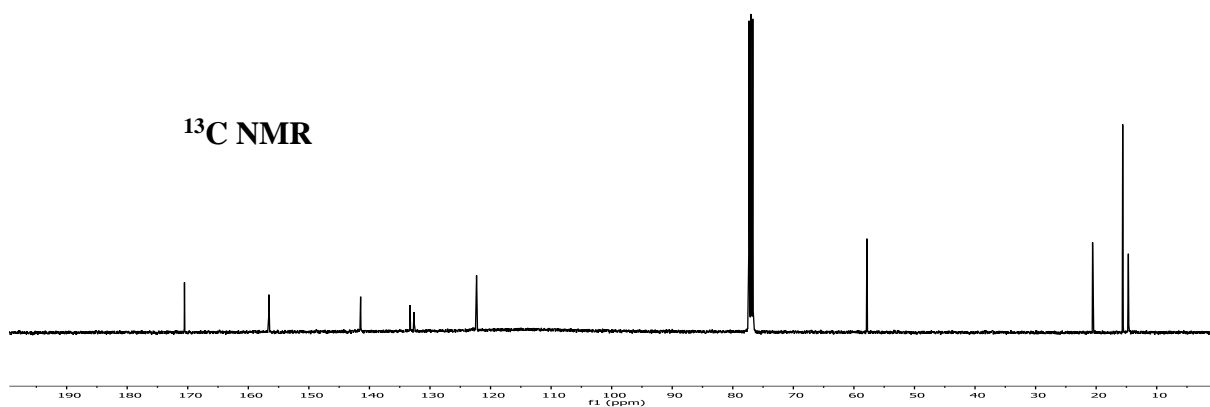
Experimental Part



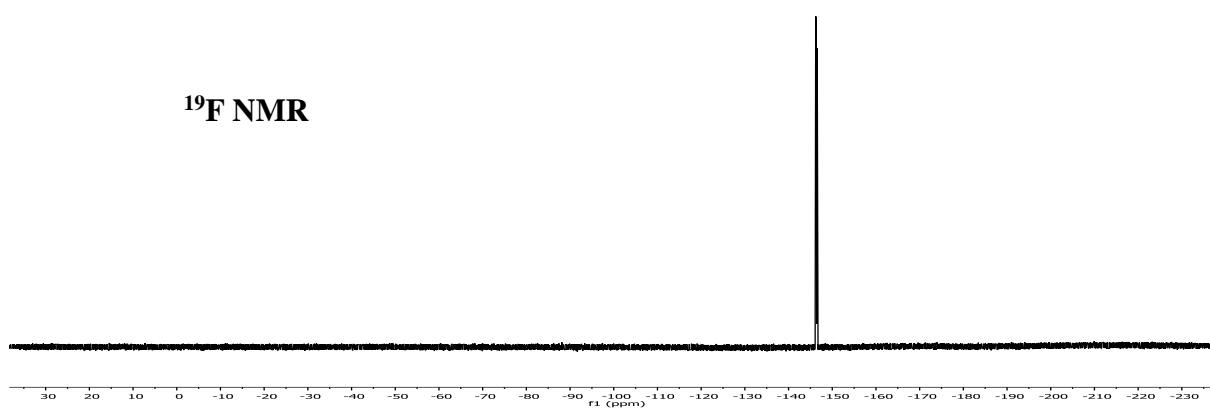
$^1\text{H}$  NMR



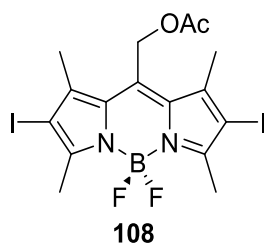
$^{13}\text{C}$  NMR



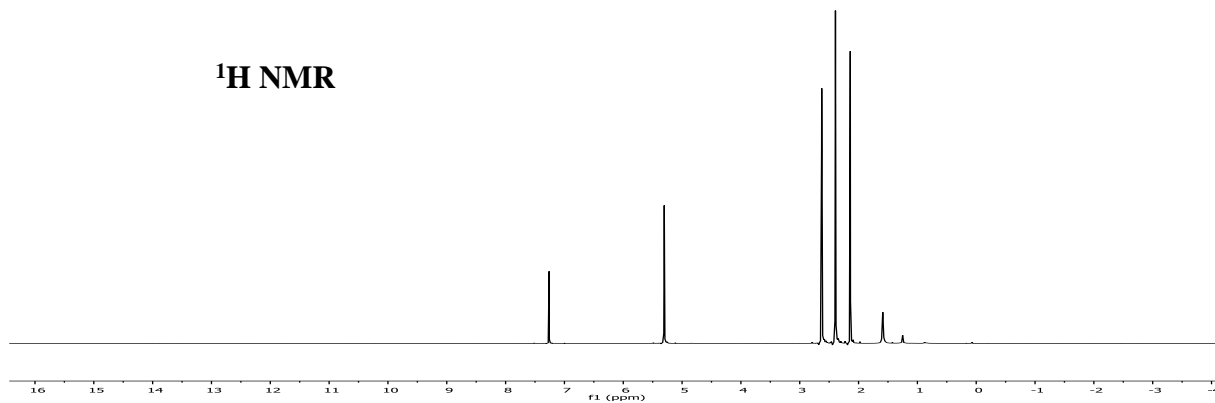
$^{19}\text{F}$  NMR



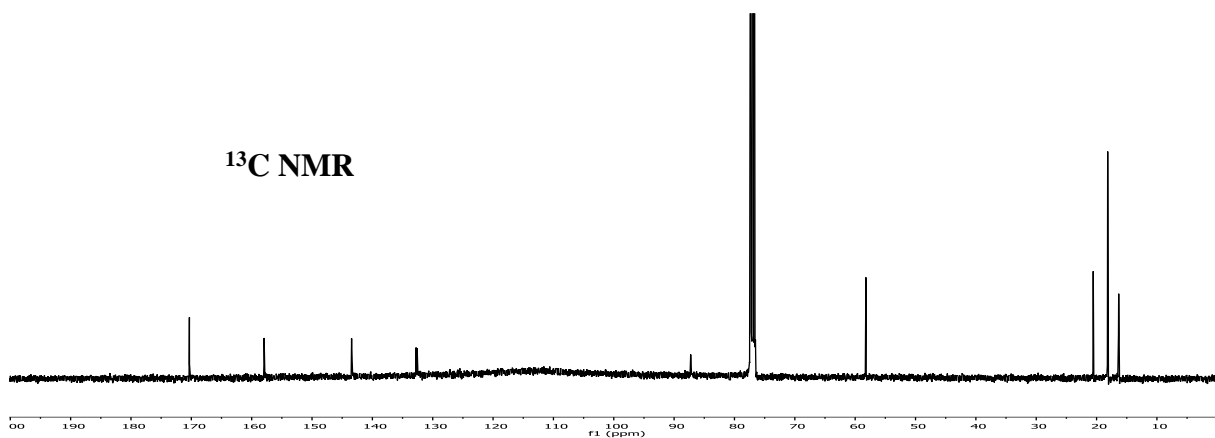
Experimental Part



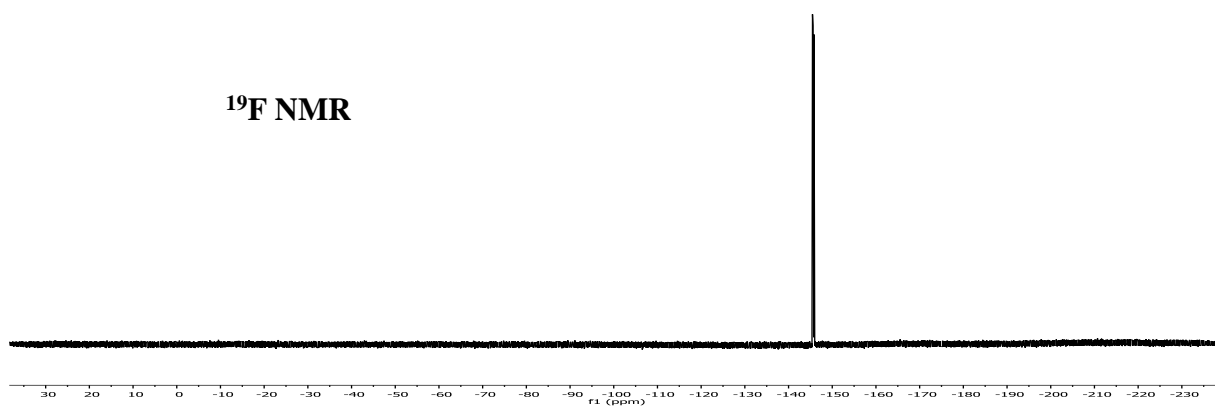
**<sup>1</sup>H NMR**



**<sup>13</sup>C NMR**



**<sup>19</sup>F NMR**

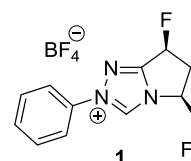




Crystal Data and Structure Refinements

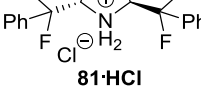
**Table Ex1:** Crystal data and structure refinement for **1**.

Identification code	GIL7080
Empirical formula	C <sub>12</sub> H <sub>12</sub> B F <sub>6</sub> N <sub>3</sub>
Formula weight	323.06
Temperature	223(2) K
Wavelength	1.54178 Å
Crystal system, space group	orthorhombic, P2 <sub>1</sub> 2 <sub>1</sub> 2 <sub>1</sub> (No. 19)
Unit cell dimensions	a = 6.1961(2) Å b = 13.5524(4) Å c = 16.3630(4) Å
Volume	1374.03(7) Å <sup>3</sup>
Z, Calculated density	4, 1.562 Mg/m <sup>3</sup>
Absorption coefficient	1.349 mm <sup>-1</sup>
F(000)	656
Crystal size	0.25 x 0.20 x 0.03 mm
Theta range for data collection	4.24 to 67.07°
Limiting indices	-7<=h<=7, -15<=k<=16, -19<=l<=19
Reflections collected / unique	6930 / 2305 [R(int) = 0.040]
Completeness to theta = 67.07	97.2 %
Absorption correction	Semi-empirical from equivalents
Max. and min. transmission	0.9606 and 0.7290
Refinement method	Full-matrix least-squares on F <sup>2</sup>
Data / restraints / parameters	2305 / 133 / 236
Goodness-of-fit on F <sup>2</sup>	1.043
Final R indices [I>2σ(I)]	R1 = 0.0438, wR <sup>2</sup> = 0.1167
R indices (all data)	R1 = 0.0455, wR <sup>2</sup> = 0.1189
Absolute structure parameter	-0.1(2)
Largest diff. peak and hole	0.175 and -0.167 e.Å <sup>-3</sup>



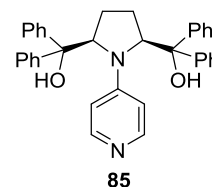
## Experimental Part

**Table Ex2.** Crystal data and structure refinement for **81·HCl**

Identification code	g101111	
Empirical formula 2.5(H <sub>2</sub> O)	3(C <sub>30</sub> H <sub>28</sub> Cl F <sub>2</sub> N),	
Formula weight	491.00	
Temperature	100(2) K	
Wavelength	0.71073 Å	
Crystal system, space group	Orthorhombic, P2(1)2(1)2(1)	
Unit cell dimensions	a = 9.3206(5) Å    alpha = 90 deg. b = 24.5318(12) Å    beta = 90 deg. c = 32.5193(18) Å    gamma = 90 deg.	
Volume	7435.6(7) Å <sup>3</sup>	
Z, Calculated density	4, 1.316 Mg/m <sup>3</sup>	
Absorption coefficient	0.192 mm <sup>-1</sup>	
F(000)	3100	
Crystal size	0.12 x 0.08 x 0.05 mm	
Theta range for data collection	1.77 to 24.82 deg.	
Limiting indices	-8<=h<=10, -19<=k<=28, -38<=l<=29	
Reflections collected / unique	25821 / 11856 [R(int) = 0.0570]	
Completeness to theta = 24.82	96.9 %	
Absorption correction	None	
Max. and min. transmission	0.9905 and 0.9773	
Refinement method	Full-matrix least-squares on F <sup>2</sup>	
Data / restraints / parameters	11856 / 6 / 990	
Goodness-of-fit on F <sup>2</sup>	1.010	
Final R indices [I>2sigma(I)]	R1 = 0.0562, wR2 = 0.0992	
R indices (all data)	R1 = 0.1071, wR2 = 0.1167	
Absolute structure parameter	-0.09(6)	
Largest diff. peak and hole	0.293 and -0.264 e.Å <sup>-3</sup>	

## Experimental Part

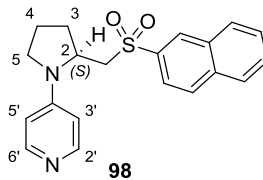
**Table Ex3:** Crystal data and structure refinement for **85**.



Identification code	g250112
Empirical formula	C <sub>35</sub> H <sub>32</sub> N <sub>2</sub> O <sub>2</sub>
Formula weight	512.63
Temperature	100(2) K
Wavelength	0.71073 Å
Crystal system, space group	Monoclinic, P2(1)/c
Unit cell dimensions	a = 12.538(3) Å    alpha = 90 deg. b = 8.998(2) Å    beta = 102.974(12) deg.
Volume	2722.9(12) Å <sup>3</sup>
Z, Calculated density	4, 1.250 Mg/m <sup>3</sup>
Absorption coefficient	0.077 mm <sup>-1</sup>
F(000)	1088
Crystal size	0.14 x 0.13 x 0.02 mm
Theta range for data collection	2.42 to 25.08 deg.
Limiting indices	-14<=h<=14, 0<=k<=10, 0<=l<=29
Reflections collected / unique	4631 / 4762 [R(int) = 0.0000]
Completeness to theta = 25.08	87.0 %
Absorption correction	None
Max. and min. transmission	0.9985 and 0.9893
Refinement method	Full-matrix least-squares on F <sup>2</sup>
Data / restraints / parameters	4762 / 0 / 358
Goodness-of-fit on F <sup>2</sup>	1.076
Final R indices [I>2sigma(I)]	R1 = 0.0968, wR2 = 0.1968
R indices (all data)	R1 = 0.1962, wR2 = 0.2362
Largest diff. peak and hole	0.347 and -0.340 e.Å <sup>-3</sup>

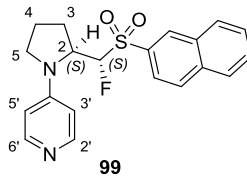
## Experimental Part

**Table Ex4:** Crystal data and structure refinement for **98**.

Identification code	GIL7159	
Empirical formula	C <sub>20</sub> H <sub>20</sub> N <sub>2</sub> O <sub>2</sub> S	
Formula weight	352.44	
Temperature	223(2) K	
Wavelength	1.54178 Å	
Crystal system, space group	monoclinic, P2 <sub>1</sub> (No. 4)	
Unit cell dimensions	a = 8.8880(9) Å b = 5.5190(5) Å    β = 96.859(4)° c = 17.6729(16) Å	
Volume	860.70(14) Å <sup>3</sup>	
Z, Calculated density	2, 1.360 Mg/m <sup>3</sup>	
Absorption coefficient	1.797 mm <sup>-1</sup>	
F(000)	372	
Crystal size	0.20 x 0.05 x 0.02 mm	
Theta range for data collection	2.52 to 66.58°	
Limiting indices	-10 ≤ h ≤ 10, -6 ≤ k ≤ 6, -20 ≤ l ≤ 20	
Reflections collected / unique	8520 / 2752 [R(int) = 0.071]	
Completeness to theta = 66.58	94.5 %	
Absorption correction	Semi-empirical from equivalents	
Max. and min. transmission	0.9649 and 0.7151	
Refinement method	Full-matrix least-squares on F <sup>2</sup>	
Data / restraints / parameters	2752 / 1 / 226	
Goodness-of-fit on F <sup>2</sup>	1.053	
Final R indices [I > 2σ(I)]	R1 = 0.0550, wR <sup>2</sup> = 0.1307	
R indices (all data)	R1 = 0.0718, wR <sup>2</sup> = 0.1465	
Absolute structure parameter	-0.03(3)	
Largest diff. peak and hole	0.219 and -0.262 e.Å <sup>-3</sup>	

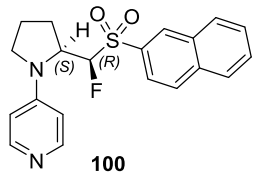
## Experimental Part

**Table Ex5:** Crystal data and structure refinement for **99**.

Identification code	GIL7149	
Empirical formula	C <sub>20</sub> H <sub>19</sub> F N <sub>2</sub> O <sub>2</sub> S	
Formula weight	370.43	
Temperature	223(2) K	
Wavelength	1.54178 Å	
Crystal system, space group	monoclinic, P2 <sub>1</sub> /c (No. 14)	
Unit cell dimensions	a = 15.6211(14) Å b = 10.6548(8) Å    β = 106.453(3) ° c = 10.9800(7) Å	
Volume	1752.7(2) Å <sup>3</sup>	
Z, Calculated density	4, 1.404 Mg/m <sup>3</sup>	
Absorption coefficient	1.879 mm <sup>-1</sup>	
F(000)	776	
Crystal size	0.13 x 0.03 x 0.01 mm	
Theta range for data collection	5.09 to 67.14°	
Limiting indices	-18<=h<=17, -12<=k<=0, 0<=l<=12	
Reflections collected / unique	12132 / 2859 [R(int) = 0.080]	
Completeness to theta = 67.14	91.1 %	
Absorption correction	Semi-empirical from equivalents	
Max. and min. transmission	0.9815 and 0.7923	
Refinement method	Full-matrix least-squares on F <sup>2</sup>	
Data / restraints / parameters	2859 / 0 / 235	
Goodness-of-fit on F <sup>2</sup>	1.044	
Final R indices [I>2σ(I)]	R1 = 0.0518, wR <sup>2</sup> = 0.1247	
R indices (all data)	R1 = 0.0881, wR <sup>2</sup> = 0.1466	
Largest diff. peak and hole	0.264 and -0.298 e.Å <sup>-3</sup>	

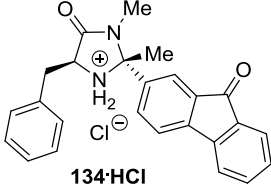
## Experimental Part

**Table Ex6:** Crystal data and structure refinement for **100**.

Identification code	GIL7033	 <p><b>100</b></p>
Empirical formula	$C_{21} H_{23} F N_2 O_3 S$	
Formula weight	402.47	
Temperature	223(2) K	
Wavelength	1.54178 Å	
Crystal system, space group	monoclinic, C2/c (No. 15)	
Unit cell dimensions	$a = 23.781(2) \text{ \AA}$ $b = 8.5624(5) \text{ \AA}$ $c = 20.0162(16) \text{ \AA}$	
Volume	$3959.5(5) \text{ \AA}^3$	
Z, Calculated density	8, 1.350 Mg/m <sup>3</sup>	
Absorption coefficient	$1.743 \text{ mm}^{-1}$	
F(000)	1696	
Crystal size	0.10 x 0.08 x 0.04 mm	
Theta range for data collection	3.83 to 66.90°	
Limiting indices	$0 \leq h \leq 27, 0 \leq k \leq 10, -23 \leq l \leq 22$	
Reflections collected / unique	21680 / 3054 [R(int) = 0.132]	
Completeness to theta = 66.90	86.8 %	
Absorption correction	Semi-empirical from equivalents	
Max. and min. transmission	0.9335 and 0.8450	
Refinement method	Full-matrix least-squares on F <sup>2</sup>	
Data / restraints / parameters	3054 / 0 / 255	
Goodness-of-fit on F <sup>2</sup>	1.038	
Final R indices [I > 2σ(I)]	R1 = 0.0603, wR <sup>2</sup> = 0.1349	
R indices (all data)	R1 = 0.1211, wR <sup>2</sup> = 0.1685	
Largest diff. peak and hole	0.263 and -0.323 e.Å <sup>-3</sup>	

*Experimental Part*

**Table Ex7.** Crystal data and structure refinement for **134·HCl**

Identification code	g170611	 <p><b>134·HCl</b></p>
Empirical formula	C <sub>25</sub> H <sub>23</sub> Cl N <sub>2</sub> O <sub>2</sub>	
Formula weight	418.90	
Temperature	100(2) K	
Wavelength	0.71073 Å	
Crystal system, space group	Monoclinic, P2(1)	
Unit cell dimensions	a = 10.2321(2) Å    alpha = 90 deg. b = 7.63910(10) Å    beta = 94.6000(10) deg.	
Volume	1031.03(3) Å <sup>3</sup>	
Z, Calculated density	2, 1.349 Mg/m <sup>3</sup>	
Absorption coefficient	0.210 mm <sup>-1</sup>	
F(000)	440	
Crystal size	0.19 x 0.11 x 0.04 mm	
Theta range for data collection	2.00 to 27.51 deg.	
Limiting indices	-13 ≤ h ≤ 13, -9 ≤ k ≤ 9, -16 ≤ l ≤ 17	
Reflections collected / unique	9328 / 4520 [R(int) = 0.0215]	
Completeness to theta = 27.51	99.5 %	
Absorption correction	SADABS, multi-scan	
Max. and min. transmission	0.9927 and 0.9611	
Refinement method	Full-matrix least-squares on F <sup>2</sup>	
Data / restraints / parameters	4520 / 1 / 363	
Goodness-of-fit on F <sup>2</sup>	0.744	
Final R indices [I > 2σ(I)]	R1 = 0.0310, wR2 = 0.0874	
R indices (all data)	R1 = 0.0375, wR2 = 0.0949	
Absolute structure parameter	0.07(5)	
Largest diff. peak and hole	0.242 and -0.181 e.Å <sup>-3</sup>	

---

## 11 References

- [1] A. J. Kirby, *Stereoelectronic Effects*, Oxford University Press, Oxford, **2011**.
- [2] P. Radermacher, *Angew. Chem.* **1973**, *85*, 410.
- [3] G. Cuevas, C. De Investigacih, *Tetrahedron* **1992**, *48*, 5019–5087.
- [4] C. Bucher, R. Gilmour, *Angew. Chem. Int. Ed.* **2010**, *49*, 8724–8728.
- [5] C. Bucher, R. Gilmour, *Synlett* **2011**, *2011*, 1043–1046.
- [6] D. O’Hagan, H. S. Rzepa, *Chem. Commun.* **1997**, 645–652.
- [7] S. Wolfe, *Acc. Chem. Res.* **1970**, *1969*, 102–111.
- [8] D. O’Hagan, *Chem. Soc. Rev.* **2008**, *37*, 308–19.
- [9] J. R. Durig, J. Liu, T. S. Little, V. F. Kalasinsky, *J. Phys. Chem.* **1992**, *8233*, 8224–8233.
- [10] C. R. S. Briggs, M. J. Allen, D. O. Hagan, D. J. Tozer, A. M. Z. Slawin, E. Goeta, J. A. K. Howard, *Org. Biomol. Chem.* **2004**, *2*, 732–740.
- [11] C. R. S. Briggs, D. O’Hagan, H. S. Rzepa, A. M. Z. Slawin, *J. Fluor. Chem.* **2004**, *125*, 19–25.
- [12] D. O’Hagan, C. Bilton, J. a. K. Howard, L. Knight, D. J. Tozer, *J. Chem. Soc. Perkin Trans. 2* **2000**, 605–607.
- [13] C. R. S. Briggs, D. O. Hagan, J. A. K. Howard, D. S. Yu, *J. Fluor. Chem.* **2003**, *119*, 9–13.
- [14] A. Sun, D. C. Lankin, K. Hardcastle, J. P. Snyder, *Chem. Eur. J.* **2005**, *11*, 1579–1591.
- [15] N. E. J. Gooseman, D. O’Hagan, A. M. Z. Slawin, A. M. Teale, D. J. Tozer, R. J. Young, *Chem. Commun.* **2006**, 3190–3192.
- [16] C. Sparr, W. B. Schweizer, H. M. Senn, R. Gilmour, *Angew. Chem. Int. Ed.* **2009**, *48*, 3065–3068.
- [17] R. W. Hoffmann, *Chem. Rev.* **1989**, *89*, 1841–1860.
- [18] D. Seebach, R. Gilmour, M. Ebert, A. K. Beck, *Helv. Chim. Acta* **2010**, *93*, 603–634.
- [19] I. G. Molnár, E.-M. Tanzer, C. Daniliuc, R. Gilmour, *Chem. Eur. J.* **2014**, *20*, 794–800.
- [20] R. Gordillo, J. Carter, K. N. Houk, *Adv. Synth. Catal.* **2004**, *346*, 1175–1185.



- [21] R. Gordillo, K. N. Houk, *J. Am. Chem. Soc.* **2006**, *128*, 3543–3553.
- [22] D. Seebach, *Helv. Chim. Acta* **2010**, *93*, 1–16.
- [23] N. A. Paras, D. W. C. Macmillan, *J. Am. Chem. Soc.* **2001**, *3*, 4370–4371.
- [24] C. Sparr, R. Gilmour, *Angew. Chem. Int. Ed.* **2010**, *49*, 6520–6523.
- [25] H. Wynberg, J. S. Svendsen, I. Marko, K. B. Sharpless, *J. Am. Chem. Soc.* **1989**, *111*, 8069–8083.
- [26] S. Jew, H. Park, *Chem. Commun.* **2009**, 7090–7103.
- [27] E.-M. Tanzer, W. B. Schweizer, M.-O. Ebert, R. Gilmour, *Chem. Eur. J.* **2012**, *18*, 2006–2013.
- [28] L. Hintermann, A. Togni, *Angew. Chemie Int. Ed.* **2000**, *39*, 4359–4362.
- [29] D. a DiRocco, K. M. Oberg, D. M. Dalton, T. Rovis, *J. Am. Chem. Soc.* **2009**, *131*, 10872–4.
- [30] J. M. Um, D. a DiRocco, E. L. Noey, T. Rovis, K. N. Houk, *J. Am. Chem. Soc.* **2011**, *133*, 11249–54.
- [31] D. Seebaeh, *Helv. Chim. Acta* **1981**, *64*, 1413–1423.
- [32] D. a DiRocco, E. L. Noey, K. N. Houk, T. Rovis, *Angew. Chem. Int. Ed.* **2012**, *51*, 2391–2394.
- [33] C. L. Chandler, B. List, *J. Am. Chem. Soc.* **2008**, *130*, 6737–6739.
- [34] H. H. Wasserman, J. L. Ives, *Tetrahedron* **1980**, *37*, 1825–1852.
- [35] F. Amat-Guerri, M. M. C. Lopez-Gonzalez, R. Martinez-Utrilla, *J. Photochem. Photobiol. A Chem.* **1990**, *53*, 199–210.
- [36] N. J. Turro, V. Ramamurthy, J. C. Scaiano, *Modern Molecular Photochemistry of Organic Molecules*, University Science Books, Sausalito, **2010**.
- [37] J. C. Koziar, D. O. Cowan, *Acc. Chem. Res.* **1978**, *71*, 334–341.
- [38] A. Kamkaew, S. H. Lim, H. B. Lee, L. V. Kiew, L. Y. Chung, K. Burgess, *Chem. Soc. Rev.* **2013**, *42*, 77–88.
- [39] D. P. Hari, B. König, *Chem. Commun.* **2014**, *50*, 6688–6699.
- [40] L. Huang, J. Zhao, *RSC Adv.* **2013**, *3*, 23377.
- [41] T. Koike, M. Akita, *Synlett* **2013**, *24*, 2492–2505.

- 
- [42] J. M. R. Narayanam, C. R. J. Stephenson, *Chem. Soc. Rev.* **2011**, *40*, 102–13.
- [43] C. K. Prier, D. a Rankic, D. W. C. MacMillan, *Chem. Rev.* **2013**, *113*, 5322–63.
- [44] D. A. Nicewicz, D. W. C. Macmillan, *Science* **2008**, *322*, 77–80.
- [45] M. Neumann, S. Földner, B. König, K. Zeitler, *Angew. Chem. Int. Ed.* **2011**, *50*, 951–954.
- [46] A. Bondi, *J. Phys. Chem.* **1964**, *68*, 441–451.
- [47] S. Paul, W. B. Schweizer, G. Rugg, H. M. Senn, R. Gilmour, *Tetrahedron* **2013**, *69*, 5647–5659.
- [48] S. Paul, W. B. Schweizer, M.-O. Ebert, R. Gilmour, *Organometallics* **2010**, *29*, 4424–4427.
- [49] C. D. Campbell, C. Concellón, A. D. Smith, *Tetrahedron: Asymmetry* **2011**, *22*, 797–811.
- [50] B. Kim, S. Park, *J. Electrochem. Soc.* **1995**, *142*, 34–40.
- [51] M. Karplus, *J. Am. Chem. Soc.* **1963**, *115*, 1962–1963.
- [52] C. Thibaudeau, J. Plavec, J. Chattopadhyaya, *J. Org. Chem.* **1998**, *3263*, 4967–4984.
- [53] C. Altona, R. Francke, *Magn. Reson. Chem.* **1994**, *32*, 670–678.
- [54] C. De Haasnoot, F. Leeuw, C. Altona, *Tetrahedron* **1980**, *27*, 564–576.
- [55] K. G. R. Pachler, *Spectrochim. Acta* **1964**, *20*, 581–587.
- [56] A. Dahbi, *Magn. Reson. Chem.* **1986**, *24*, 337–342.
- [57] A. C. Spivey, S. Arseniyadis, *Angew. Chem. Int. Ed.* **2004**, *43*, 5436–5441.
- [58] L. M. Litvenenko, A. I. Kirichenko, *Dokl. Chem.* **1967**, 763.
- [59] R. P. Wurz, *Chem. Rev.* **2007**, *107*, 5570–5595.
- [60] N. De Rycke, F. Couty, O. R. P. David, *Chem. Eur. J.* **2011**, *17*, 12852–12871.
- [61] J. C. Ruble, H. A. Latham, G. C. Fu, *J. Am. Chem. Soc.* **1997**, *7863*, 1492–1493.
- [62] A. C. Spivey, A. Maddaford, D. P. Leese, A. J. Redgrave, *J. Chem. Soc. Perkin Trans. 1* **2001**, 1785–1794.
- [63] T. Kawabata, M. Nagato, K. Takasu, *J. Am. Chem. Soc.* **1997**, *7863*, 3169–3170.

- [64] G. Priem, S. J. F. Macdonald, M. S. Anson, I. B. Campbell, *J. Org. Chem.* **2003**, *68*, 3844–3848.
- [65] E.-M. Tanzer, L. E. Zimmer, W. B. Schweizer, R. Gilmour, *Chem. Eur. J.* **2012**, *18*, 11334–42.
- [66] Y. P. Rey, L. E. Zimmer, C. Sparr, E.-M. Tanzer, W. B. Schweizer, H. M. Senn, S. Lakhdar, R. Gilmour, *Eur. J. Org. Chem.* **2014**, *2014*, 1202–1211.
- [67] H. Mayr, T. Bug, M. F. Gotta, N. Hering, B. Irrgang, B. Janker, B. Kempf, R. Loos, A. R. Ofial, *J. Am. Chem. Soc.* **2001**, *123*, 9500–9512.
- [68] F. Brotzel, B. Kempf, T. Singer, H. Zipse, H. Mayr, *Chem. Eur. J.* **2007**, *13*, 336–345.
- [69] H. Kagan, J. Fiaud, in *Top. Stereochem. Vol. 18*, John Wiley & Sons, Inc., **1988**, pp. 249–330.
- [70] R. P. Wurz, E. C. Lee, J. C. Ruble, G. C. Fu, *Adv. Synth. Catal.* **2007**, *349*, 2345–2352.
- [71] J. Huang, G. Grasa, S. P. Nolan, *Org. Lett.* **1999**, *1*, 1307–1309.
- [72] V. K. Aggarwal, F. Sandrinelli, J. P. H. Charmant, *Tetrahedron: Asymmetry* **2002**, *13*, 87–93.
- [73] W. J. Lees, R. Singh, G. M. Whitesides, *J. Org. Chem.* **2011**, *56*, 7328–7331.
- [74] M. Von Raumer, P. Suppan, E. Haselbach *Helv. Chim. Acta* **1997**, *80*, 719–724.
- [75] S. Syu, T.-T. Kao, W. Lin, *Tetrahedron* **2010**, *66*, 891–897.
- [76] K. Krumova, G. Cosa, *J. Am. Chem. Soc.* **2010**, 17560–17569.
- [77] A. Loudet, K. Burgess, *Chem. Rev.* **2007**, *107*, 4891–932.
- [78] A. Lamola, S. Hammokd, *J. Am. Chem. Soc.* **1964**, *5*, 1962–1965.
- [79] E. L. Clennan, A. Pace, *Tetrahedron* **2005**, *61*, 6665–6691.
- [80] M. Prein, W. Adam, *Angew. Chemie Int. Ed.* **1996**, *35*, 477–494.
- [81] L. Wang, J.-W. Wang, A. Cui, X.-X. Cai, Y. Wan, Q. Chen, M.-Y. He, W. Zhang, *RSC Adv.* **2013**, *3*, 9219.
- [82] A. Barba-Bon, A. M. Costero, S. Gil, A. Harriman, F. Sancenón, *Chem. Eur. J.* **2014**, *20*, 6339–6347.
- [83] C. Hansch, A. Leo, R. Taft, *Chem. Rev.* **1991**, 165–195.
- [84] J. Karolin, *J. Am. Chem. Soc.* **1994**, 7801–7806.

- [85] G. Ulrich, R. Ziessel, *J. Org. Chem.* **2004**, 2070–2083.
- [86] K. R. Kopecky, H. J. Reich, *Can. J. Chem.* **1965**, *43*, 2265–2270.
- [87] J. E. Hawkins, G. T. Armstrong, *J. Am. Chem. Soc.* **1954**, *76*, 3756–3758.
- [88] C. W. Jefford, C. G. Rimbault, M. H. Laffer, *Helv. Chim. Acta* **1973**, *56*, 2649–2656.
- [89] J. M. Carney, R. J. Hammer, M. Hulce, C. M. Lomas, D. Miyashiro, *Tetrahedron Lett.* **2011**, *52*, 352–355.
- [90] T. States, *J. Am. Chem. Soc.* **1993**, *115*, 12144–12151.
- [91] S. Banfi, G. Nasini, S. Zaza, E. Caruso, *Tetrahedron* **2013**, *69*, 4845–4856.
- [92] M. N. Hopkinson, B. Sahoo, J.-L. Li, F. Glorius, *Chem. Eur. J.* **2014**, *20*, 3874–3886.
- [93] M. M. Maturi, T. Bach, *Angew. Chem. Int. Ed.* **2014**, *53*, 7661–7664.
- [94] A. V. Bezdudny, A. N. Alekseenko, P. K. Mykhailiuk, O. V. Manoilenko, O. V. Shishkin, Y. M. Pustovit, *Eur. J. Org. Chem.* **2011**, 1782–1785.
- [95] C. Sparr, E.-M. Tanzer, J. Bachmann, R. Gilmour, *Synthesis* **2010**, *2010*, 1394–1397.
- [96] N. A. Paras, D. W. C. Macmillan, *J. Am. Chem. Soc.* **2002**, *124*, 7894–7895.
- [97] S. Ribeiro, a Serra, a Rochagonsalves, *J. Catal.* **2008**, *256*, 331–337.
- [98] J. Carney, R. Hammer, M. Hulce, C. Lomas, D. Miyashiro, *Synthesis* **2012**, *44*, 2560–2566.
- [99] G. Duran-Sampedro, A. R. Agarrabeitia, I. Garcia-Moreno, A. Costela, J. Banuelos, T. Arbeloa, I. Lopez Arbeloa, J. L. Chiara, M. J. Ortiz, *Eur. J. Org. Chem.* **2012**, 6335–6350.

## Curriculum Vitae

**Yannick Pierre Rey**

**Born 10.11.1985**

**Citizen of Geltwil (AG), Switzerland**

---

- Since February 2011** **Swiss Federal Institute of Technology (ETH) Zürich, Switzerland** and **Westfälische-Wilhelms-Universität (WWU) Münster, Germany.**  
Ph.D studies with Prof. Gilmour on asymmetric organocatalysis.
- Fall Semester 2010** **Swiss Federal Institute of Technology (ETH) Zürich, Switzerland.**  
Master Thesis in the group of Prof. Gilmour on “*The Design and Synthesis of a Metal Free Photoredox Catalyst for Enantioselective  $\alpha$ -Functionalisation of Aldehydes*”.
- Novartis Master Fellowship in Organic Chemistry (ETH Zürich).**
- Spring Semester 2010** **Swiss Federal Institute of Technology (ETH) Zürich, Switzerland.**  
Semester work in the group of Prof. Diederich on “*The Design and Synthesis of Potential Inhibitors for IspD*”.
- Spring Semester 2009** **Swiss Federal Institute of Technology (ETH) Zürich, Switzerland.**  
Advanced Organic Chemistry Laboratory, OCP II.
- 2005 – 2010** **Swiss Federal Institute of Technology (ETH) Zürich, Switzerland.**  
Bachelor and Master studies of Chemistry at ETH Zürich.
- 2004 – 2005** **Military Service and language stay in Vancouver, Canada.**
- 2000 – 2004** **Gymnasium in Pfäffikon SZ, Switzerland.**
- 1998 – 2000** **Secondary School in Freienbach, Switzerland.**
- 1992 – 1998** **Primary School in Pfäffikon SZ, Switzerland.**

### Teaching experience:

**Fall Semester 2011** Teaching Assistant Organic Chemistry I Practical Lab Course